FLAMMABILITY STUDIES ON BIOPOLYMERS AND THEIR BLENDS

by

MFISO EMMANUEL MNGOMEZULU (M.Sc.)

2002121057

Submitted in accordance with the requirements for the degree

PHILOSOPHIAE DOCTOR (Ph.D.) in Polymer Science

Department of Chemistry

Faculty of Natural and Agricultural Sciences

at the

UNIVERSITY OF THE FREE STATE (QWAQWA CAMPUS)

SUPERVISORS: DR M.J. JOHN and PROF A.S. LUYT

CO-SUPERVISOR: DR N.V. JACOBS

***The financial assistance of the National Research Foundation towards this research is hereby acknowledged. Opinions expressed and conclusions arrived at, are those of the author and are not necessarily to be attributed to the NRF*.**

January 2016

DECLARATION

I declare that the dissertation hereby submitted by me for the Doctor of Philosophy degree at the University of the Free State is my own independent work and has not previously been submitted by me at another university/faculty. I furthermore, cede copyright of the dissertation in favour of the University of the Free State.

_____

MngomezuluM.E. (Mr)

DEDICATIONS

This thesis is dedicated to ugogo Tholoana Cathrine MaMotaung Yika, ukhulu Nozimvu Grace MaMngomezulu Magubani, ugogo Ntombizodwa MaGamede Yika, umkhulu Lehlohonolo Petrus Monareng, ubabekazi Nomakhosi Violet MaMngomezulu Motaung bonke asebendele kwelamathongo.

It is also dedicated to the following people for, their incessant love and reminder that LIFE IS NOW!

- My friend and soulmate Ma-ka-Ngonyama “Mango” MaMosia Mngomezulu (wife), Zamafiso “Zamzeni” Jemina Nonhlonipho and Nokukhanya “Khanyo” Violet Nandi Mngomezulu (daughters).
- My parents ubaba Vusimuzi Josiah and umama Ma-ka-Mfiso Jemina MaMonareng Mngomezulu, ubaba Mokete Joseph (osekwelamathongo) and umama ′MaTankiso MaGamede Mosia as well as Mngomezulu and Mosia families.
- My grandparents ukhulu Teboho Linah MaYika and ubabamkhulu Christmas Meshaek “umcansa ongakhwelwa ‘mbongolo, Mashobane” Mngomezulu and ukhulu Kukkie Violet MaKhumalo and ubabamkhulu Lehlohonolo Petrus Monareng.
- My siblings and nephews: Thokozile Grace, Teboho Linah, Chrismas Khehla, Lehlohonolo Thamsanqa, Lebohang “Mohlomphehi”, Mpho and Tshepo Makhalemele
- Mme Moipone Alice Malimabe.

ACKNOWLEDGEMENTS

The preparation of this thesis would not have been possible without the will of the Almighty God and the support, hard work and endless efforts of a large number of individuals and institutions.

I would like to thank my supervisors/co-supervisors, **Dr Maya Jacob John and Prof. Adriaan Stephanus Luyt** for their great efforts to explain things clearly and simply, and their guidance during my research. I express my deep sense of gratitude for their guidance, cloudless source of inspiration and constant support all through the course of the study. Throughout my thesis-writing period, they provided encouragement, sound advice, good teaching, good company and lots of good ideas. Their overly enthusiasm and integral view on research and their mission for providing 'only high-quality work and not less', has made a deep impression on me. They could not even realize how much I have learned from them.

I would like to gratefully acknowledge my enthusiastic co-supervisor **Dr Nokwindla Valencia Jacobs** and my mentor **Mr. Steve A Chapple,** during this work, who shared with me a lot of their expertise and research insight.

I acknowledge the University of the Free State and CSIR at large by proving me with an opportunity to study.
I would like to acknowledge the financial support by the National Research Foundation (NRF) and Department of Science and Technology (DST) under the Professional Development Programme (PDP). Acknowledgements are also extended to my colleagues for their undivided attention and support.

Many thanks are due to Dr. Vladimir Djoković and my fellow polymer science research group members from the CSIR, NMMU and UFS: Dr. B. Hlangothi, Dr SP Hlangothi, Dr. Tshwafo Motaung, Dr. Mokgaotsa Mochane, Dr Puseletso Mofokeng, Dr Thabang Mokhothu, Dr Doice Moyo, Dr Christopher Ogunleye, Prof Oriel Thekisoe, Dr Mohammad Essa Ahmad, Dr. Asanda Mtibe, Mr. Teboho Mokhena, Miss Tshepiso Molaba, Dr. Shale Sefadi, Mr. Rantoa Moji, Dr Linda Linganiso, Mr. Osei Ofosu, Dr Dusco Dudic, Mr. Mahase from Geography department (UFS) and the rest, for their support throughout the study. Thank you very much!

ABSTRACT

The effect of commercial expandable graphite (EG) on the flammability and thermal decomposition characteristics of two systems based on poly(lactic acid) (PLA) and poly(lactic acid)/poly(ε-caprolactone) (PLA/PCL) blend was investigated. Furthermore, the morphology, structure, melting and crystallization behaviour as well as the dynamic mechanical properties of flame retardant PLA/EG and PLA/PCL/EG composites were also studied. The flame retardant PLA/EG and PLA/PCL/EG composites were prepared by melt-mixing using the Brabender-Plastograph and were melt-pressed using the electrical hydraulichot melt press. The samples were characterized for their flammability performance and thermal stability via cone calorimeter and thermogravimetric analyser (TGA), respectively. They were also characterized for their volatile pyrolysis products during thermal degradation using simultaneous TGA-Fourier transform infrared spectroscopy (TGA-FTIR). The char residues obtained after combustion by cone calorimeter were further analysed with environmental scanning electron microscopy (ESEM). Furthermore, X-ray diffraction (XRD) and scanning electron microscopy (SEM) were used to elucidate the structure and morphology of the flame retardant PLA/EG and PLA/PCL/EG composite systems. Their thermal behaviour (i.e. melting and crystallization) as well as their thermo-mechanical properties were respectively analysed by differential scanning calorimetry (DSC) and dynamic mechanical analysis (DMA) techniques.

For the PLA/EG composite system, the thermal decomposition stability of the composites was improved in the presence of EG. However, the char content was less than expected as per the sum of the wt.% EG added into PLA and % residue of PLA after thermal decomposition. The flammability performance of the PLA/EG composites was improved, especially at 15 wt.% EG content, due to a thick and strong worm-like char structure. The peak heat release rate (PHRR) was improved by 74%, the total smoke production (TSP) was improved by 40% and the specific extinction area (SEA) by 55%. These improvements were due to the ability of EG to exfoliate at increased temperatures during which three effects occurred: i) cooling effect due to an endothermic exfoliation process; ii) dilution effect due to the release of H_2O, SO_2 and CO_2 gases and iii) formation of a protective intumescent char layer. However, both the CO and CO_2 yields were found to be unfavourably high due to the presence of EG. The graphite layers still existed in an aggregate structure with poor filler dispersion and lack of interfacial adhesion between EG and the PLA matrix. The presence of EG micro-particles: i) did not favour the

crystallization of PLA, ii) increased the glass transition temperature and iii) showed a reduction in the crystallinity of the composites. The composites showed enhanced storage and loss moduli, especially at high EG contents (i.e. 10 and 15 wt.%). The glass transition from the loss modulus and damping factor varied inconsistently with the EG content. The use of commercial expandable graphite as filler in PLA could preserve the thermal properties of injection molding grade Cereplast PLA, while improving the fire resistance of PLA/EG flame retardant composites.

In the case of PLA/PCL/EG flame retardant composite system, the thermal degradation stability of the composites was improved and the char content was found to have increased. Although the char content of the composites increased generally with EG loadings, the combined % residue from both the blend and wt.% EG initially added into the blend was higher than the observed % residue because of the thermal degradation mechanism that favoured the formation of CO and CO_2 volatile gases rather than carbon. The flammability performance results indicated that the PLA/PCL blend was successfully modified with the EG micro-filler that resulted in fire resistant composites, especially at high filler loadings, due to the formation of intumescent carbonaceous char. This was confirmed by reductions of up to 64% in both the peak heat release rate (PHRR) and the total smoke release (TSR) and 54% in the specific extinction area (SEA). This was due to the EG acting mainly through a physical mode by cooling and fuel dilution and through the formation of an intumescent char layer. However, the effective heat of combustion (EHC) and carbon monoxide (CO) yields did not favourably improve. It was found that the melt mixing process could not separate the graphite layers, which existed as aggregate structures (i.e. EG layered stacks and/or lumps). In the composites, PCL was favoured to crystallize mainly on the surface of the microspheres and EG. The PLA/PCL blend showed an immiscibility feature, even in the presence of EG filler. Incorporation of EG in PLA/PCL blend influenced the melting and crystallization behaviour of PCL than that of the PLA component. Both the PCL and EG hindered the crystallization of the PLA component. From DSC and DMA, the glass transition of the composites occurred at high temperatures, suggesting that PLA polymer chains were immobilized in the presence of EG micro filler. The storage and loss moduli values were low for the composites when compared to PLA/PCL. The results suggest that the PLA/PCL/EG flame retardant composites have low thermal and thermo-mechanical properties due to the aggregation of EG and lack of interfacial adhesion between EG lumps and the polymer blend matrix.

CONFERENCES AND PUBLICATIONS

Conferences

1. ME Mngomezulu, MJ John, V Jacobs, AS Luyt. Flammability and thermal properties of polylactic acid based blends. ICCBN2013, 02-04 December 2013, Durban University of Technology (DUT), Durban, South Africa.
2. ME Mngomezulu, MJ John, V Jacobs, AS Luyt. Flammability and thermal properties of polylactic acid based blends. Fire Retardant Technologies 2014 (FRT14), 14-16April 2014, University of Central Lancashire, Preston, UK. (Poster presented on my behalf by Mr. Steve Chapple). Awarded Best Student Poster, 2nd prize.
3. ME Mngomezulu, MJ John, V Jacobs, AS Luyt. Flammability, thermal, morphology and visco-elastic characteristics of natural silicate filled-polylactic acid/poly(ε-caprolactone) (PLA/PCL) biobased blends.MAM-14, International Symposium on Macro- and Supramolecular Architectures and Materials, 23-27 November 2014, Emperors' Palace, Johannesburg, South Africa.

Publications

1. Mngomezulu, M.E., John, M.J., Jacobs, V., Luyt, A.S. (2014). Review on flammability of biofibres and biocomposites. *Carbohydrate Polymers*, 111:149-182. DOI: 10.1016/j.carbpol.2014.03.071
2. Mngomezulu, M.E., John, M.J. (2015). Thermoset-cellulose nanocomposites; Flammability characteristics; Chapter 7, In Handbook of Thermoset-Cellulose Nanocomposites (Submitted for review). Handbook to be published by Wiley-VCH in 2016.

Papers under preparation

1. Thermal degradation kinetics of fire resistant poly(lactic acid)/expandable graphite (PLA/EG) composites

2. Effect of expandable graphite (EG) on the fire resistance and thermal degradation stability of poly(lactic acid)/poly(ε-caprolactone)/vermiculite (PLA/PCL/VMT) composites
3. Morphology, thermal, static and mechanical characteristics of fire resistant poly(lactic acid)/poly(ε-caprolactone)/vermiculite/expandable graphite (PLA/PCL/VMT)/EG composites
4. Preparation and characterization of diammonium phosphate (DAP) flame retarded poly(lactic acid)/poly(ε-caprolactone) (PLA/PCL) blend
5. Flammability, thermal decomposition and morphology of char residues of diammonium phosphate (DAP) flame retarded poly(lactic acid)/poly(ε-caprolactone)/vermiculite (PLA/PCL/VMT) composites
6. Structure and properties of flame retardant poly(lactic acid)/poly(ε-caprolactone)/vermiculite/diammonium phosphate (PLA/PCL/VMT)/DAP composites

TABLE OF CONTENTS

LIST OF TABLES

LIST OF FIGURES

LIST OF ABBREVIATIONS

APP	Ammonium polyphosphate
ASTM	American society for testing and materials
ATH	Aluminium tri-hydrate
av-MLR	Average specific mass loss rate
BAl	Boehemite aluminium
BDP	Bisphenyl A bis(diphenyl phosphate)
DMA/DMTA	Dynamic mechanical analysis/ thermal analysis
DNA	Deoxyribonucleic acid
DSC	Differential scanning calorimetry
DTG	Derivative thermogravimetric analysis
EG	Expandable graphite
EG	Expandable graphite
EVA	Ethylene-co-vinyl acetate
EVA	Ethylene vinyl acetate
EVAL	Ethylene-vinyl alcohol copolymer
FPI	Fire performance index
FRAs	Flame retardant agents/additives
FRs	Flame retardants
HBCD	Hexabromocyclododecane
HDPE	High density polyethylene
HPCA	Hyperbranched polyamine charring agent
HRC	Heat release capacity (η_c)
HRR	Heat release rate
IFR	Intumescent flame retardant
LDPE	Low-density polyethylene
LDPE	Low density polyethylene
LLDPE	Linear low-density polyethylene
LOI	Limited oxygen index
MA	Melamine
MA-*g*-PP	Maleic acid grafted polypropylene
MARHE	Maximum average rate of heat emission
MCC	Microscale combustion calorimetry

MFI	Melt flow injection
MH or MDH	Magnesium hydroxide or Magnesium dihydroxide
MLR	Mass loss rate
MMB	Melamine borate
MMP	Melamine phosphate
MMT	Montmorillonite
MPD	methacryloyloxyethylorthophosphorotetraethyl diamidate
MWNTs	Multi walled nanotubes
NAs	Normal additives
NFRBC	Natural fibre reinforced biopolymer composites
NFs	Natural fibres
OMT	Organophilic montmorilonite
OSU	OhioStateUniversity
PA6	Polyamide 6
PBAT	Poly(butylene adipate-co-terephthalate)
PBDE	Polybromodiphenyl ether
PBT	Poly(butylene terephthalate)
PC	Polycarbonate
PC	Polycarbonate
PCFC	Pyrolysis combustion flow calorimetry
PCL	Polycaprolactone
PE	Polyethylene
PE	Polyethylene
PEBAX	Polyether blockamide
PHBV	Poly(3-hydroxybutyrate-co-3-hydroxyvalerate)
PHRR	Peak heat release rate
PLA	Polylactic acid
PMMA	Polymethyl methacrylate
POSS	Polyhedral oligomeric silsesquioxane
PP	Polypropylene
PP	Polypropylene
PPTA	Poly(p-phenylenediamineterephthalamide)
PS	Polystyrene
PS	Polystyrene

PTT	Poly(trimethylene terephthalate)
PU	Polyurethane
PU	Polyurethane
RAs	Reactive additives
RTM	Resin transfer moulding
SBS	Styrene-butadiene-styrene
SEA	Soot extinction area
SEBS	Styrene-ethylene-butylene-styrene
SEM	Scanning electron microscopy
SEM	Scanning electron microscopy
SPDPM	Spirocyclic pentaerythritol bisphosphorate disphosphoryl melamine
SPR	Smoke production rate
SWNTs	Single walled nanotubes
TBBPA	Tetrabromobisphenol A
TBPA	Tetrabromophthalic anhydride
TGA	Thermogravimetric analysis
THR	Total heat release
TPOSS	Trisilanolphenylpolyhedral oligomeric silsesquioxane
TTI	Time to ignition
UL 94	Underwriter laboratories 94
UV	Ultraviolet
UV	Ultraviolet
Viz.	(*videlicet*) Namely
X_c	Degree of crystallinity
ZB	Zinc borate

Chapter 1

Introduction

1.1 General background

The flammability and/or reaction-to-fire characteristics of biodegradable polymers (e.g. poly(lactic acid) (PLA)) and their blends (e.g. poly(lactic acid)/poly(ε-caprolactone) (PLA/PCL)) are becoming important of recent. This is as a consequence of the current trends in the plastics industry whereby there is a shift from petroleum-based polymeric materials to biodegradable materials. The shift is encouraged by various factors, such as: shortage and high cost of fossil fuel, as well as environmental concerns. Since biodegradable polymers are produced, for instance, from bio-based agricultural resources, they possess supportive features to the environment (i.e. biodegradation, compostability and environmental friendliness). Additionally, they have chemical and physical properties comparable to those of petroleum-based polymers. Similar to the latter, biodegradable polymers are hydrocarbons which, when exposed to fire, may quickly ignite and combust releasing *inter alia* carbon dioxide, water and large amounts of heat. Their release of large quantities of heat creates a challenge to their applications in advanced engineering fields (e.g. aerospace, automotive, construction, electric and electronics), since they are potential fire hazards and can pose risk to infrastructures and lives. Consequently, there is a need to investigate the possible and cost effective ways of improving reaction-to-fire properties of biodegradable polymers and their blends [1-6].

Studies on fire retardancy properties of biodegradable polymers are necessary in order to extend their usefulness. Fire retardancy may be defined as a phenomenon whereby a polymeric material may be rendered less likely ignitable with the use of micro or nanoscale additive/filler materials, termed flame retardants. In case a material is ignitable, the presence of flame retardants should encourage such a material to burn with less efficiency. Fire retardancy may be accomplished by various approaches, including chemical and physical treatments of polymeric materials. The physical approach of fire retardancy may be exemplified by the use of flame retardant fillers, such as carbon-based materials (e.g. expandable graphite (EG)) [1,5,7]. Further and elaborate discussions are provided in Chapter 2.

EG is an intercalated compound produced by the chemical or electrochemical intercalation of molecular or atom guests (e.g. sulphuric acid) between the layers of graphite. Its structure consists of graphene layers (see Figure 1.1A) within which chemical compounds (i.e. oxidants, such as H_2SO_4 or HNO_3 and $KMnO_4$) are intercalated. When exposed to high temperatures (i.e. >190 °C), EG layers are able to exfoliate and expand rapidly in an accordion-like pattern (see Figures 1.1B & C). This is due to the decomposition of the intercalating medium (e.g. sulfuric acid, H_2SO_4) into water (H_2O) and sulphur dioxide (SO_2) gases. EG also undergoes oxidation by H_2SO_4 with the production of CO_2 in addition to SO_2 according to Equation 1.1 [8-12].

$$C + 2H_2SO_4 \rightarrow CO_2 + 2SO_2 + 2H_2O \qquad (1.1)$$

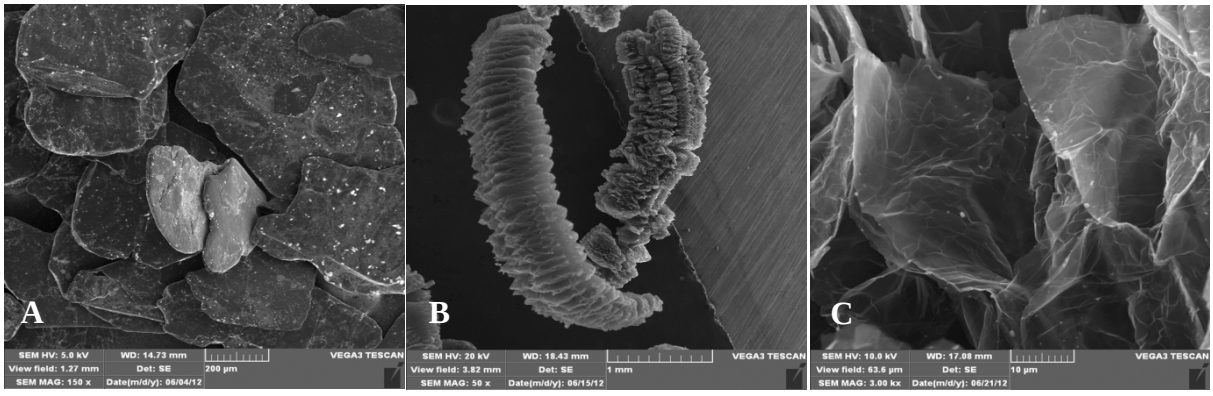

Figure 1.1 Scanning electron microscopy (SEM) images of (A) EG, (B) exfoliated and/or intumesced graphite and (C) intumesced graphite layers at high magnification

The exfoliation of EG during exposure to high temperatures is an endothermic process. Thus, when it is used as a flame retardant in polymeric materials, the temperature in the system is decreased to below polymer combustion temperatures. The decomposition of an acid as well as the redox reaction between an acid and graphite result in the production of inert gases (i.e. H_2O, CO_2 and SO_2), which may lead to favourable dilution of a mixture of combustible gases. These inert gases limit both the concentration of reagents and the possibility of materials to ignite when exposed to fire. Additionally, the resultant carbonaceous intumescent char (see Figures 1.1B and C) would form a protective layer between the gaseous and solid combustible phases. Consequently, the transfer of combustible volatile gases is limited and the oxygen necessary for combustion is excluded so that the amount of decomposition gases is reduced [13,14]. This is considered as a physical mode of action, expressed by the cooling and fuel

dilution effects, as well as the formation of a protective barrier [1]. When EG is used as a filler in a polymer matrix and the polymer/EG composite material is exposed to heat, it produces a protective exfoliated graphite covering the burning polymer surface. Since EG begins to exfoliate at temperatures below the onset of thermal decomposition temperature of polymers such as PLA at ~280 °C, EG will act before the degradation of the biopolymer. It may, therefore, modify the thermal degradation pathway of PLA to yield some char and probably lower the evolution of flammable pyrolysis products [9,2,14].

Biodegradable polymers in general, PLA and PCL in particular, have been subjects of various studies, either in i) composites or ii) blends. The modification of PLA, specifically through these two ways, comes as a result of some inherent limitations due to its chemical structure.

PLA belongs to the family of aliphatic polyesters generally made from α-hydroxy acids. The latter include polyglycolic acid or polymandelic acid. It is produced from a bio-based 2-hydroxy propionic acid (i.e. lactic acid) monomer by classical synthesis and it is therefore biodegradable and compostable. Lactic acid may be produced by either i) bacterial fermentation of carbohydrates or ii) chemical synthesis with the former being a predominant route. The bacterial fermentation of carbohydrates uses homolactic organisms, such as different types of optimized or modified strains of the genus *Lactobacilli* which exclusively forms lactic acid. The various types of carbohydrates used in the fermentation are obtained from agricultural by-products and include i) glucose, maltose and dextrose from corn or potato starch, ii) sucrose from cane or beet sugar and iii) lactose from cheese whey. PLA is applied in various fields, such as: medical and pharmaceuticals, textiles, packaging and composites. It is the most highly produced degradable aliphatic polyester at relatively reasonable cost. It has several advantages, which include: eco-friendliness, biocompatibility, processability and energy efficiency during production [15-18]. Several limitations inherent to PLA were identified from literature and these include: poor toughness, hydrophobicity, slow crystallization rate, lack of side-chain groups and poor flammability performance [1,9,17,19-22].

As a consequence of the aforementioned limitations, there is a need to modify PLA, *via* i) the use of fillers, such as EG to form polymer composites and ii) blending it with other biodegradable polymers, such as PCL to form polymer blends [1,9,17,19-22]. Similar to PLA, PCL is also a biodegradable, semi-crystalline linear aliphatic commercial polyester. It is

obtained by ring opening polymerization (ROP) from ε-caprolactone. PCL has a low tensile strength, high elongation-at-break and its processing temperatures are similar to those of PLA. It is therefore expected that PCL can act as a plasticizing agent when blended with PLA [23].

Blending of existing polymers lowers the need for the synthesis of new materials. It provides an economic advantage over the development of new polymers. Numerous blend systems have been developed and commercialized. They include: chemical blends, solution cast blends, latex blends, mechano-chemical blends and thermo-mechanical blends. In the last type of blending, polymers are mixed at temperatures above the glass transition (T_g) or melting (T_m) temperatures for amorphous and semicrystalline polymers, respectively. This is also known as a melt-mixing/blending process and it is the approach chosen in this study for the preparation of PLA/EG and PLA/PCL/EG flame retardant blend systems, because it is relatively easy and less costly [24,25]. Blending PLA with PCL provides an important property complementarity. In this case, glassy PLA with low thermal stability and high degradation rate exhibits better tensile strength, while the rubbery PCL with high thermal stability and relatively slower degradation rate shows better toughness [23,26-31]. Generally, studies on PLA/PCL blends have been mainly focused on biodegradation, structure, morphology, static and dynamic mechanical, rheology and thermal properties. So far, there is little, if any, work done on the flammability properties of PLA/PCL with EG as filler [21,22].

A filler may be defined as a material that is added into a polymeric material to modify its strength and working properties, or sometimes to lower its cost. The incorporation of a filler may give rise to high heat resistance, high mechanical strength, low moisture absorption and good electrical and flammability properties. Fillers are abundantly available at low cost, they are expected to be compatible with polymer matrices as well as other additives and they should not have abrasive or chemical action on the mould [25]. When a filler is compounded with a polymer, a composite is produced. Composites are materials made-up of distinct phases with different physical properties. They often consist of a soft continuous flexible matrix (e.g. PLA or PLA/PCL) reinforced by a stiffer component (e.g. EG). Similar to blends, the development of polymer composites is motivated by property improvement and cost. They may be classified into three main categories, including: i) particulate composites, ii) discontinuous fibre composites and iii) continuous fibre composites. In the last category, fibres may be aligned uniaxially, while in the second category, fibres may be aligned or randomly placed at various positions in the composite. In particulate composites, particles may be spherical but usually

have non-uniform shapes and are sometimes elongated or even plate-like, such as EG (see Figure 1.1A) [24]. Generally, composites may be prepared either by solution mixing, melt extrusion/blending, milling or injection moulding. They are formulated for various purposes, *inter alia*, for improved fire resistance and better thermal stability characteristics. For example, PLA is reported to be flammable and burning with intense dripping during combustion; however, the incorporation of clay and/or expanded graphite rendered PLA-based composites to be fire resistant [9]. Similarly, EG, either alone or with other additives (e.g. ammonium polyphosphate, zinc borate, phosphorus-nitrogen compounds), has been used as a flame retardant in various polymer matrices. It has been mostly used in petroleum-based polymers (e.g. polyolefins, polyurethanes, and polyamide), but less used in biodegradable polymers (e.g. PLA) [8,25,32-41].

There have been few studies conducted on the use of EG as a flame retardant in a PLA matrix [32,40,41]. From these, improved reaction-to-fire behaviour was reported. For instance, extruded PLA/EG composites with the highest V-0 ranking (UL-94 flammability test) at low filler loadings and lowered rate of combustion, were reported [32]. Furthermore, improved thermal stability, flame retardancy, synergistic effect and anti-dripping performance of melt blended PLA/EG/{poly(bis(phenoxy)phosphazene)} and EG/ammonium polyphosphate (APP) (1:3) filled-PLA composites were also reported [40,41]. In addition to EG, ammonium polyphosphate, boehmite, clays, halloysite, talc and silica have also been investigated as fillers for PLA. The resulting flame retarded PLA materials were characterized and were reported to have better thermal, mechanical and fire resistance performance [1,9,33-43]. It is also noted that PLA, in addition to poor flammability performance, has low rigidity for applications, such as: in electric and electronics (e.g. housings for notebook computers) [44]. In addition to improving its flame resistance, it may also be blended with other petroleum-based polymers, such as: polystyrene, polyethylene and polypropylene for better rigidity. Such developed PLA-based materials exhibit optimal physical and flammability properties, qualifying them for the intended purpose. Consequently, blending of PLA and other polymers with the simultaneous incorporation of flame retardant fillers becomes evidently important. However, in order to uphold the eco-friendliness character of the resulting composites, it may be necessary to use biodegradable polymers (e.g. PCL) instead.

The flammability properties of blends (e.g. ethylene vinyl acetate/low-density polyethylene (EVA/LDPE), poly(lactic acid)/polycarbonate (PLA/PC), poly(3-hydroxybutyrate-co-3-

hydroxyvalerate)/poly(butylene adipate-co-terephthalate) (PHBV/PBAT)) may also be improved through the use of various additives, including: clays, graphite, aluminium hypophosphate and glass fibres [9,45-47]. The incorporation of EG with phosphorus-based compounds and zinc borate in EVA/LDPE blends yields flame retardant polyolefin materials of good mechanical and flammability properties. This is attributed to the synergy between flame retardants and EG [45]. Furthermore, the use of synthetic glass fibre as reinforcement in a 70/30 w/w PLA/PC blend filled with aluminium hypophosphite led to improved mechanical properties, heat and fire resistance [46]. Although little work has been done on the fire retardancy of biodegradable polymer blends, a successful work on improved flame retardancy of the system composed of a commercial PHBV/PBAT blend with aluminium phosphinate and metal oxides (i.e. antimony oxide, Sb_2O_3, and iron oxide, Fe_2O_3) nano-particle fillers was reported [47].

It is therefore against this brief background that the question is formulated: What influence will commercial EG have on the flammability, morphology, as well as thermal and thermo-mechanical characteristics of Cereplast PLA (i.e. PLA/starch blend with other bio-based additives) [2,48] and its blend with PCL (i.e. PLA/PCL)? The current study was aimed at the extension of the possible applications of PLA/EG and PLA/PCL/EG composites and the addition to the knowledge base in the polymer composites field.

1.2 Aims and objectives

The aims of this study are: i) to investigate whether the incorporation of commercial EG in PLA and a PLA/PCL blend can improve their flammability properties and thermal stability, ii) to determine the influence of blending PLA with PCL on the foregoing properties and iii) to determine the melting and crystallization, morphology, structure and thermo-mechanical properties of the PLA/EG and PLA/PCL/EG composites prepared. The objectives are, therefore: i) to develop PLA/EG and PLA/PCL/EG flame retardant composites and ii) to characterize the composites developed for their flammability performance, thermal decomposition stability, pyrolysis volatile products, morphology, structure, melting and crystallization behaviour and dynamic mechanical properties.

1.3 Thesis outline

The outline of this thesis is as follows:

Chapter 1: Introduction

Chapter 2: Review on flammability of biofibres and biocomposites

Chapter 3: Flammability, thermal decomposition and morphology of char residues of expandable graphite flame retardant poly(lactic acid) (PLA) composites

Chapter 4: Morphology, thermal and dynamic mechanical properties of poly(lactic acid)/expandable graphite (PLA/EG) flame retardant composites

Chapter 5: Effect of expandable graphite on fire resistance and thermal stability of PLA/PCL blend

Chapter 6: Morphology, thermal and dynamic mechanical characteristics of fire resistant poly(lactic acid)/poly(ε-caprolactone)/expandable graphite (PLA/PCL/EG) composites

Chapter 7: Conclusions

References

1. Mngomezulu, M.E., John, M.J., Jacobs, V., Luyt, A.S. (2014). Review on flammability of biofibres and biocomposites. *Carbohydrate Polymers*, 111:149-182. DOI: 10.1016/j.carbpol.2014.03.071
2. Chapple, S., Anandjiwala, R., Ray, S.S. (2013). Mechanical, thermal, and fire properties of polylactide/starch blend/clay composites. *Journal of Thermal Analysis and Calorimetry*, 113:703-712. DOI: 10.1007/s10973-012-2776-6
3. Chapple, S., Anandjiwala, R. (2010). Flammability of natural fibre-reinforced composites and strategies for fire retardancy: A review. *Journal of Thermoplastic Composite Materials*, 23:871-893. DOI: 10.1177/0892705709356338
4. Nikolaeva, M., Kärki, T. (2011). A review of fire retardant processes and chemistry, with discussion of the case of wood-plastic composites. *Baltic Forestry*, 17(2):314-326. ISSN: 1392-1355

5. Laoutid, F., Bonnaud, L., Alexandre, M., Lopez-Cuesta, J.-M., Dubois, Ph. (2009). New prospects in flame retardant polymer materials: From fundamentals to nanocomposites. *Materials Science and Engineering R*, 63:100-125.
DOI: 10.1016/j.mser.2008.09.002
6. Bourbigot, S., Fontaine, G. (2010). Flame retardancy of polylactide: An overview. *Polymer Chemistry*, 1:1413-1422.
DOI: 10.1039/c0py00106f
7. Price, D., Anthony, G., Carty, P. (2001). Introduction: polymer combustion, condensed phase pyrolysis and smoke formation. In Horrocks, A.R. and Price, D. (Eds.), Fire Retardant Materials. Woodhead Publishing Limited, England.
8. Bai, G., Guo, C., Li, L. (2014). Synergistic effect of intumescent flame retardant and expandable graphite on mechanical and flame-retardant properties of wood flour-polypropylene composites. *Construction and Building Materials*, 50:148-153.
DOI: 10.1016/j.conbuildmat.2013.09.028
9. Fukushima, K., Murariu, M., Camino, G., Dubois, P. (2010). Effect of expanded graphite/layered-silicate clay on thermal, mechanical and fire retardant properties of poly(lactic acid). *Polymer Degradation and Stability*, 95:1063-1076.
DOI: 10.1016/j.polymdegradstab.2010.02.029
10. Lee, J.D. (1995). Concise Inorganic Chemistry. 4th Edition. Chapman & Hall Ltd. Singapore.
11. Sengupta, R., Bhattacharya, M., Bandyopadhyay, S., Bhowmick, A.K. (2011). A review on the mechanical and electrical properties of graphite and modified graphite reinforced composites. *Progress in Polymer Science*, 36:638-670.
DOI: 10.1016/j.progpolymsci.2010.11.003
12. Focke, W.W., Badenhorst, H., Mhike, W., Kruger, H.J., Lombaard, D. (2014). Characterization of commercial expandable graphite fire retardants. *Thermochimica Acta*, 584:8-16.
DOI: 10.1016/j.tca.2014.03.021
13. Wang, Z., Han, E., Ke, W. (2007). Influence of expandable graphite on fire resistance and water resistance of flame-retardant coatings. *Corrosion Science*, 49:2237-2253.
DOI: 10.1016/j.corsci.2006.10.024
14. Kopinke, F.-D., Remmler, M., Mackenzie, K., Milder, M., Wachsen, O. (1996). Thermal decomposition of biodegradable polyesters – II. Poly(lactic acid). *Polymer Degradation and Stability*, 43:329-342.

PII: S0141-3910(96)00102-4

15. Garlotta, D. (2001). A literature review of poly(lactic acid). *Journal of Polymers and the Environment*, 9(2):63-83.
DOI: 10.1023/A:1020200822435

16. Gupta, A.P., Kumar, V. (2007). New emerging trends in synthetic biodegradable polymers – Polylactide: A critique. *European Polymer Journal*, 43:4053-4074.
DOI: 10.1016/j.eurpolymj.2007.06.045

17. Rasal, R.M., Janorkar, A.V., Hirt, D.E. (2010). Poly(lactic acid) modifications. *Progress in Polymer Science*, 35:338-356.
DOI: 10.1016/j.progpolymsci.2009.12.003

18. Saeidlou, S., Huneault, M.A., Li, H., Park, C.B. (2012). Poly(lactic acid) crystallization. *Progress in Polymer Science*, 37:1657-1677.
DOI: 10.1016/j.progpolymsci.2012.07.005

19. Huang, G., Gao, J., Wang, X., Liang, H., Ge, C. (2012). How can graphene reduce the flammability of polymer nanocomposites? *Materials Letters*, 66:187-189.
DOI: 10.1016/j.matlet.2011.08.063

20. Murariu, M., Dechief, A.L., Bonnaud, L., Paint, Y., Gallos, A., Fontaine, G., Bourbigot, S., Dubois, P. (2010). The production and properties of polylactide composites filled with expanded graphite. *Polymer Degradation and Stability*, 95:889-900.
DOI: 10.1016/j.polymdegradstab.2009.12.019

21. Vogel, C., Siesler, H.W. (2008). Thermal degradation of poly(ε-caprolactone), poly(L-lactic acid) and their blends with poly(3-hydroxy-butyrate) studies by TGA/FT-IR spectroscopy. *Macromolecular Symposia*, 265:183-194.

22. Wu, D., Zhang, Y., Zhang, M., Zhou, W. (2008). Phase behaviour and its viscoelastic response of polylactide/poly(ε-caprolactone) blend. *European Polymer Journal*, 44:2171-2183.
DOI: 10.1016/j.eurpolymj.2008.04.023

23. Cabedo, L., Feijoo, J.L., Villanueva, M.P., Lagarón, J.M., Giménez, E. (2006). Optimization of biodegradable nanocomposites based on aPLA/PCL blends for food packaging applications. *Macromolecular Symposia*, 233:191-197.
DOI: 10.1002/masy.200650124

24. Young, R.J., Lovell, P.A. (2011). Introduction to Polymers. 3rd Edition. CRC Press, Tylor and Francis Group. Boca Raton.

25. Mngomezulu, M.E. (2009). Phase change materials based on polyethylene, paraffin wax and wood flour. Master of Science thesis, University of the Free State, Qwaqwa Campus.
26. Takayama, T., Todo, M., Tsuji, H. (2011). Effect of annealing on the mechanical properties of PLA/PCL and PLA/PCL/LTI polymer blends. *Journal of the Mechanical Behavior of Biomedical Materials*, 4:255-260.
DOI: 10.1016/j.jmbbm.2010.10.003
27. Patrício, T., Domingos, M., Gloria, A., Bártolo, P. (2013). Characterisation of PCL and PCL/PLA scaffolds for tissue engineering. *Procedia CIRP*, 5:110-114.
DOI: 10.1016/j.procir.2013.01.022
28. Patrício, T., Bártolo, P. (2013). Thermal stability of PCL/PLA blends produced by physical blending process. *Procedia Engineering*, 59:292-297.
DOI: 10.1016/j.proeng.2013.05.124
29. Todo, M., Park, S.-D., Takayama, T., Arakawa, K. (2007). Fracture micromechanisms of bioabsorbable PLLA/PCL polymer blends. *Engineering Fracture Mechanics*, 74:1872-1883.
DOI: 10.1016/j.engfracmech.2006.05.021
30. Li, H., Huneault, M.A. (2011). Comparison of sorbitol and glycerol as plasticizers for thermoplastic starch in TPS/PLA blends. *Journal of Applied Polymer Science*, 119:2439-2448.
DOI: 10.1002/app.32956
31. Chavalitpanya, K., Phattanarudee, S. (2013). Poly(lactic acid)/polycaprolactone blends compatibilized with block copolymer. *Energy Procedia*, 34:542-548.
DOI: 10.1016/j.egypro.2013.06.783
32. Wei, P., Bocchini, S., Camino, G. (2013). Flame retardant and thermal behavior of polylactide/expandable graphite composites. *Polimery*, 58(5):361-364.
DOI: 10.14314/polimery.2013.361
33. Focke, W.W., Kruger, H.J., Mhike, W., Taute, A., Roberson, A., Ofosu, O. (2014). Polyethyelene flame retarded with expandable graphite and a novel intumescent additive. *Journal of Applied Polymer Science*, 40493:1-8.
DOI: 10.1002/app.40493
34. Focke, W.W., Muiambo, H., Mhike, W., Kruger, H.J., Ofosu, O. (2014). Flexible PVC flame retarded with expandable graphite. *Polymer Degradation and Stability*, 100:63-69.

DOI: 10.1016/j.polymedegradstab.2013.12.024

35. Uhl, F.M., Yao, Q., Nakajima, H., Manias, E., Wilkie, C.A. (2005). Expandable graphite/polyamide-6 nanocomposites. *Polymer Degradation and Stability*, 89:70-84. DOI: 10.1016/j.polymdegradstab.2005.01.004

36. Pang, X.-Y., Weng, M.-Q. (2014). Preparation of expandable graphite composite under the auxiliary intercalation of zinc sulfate and its flame retardancy for ethylene/vinyl acetate copolymer. *International Journal of ChemTech Research*, 6(2):1291-1298.

37. Gao, L., Zheng, G., Zhou, Y., Hu, L., Feng, G., Xie, Y. (2013). Synergistic effect of expandable graphite, melamine polyphosphate and layered double hydroxide on improving the fire behavior of rosin-based rigid polyurethane foam. *Industrial Crops and Products*, 50:638-647. DOI: 10.1016/j.indcrop.2013.07.050

38. Gao, L., Zheng, G., Zhou, Y., Hu, L., Feng, G., Zhang, M. (2014). Synergistic effect of expandable graphite, diethyl ethylphosphonate and organically-modified layered double hydroxide on flame retardancy and fire behavior of polyisocyanurate-polyurethane foam nanocomposite. *Polymer Degradation and Stability*, 101:92-101. DOI: 10.1016/j.polymdegradstab.2013.12.025

39. Qian, L., Feng, F., Tang, S. (2014). Bi-phase flame-retardant effect of hexa-phenoxy-cyclotriphosphazene on rigid polyurethane foams containing expandable graphite. *Polymer*, 55:95-101. DOI: 10.1016/j.polymer.2013.12.015

40. Mu, X., Yuan, B., Hu, W., Qiu, S., Song, L., Hu, Y. (2015). Flame retardant and anti-dripping properties of polylactic acid/poly(bis(phenoxy)phosphazene)/expandable graphite composite and its flame retardant mechanism. *RSC Advances*, 5:76068-76078. DOI: 10.1039/c5ra12701g

41. Zhu, H., Zhu, Q., Li, J., Tao, K., Xue, L., Yan, Q. (2011). Synergistic effect between expandable graphite and ammonium polyphosphate on flame retarded polylactide. *Polymer Degradation and Stability*, 96:183-189. DOI: 10.1016/j.polymdegradstab.2010.11.017

42. Das K., Ray, S.S., Chapple, S., Wesley-Smith, J. (2013). Mechanical, thermal, and fire properties of biodegradable polylactide/boehmite alumina composites. *Industrial & Engineering Chemistry Research*, 52:6083-6091.

DOI: 10.1021/ie4004305

43. Mhike, W., Focke, W.W., Mofokeng, J.P., Luyt, A.S. (2012). Thermally conductive phase-change materials for energy storage based on low-density polyethylene, soft Fischer-Tropsch wax and graphite. *Thermochimica Acta*, 527:75-82.
DOI: 10.1016/j.tca.2011.10.008

44. Kimura K., Horikoshi Y. (2005). Bio-based polymers. *Fujitsu Scientific and Technical Journal*, 41(2):173-180.

45. Xie, R., Qu, B. (2001). Synergistic effects of expandable graphite with some halogen-free flame retardants in polyolefin blends. *Polymer Degradation and Stability*, 71:375-380.
PII: S0141-3910(00)00188-9

46. Lin, L., Deng, C., Lin, G.-P., Wang, Y.-H. (2014). Mechanical properties, heat resistance and flame retardancy of glass fiber-reinforced PLA-PC alloys based on aluminum hypophosphite. *Polymer-Plastics Technology and Engineering*, 53:613-625.
DOI: 10.1080/03602559.2013.866244

47. Gallo, E., Schartel, B., Acierno, D., Russo, P. (2011). Flame retardant biocomposites: Synergism between phosphinate and nanometric metal oxides. *European Polymer Journal*, 47:1390-1401.
DOI: 10.1016/j.eurpolymj.2011.04.001

48. http://trellisbioplastic.com/wp-content/uploads/2014/08/Sustainable-1001-Property-Guide.pdf (26/10/2015).

Chapter 2

Review on flammability of biofibres and biocomposites

This chapter has been published as:

Mfiso E. Mngomezulu, Maya J. John, Valencia Jacobs, Adriaan S. Luyt. Review on flammability of biofibres and biocomposites. Carbohydrate Polymers, 2014; 111:149-182. DOI: 10.1016/j.carbpol.2014.03.071 (Reuse by permission from Elsevier)

Abstract

It is our belief that the subject on flammability properties of natural fibre-reinforced biopolymer composites has not been broadly researched. This is not only evidenced by the minimal use of biopolymer composites and/or blends in different engineering areas where fire risk and hazard to both human and structures are of critical concern, but also the limited amount of published scientific work on the subject. Therefore, it is necessary to expand knowledge on the flammability properties of biopolymers and add value in widening the range of their application. This paper reviews the literature on the recent developments on flammability studies of bio-fibres, biopolymers and natural fibre-reinforced biocomposites. It also covers the different types of flame retardants (FRs) used, their mechanisms and it discusses the principles and methodology of various flammability testing techniques.

2.1 Introduction

In recent years, research on bio-fibre reinforced biopolymer composites has advanced. This development is motivated by factors, such as: shortage of and high fossil energy cost and the current shift towards environmentally-tolerant or "green" composite materials. The shift towards environmentally-friendly biocomposite materials is due to the environmental legislations, the REACH Act (Registration, Evaluation, Authorization and Restriction of Chemical substances), comparable properties to synthetic fibre counterparts, green attribution and low cost. Most of the components in biocomposites are based on agricultural products, as sources of raw materials. Thus, their use provides solution for waste disposal, reduction in agricultural residues and hence environmental pollution resulting from the burning of these

agricultural products. Additionally, it offers an economical solution to the farming communities and especially, the rural areas of the developing countries [1-9].

Bio-fibre reinforced biopolymer composite materials largely have appealing properties. They are renewable, recyclable (partially or completely), relatively cheap, biodegradable and thus environmentally-friendly. However, there are some inherent disadvantages, such as their hydrophilic nature and poor flammability properties (i.e. poor fire resistance). The attractive properties clearly outweigh the undesirable ones and the latter have remedial measures. For example, remedies may be chemical and/or physical modifications, such as the incorporation of flame retardant additives (FRAs) in order to improve flammability of biocomposites [6].

Previous research observed limitations in the use of bio-fibre reinforced biopolymer composites, especially in areas that pose fire hazard and risk. This is because natural fibre reinforced biopolymer composites are largely used in the packaging and automotive industries, where fire safety regulatory requirements are not as stringent as those in the aerospace industry. Therefore, in order to broaden the range of applications of these biocomposites into other sectors of advanced engineering (i.e. aerospace, marine, electronics equipment and construction), both their flammability characteristics and fire retardance strategies need more research [2,7,10].

There are different strategies that can be demonstrated for fire retardancy of biocomposites. Fire retardancy is the phenomenon in which materials, such as plastics and/or textiles are rendered less likely to ignite or, if they are ignitable, should burn with less efficiency [11]. It may be achieved by use of several approaches. These may be chemical modification of existing polymers, application of surface treatment to the polymers, use of inherently fire resistant polymers or high performance polymers and the direct incorporation of flame retardants (FRs) and/or micro or nanoparticles in materials. The direct incorporation of flame retardants is achieved through use of various additives. These flame retardance strategies may range from the use of phosphorus additives (e.g. intumescent systems), halogen additives (e.g. organobromine), silicon additives (e.g. silica), nanometric particles (e.g. nanoclays) and minerals based additives (e.g. metal hydroxide). The broader information on flame retardant additives (FRAs) in natural polymers, wood and lignocellulosic materials has been reviewed by Kozlowski and Wladyka-Przybylak [12]. Thus, the primary duty of flame retardant systems is to prevent, minimize, suppress or stop the combustion of a material [11,13-15].

Flame retardant systems can either act chemically or physically in the solid, liquid or gas phase. Their mechanisms are dependent on the nature of the flame retardant system. The chemical mode of action may be manifested by reaction in the gaseous and condensed phases, whereas the physical mode occurs by a cooling effect, formation of a protective layer or by fuel dilution. FRs may be classified into three classes. They are normal additives (NAs), reactive additives (RAs) and a combination of FRs [11,13,15].

The flammability of fire retarded materials may be tested using different fire testing techniques. The most widely used laboratory flammability testing techniques have been reported in literature [11,13,15]. A number of small, medium and full scale flammability tests are used in both academic and industrial laboratories. They are employed for either screening the materials during production or testing the manufactured products. These techniques are cone calorimetry, pyrolysis combustion flow calorimetry (PCFC), limiting oxygen index (LOI), and underwriters' laboratories 94 (UL-94) and Ohio State University (OSU) heat release rate tests. These techniques involve the measurement of various flammability parameters by appropriate tests, depending on the targeted application of a polymeric material. The flammability of polymers can be characterized by parameters, such as: ignitability (ignition temperature, delay time, critical heat flux), burning rates (heat release rate, solid degradation rate), spread rates (flame, pyrolysis and smoulder), product distribution (emissions of toxic products) and smoke production [11,13,16].

The flammability properties of natural fibre reinforced biopolymer composites have not been studied extensively. The aim of this chapter is to review the current research and developments relating to the flammability of bio-fibre reinforced biopolymer composites in the period 2000 to 2013. This review will explore aspects, such as the different types of flame retardants, laboratory flammability testing techniques and recent studies on the flammability of biopolymers and biocomposites.

2.2 Flame retardants

FRs impart flame retardancy character to materials, such as: coatings, thermoplastics, thermosets, rubbers and textiles. These FRs may prevent, minimize, suppress or stop the combustion process of materials. They act to break the self-sustaining polymer combustion

cycle shown in Figure 2.1 and consequently reduce the burning rate or extinguish the flame in several ways [11-15,17-21].

The possible ways to reduce the burning rate or extinguish the flames are: i) the modification of the pyrolysis process in order to lower the quantity of evolved flammable volatiles, which normally increases the formation of char (less flammable), hence serving as barrier between the polymer and flame (stage 'a', Figure 2.1), ii) the isolation of the flame from the oxygen/air supply (stage 'b'), iii) introduction into the polymer formulations those compounds that will release efficient flame inhibitors (e.g. chlorine and bromine) (stage 'c') and iv) the lowering of thermal feedback to the polymer to prevent further pyrolysis (stage 'd') [11].

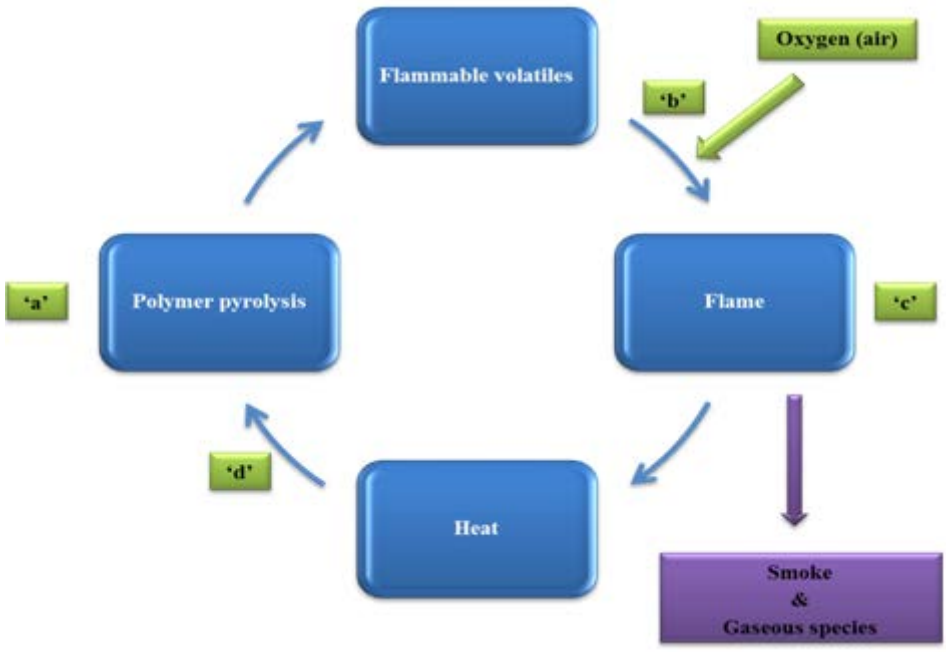

Figure 2.1 Demonstration of the self-sustaining polymer combustion cycle, a–d represent the potential modes of flame retardants (adapted from [11])

In order to flame retard polymer materials or to protect them from fire, there are three main approaches to be considered. These are: the engineering approach, use of inherently low flammable polymers and the use of flame retardant additives (FRAs) [14].

The engineering approach is cost-effective and relatively easy to implement. It requires the use of a fire protection shield. However, the method has some limitations, such as: tearing and/or ripping off (of fire proof fabric), loss of adhesion (in metal fire protection) and scratching away

and falling-off due to impact or ageing (of intumescent paint). Consequently, the underlying material may be left exposed to fire damage.

Inherently flame retarding polymers can be made in various forms and are easy to implement in different applications. Their use, however, can be limited by high cost and difficulty to recycle (i.e. fibre reinforced polymer composites). As a result, low flammability polymers are less used except for applications demanding their use (e.g. aerospace and military sectors).

The use of FRAs is a well-known approach, cost-effective and relatively easy to incorporate into polymers. The challenges with this approach, however, include the potential for leaching into environment, difficulty with recycling and a compromise in reaching a balance in the properties of a polymer. Regardless of these problems, FRAs are still used.

FRs are classified into three categories. They are normal additives (NAs) flame retardants, reactive additives (RAs) flame retardants and combinations of FRs. NAs are incorporated during polymerization or during melt mixing processing and they react with the polymer only at high temperatures at the start of a fire. They are common flame retardant additives and their interaction with the substrate, is physical. NAs usually include mineral fillers, hybrids or organic compounds that can include macromolecules. RAs, on the other hand, are usually introduced into polymers during polymerization or in a post reaction process. During polymerization, RAs are introduced as monomers or precursor polymers, whereas in a post reaction process their introduction is by chemical grafting. These flame retardants chemically bond to the polymer backbone. Combinations of NAs and RAs can produce an additive (sum), synergistic (high) or antagonistic (low) effect. A synergistic effect typically occurs when they are used together with specific flame retardants [11,12,14,22].

2.2.1 Mode of action of flame retardants

Flame retardant systems can act either chemically or physically in the solid, liquid or gas phase. Such actions do not occur singly but should be considered as complex processes in which various individual stages occur simultaneously, with one of these proceses dominating. They are dependent on the nature of flame retardant system in place [11,13-15,22,23]. Various modes of flame retardants are discussed in subsequent sections.

2.2.1.1 Physical action

The physical mode occurs by (i) cooling effect, (ii) fuel dilution or (iii) via formation of a protective layer (coating) [2,5,7,11,13,15,22].

(i) Cooling effect: Some FRAs (e.g. hydrated trialumina and magnesium hydroxide) decompose by an endothermic process and trigger temperature decrease in the system. Cooling of the medium, to below the polymer combustion temperatures, is effected. Such endothermic reaction is known to act as a heat sink.

(ii) Fuel dilution: During decomposition of flame retardants (e.g. aluminum hydroxide), the formation of gases such as H_2O, CO_2 and NH_3 lead to dilution of the mixture of combustible gases. Consequently, this limits the concentration of reagents and the possibility of materials to ignite.

(iii) Formation of a protective layer (coating): Some FRAs (e.g. phosphorus and boron compounds) form a protective solid or gaseous layer between the gaseous and solid combustible phases. This limits the transfer of combustible volatile gases, excludes oxygen that is necessary for combustion and thus reducing the amount of decomposition gases.

2.2.1.2 Chemical action

The chemical mode of action may be manifested by reaction in the (i) gaseous and (ii) condensed phase [2,5,7,11,13,15,22].

(i) Gaseous phase: By incorporation of FRAs that favour the release of specific radicals (e.g. halogen flame retardants, Cl• and Br•) in the gas phase, the free radical mechanism of the combustion process can be stopped. These radicals can react with highly reactive species, such as: H• and OH• in order to form less reactive or inert molecules. The exothermic reactions are then stopped and the system cools down as the supply of flammable gases is subsequently reduced.

(ii) Condensed phase: Two types of chemical reaction initiated by FRAs are possible: (a) flame retardants can speed up the rupture of polymer chains and the polymer will drip, thus moving

away from the flame action zone; (b) FRs can cause the formation of a carbonized or vitreous layer at the surface of the polymer. This occurs by chemical transformation of degraded polymer chains. The char and/or vitreous layer formed acts as a physical insulating barrier between the gas and condensed phases.

2.2.2 Types of flame retardant agents

FRAs are based on various chemical compounds. This subsection discusses chemical compounds based on phosphorus, halogen, silicon, nanometric particles and mineral additives. The phosphorus based additives include organic phosphorus, inorganic phosphorus, red phosphorus and intumescent flame retardant systems. The silicon based additives consist of silica and silicones, the nanometric particles-based types may be carbon nanotubes, nanoclays and nanoscale particulate additives and the minerals based flame retardant additives are hydrocarbonates, metal hydroxides and borates.

2.2.2.1 Phosphorus based flame retardants

Phosphorus-based FRs include phosphorus into their structure. Their structure can vary from inorganic to organic forms and with oxidation states of 0, +3, or +5. Phosphorus-based FRs consist of phosphates, phosphonates, phosphinates, phosphine oxide and red phosphorus. These FRAs are used as NAs or RAs, incorporated into the polymer chain during synthesis. They are effective with oxygen or nitrogen-containing polymers (cellulose, polyesters and polyamides). Phosphorated FRs are unique in that they can be in the condensed phase or vapour phase FRs, depending on their chemical structure and their interaction with the polymer under fire conditions [3,5,13].

In the *condensed phase*, FRs thermal decomposition leads to the production of phosphoric acid that readily condenses to give phosphorylated structures and gives off water. Released water dilutes the oxidizing gas phase (physical action: fuel dilution). Additionally, phosphoric acid and pyrophosphoric acid can facilitate a dehydration reaction, resulting in the formation of carbon to carbon double bonds and charring. This can then lead to the generation of cross-linked or carbonized structures at high temperatures [3,5,13,14,22].

At high temperatures, ortho and pyrophosphoric acid are turned into metaphosphoric acid (OPOOH) and their corresponding polymers $(PO_3H)_n$. Phosphate anions (pyro and polyphosphates) then partake in char formation (with carbonized residue). This carbonized layer isolates and protects the polymer from the flames, limits the volatilization of fuel, prevents formation of new free radicals, limits the diffusion of oxygen thus reducing combustion and insulates the polymer underneath from the heat [3,5,13,14,22].

Phosphorus based flame retardants can also volatilize into *vapour phase*, forming active radicals (PO_2•, PO• and HPO•) and acting as scavengers of H• and OH• radicals. Volatile phosphorated compounds are among the effective inhibitors of combustion when compared to bromine and chlorine radicals. Since phosphorus-based flame retardants are significantly effective in oxygen and nitrogen-containing polymers, it is thus important to have these atoms in the polymer chain. In case the polymer of interest lacks these atoms in its chain and cannot contribute to charring, a highly charring co-additive {e.g. polyol (pentaerythritol)} has to be introduced in combination with the phosphorated flame retardant. Polymers, such as polyamides and polyurethane can also be used as charring agents in intumescent flame retardant systems [3,5,13,14,22].

Organic phosphorus

Many organic phosphorus derivatives show flame retardancy properties. But, those of commercial importance are limited by the processing temperature and the nature of the polymer to be modified. Organic phosphorus-based FRs can act as NAs or as RAs monomers or co monomers/oligomers. Their main groups are phosphate esters, phosphonates and phosphinates. Due to their high volatility and relatively low fire retardant efficiency, the use of alkyl substituted triaryl phosphate (i.e. triphenyl phosphate, TPP, cresyl diphenyl phosphate, isopropylphenyl diphenyl phosphate, tertbutylphenyl diphenyl phosphate or tricresyl phosphate) is limited in plastics engineering. Oligomeric phosphates with lower volatility and higher thermal stability than triaryl phosphate can be used in plastics engineering. These may be resorcinol bis(diphenyl phosphate) (RDP) and bisphenol A bis(diphenyl phosphate (BDP). The combination of volatile and nonvolatile phosphates can also lead to a synergistic effect. This may be a positive combination of the condensed phase and gas phase of phosphates. The use of reactive phosphorus flame retardants is also a solution for avoiding volatilization during thermal decomposition and migration towards the surface of a polymer. They can be

incorporated directly within the polymer chain structure and can be used either as monomers for copolymerization with one or two co-monomers in order to obtain phosphorated polymers or as oligomers that can react with polymers to form branched or grafted phosphorated polymers [3,5,13,14].

Inorganic phosphorus

A typical example of an inorganic phosphorus salt is a combination of polyphosphoric acid and ammonia called ammonium polyphosphate (APP). It is either a branched or unbranched polymeric compound with variable chain length (*n*). For short and linear chain APPs (where *n* is less than 100, crystalline form I), they are more water-sensitive and less thermally stable, whereas APPs with longer chain (*n* is greater than 1000, crystalline form II) exhibit very low water solubility (< 0.1 g/100 ml)and more stable, thermally [5,13].

The APPs are stable and nonvolatile compounds. Those with long chains start decomposing at temperatures above 300 °C, giving polyphosphoric acid and ammonia, whereas the short chain types decompose at 150 °C. It is thus, important to adapt a crystalline form of APP to the decomposition temperature of a polymer. When an APP is incorporated into a polymer that contains oxygen and/or nitrogen atoms, polymer charring occurs. Thermal degradation of APP creates free acidic hydroxyl groups that condense by thermal dehydration, yielding a structure of ultraphosphate and polyphosphoric acid with a highly cross-linked structure. Polyphosphoric acid reacts with oxygen and/or nitrogen containing polymers and catalyses their dehydration reaction and char formation. However, the effectiveness of an APP is dependent on the loading concentration. Low concentrations of APP are not efficient in aliphatic polyamides, but at high concentrations it becomes efficient. In non-self-charring polymeric materials, the APP can modify the degradation mechanism of the polymer [10,21,24].

Red phosphorus

This is the most concentrated source of phosphorus for flame retardancy and it is used in small quantities (i.e. < 10%). It is effective in oxygen and nitrogen-containing polymers (i.e. polyesters, polyamides and polyurethanes). For oxygen-containing polymers only, the mode of action involves specific scavenging of oxygen-containing radicals, leading to the generation of

gaseous fuel species. For oxygen- and nitrogen-containing polymers, red phosphorus turns into phosphoric acid or phosphoric anhydride, which gives polyphosphoric acid upon heating. This happens through thermal oxidation and the polyphosphoric acid formed catalyses the dehydration reaction of the polymer chain ends and triggers char formation [13,25].

Additionally, red phosphorus is also effective in non-oxygenated polymers (e.g. polyethylene). Consequently, red phosphorus depolymerizes into white phosphorus (P_4). This white phosphorus can volatilize at high temperatures and act in the gaseous phase or it can diffuse from the bulk of the polymer to the burning surface, where it oxidizes to phosphoric acid derivatives. These can come into close contact with flame and form phosphoric acid. This acid can act as a char forming agent and therefore, physically limiting oxygen access and fuel volatilization [13].

Red phosphorus is active in both the gas and condensed phase in polyethylene. In the gas phase, the PO• radicals produced quench the free radical process. In the condensed phase, red phosphorus lowers the heat of oxidation and also traps the free radicals. This results in improved thermal stability leading to a decrease in fuel production during burning of a material [13].

The disadvantage of red phosphorus is that it releases toxic phosphine (PH_3) through its reaction with moisture, due to its poor thermal stability. However, phosphine formation can be avoided by prior encapsulation of red phosphorus in order to improve its effectiveness as a flame retardant. Alternatively, phosphine formed at high temperatures can be trapped by taking advantage of its capacity to react with metallic salts (e.g. $AgNO_3$, $HgCl_2$, MoS_2, HgO, PbO_2, CuO, $FeCl_3 \cdot H_2O$) [13].

Intumescent flame retardant system

Intumescent flame retardant systems were initially developed to protect fabrics, wood and coatings for metallic structures from fire. Intumescent materials are classified into thick or thin film intumescent coatings. The thick films, usually based on epoxy resins, contain agents that intumesce when exposed to heat and are available as solvent free systems. Thin films are available as solvent- or water-based systems and are applied by spray or brush roller in thin film coats. An intumescent system is based on the formation of an expanded carbonized layer

on the surface of a polymer during thermal degradation. This layer acts as an insulating barrier by reducing the heat transfer between the heat source and the polymer surface, hence limiting the fuel transfer from the polymer towards the flame and limiting the oxygen diffusion into a material. The formulation of an intumescent system consists of three components: an acid source, a carbonizing agent and a blowing agent. Table 2.1 shows examples of each component category [23]. The intumescent FRs are widely used due to their advantages of low smoke and low toxicity [13,14,21,26].

Table 2.1 Examples of components of intumescent systems. Reprinted from [23], Copyright 2007, with permission from Royal Society of Chemistry

Inorganic acid source	**Carbonizing agent**	**Blowing agents**
Phosphoric	Starch	Urea
Sulfuric	Dextrins	Urea-formaldehyde resin
Boric	Sorbitol, mannitol	Dicyandiamide
Ammonium salts	Pentaerythritol, monomer,	Melamine
Phosphates, polyphosphates	dimer, trimer	Polyamides
Borates, polyborates	Phosphates, polyphosphates	
Sulfates	Phenol-formaldehyde resins	
Halides	Methylol melamine	
Phosphates of amine or amide	Char former polymers (PA-	
Products of reaction of urea or guanidyl urea with phosphoric acids	6, PA-6/clay nanocomposite PU, PC, etc.)	
Melamine phosphate		
Product of reaction of ammonia with P_2O_5		
Organophosphorus compounds		
Tricresyl phosphate		
Alkyl phosphates		
Haloalkyl phosphates		

An *acid source* promotes dehydration of the carbonizing agent and results in the formation of a carbonaceous layer. It has to be liberated at a temperature below the decomposition

temperature of a carbonizing agent and its dehydration should happen around the decomposition temperature of a polymer. A *carbonizing agent* is generally a carbohydrate that can be dehydrated by an acid to form a char. Its effectiveness relates to the number of carbon atoms and the reactive hydroxyl sites containing carbon source agent molecules. The quantity of char produced is dependent on the number of carbon atoms present. Reactive hydroxyl (OH) sites determine the rate of the dehydration reaction and thus the rate of formation of the carbonized structure. A *blowing agent* decomposes and releases gas, leading to expansion of the polymer and formation of swollen multicellular layer. The gas must be released during thermal decomposition of a carbonizing agent in order to trigger the expansion of the carbonized layer [13,14,21,23,26].

2.2.2.2 Halogen based flame retardants

Halogenated FRs are molecules that include elements from group VII of the periodic table (F, Cl, Br and I). Their effectiveness increases in the order F < Cl < Br < I. The type of halogen dictates the effectiveness of the halogenated flame retardant. However, fluorine (F) and iodine (I) are not used because they do not interfere with the polymer combustion process. Fluorinated compounds are more thermally stable than most polymers and do not release halogen radicals at the same temperature range or below the decomposition of the polymers. Iodine compounds are less thermally stable than most commercial polymers and therefore release halogen species during polymer processing. Bromine and chlorine can readily be released and partake in the combustion process because of their low bonding energy with carbon atoms [13,14,22,27].

Halogenated flame retardant additives

Halogenated FRs differ in chemical structure from aliphatic to aromatic carbon substrates or can come in inorganic forms. Of these, the organohalogen compounds are the most commonly used as FRs for polymers due to their effectiveness. Organochlorine and organobromine are the most used, with organobromine compounds being the most commonly used of the two. This is because the C–Br bond is stable enough for environmental exposure and yet heat can easily break it to release bromine under fire conditions in order to inhibit free radical reactions. It is these unique bond strengths that make halogen-based FRs, mostly the vapour phase FRs [13,14,27].

Halogenated FR technology has been used since the 1930's due to its advantages of low cost, processability, miscibility and low reduction on the physical/mechanical properties of the FR systems. However, its flaws include increased smoke release under fire conditions, the release of corrosive gases (i.e. HBr in case of brominated FRs) during burning, which leaches to the environment and thus brominated products are currently under environmental scrutiny. The increased smoke and corrosive gas release of these compounds are rooted to their flame retardant chemistry. Since it inhibits combustion through the formation of HBr gas, it causes the formation of partially combusted polymer decomposition products as well as carbon monoxide (CO). Halogenated FR systems do not always perform well under very high heat flux conditions because once a halogen is consumed by fire any remaining polymer will burn if exposed to additional heat. This will happen unless a lot of halogen is present in a polymer, which will result in high smoke production and corrosive gas release [13,14].

Mode of action

The thermally induced polymer decomposition (during polymer combustion) releases very reactive free radical species (i.e. H• and OH•). These maintain a combustion process by a series of chain reactions in the gas phase.

$$H\bullet + O_2 \rightarrow OH\bullet + O$$

$$O + H_2 \rightarrow OH\bullet + H\bullet$$

The reactive free radical species H• and OH• formed by chain branching are removed by halogenated FR. Initially the flame retardant breaks down into a halogen radical (see below reaction, where X is either Cl or Br):

$$RX \rightarrow R\bullet + X\bullet$$

The halogen radical formed reacts to form a hydrogen halide:

$$X\bullet + RH \rightarrow R\bullet + HX$$

This hydrogen halide consequently interferes with the radical chain mechanism:

$$HX + H\bullet \rightarrow H_2 + X\bullet$$

$$HX + OH\bullet \rightarrow H_2O + X\bullet$$

The highly reactive H• and OH• free radical species are removed by reaction with HX and replaced with the less reactive X radicals. The actual flame retardant effect is therefore produced by HX. The hydrogen halide consumed is regenerated by reaction with hydrocarbon:

$$X\bullet + RH \rightarrow R\bullet + HX$$

As a result, HX is an effective FR species. It is non-flammable and can have physical action on the combustion mechanism by forming a protective gaseous layer and/or dilution of fuel gases. Furthermore, HX can catalyse the oxidation of the solid phase and the oxidation products tend to cyclize, leading to the formation of a solid protective layer [13,22]. The most common halogen FRA compounds are tetrabromobisphenol A (TBBPA), polybromodiphenyl ether (PBDE), hexabromocyclododecane (HBCD) and tetrabromophthalic anhydride (TBPA) [13,14,22,27].

Halogenated monomers and copolymers

The advantages of reactive additive FRs are their ability to be used in relatively low concentrations and they can be directly incorporated in the polymer structure. Consequently, they can increase the compatibility between a polymer and an FRA, they can limit the damage caused by heterogeneous additives to the mechanical properties of the resulting materials and can reduce the migration of FRAs onto the material surface [13].

Nevertheless, they need an additional synthetic step that may be a limiting factor on an industrial scale. They can be used as condensation free radical polymerization monomers, copolymerized with virgin monomers or grafted onto the polymer chain. Their action is very similar to other halogenated FRAs. In some cases, other mechanisms can be added to the conventional effect of halogenated derivatives and thus changing the degradation pattern of a polymer. The effectiveness of a halogenated monomer depends on the composition of the monomer and the copolymer. Increasing the content of halogen atoms in the monomer leads to more efficient fire retardance [13,14].

Reactive halogenated FRAs may be an alternative to halogenated FRAs that seem to pose some toxicological risk to the environment. However, they are less used due to high cost and most of them are limited to a few polymers, such as: styrenics, acrylates, urethanes and epoxies [14].

2.2.2.3 Silicon based flame retardants

The addition of a relatively low amount of silicon-based compounds to polymers, substantially improves their fire retardancy. These silicon-based compounds are silicones, silicas, organosilicates, silsesquioxanes and silicates. They can be used as fillers incorporated into polymers, as copolymers or as main polymer matrices and they are discussed in the following sections.

Silicones

Silicones {typically polydimethylsiloxane (PDMS) polymers} are known to have excellent thermal stability, high heat release (i.e. 60 to 150 kW m^{-2}) and very limited release of toxic gases (i.e. CO) during thermal decomposition. They exhibit a slow burning rate without a flaming drip and when pure, they do not emit toxic smokes. Silicones have been commercialized since the 1940's. They are used in various applications in civil engineering, construction building, electrical, transportation, aerospace and defence, textile and cosmetics industries. They can be used as flame retardants through direct blending with a polymer matrix or by synthesizing block/graft copolymers including silicone segments. Their superior flame retardant behaviour is the result of excellent dispersion in polymer matrices and migration towards the material surface during combustion, followed by the formation of a highly flame retardant char. Their main advantage as flame retardants is that they have a minimal environmental effect due to their inorganic structure. They are expensive and hence used sparingly [13,14,27,28].

Silica (silicon dioxide, SiO_2)

The flammability reduction mechanism of silica is based on a physical process rather than a chemical reaction. Its effectiveness is dependent on several factors, including: pore size, particle size, surface silanol concentration, surface area, density and viscosity. Large pore volumes may accommodate macromolecular polymer chains, or the presence of silica may increase the melt viscosity during pyrolysis, which can trap and/or slow down volatilization and evolution of degradation products. The balance between density and surface area of the additive, together with the polymer melt viscosity, determine whether the additive accumulates near the surface of a sample or sinks through the polymer molten layer. If additives accumulate

near the sample surface, the possibility is that the additive acts as a thermal insulation layer and also reduces the polymer concentration near the surface in contact with the flame. The specific area and porous volume can modify the viscosity of the system in the molten state. The control over viscosity seems to be the key factor in the formation of a protective layer [13,27,29].

Several studies have been conducted where silica was used as flame retardant in thermoplastics [29-31]. Kashiwagi *et al*. [29] used various types of silica (i.e. silica gel, fumed silica and fused silica) in polypropylene (PP) and polyethylene oxide (PEO). Their effectiveness and mechanisms were determined. Li *et al*. [30] synthesized flame retardants that contain silicon elements (together with phosphorus and nitrogen), applied them in PP, and investigated their fire performance. Zhang *et al*. [31] investigated the use of silica and ammonium polyphosphate flame retarded wood fibre in polypropylene/wood fibre composites. In all these studies, the silica flame retarded systems showed reduced heat release and burning rates. The mechanism of the reduction in the heat release rate and mass loss rate was due to physical action of the silica in the condensed phase.

2.2.2.4 Nanometric particles

Nanometric particles contribute to the enhancement of thermal, mechanical or fire resistance properties when used separately and well dispersed within polymer matrices. They allow considerable reduction in loading content as the interfacial area between the polymer and nanofiller is greatly increased. The contribution of each type of nanoparticles to flame retardancy varies and depends on its chemical structure and geometry. These nano-metric particles are classified as layered, fibrous and particulate materials [13].

Layered materials: represented by nanoclays (e.g. montmorilonite, MMT); one nanometric dimension.

Fibrous materials: e.g. carbon nanotubes (CNTs), sepiolite; elongated structured materials with two nanometric dimensions.

Particulate materials: e.g. nano scale particulate additives; polyhedral oligosilsesquioxane (POSS), spherical silica nanoparticles; three nanometric dimensions.

Nano-clays

A lot of work has been done on nanoclay-based polymer composites and some reviews have been published [32-36]. Morgan [32] reviewed the flame retarded polymer layered silicate nanocomposites for commercial systems. Bordes *et al*. [33] discussed the recent research and developments in biopolyester/nanoclay systems, whereas Kiliaris and Papaspyrides [34] presented recent developments on the use of layered silicates (clay) for designing polymer nanocomposites with enhanced flame retardancy. Natural clays must be chemically modified in order to favour the dispersion of clay nanolayers within the polymer matrix. This is achieved by using organic cations, such as: alkylammonium, alkyl phosphonium and alkyl imidazol(idin)ium which leads to the formation of organo-modified nanoclays [13].

Incorporation of low amounts (~10 wt.%) of organomodified nanoclay in a polymer matrix creates a protective layer during combustion. During heating, the viscosity of a molten polymer/layered silicate nanocomposite decreases with increasing temperature. This facilitates the migration of clay nanolayers to the surface. Heat transfer promotes thermal decomposition of an organomodifier and creates strongly protonic catalytic sites onto the clay surface, which can catalyse the formation of a stable char residue [13,34].

Consequently, the accumulation of clay on the surface of a material acts as a protective barrier that limits the heat transfer into the material, limits the volatilization of combustible degradation products, as well as the diffusion of oxygen into the material. Additionally, nanoclay migration is enhanced by the formation of gas bubbles initiated by the decomposition of both quaternary ammonium organomodifiers and polymer chains. Such gas bubbles may be nucleated by the surfaces of the nanoclay sheets and could also help in the convection of nanoclay sheets to the surface [13,34].

There are several factors that play a key role in determining the flammability behaviour of polymer/silicate layered nanocomposites. These may be char formation, morphology of the nanocomposites (intercalated or exfoliated) and the ability of nanoclays to disperse, contents of organomodifier in nanoclays, nanoclay loading and melt viscosity. The main fire retardancy mechanisms in polymer/silicate layered nanocomposites are believed to be the formation of a barrier against heat and volatiles by the migration of clay nanolayers towards the material surface, followed by char formation together with increased melt viscosity for exfoliated

nanocomposites. These mechanisms can modify the fire properties of the nanocomposites differently depending on the fire test applied. In general, the incorporation of nanoclays retards and reduces the peak heat release rate (PHRR), but does not lower the total heat release (THR). This means that almost all the fuel released is combusted, hence ther will be little or no change in THR. However, fuel is released so slowly that the HRR stays same throughout the burning process [32]. It may also reduce the time to ignition (TTI). In addition, it reduces the melt viscosity in the exfoliated nanocomposites and thus prevents dripping and promotes char formation [13,19].

Manfredi *et al*. [37] investigated the various properties (including fire resistance) of organically modified clay on jute reinforced vinyl ester and resol composites. The composites showed an improvement in their fire performance when compared to unmodified clay ststem. Lower fire risk and low heat evolution were observed. Barbosa *et al*. [38] used Brazilian clay [montmorillonite (MMT)] and two types of commercial flame retardants with a polyethylene matrix and evaluated their flammability behaviour. Polyethylene flame retarded nanocomposites were produced via direct melt intercalation. The flammability resistance of PE/Brazilian clay nanocomposites was improved due to the barrier effect of the organoclay during the combustion. The nanocomposites were more effective than conventional PE/flame retardants systems and only 3 wt.% MMT reduced the burning rate of the nanocomposites by 17%.

Wei *et al*. [39] addressed the combustion behaviour of PLA nanocomposites, based on organomodified MMT clays (i.e. Closite 30B and 20A) with N-alkoxy hindered amine as a flame retardant. Si *et al*. [40] prepared self-extinguishing polymer nanocomposites using Closite 20A with PMMA matrix, decabromodiphenyl ether and antimony oxide as flame retardants. Ribeiro *et al*. [41] employed some organic chemical treatments on natural Brazilian MMT clay and then evaluated the effect of treatments on the flame retardancy potential of ethylene-butyl acrylate copolymer composites in the presence of APP and PER (pentaerithritol). In these studies, samples were prepared by melt mixing process and then subjected to various characterization tests: morphological, thermal, mechanical and flammability performance (i.e. UL-94, LOI, cone calorimetry).

From these studies, it is reported that the incorporation of clays into polymer matrices led to reduced burning rate with respect to neat polymers. The effect was attributed to the ability of

clay to form stable char on the surface of the burning nanocomposites. This insulated the underlying polymer from heat transfer due to flames, thus lowering the rate of volatilization [39]. Furthermore, Wei *et al*. [39] concluded that the combination of nanoclays and flame retardant did not exhibit remarkable additional influence on fire behaviour of PLA nanocomposites, except for the improved resistance to self-sustained combustion. However, Ribeiro *et al*. [41] and Si *et al*. [40] concluded that the combination resulted to lower PHRR, average MLR and HRR than those with only clay or the FRAs. This indicated some synergistic effect between nanoclays and FRAs. Ribeiro *et al*. [41] also reported that the modifications of natural Brazilian MMT clay did not change their flame retardancy performance.

Tai *et al*. [42] incorporated organic nanoclay into polyphosphoramide (PDEPD) by in-situ polycondensation in order to prepare flame retardant/clay nanocomposites. These were then introduced to polystyrene (PS) and polyurethane (PU) separately by solvent blending method. From the MCC tests, it was found that both PDEPD and mostly PDEPD/clay nanocomposites FRAs improved the flammability performance of PS and PU matrices by reducing both PHRR and THR. Moreover, the reduction in THR with the inclusion of PDEPD was attributed to the enhancement of char residues after combustion, thus leading to less evolution of combustible fuel gases.

Carbon nanotubes

Carbon nanotubes (CNTs) are the most widely studied nanofibrous materials with respect to polymer flame retardancy [13,35,43,44]. They may be synthesized in several ways, such as: arc discharge, laser ablation and thermal or plasma enhanced chemical vapour growth deposition (CVD). Direct arc discharge and laser ablation require the use of small quantities of a metal catalyst and very high temperatures. The CVD technique, on the other hand, enables the synthesis of CNTs at low temperatures, however the process leaves significant amounts of catalyst residues on the recovered sample. These nanotubes show exceptional properties that can be used in many applications, ranging from macroscopic material composites to nanodevices. They have high aspect ratios and as a result, percolate to form networks at very low loadings in a polymer matrix. This leads to a substantial improvement in a number of properties, e.g. mechanical, rheological and flame retardancy [13].

There are two different types of carbon nanotubes, i.e. small diameter (1-2 nm) single walled nanotubes (SWNTs) and large diameter (10-100 nm) multi walled nanotubes (MWNTs). CNTs are an interesting alternative to the use of conventional flame retardants and nanoclays. Their incorporation at low contents (< 3wt.%) can result in enhanced flammability for several polymers {PP, polystyrene (PS), ethylene vinyl acetate (EVA), polymethyl methacrylate (PMMA), low density polyethylene (LDPE) and polyamide 6 (PA 6)}. Several factors, including: nanotube dispersion, nanotube loading rate, mean size of nanotubes and large aspect ratio influence the flame retardant properties of polymeric material nanocomposites. Large aspect ratio can lead to the formation of an efficient and compact layer [13].

The presence of CNTs can increase thermal conductivity of a polymer and thus increase the time to ignition (TTI) and peak heat release rate (PHRR) where MWNTs are used. Several studies, based on CNTs with nanoclays in different thermoplastic matrices, were reported. Gao *et al*. [43], Hapuarachchi and Peijs [35] and Ye *et al*. [44] investigated the role of MWNTs with clays [35,44] and magnesium hydroxide (MH) [43] in the fire retardancy of PLA and EVA nanocomposites. In these studies, it was reported that the incorporation of MWNTs in the presence of other additives resulted in a remarkable reduction in heat release rate (HRR), PHRR, mass loss rate (MLR) as well as a prolonged combustion in the cone calorimetry test. Ye *et al*. [44] concluded that there was a synergistic effect which was driven by factors, such as: increased melt viscosity, improved thermo oxidation stability and the formation of compact charred layers due to MWNTs acting as heat barriers and insulation. Furthermore, Gao *et al*. [43] concluded that the addition of clay into a CNTs/EVA composite enhanced the formation of graphitic carbon. Additionally, nanotubes reduced the surface cracks of chars and hence increase the barrier resistance to the evolution of flammable volatiles and the oxygen ingress into the condensed phase.

Peeterbroeck *et al*. [45,46] used MWNTs with EVA copolymers, in the presence of commercial organoclays [45] and high density polyethylene (HDPE) coated-MWNTs [46]. In the latter study, the authors demonstrated the significant effect of the HDPE coating on the mechanical properties of nanocomposites and explained the flame retardant efficiency of MWNTs in EVA matrix. Furthermore, improved flammability performance of coated MWNTs containing EVA nanocomposites was reported. This followed the reduction in HRR and enhanced cohesion of the combustion residue, which was attributed to high quality of dispersion of HDPE-coated nanotubes and the chemical structure of the combustion products. In the former study [45], it

was concluded that simultaneous addition of modified clay and CNTs displayed a synergistic effect. Enhanced thermal and mechanical properties, in the presence of nanofillers, were also reported.

When the synergistic effect of CNTs, MMTs and decabromodiphenyl oxide/tin oxide in enhancing flame retardancy performance of PS was investigated, Lu and Wilkie [47] found that nanotubes were more efficient than clay in improving flame retardancy of materials. CNTs are believed to promote carbonization in the polystyrene matrix. On the other hand, Isitman and Kaynak [48] evaluated the potential synergistic flame retardancy action of filler nanoparticles (i.e. nanoclays and CNTs) combined with organophosphorus flame retardant in PMMA. In this case, it is reported that nanoclays showed improved effect on fire properties of intumescent nanocomposites compared to CNTs containing ones. This was explained in terms of suppressed intumescent character of organophosphorus FRA exerted by strong and continuous CNTs networks formed on the flaming surface during combustion. Nanoclays on the other hand, physically reinforced and consolidated the phosphate barriers without interfering with its intumescent character.

Graphene

Graphene is an emerging two dimensional material with unique mechanical, electrical and thermal properties. It consists of monolayer of sp^2-hybridized carbon atoms (carbon-carbon bond length of ~142 pm) packed in a honeycomb lattice. Its current scientific research interest results from marked enhancement in polymer properties at low filler contents. This is due to the high aspect ratio of graphene platelets, homogenous dispersion of graphene platelets in a polymer matrix and the filler-polymer interactions at interface. Similar to other types of nanofillers, such as CNTs and MMTs, it is also used to impart flame retardancy character to polymeric materials. This beneficial flame retardancy property is attributed to the physical barrier effect of layered graphene that slows down the release of volatile flammable gases and protects the underlying material from further burning [49-52].

Numerous works have been done on graphene-based nanocomposites with focus mainly on various properties other than flammability. The graphene-based nanocomposites are manufactured in four main routes. These are: a) template synthesis, b) intercalation from solution, c) in situ intercalative polymerization and d) melt intercalation. Mittal [49] reviewed

graphene materials in functional polymer nanocomposites and has elaborated on these fabrication methods. Premkumar and Geckeler [50] looked at graphene-DNA hybrid materials. Most studies on graphene nanocomposites mainly involved petroleum-based polymer matrices, such as: EVA, PP, PVA, PMMA and epoxy [51-56], whereas studied on biopolymers, included: poly(D, L-lactic-co-glycolic acid), chitosan and cellulose [57-61]. Form these studies, the flammability performance of graphene nanocomposites were based on petroleum polymer matrices and so far none on biopolymer matrices.

Huang *et al*. [53-55] investigated the flame retardant properties of graphene-containing nanocomposites in EVA and PVA polymer matrices. In these studies, the authors used graphene alone [53] and incorporated flame retardant additives, such as melamine polyphosphate (MMP) [54] as well as an intumescent FR (i.e. poly(piperazine spyrocyclic pentaerythrito bisphosphonate) (PPSPB) grafted onto the surface of graphene oxide [55]. From these studies, the presence of graphene and other FRAs led to improved flammability character of the nanocomposites investigated. This was indicated by increased TTI and reduction of values of PHRR, THR, ASEA and average MLR [53,54] when compared to neat PVA. This was attributed to the condensed phase flame retardancy through the formation of a compact, dense and uniform char during combustion [53]. Furthermore, the combination of MMP with graphene in PVA achieved a LOI value of 29.6 vol.% and UL-94 V-0 grade [54]. Similarly, graphene grafted PPSPB was reported to have enhanced the flammability performance of EVA by reducing the PHRR of the nanocomposites by about 56% at 1 wt.% filler content [55].

Dittrich *et al*. [56] used various carbon additives with different particle sizes and shapes to investigate their influence on the flammability and mechanical properties of isotactic PP. The authors compared the thermally reduced graphite oxide and multi-layer graphene with carbon black, MWNTs and expanded graphite. The flammability properties of PP were mainly enhanced in the presence of the thermally reduced graphite and multi-layer graphene, which formed residue layers that protected the underlying polymer during combustion. These led to a reduction PHRR up to 74% with respect to neat polymer.

Nano scale particulate additives

Nano scale particulate additives form another family of dditives that are made up of nanoparticles of metal oxides, silica and polyhedral oligomeric silsesquioxane (POSS). They are distinguished by their isometric dimensions.

Silsesquioxane

Polyhedral oligomeric silsesquioxane (POSS) cluster is an inorganic silica-like nanocage (general formula $RSiO_{3/2})_n$, where $6< n <18$. The inorganic core of POSS is surrounded by organic ligands (i.e. hydrogen, halogen, alkyl groups, organofunctional groups) that are covalently bonded to Si atoms, placed at the vertices of the polyhedral cage. A general concern about POSS is its high level of interactions, existing between clusters. This makes some POSS immiscible with some monomers or polymers. Consequently, the nature of the organic ligands of POSS clusters is an important element to choose, since it controls the behaviour of the clusters during processing and polymerization and thus allows tailoring the desired microstructure for the POSS hybrid polymer systems. POSS is depicted by the methyl phenyl polysilsesquioxane, aluminumisobutyl silsesquioxane (Al-POSS) and zinc isobutyl silsesquioxane (Zn-POSS). They do play a role as metal dispersing agents and it is possible to include a metal atom at one corner of the POSS nanocage structure. These inorganic nanocages are also referred to as preceramic compounds [62,63].

There are two types of POSS that have been studied with respect to flame retardancy i.e. those that bear either i) eight identical R groups (R = methyl, phenyl, isobutyl or isooctyl), or ii) seven R groups of the same nature and one functional R′ group (R′ = ester, silane, isocynate, methacrylate, alcohol, epoxide or amine). This wide range of R and R′ groups allows for the selective use of functionalized POSS according to the chemical nature of the polymer matrix. The functionality of the R′ group can improve the compatibility between the dispersed nanocages and the polymer matrix. It can also allow either chemical grafting of reactive polymer chains or initiation of polymerization reactions from POSS surface via the so-called “grafting from” technique [13,62-64]. Devaux *et al*. [64] used montmorillonite (MMT) clay together with POSS to process polyurethane nanocomposites and they concluded that the nano-additives appreciably reduced the harmful effects of fire. Additionally, the study showed the importance of the choice of nano-additives on the results of fire retardant behaviour with two

notable factors: the nature of the chemical groups grafted onto POSS and the conditions of the coating synthesis.

The presence of POSS in polymers modifies the viscosity and mechanical properties of the molten polymer. It also affects the thermal stability and fire performance by reducing the amount of heat released upon combustion. On combustion, POSS acts like a precursor forming thermally stable ceramic materials at high temperatures. For example, Franchini *et al*. [62] showed that POSS nanoclusters resulted in the improvement of fire retardancy of epoxy materials and the mechanism involved the formation of a rigid char structure during combustion. Furthermore, He *et al*. [65] prepared a series of flame retardant hybrids based on bisphenol A polycarbonate (PC), trisilanolphenylpolyhedral oligomeric silsesquioxane (TPOSS) and oligomeric bisphenyl A bis(diphenyl phosphate) (BDP) via a melt blending method. The group found enhanced thermal oxidative stability and fire resistance of the char layer which gathered or accumulated on the surface of the burning polymer when BDP and TPOSS were introduced. A synergistic effect was established in a system consisting of 2 wt.% TPOSS and 3 wt.% BDP.

In their investigation, Glodek *et al*. [66] reported a slightly improved fire retardancy and material property when POSS and talc fillers were incorporated in vinyl ester resins and tested for different properties including flammability. There was a slight increase in fire resistance of methacryl POSS relative to other fillers and this was attributed to the successful dispersion and reaction of this POSS into the polymer matrix. However, its overall fire resistance performance was reported as poor, relative to the brominated FRAs used in the study. Fina *et al*. [67] prepared PP/POSS blends by melt mixing method using POSS with different organic groups (methyl, vinyl or phenyl). The authors reported improved performances in the thermal and combustion rate. This was attributed to the formation of a ceramic superficial layer that protected the underlying material from degradation. The conclusion arrived at was that better results were obtained when vinyl-POSS was used as exemplified by the maximum HRR reduction and increased LOI value. In another study on the effect of flame retardance of isotactic PP/aminopropylisobutyl POSS composites, Bouza *et al*. [68] reported improved fire retardance, as determined by LOI test. In this study, the authors incorporated maleic anhydrite grafted PP (MA-g-PP) coupling agent and the resulting composites led to a remarkable increase in the LOI values when 2% POSS and 10% MA-g-PP were compounded with PP matrix.

Furthermore, the presence of these additives in PP matrix resulted in composites with high thermal stability than neat matrix, as reported from TGA test.

When biopolymers, such as poly(butylenes succinate) (PBS) [69] and PLA [70] were used with POSS materials, improved material properties were reported. Wang *et al*. [69] used POSS and graphene as nanofillers to flame retard PBS prepared by melt blending. It was reported that the addition of graphene led to superior flame retardance to POSS. The authors concluded that the presence of POSS and graphene improved the char yield with graphene incorporation into PBS, leading to better thermo-oxidative resistance in char layer. In a recent study by Fox *et al*. [70] PLA was extruded with intumescent FRAs based on APP, nanofibrillated cellulose fibre, POSS modified nanofibrillated cellulose fibre and PER. The authors found that the cross-linked network formed between cellulose, POSS and PLA produced composites with superior flame retardant, rheological and mechanical properties with respect to other intumescent formulations.

Metallic oxide particles

Metal oxide particles have been used as reinforcing fillers for polymeric materials. These particles may be nanometric titanium oxide (TiO_2), ferric oxide (Fe_2O_3), aluminum oxide (Al_2O_3) or antimony oxide (Sb_2O_3) particles. Flammability performance of these metallic oxide nanoparticles is dependent on the filler content, particle size and surface area of the nanoparticles [13,71-75].

Laachachi *et al*. [71,72] looked at the influence of different nanoparticles (Al_2O_3, TiO_2 and Fe_2O_3), in combination with organoclays (organomodified MMT) and phosphinate additives, on the thermal stability and fire retardancy of poly(methyl methacrylate). In both studies, the synergistic effect on the thermal stability and fire performance of these systems were reported. This resulted in enhanced ignition times, reduced total heat, reduced smoke release and a significant increase in the total burning period. The metal oxide particles are believed to have promoted the formation of carbonaceous layer/char. They also modified the heat transfer properties of the polymer nanocomposites due to their good thermal properties and large specific area. Depending on the system, the metal oxide particles may [71] or may not [72] improve the fire performance of the composites.

Gallo *et al*. [73,74] investigated the flame retardancy synergy between aluminium phosphinate and metal oxides for different polymers. In the first study [73], Al_2O_3 and TiO_2 were used for poly(butylene terephthalate) PBT. In the second study [74], they used Fe_2O_3 and Sb_2O_3 for a commercial poly(3-hydroxybutyrate-co-3-hydroxyvalerate)/poly(butylene adipate-co-terephthalate) PHBV/PBAT biodegradable blend system. They reported better fire retardancy which was ascribed to increased intermediate char formation. A synergistic effect due to the phosphorus and the nanofiller components was observed in the flame retardancy mechanism, where the phosphorus acted as flame inhibition in the gas phase and the nanofiller promoted crosslinking in the solid phase [73]. In both studies, a combination of metal oxides and aluminium phosphinate resulted in better classification in the UL-94 test due to the combination of the different mechanisms.

Wang *et al*. [76] prepared flame retardant nanocoatings of nanometer scale layer double hydroxides (nano-LDHs) and titanium oxide nanoparticles to ammonium polyphosphate-pentaerythritol-melamine intumescent FR system. The authors reported the improvement of nanoparticles in fire resistance and anti-ageing properties of the intumescent flame retarded system. It was reported that the thermal decomposition of nano-LDHs promoted the formation of char by the IFR system, which was said to be an intercalated nanostructure with mixed resultant metal oxides (Al_2O_3 and $MgAl_2O_4$). This intercalated structure was thought to have improved the anti-oxidation character of the char structure. It was further reported that the inclusion of nano titanium oxide particles improved the anti-ageing of the IFR coated system. The conclusion arrived at was that nanocoating has the good expanding effect and fire resistance property, even after 500 hours accelerated ageing.

Shen *et al*. [77] and Li *et al*. [78] used PP to investigate the influences of metal oxides on the flammability properties of nanocomposites. Lanthanum oxide in the presence of magnesium hydroxide were extruded with PP matrix and their flammability performance tested via LOI and microscale combustion calorimeter [77]. On the other hand, Li *et al*. [78] compounded an intumescent system, based on APP and PER, with antimony oxide by melt mixing method. LOI and UL-94 were employed for flame resistance tests. In this study, the authors reported increased LOI values from 27.8 to 36.6 vol.% in the presence of antimony oxide. The FR system also recorded UL-94 V-0 rating at the 2 wt.% content of Sb_2O_3. This was attributed to the reaction of antimony oxide with APP to form cross-linked charred layers. Lowered mechanical properties were also reported in the presence of a metal oxide due to the poor

compatibility between PP and Sb_2O_3. In the former study [77], it was found that the presence of La_2O_3, can remarkably improve the flame retardancy of magnesium hydroxide filled PP flame retarded composites. It was indicated by the UL-94 V-0 rating and reduced HRR, THR and HRC values obtained for the PP/MH/La_2O_3 composites. This was attributed to enhanced quality of condensed phase charred layers deposited on the surface of magnesium oxide particles formed through the participation of PP chains in char formation due to the catalytic effect of lanthanum oxide. The authors further proposed some flame retardancy mechanisms which may be obtained from the source.

In general, the incorporation of nanoparticles (organoclays, CNTs, or POSS) decreases polymer flammability through several mechanisms. Amongst others, limiting the fuel transfer, formation of protective layers (char and/or ceramic like materials) and the prevention of dripping via reduced melt viscosity can be obtained. These polymer nanocomposites still burn with little reduction in the THR and TTI is, generally, not improved, which can even decrease for some nanocomposites. This may, somehow, necessitate the use of nanoparticles in combination with other flame retardant agents for a synergistic effect.

Hybrid nanofillers

Hybrid materials refer to the class of materials whereby inorganic and organic components are mixed intimately at a nanometric or molecular scale. Hybrids may be either homogeneous systems of miscible organic and inorganic components or can be heterogeneous. The properties of the resultant material do not only depend on the individual properties of the materials, but also on the scale of interaction between the two components that contributes noticeably to the properties of the resultant material. These materials have the potential to improve, amongst others, thermal, mechanical and photochemical stability [79].

A number of studies have been done on the use of hybrid materials for the improvement in the thermal, mechanical and flame resistance performance of the polymer composites [52,80-85]. There are different hybrid materials, such as graphene, phosphorus, layered silicate, silane-PCL, and brucite-polyphosphate-amine based inorganic-organic materials. Messori *et al*. [80] prepared organic-inorganic hybrid materials from tetraethoxysilane and α and α, ω-triethoxysilane terminated poly(ε-caprolactone) (PCL-Si), using the sol-gel process. PMMA slabs were dip-coated with PCL-Si/silica hybrids and increased flame resistance was reported

with respect to neat matrix. This was attributed to a preferential segregation of silica onto the outer surface of the nanocomposites. Bonnet *et al*. [81] prepared EVA-based hybrid material containing silicon and phosphorus in order to improve flame retardancy. The authors found synergistic effect between silicon and phosphorus on the fire properties at 1.3 wt.% silicon and 1.4 wt.% of phosphorus loadings. A reduction by 35% in the PHRR, measured in a cone calorimeter for EVA-hybrid materials was observed when compared to pure EVA. This was attributed to the formation of compact charred layer.

2.2.2.5 Mineral flame retardants

Mineral FRs have been researched and reviewed by numerous investigators [13,86-104]. These inorganic fillers can influence the reaction of polymers, including inert types. They reduce the contact of combustible products, modify the thermal conductivity and all its thermophysical properties and change the viscosity of the resulting materials. These have indirect incidence on the fire performance of a polymer. Some minerals (see Table 2.2) are specifically used as FRs due to their behaviour at high temperatures [13,86,87].

Table 2.2 Physical properties of potential fire retardant mineral fillers. Reprinted from [96], Copyright 2011, with permission from Elsevier

Filler	Formula	T_{decomp}/ °C	ΔH_{decomp}/kJ g^{-1}
Aluminium hydroxide	$Al_2O_3 \cdot 3H_2O$	180-200	1300
Magnesium hydroxide	$Mg(OH)_2$	300-320	1450
Calcium hydroxide	$Ca(OH)_2$	430-450	1150
Nesquehonite	$MgCO_3 \cdot 3H_2O$	70-100	1750
Hydromagnesite	$Mg_5(CO_3)_4(OH)_2 \cdot 4H_2O$	220-240	1300
Huntite	$Mg_3Ca(CO_3)_4$	400	980
Ultracarb	Hydromagnesite/Huntite	220-400	1172
Boehmite	60/40 AlO(OH)	340-350	560

The most commonly used mineral flame retardants are hydrocarbonates [13,88,89,94-96], metal hydroxide (aluminum and magnesium) [13,18,86,87,90-92,95,98,100-102,104] and borates [13,18,92,99,102]. Inorganic fillers have a physical flame retardant action. As the temperature of the system rises, fillers decompose endothermically and consequently absorb

energy. Furthermore, they release non-flammable molecules, such as H_2O and CO_2. These molecules serve to dilute combustible gases and can also promote the formation of a protective ceramic or vitreous layer due to their release which leaves behind such a layer [13,86,87,89].

Hydroxycarbonates

All carbonates release CO_2 at high temperatures, except for magnesium and calcium carbonates that release CO_2 at temperatures below 1000 °C. Magnesium carbonate is the carbonate that releases carbon dioxide at the lowest temperature of about 550 °C [95]. In comparison with other conventional flame retardants, hydrocarbonates are less widely used but remain an alternative to metal hydroxides. Natural magnesium carbonate (magnesite) and synthetic magnesium hydrocarbonate (hydromagnesite) release water, break down endothermically and liberate CO_2 at high temperature. The thermal decomposition of hydromagnesite ($4MgCO_3 \cdot Mg(OH)_2 \cdot 4H_2O$ or $5MgO \cdot 4CO_2 \cdot 5H_2O$) in air is represented thus [13,88,89,94-96]:

$$4MgCO_3 \cdot Mg(OH)_2 \cdot 4H_2O \rightarrow 4MgCO_3 \cdot Mg(OH)_2 + 4H_2O$$

$$4MgCO_3 \cdot Mg(OH)_2 \rightarrow 4MgCO_3 \cdot MgO + H_2O$$

$$4MgCO_3 \cdot MgO \rightarrow 5MgO + 4CO_2 \qquad (800kJ\ kg^{-1})$$

Hydromagnesite releases water and carbon dioxide over a wider temperature range than aluminum trihydroxide (ATH) and magnesium dihydroxide (MDH) (also called magnesium hydroxide, MH) (see section on metal hydroxides). It has been used as flame retardant in polypropylene (PP), ethylene vinyl acetate (EVA) [94] and low density polyethylene (LDPE)/ethylene vinyl acetate (EVA) blends [94,95]. It releases water and carbon dioxide between 200 and 550 °C in comparison with ATH (180 to 200 °C) and MDH (300 to 340 °C), suggesting that it may have similar or even better flame retardancy effectiveness than ATH and MDH [13].

Some studies have been conducted on magnesium carbonate [93] and hydromagnesite [88,89,94-96]. Haurie *et al*. [94,95] investigated the flammability and thermal stability of hydromagnesite alone in polyethylene [94] and combined with aluminum hydroxide, magnesium hydroxide and montmorillonite mixtures in polyethylene/ethylene vinyl acetate blends [95]. Laoutid *et al*. [89] compared the flame retardancy of a combination of hydromagnesite/organomodified montmorillonite (MMT) with a magnesium hydroxide (MH

and/or MDH)/MMT flame retardant system. In these studies, improved fire resistance (i.e. reduced peak heat release rate, auto extinguishability and increased time to ignition) was generally reported. The conclusions made were, namely, reduction in mineral filler content as well as improved mechanical properties due to the presence of nanoclays.

Metal hydroxides

Metal hydroxides are the largest group of mineral fire retardants. They act as flame retardants for polymers by releasing water vapour through endothermic decomposition and leave a thermally stable inorganic residue. This has to occur at temperatures higher than the polymer processing temperature range and around the polymer decomposition temperature. Aluminum trihydroxide, $Al(OH)_3$ (ATH) and magnesium dihydroxide, $Mg(OH)_2$ (MDH) are the most commonly used metal hydroxides. They are used as smoke suppressants and have been incorporated in wood products as flame retardants [13,18,86,87].

The endothermic decomposition of ATH occurs between 180 and 200 °C, depending on the particle size and physical form, leading to the release of water and formation of alumina:

$2Al(OH)_{3(s)} \rightarrow Al_2O_{3(s)} + 3H_2O_{(g)}$ (1050 kJ kg^{-1})

The decomposition reaction of ATH has several effects on the combustion of a polymer, namely it absorbs 1050 kJ kg^{-1} of energy and then cools down the polymer material, the solid alumina (Al_2O_3) formed provides a thermally insulating protective coating and the water vapour released dilutes the combustible gases and forms a protective gas layer. The use of ATH lowers fire growth in cone calorimetry and markedly reduces smoke production. However, the fire properties of ATH-filled polymers are only of interest at high loading levels i.e. 60 wt.%. Such high loadings have a negative effect on the mechanical properties of the composites. This limits the application of mineral flame retardants. Due to its low processing temperature, ATH is limited to polymers such as EVA and LDPE with low processing temperatures [13,86,87,91,95,104].

The use of ATH as a flame retardant was explored in different studies [90,91,95,98,104] where it was used in combination with other additives. Haurie *et al*. [95] used hydromagnesite, MDH, ATH and montmorillonite in LDPE/EVA blends, Cárdenas *et al*. [91] and Witkowski *et al*. [104] investigated the influence of ATH (different particle sizes and surface treatments) and

ATH and MDH, respectively, on the fire retardant properties of EVA/nanoclay composites. As a way to minimize the negative effects of high loads of metallic hydroxides, Nachtigall *et al*. [98] incorporated interfacial coupling agents for polypropylene (PP)/ATH composites. The effect of a combination of ATH and zinc borate on a PP matrix was investigated by Ahmad Ramazani *et al*. [90]. In these investigations, it was generally concluded that there is synergy between the ATH and other additives (i.e. nanoclays, MDH and zinc borate), resulting in improved fire retardancy and mechanical properties.

Magnesium dihydroxide (MDH) acts in the same way as ATH, except that its endothermic decomposition occurs at temperatures above 300 °C. This makes MDH an interesting additive with respect to extrusion and injection moulding processes of some polymers [13,101].

$2Mg(OH)_{2(s)} \rightarrow 2MgO_{(s)} + 2H_2O_{(g)}$ (1300 kJ kg^{-1})

Its flame retardant action is effective up to 400 °C. Beyond this temperature, the exothermic character of degradation predominates. On decomposition, MDH may have a catalytic effect on the carbonized residues, produced by combustion. This leads to an afterglow effect, which could be cancelled by incorporating additional additives in order to acquire effective barrier formation [13,93].

Various polymer matrices, viz: PP [102], EVA [44,89,92,100] and unsaturated polyester resins [103] were compounded with MDH filler and their flammability and mechanical properties were investigated. Sain *et al*. [102] studied the flammability of sawdust and rice husk-filled PP with magnesium hydroxide, combined with boric acid and zinc borate as flame retardant systems. MDH (25 wt.%) lowered the burning rate (using a horizontal burning test) of the composites by 50% relative to the untreated materials. It was further reported that there was no flame resistance synergy observed between MDH and other additives. Grexa and Lübke [18] investigated the effect of magnesium hydroxide (type A) on the flammability properties of wood particle boards. This was compared to combinations of monoammonium phosphate with ATH (type B) and monoammonium phosphate with boric acid (type C). The group reported decreased peak values of HRR (using a cone calorimeter) as a function of MDH content (see Figure 2.2, where A1, A2 and A3 = 8, 15 and 24 wt.%, respectively) indicating the possibility of improving the overall fire performance of wood particle board using this flame retardant.

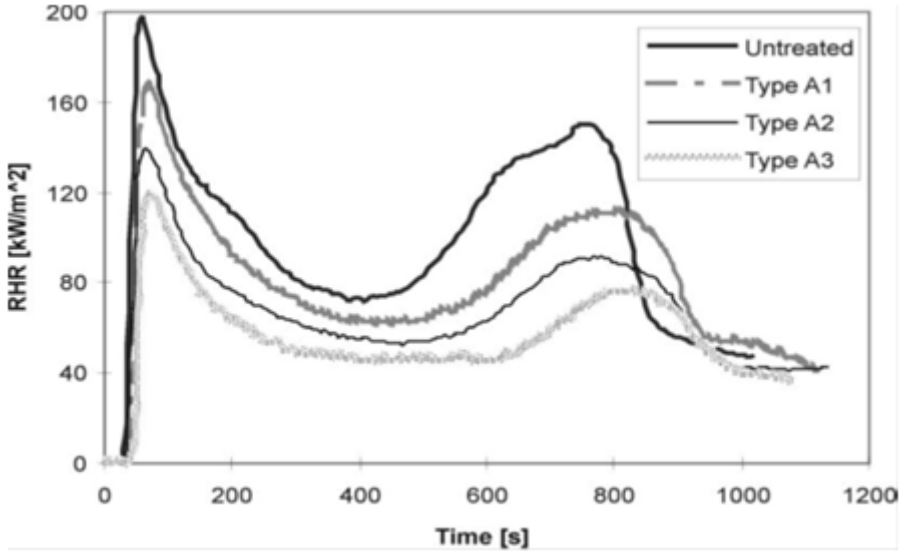

Figure 2.2 HRR as a function of time for untreated and FR-treated particle board with the use of magnesium hydroxide. Reprinted from [18], Copyright 2001, with permission from Elsevier

MDH nanoparticles have also been considered as flame retardant agents [100]. They can be obtained by several methods, including the sol-gel technique followed by a hypercritical drying procedure, hydrothermal reaction, using various precursors and solvents or theprecipitation of magnesium salts with alkaline solution. This last method allows for the control of nanoparticles morphology by fine-tuning of experimental parameters, such as: the chemical nature of a base used as precipitant, type of counter-ion, temperature as well as hydrothermal treatment. The use of nanometric MDH led to good fire performance at low loading levels [13]. This was also shown by Qui *et al*. [100] who prepared and characterized MDH nanoparticles as flame retardant for EVA nanocomposites. They attributed this to the good dispersion of the nanoparticles, resulting in the formation of more compact and cohesive char during combustion tests (i.e. limiting oxygen index, LOI).

Borates

Borates are another family of inorganic additives with flame retardance properties. The most frequently used borate is zinc borate ($2ZnO{\cdot}3B_2O_3{\cdot}3.5H_2O$). It undergoes endothermic decomposition (503 kJ kg^{-1}) between 290 and 450 °C and liberates water (H_2O), boric acid (H_3BO_3) and boron oxide (B_2O_3). Boron oxide softens at 350 °C and flows above 500 °C, leading to the formation of a protective vitreous layer. In the case of polymers with oxygen

atoms, the presence of boric acid causes dehydration, leading to the formation of a carbonized layer. This layer protects the polymer from heat and oxygen, thus reducing the amount of combustible gases released [13,18,92,99,102].

2.3 Flammability testing techniques

Flammability of polymers can be characterized by the ignitability, flame spread rate and heat release. A number of small, intermediate and/or full scale flammability tests are used in industrial and/or academic laboratories. They are used for either screening materials during production or testing manufactured products. This section discusses the commonly used flammability testing techniques, such as: cone calorimetry, pyrolysis combustion flow calorimetry (PCFC), limiting oxygen index (LOI), underwriters' laboratories (UL-94) and Ohio State University (OSU) heat release rate [4,11,16].

2.3.1 Cone calorimetry

Cone calorimetry is a technique used to quantify the flammability of materials by determining various flammability parameters. It was first reported on in 1982 by the National Bureau of Standards (NBS), now known as the National Institute of Standards and Technology (NIST). This came after several attempts were made to design a reliable bench scale engineering device for measuring heat release rate (HRR). Although there were such tools already built for this purpose in the late 1970's and early 1980's by NBS and other institutions, none was appropriate for normal engineering laboratory use. It was during this time that the concept of oxygen consumption was developing and becoming familiar. From this concept, the successful bench scale heat release rate (HRR) apparatus was developed and the method was termed cone calorimetry. There have been numerous improvements made on the cone calorimeter since its introduction. However, its basic principle has remained unchanged. The greatest changes were introduced in 1987 with the inclusion of systems for measuring smoke optically and soot yield gravimetrically. Most other changes involved parts redesign for ease of use and reliability of operation [15,105,106]. Figure 2.3 shows a photograph of a cone calorimeter apparatus.

Figure 2.3 Cone calorimeter apparatus (from the Council for Scientific and Industrial Research (CSIR) fire testing laboratory)

Cone calorimetry is one of the most effective medium sized fire behaviour tests used to study the rate of heat released by materials exposed to radiant heat flux. Its principle is based on the measurement of decreasing oxygen concentration in the combustion gases of the sample that is subjected to a given heat flux (10 to 100 kW m^{-2}). It has been standardized in the United States (ASTM E 1354) and now it is an international standard (ISO 5660) [13,15-17].

Figure 2.4 shows an experimental schematic representation of a cone calorimeter. A sample of 100 mm x 100 mm dimensions is horizontally (occasionally vertically) placed in a sample holder on a load cell for evaluation of the mass loss during the experiment. The sample is aluminum foil-wrapped on the sides and at the bottom. It is put in a retainer frame over low density ceramic wool and the retainer frame is secured to the specimen holder. A conical radiant electrical heater uniformly irradiates the sample from above and combustion is triggered by an electrical spark. The combustion gases that are produced pass through the cone and are removed by means of an exhaust duct system with a centrifugal fan and an extraction hood. The centrifugal fan is situated in the combustion gas line in order to set the flow rate of the combustion products. Along the combustion gas line, there is a gas sampling ring positioned before the fan. The gas sampled in the ring is first passed through two filters in order to remove particles. It is then passed through a cold trap and a drying agent in order to remove possible water. Finally, it reaches the gas analyzers. Between the gas sampling ring and the fan, there is

also a smoke measurement system. This system determines the amount of smoke produced using a laser photometric beam [13,15-17,106].

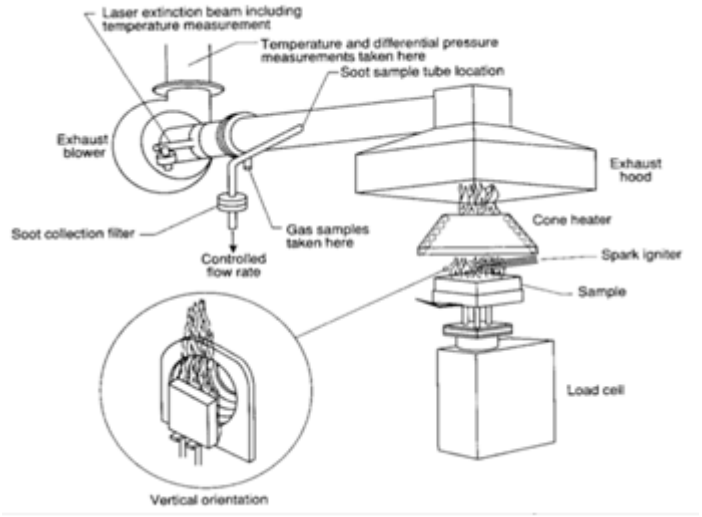

Figure 2.4 Schematic representation of an experimental set-up in a cone calorimeter. Reprinted from [107], Copyright 1992, with permission from Elsevier

In order to perform the basic cone calorimeter experiments, only an oxygen analyser is required. Furthermore, in order to better understand the burning process and minimize the uncertainties in the results, additional analyzers are usually fitted. These may be CO and CO_2 analyzers. In order to further analyse combustion products and gaseous species, a Fourier transform infrared (FTIR) spectrometer can be coupled through a heated line [106].

Measurements of gas flow and oxygen concentration are used to calculate the quantity of heat released per unit of time and surface area (heat release rate, HRR), expressed in kW m^{-2}. The development of HRR over time i.e. the value of its peak maximum (PHRR) or HRR maximum is considered in order to assess the fire properties of materials. The calculation of HRR is based on Huggett's observation in a study of the estimation of HRR via oxygen consumption measurements [108]. Huggett observed that most organic materials release an amount of heat that is practically proportional to the amount of oxygen consumed while burning. The proportionality factor is constant from one material to another and is equal to 13.1 kJ g^{-1} consumed oxygen, with an accuracy of approximately 5%. Integration of the heat release rate (HRR) versus time curve, gives the total heat release (THR) expressed in MJ m^{-2} [13,15-17].

Cone calorimetry, in addition to the aforementioned parameters, also enables the characterization of time to ignition (TTI), time to flame out (TFO), mass loss rate, levels of oxygen, carbon monoxide and carbon dioxide and total smoke released (TSR). Furthermore, it provides more detailed fire characteristics, with HRR being the most widely used parameter for evaluating the fire properties. Some conditions, such as ignition and flammability of weakly reacting materials, conditions of low or fluctuating oxygen concentration and variable material thickness and composition, pose difficulty for proper examination of samples [13,15-17]. In essence , cone calorimetry is regarded as the most versatile medium sized fire testing method ever invented.

2.3.2 Pyrolysis combustion flow calorimetry (PCFC)

Pyrolysis combustion flow calorimetry (PCFC) is a fire testing method for evaluating the combustibility of milligram sized samples. It is also known as microscale combustion calorimetry (MCC). This was originally developed by the Federal Aviation Administration (FAA) in the United States. The intent was to identify inherently fire resistant polymers for use in commercial aeroplanes. Later on the FAA adopted the method to screen new polymers for heat release rate in flaming combustion. Recently, PCFC has been used to assess the flammability of flame retarded polymers. It is now a standardized technique, classified as ASTM D7309-07 [109-114].

PCFC simulates the burning of a polymer solid. It separately reproduces the solid state and gas phase processes of flaming combustion in a non-flaming test. This is achieved by controlled pyrolysis of the sample in an inert gas stream, followed by high temperature oxidation of the volatile pyrolysis products. The heat of combustion of the pyrolysis products is measured by the use of oxygen consumption calorimetry. This method combines the constant heating rate and flow characteristics of thermal analysis (i.e. thermogravimetry) with the ability to determine the heat of combustion, typical of oxygen bomb calorimetry. Nonetheless, PCFC determines the heat release and heat release rate using an oxygen consumption method. Consequently, PCFC is more of a fire calorimetry parallel rather than a thermal analysis [110,114].

The PCFC technique attempts to improve on the laboratory pyrolysis combustion methods by providing a dynamic capability for solids without the need to measure mass loss rate during

the test. It helps in measuring the maximum specific heat release rate, Q_{max} (HRR, W g^{-1}) at a heating rate, β, the total amount of heat release for complete combustion, h_c^0 (THR, J g^{-1}), and the temperature at maximum pyrolysis rate, T_{max} (°C) of polymers, using only a milligram size samples. For polymeric materials that thermally decompose to fuel gases and possibly forming char in a single step, the pyrolysis temperature interval, ΔT_p is given by equation 2.1:

$$\Delta T_p(°C) = eRT_{max}^2/E_a \quad (2.1)$$

where E_a (J mol^{-1}) is the global activation energy for pyrolysis, e is the natural number and R is the universal gas constant. These combustion parameters help to define a heat release capacity, η_c (HRC, J g^{-1} K^{-1}), given by equation 2.2:

$$\eta_c = Q_{max}/\beta = h_c^0/\Delta T_p \quad (2.2)$$

The heat release capacity is the maximum potential of the material to release combustion heat in a fire. From the above equation, the heat release capacity (η_c) is a combination of material properties, consequently, it is in itself a material property as measured in PCFC [111,114-116]. According to Schartel *et al*. [114], the use of HRC as a measure of fire risk is based on the assumption that the maximum specific heat release rate at the decomposition temperature reached at constant heating rate that correlates with the mass loss rate during pyrolysis in a fire, characterized by a transient temperature gradient.

The apparatus construction and calibration method are well described by Lyon and Walters [109,110] and its schematic representation is shown in Figure 2.5a. PCFC is based on linear programmed heating of a milligram sample in an inert atmosphere in order to separate the solid and gas phase processes of flaming combustion as would normally be the case in a fire situation [113].

The principles of this technique are as follows: A solid sample is subjected to heating at a constant rate, (β) of temperature rise under an inert (N_2) gas flow. The heating goes to a maximum temperature (T_{max}) and the sample is held at this maximum temperature for between 10 and 120 s in order to stimulate pyrolysis. The volatile pyrolysis products generated during the temperature rise are removed from the pyrolyser by the nitrogen purge gas and O_2 gas is added to the pyrolyzate/nitrogen gas stream at the inlet to the combustor. Combustion products, such as: carbon dioxide, water and acid gases that exit the combustor are removed by the scrubbers and the dry nitrogen and the residual oxygen pass through the flow meter and oxygen

analyser. Deconvolution of the oxygen consumption signal is performed numerically during the test and the heat release rate, heat release capacity and total heat of combustion are calculated and displayed. In order to determine the residual mass of the sample, the quartz tube is weighed after the test. Figure 2.5b shows the experimental setup of the PCFC in comparison with the flaming combustion of a polymer. This figure illustrates how the condensed phase (pyrolysis) and gas phase (combustion) processes of flaming combustion are separately reproduced in a non-flaming combustion test, using the flaming polymer combustion as a reference [109,110,113-116].

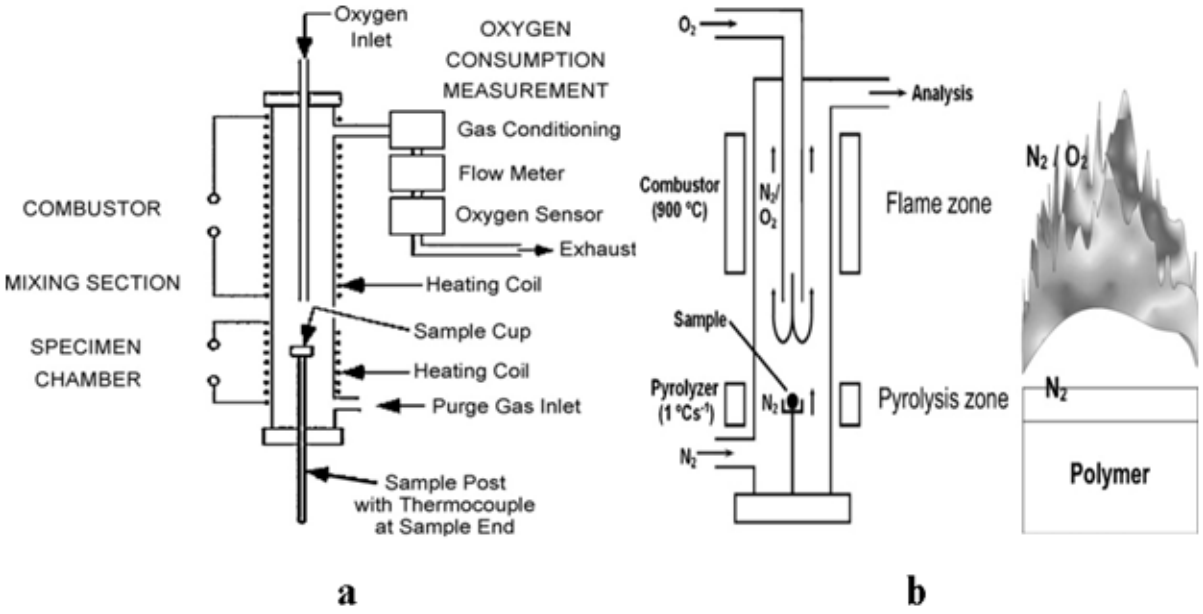

Figure 2.5 Schematic representation of pyrolysis combustion flow calorimetry (PCFC): (a) basic section of the apparatus. Reprinted from [113], Copyright 2009, with permission from Elsevier.
(b) Experimental set-up of the PCFC (left) in comparison with the flaming combustion of a polymer (right). Reprinted from [114], Copyright 2007, with permission from Elsevier

The total heat of combustion of the solid, as opposed to the pyrolysis gases, can be measured by switching the purge gas from nitrogen to air after the temperature ramp or by using air as the purge gas during the ramp and hold cycles. Thus, selective thermooxidative degradation of the solid or char can be accomplished and the oxygen consumption can be measured in order to determine the heat of complete combustion, since any residual organic material will be oxidized in air at a maximum temperature (T_{max}) [110].

The pyrolysis combustion flow calorimetry (PCFC) method has some advantages. This technique requires small sample size of between 5 to 50 mg, ideal for research work, giving small product yields during synthesis. When a sample is reacted in an air atmosphere, it can separate oxide-forming reactions from nitride-forming reactions. PCFC has the capability of separately measuring the combustion of volatile and nonvolatile components [110].

2.3.3 Limiting oxygen index (LOI)

Limiting oxygen index (LOI) is the minimum concentration of oxygen in a mixture of oxygen and nitrogen that is needed to support the flaming combustion of a material. It is expressed in volume percent (vol.%). It was first introduced in 1966 by Fenimore and Martin [111,117]. It is used to indicate the relative flammability of materials. It is standardized in the United States (ASTM D 2863) and in France (NF T 51-071), as well as internationally (ISO 4589). The principle of the method is that a sample is placed vertically within a controlled atmosphere and its top inflamed with a burner. LOI, the minimum concentration of oxygen in a mixture of oxygen and nitrogen that either maintains flame combustion of a material for 3 minutes or consumes a length of 5 cm of a sample, is expressed as:

$$LOI = 100 \text{ x } [O_2]/([O_2] + [N_2]) \qquad (2.3)$$

where $[O_2]$ and $[N_2]$ are the concentrations of oxygen and nitrogen gases, respectively. According to ISO 4589, LOI is measured on specimen (dimensions: 80 x 10 x 4 mm) vertically placed at the centre of a glass chimney, as illustrated in Figure 2.6. A mixture of gases flows upstream via this chimney and it is homogenized by passing through layers of glass beads. After 30 s purge of the column, the top of a specimen is ignited like a candle [7,13,15].

As air contains 21% of oxygen, materials with LOI values less than this are classified as combustible, but those with LOI greater than 21 are classed as self-extinguishing since their combustion cannot be sustained at ambient temperature without an external energy contribution. It therefore, means that high LOI value materials will generally exhibit a better flame retardant property. This method remains one of the most important screening and quality control tools in the plastics industry, used to characterize both the ignitability and flammability resistance. However, LOI measurements are taken at room temperature and LOI values decrease as temperature increases. This means that self-extinguishing cannot be considered a fast rule since materials with high LOI values at room temperature may burn without self-extinguishing under intense fire conditions. It should be noted that melting and dripping of a

polymer during the LOI test may cause a specimen to extinguish and thus give misleading high LOI values. In addition, LOI has a limitation as a test for nanocomposites in that organomodified nanoclay reinforced polymer nanocomposites exhibit decreased LOI values due to an increased flame spread rate over the surface of the specimen, while inside the material, nanoclays form a barrier layer that limits the propagation of fire [2,13,15,19].

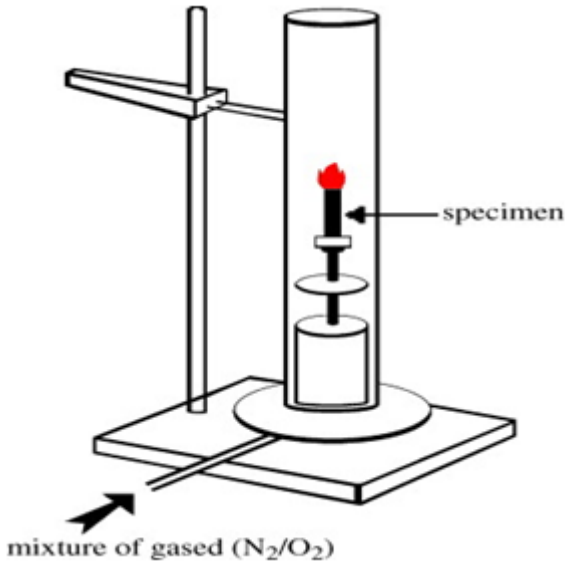

Figure 2.6 Schematic representation of a limiting oxygen index (LOI) test setup. Reprinted from [13], Copyright 2009, with permission from Elsevier

The advantages of LOI are that it provides a convenient, reproducible means of determining a numerical measure of flammability. Furthermore, the test equipment is inexpensive and only a small sample size is required for testing [118].

2.3.4 Underwriters Laboratories 94 (UL-94)

UL-94 is a set of tests approved by Underwriters Laboratories Inc. as flame tests for plastics materials materials of parts in devices and appliances. It includes a range of tests, such as small and large flame vertical (V) tests, horizontal (H) tests for bulk and foamed materials, as well as radiant panel flame spread test. The commonly used test, is the UL-94 V in terms of practice and usage. It measures ignitability and flame spread of vertical bulk materials exposed to small flame. It is equivalent to international standard IEC 60695-11-10 (Test method B) for small flames (50W) and ASTM D3801-10 [13,119,120].

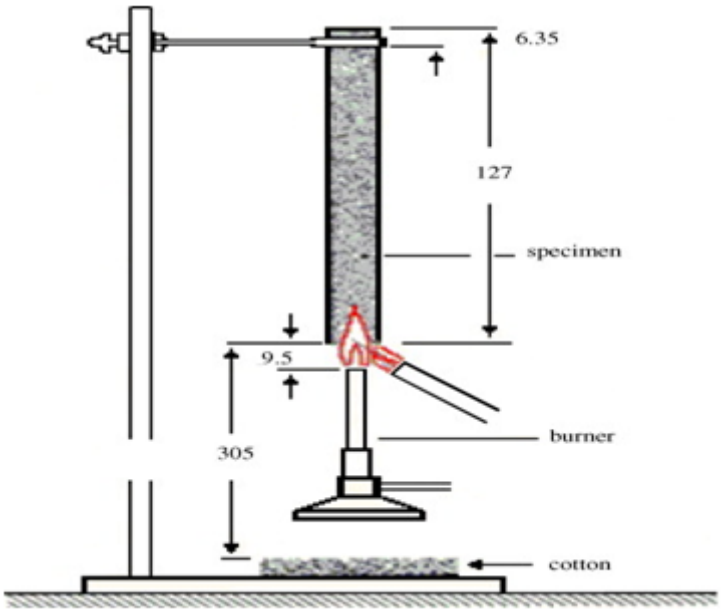

Figure 2.7 Schematic representation of UL-94 vertical test. Reprinted from [13], Copyright 2009, with permission from Elsevier

As shown in Figure 2.7, the burner is adjusted in order to produce a blue flame with 20 mm high central cone and a power of 50W. The flame is applied to the bottom of a specimen with the top of the burner located approximately 10 mm from the bottom edge of the specimen. The flame is applied for 10 s and removed and the time required for flaming combustion to cease (after flame time) is noted as t_1. After flaming combustion has ceased, the flame is applied for another 10 s and after flame time, t_2 is noted together with afterglow time, t_3. The distance between the burner and specimen must remain constant during flame application. If some drops fall from the specimen, the burner is tilted to a maximum angle of 45° and slightly removed from the edge of the specimen. During the test, the presence of burning drops and any ignition of a piece of cotton placed under the specimen must be noted. The standard specification is that at least 5 specimens must be tested. The classification is made via V-0, V-1 and V-2 rating and criteria as shown in Table 2.3 [13,119,120].

The UL-94 test is widely used both in industry and academic research centres. It is intended to meet industrial requirements as well as classify polymeric materials hierarchically. The information obtained remains limited due to its basic and unrefined character. For specimens that flow, the test seems less appropriate than for more cohesive materials [13,119,120].

Table 2.3 UL-94 V ratings and criteria. Reprinted from [119], Copyright 2011, with permission from John Wiley and Sons

Sample classified to the following criteria	V-0	V-1	V-2
After flame time for each individual specimen t_1 or t_2	≤10 s	≤30 s	≤30 s
Total after flame for any set (t_1 plus t_2 for five specimens)	≤50 s	≤250 s	≤250 s
After flame/glow time for each specimen after second application ($t_1 + t_3$)	≤30 s	≤60 s	≤60 s
After flame glow of any specimen up to clamp	No	No	No
Cotton indicator ignited by flaming drips	No	No	Yes

s stands for seconds

2.3.5 Ohio State University heat release apparatus (OSU)

The OSU is a technique developed to describe how a material burns. It is a quantitative method of analysis that was available in its basic form in the early 1970's. The technique is used to measure the rate of heat release (RHR) of materials and products in a forced flaming combustion. Originally, RHR is determined by measuring the temperature change (ΔT) of a constant mass flow of air (m_a) through the apparatus, caused by the heat released from the burning sample. The change in enthalpy of the air is calculated using the usual relation 2.4:

$$\Delta H = m_a c_p \Delta T \qquad (2.4)$$

where c_p is the heat capacity of air [121].

The fundamental principles of the OSU heat release apparatus are outlined in the Federal Aviation Administration (FAA), FAR 25.853 (ASTM E906/E906M-10, 2010) and the American Society of Testing and Materials (ASTM), ASTM E906 [122,123] test methods. This apparatus is used in two configurations A and B. Configuration A is used by FAA under the designation FAR 25.853 as a regulatory tool in determining the fire properties of materials of aircraft interior cabin. The FAA requirements are exclusively based on heat release. In order for a material to satisfy the requirements, it must have an average maximum heat release of < 65 kW m^{-2}, during 5 minutes of the test and an average total heat release of < 65 kW min m^{-2} within the first 2 min of the test, when the incident heat flux is set at 35 kW m^{-2} [124,125]. Configuration B, under the designation ASTM E906, is intended for use in research and

development and not as a basis for rating, regulatory, or code purposes. Figure 2.8 shows the OSU rate of heat release apparatus [126].

In the standard method (ASTM E906, configuration B), the OSU determines the rate of heat release (RHR) (also heat release rate, HRR) of a material from the sensible enthalpy (temperature) rise of the air. The specimen is injected into an environmental chamber through which a constant flow of air passes. The specimen's orientation varies from vertical (configuration B) to horizontal (configuration A). The air flows past a 150 mm x 150 mm specimen with maximum thickness of 45 mm. The OSU monitors the temperature difference between the air entering and exiting the environmental chamber by a thermopile. The specimens of materials or products are exposed to different levels of radiant heat at incident fluxes up to 100 kW mm^{-2}. Combustion is initiated by piloted ignition. The combustion products leaving the chamber are monitored and the change in temperature (enthalpy) due to these, is used to calculate the rate of heat release [124-126]

Numerous modifications had been proposed to the OSU technique [127-129]. This was because the standard thermal mode had some errors caused by the heat losses that were not accounted for, as well as the fact that the mass flow rate is controlled [130]. Consequently, the oxygen consumption mode was put in place in addition to the standard thermal mode within the OSU apparatus. For example, Tran and White [129] modified OSU with the aim to improve its accuracy during the investigation of the burning characteristics of wood. They employed four techniques in this regard: a) addition of oxygen consumption calorimetry, b) addition of an auxiliary heat flux meter, c) gas phase piloted ignition of the sample and d) a mass loss determining system using an injection shaft as a lever. According to Tran [128], the common finding was that the HRR measurements obtained by the OSU standard thermal mode are lower than those obtained by the OSU oxygen consumption method in the same apparatus, despite some differences in the way gas samples are taken. The oxygen consumption mode is based on the fact that the quantity of the net heat released by complete combustion per unit of oxygen consumed is almost constant over a wide range of materials (i.e. 13.1 kJ g^{-1}) [108,127]. It is through the measurement of the quantity of oxygen consumed that the amount of heat release is calculated. The heat release rate (HRR) measured through OSU and cone calorimeter were investigated and compared in some studies [127,131]. The general conclusion made by Tran [128] was that there is some agreement of the HRR results from these two different test methods when a modified OSU was used. However, the HRR results from these two test methods did

not agree in most cases according to Filipczak *et al*. [131], who used a single ply fibre glass reinforced epoxy thin composite materials.

Figure 2.8 Ohio State University heat release (OSU) apparatus. Reprinted from [126], with permission from Fire Testing Technology Limited

The other modification is, essentially for the determination of the smoke release rate. This is done by an optical method, with a white light source and a photo detector fitted above the exhaust stack, close to the thermopile [124]. Heat and smoke release rates are measured from the moment the specimen is injected into a controlled exposure chamber. Measurements are continued during the period of ignition and to such a time that the test is terminated.

Although the OSU heat release apparatus is a good tool for flammability testing, there are known limitations of this test method [126,132]:

- The heat and smoke release depend on several factors, such as: formation of surface char, formation of adherent ash, sample thickness and method of mounting.
- Heat release values are a function of the exposed tested area of the specimen.
- The test method is restricted to the specified specimen size of materials, products or assemblies. In the case of products, the test specimen (i.e. prototype) is representative of the product in actual size.
- At very high specimen heat release rates, flaming above the stack is possible, hence making the test invalid.

- There is no established general relationship between heat release rate values obtained from horizontally and vertically oriented specimens. Specimens that melt and drip in a vertical position are tested horizontally.
- Vertical testing remains a problem for testing thermoplastic materials in the OSU. Moreover, the reflector used for horizontal testing leads to serious reproducibility errors in the heat flux input to the horizontal sample.

Other analytical techniques, including thermogravimetric analysis (TGA), differential thermal analysis (DTA) and differential scanning calorimetry (DSC), are useful in broadening the understanding of the response of different materials under fire circumstances. Furthermore, TGA coupled with FTIR is also a useful tool for identifying gases being emitted during the thermal decomposition process. For example, TGA provides valuable information on char residue that remains after thermal degradation of a material, which helps to clarify some flame retardancy mechanisms that are based on the formation of a protective char and/or vitreous layer by different materials (i.e. intumescent flame retardants). DTA aids at giving the amount of heat liberated or absorbed by materials during any physical transition or chemical reaction. Consequently, it is useful in measuring heat capacity, provides kinetic data and gives transition temperatures. Similarly, DSC provides information on enthalpies of various transitions and chemical reactions [133].

2.4 Flammability of biofibres and biocomposites

The properties of biofibre (natural fibre) reinforced biocomposites have been reviewed by numerous authors[2,7,10,11,134]. This section is divided into three subsections, namely, flammability studies on biofibres, biopolymers and biofibre reinforced biopolymer composites.

2.4.1 Biofibres (natural fibres)

Biofibres are natural lignocellulosic composites composed of highly crystalline and spirally wound cellulose fibrils embedded in an amorphous hemicellulose, lignin, pectin and wax matrix [7]. They have rounded and elongated structures with hollow cross sections that are spread over the whole plant [135]. Generally, their composition consists of cellulose, lignin, hemicellulose, pectin and wax. Depending on their origin, they may be classified as plant, animal and minerals based fibres. The minerals based fibres (e.g. asbestos) are scarcely used

due to their negative effects on health. The examples of animal-based fibres are wool, hair and silk. Table 2.4 gives the list of important plant-based natural fibres, which may be classified according to the anatomical origin, such as: stem, leaf, wood and fruit. There is plenty of published literature on natural fibres and its composites, based either on thermoplastics, thermosets or biopolymers as composites matrices [3,6,8,9,135].

Biofibres offer numerous advantages, such as: energy efficiency, low cost, low density, high toughness, appreciable specific strength and biodegradability. However, they are hydrophilic in nature and have poor fire resistance. These disadvantages limit their application in outdoor panels (i.e. construction) and in areas that pose fire hazard to humans (i.e. aerospace and marine) [136].

Biofibres are non-thermoplastic materials and their thermal degradation temperatures are lower than their glass transition (T_g) and/or melting (T_m) temperatures. When natural fibres are exposed to fire or a high intensity heat source, they are subject to thermal decomposition and combustion, depending on the prevailing conditions. Conditions, such as: direct contact with air and physical, chemical and microbiological stimuli associated with heat release, can make the combustion of natural fibres possible. In addition, the intensity of heat stimulus, oxygen concentration and circulation around the combustion area and the intensity of the combustion process, influence the time to ignition (TTI) of natural fibres. The thermal degradation of plant fibres involves a number of processes: a) dehydration of adsorbed water molecules, b) depolymerisation and decarboxylation of cellulose chains with evolution of water to form dehydrocellulose, c) decomposition of the dehydrocellulose formed to yield char and volatiles, d) formation of levoglucosan (an intermediate nonvolatile liquid product) and e) decomposition of the levoglucosan to yield lower molecular weight and highly flammable volatiles, nonflammable volatiles and gases, tar and char [2,7].

Table 2.4 List of important biofibres. Reprinted from [6], Copyright 2008, with permission from Elsevier

Fibre source	Species	Origin
Abaca	*Musa textilis*	Leaf
Bagasse	–	Grass
Bamboo	(*>1250 species*)	Grass
Banana	*Musa indica*	Leaf
Broom root	*Muhlenbergia macroura*	Root
Cantala	*Agave cantala*	Leaf
Caroa	*Neoglaziovia variegata*	Leaf
China jute	*Abutilon theophrasti*	Stem
Coir	*Cocos nucifera*	Fruit
Cotton	*Gossypium sp.*	Seed
Curaua	*Ananas erectifolius*	Leaf
Date palm	*Phoenix Dactylifera*	Leaf
Flax	*Linum usitatissimum*	Stem
Hemp	*Cannabis sativa*	Stem
Henequen	*Agave fourcroydes*	Leaf
Isora	*Helicteres isora*	Stem
Istle	*Samuela carnerosana*	Leaf
Jute	*Corchorus capsularis*	Stem
Kapok	*Ceiba pentranda*	Fruit
Kenaf	*Hibiscus cannabinus*	Stem
Kudzu	*Pueraria thunbergiana*	Stem
Mauritius hemp	*Furcraea gigantea*	Leaf
Nettle	*Urtica dioica*	Stem
Oil palm	*Elaeis guineensis*	Fruit
Piassava	*Attalea funifera*	Leaf
Pineapple	*Ananus comosus*	Leaf
Phormium	*Phormiumtenas*	Leaf
Roselle	*Hibiscus sabdariffa*	Stem
Ramie	*Boehmeria nivea*	Stem
Sansevieria (Bowstring hemp)	*Sansevieria*	Leaf
Sisal	*Agave sisilana*	Leaf
Sponge gourd	*Luffa cylinderica*	Fruit
Straw (Cereal)	–	Stalk
Sun hemp	*Crorolaria juncea*	Stem
Cadillo/urena	*Urena lobata*	Stem
Wood	(*>10,000 species*)	Stem

These processes occur during the course of the three stages of heat action on natural fibres and natural polymers, as detailed by Kozlowski and Wladyka-Przybylak [12], i.e. *preliminary flameless stage*, followed *by main flame stage* and then the *final flameless stage*. Generally, these stages may be briefly described as follows:

Preliminary stage involves the dehydration (up to 105 °C) and release of liquid and volatiles and further heating of natural fibre leads to their decomposition temperature. At this

stage, reactions are slow and endothermic. Above 105 °C, the fibre components begin to decompose with gaseous products being released within the temperature range of between 150 to 200 °C. The bonds between natural fibre components become weak.

The *main flame stage* includes ignition of thermal decomposition products, flame spread by combustible gases and increase in heat release and mass loss rates. This is an active process of decomposition occurring in the temperature range of between 260 to 450 °C.

The *final flameless stage* includes the slow burning of residue and the formation of ash from the remaining matter, which occurs above 500 °C.

The mechanism of thermal degradation of plant fibres may be similar from a thermogravimetric analysis point of view. However, the flammability behaviour of plant fibres is different. This is motivated by factors, such as: chemical composition, fine structure, degree of polymerization and fibrillar orientation. The decomposition of the major constituents (cellulose, hemicellulose and lignin) making up natural fibre, may be described as follows:

Lignin: Lignin begins to decompose in the temperature range of between 160 to 400 °C. At lower temperatures, relatively weak bonds break, whereas at higher temperatures phenols result from cleavage of ether and carbon-carbon linkages. This results into more char than in the case of either cellulose or hemicellulose. Lower lignin content in natural fibre contributes to higher decomposition temperatures but lower resistance to oxidation, which is provided by the aromatic structure of lignin.

Hemicellulose: The decomposition of this low molecular weight polysaccharide begins at 180 °C, releasing more incombustible gases and fewer tar substances. Released gases usually contain 70% of incombustible CO_2 and about 30% of combustible CO. Depending on the availability of oxygen, subsequent reactions may be exothermic or endothermic. Between 200 and 260 °C, exothermic reactions start and are characterized by increased emission of gaseous products of decomposition, release of tar substances and the appearance of local ignition areas of hydrocarbons with low boiling points. No spontaneous ignition at these temperatures may occur, but under favourable conditions ignition can start from a pilot flame.

Cellulose: Cellulose decomposes in the temperature range of between 260 to 350 °C, primarily yielding flammable volatiles and gases, non-combustible gases, tars and some char. The thermal degradation of cellulose can be catalysed in the presence of water, acids and oxygen. Consequently, natural fibres turn brown and a carbonaceous char (pyrophoric carbon) is formed. The reaction below 260 °C is still low. High contents of cellulose are likely to increase flammability of a fibre, whereas high contents of lignin are likely to reduce it [2,7,12].

The fine structure of the fibre also plays a role in influencing the flammability characteristics of a fibre. Fibres rich in cellulose, have high levels of crystallinity. This results in high levels of levoglucosan during pyrolysis, thereby leading to increased flammability. Additionally, this increased level of crystallinity, requires more activation energy (E_a) of pyrolysis of cellulose in order to decompose the crystalline structure, consequently leading to higher ignition temperatures [2,137].

The degree of polymerization and fibrillar orientation also dictate the fibre flammability. Increased degree of polymerization and orientation results in decreased pyrolysis. Fibrillar orientation controls the quantity of oxygen that can penetrate into the fibre, thus the higher the orientation, the lower the permeability of the fibre to oxygen [2,137]. In their review on the flammability of natural fibre-reinforced composites and strategies for fire retardancy, Chapple and Anandjiwala [2] made an important conclusion that, from a flammability perspective, natural fibres with low crystallinity, high degree of polymerization and high fibrillar orientation will be an ideal choice to use as reinforcement in composite materials.

The flammability properties of natural fibres were reported [5,18,35,102,136,138-141] and mostly the biofibres were compounded with different polymer matrices [i.e. poly(lactic acid) (PLA), polypropylene (PP) and epoxy resin] in the presence of flame retardants. In some studies, fibres alone were treated with flame retardants and characterized. The different flame retardant additives used for lignocellulosic materials, include: ammonium salts of phosphoric acid (i.e. melamine phosphate, ammonium polyphosphate), boric acid, zinc chloride, zinc borate, salts of sulphuric acid, vermiculite, magnesium hydroxide, aluminumhydroxide, expandable graphite and pentaerythritol (as the carbon source for intumescent systems) [18,92,136,139-141]. The preparation of flame retardant-treated natural fibres is achieved in different ways, including: a) impregnation of fibres with a solution of the flame retardant, b) incorporation of the flame retardant into the adhesive system, c) surface treatment of the fibres and d) mixing of the fibres with the flame retardant before the addition of an adhesive (e.g. melamine urea formaldehyde condensate, pea protein) [18,136,140].

Grexa and Lübke [18] and Grexa *et al*. [136] reported on the flammability of lignocellulosic particleboard using a cone calorimeter. In both studies, samples were conditioned to equilibrium at 55% relative humidity (RH) and 23 °C prior to testing. In the first study [18],

the authors looked at the effect of magnesium hydroxide loading and that of other flame retardants (i.e. monoammonium phosphate (MAP), aluminum hydroxide and boric acid), whereas in the second study [136], they dealt with an intumescent system for wood-based panels. The RHR (see Figure 2.2, section on metal hydroxides), average specific extinction area of smoke and the rate of smoke release (Figure 2.9) were generally improved with increasing amount of magnesium hydroxide flame retardant (type A) (where A1, A2 and A3 are 8, 15 and 24 wt.% respectively). In addition to smoke production improvement, carbon monoxide yield was also improved due to this flame retardant [18].

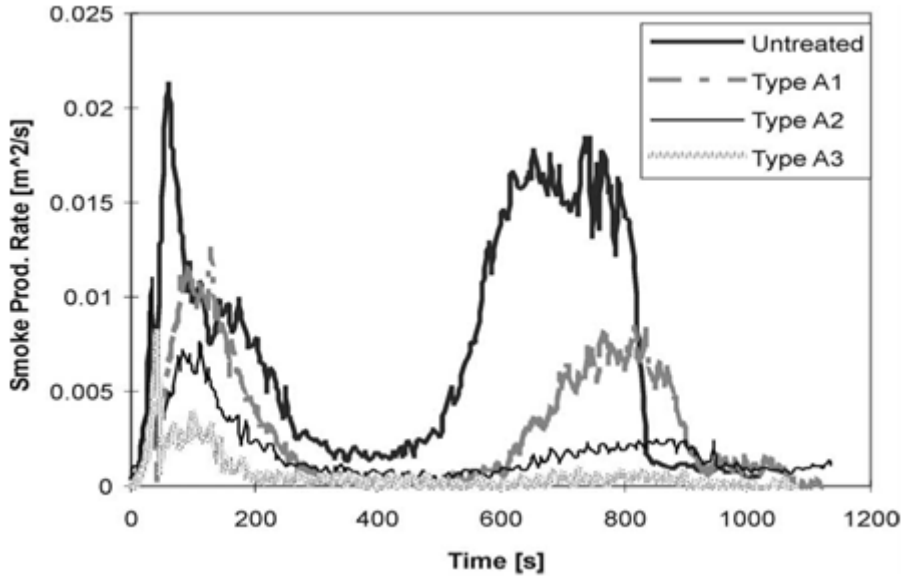

Figure 2.9 Smoke production rate versus time for non-treated and magnesium hydroxide-treated particleboard. Reprinted from [18], Copyright 2001, with permission from Elsevier

Furthermore, when different flame retardant combinations [i.e. monoammonium phosphate (MAP) 17 wt.% + aluminium hydroxide 8 wt.% (type B) and MAP 20 wt.% + boric acid 5 wt.% (type C)] were used and compared, the authors concluded that the combination of MAP/boric acid (type C) was the most effective system. As seen in Figure 2.10, the type C flame retardant system did not only lower the RHR, but also eliminated the second peak and shortened the time of burning with respect to other modifications, including magnesium hydroxide. The mass loss was reduced for the flame retardant treated systems, especially type C (i.e. from 72% to 17%), but the mass loss rate was almost the same for all the studied materials. In this study, the authors distinguished between the yield of CO and the production of CO and concluded that the stronger retardant effect may give better results on the total CO

production than the weaker retardant effect, even though the CO yield per burned portion of the pure material increased [18].

In the second study [136], ammonium phosphate and expandable graphite intumescent flame retardant systems formed a protective char layer on the surface of wood. Similar to the previous study [18], the RHR was reduced by between 55-66% over the untreated material. The time to ignition (TTI) remained unchanged with the presence of the flame retardant and theauthors concluded that the flammable particles of wood on the surface were not directly protected. The intumescent flame retardant system, based on expandable graphite, showed better flammability performance at low loadings than the phosphate-based systems, which required high contents (i.e. 30 wt.%). This was explained in terms of the difference in the presence of the expanding charring foam layer on the pyrolysis surface. The other important aspect is that CO emissions increased for expandable graphite at the lowest loadings and increased noticeably for the phosphate-based system at 13 wt.% and higher.

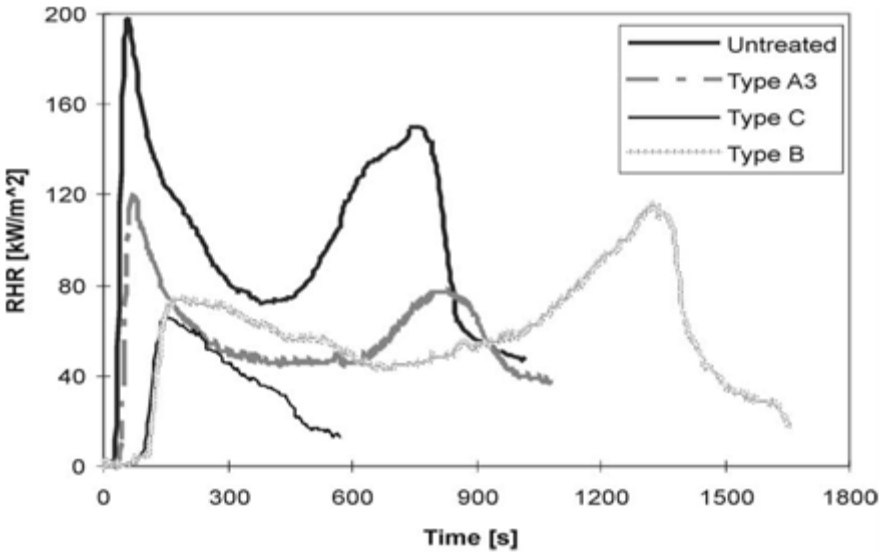

Figure 2.10 HRR versus time for untreated and flame retardant treated particle board with the use of different flame retardant combinations. Reprinted from [18], Copyright 2001, with permission from Elsevier

The flammability properties of flax fibres were investigated by Lazko *et al*. [140]. They employed a wet process to prepare the flame retardant insulating agro materials made of short flax fibres with pea protein binder. It was reported that the incorporation of different flame retardants (i.e. aluminum hydroxide (ATH), zinc borate (ZB), melamine phosphate (MMP) and melamine borate (MMB)), did not interfere with the expanded structure and the open porosity

of the lignocellulosic matrix. This was shown by macroscopic and SEM results (see Figure 2.11). Two conclusions arose from these: a) the appropriate choice of process parameters allowed a coherent set of materials with comparable morphologies and densities and b) the use of pea protein binder, permitted all flame retardants to be fixed firmly and permanently onto the flax fibre matrix. The presence of FRs lowered the flexural strength by 50% and the flexural modulus by 65% (see Table 2.5), except for ATH, for which the properties remained at the same levels as the reference. Different flax fibre flame retardant treatments led to lowered peak and total HRR (especially for ZB, MMP and MMB) relative to the untreated short flax fibres. Similar to the studies by Grexa *et al*. [136], the TTI remained unchanged including the resistance to ignition.

Table 2.5 Density and flexural properties of non FR treated short flax fibres with pea protein binder (i.e. reference) and FR treated materials. Reprinted from [140], Copyright 2013, with permission from Elsevier

Composition	Density [g/cm^3]	Flexural strength [MPa]	Flexural modulus [MPa]
Reference	0.07 ± 0.01	0.34 ± 0.02	14.4 ± 2.5
ATH 20%	0.09 ± 0.01	0.39 ± 0.03	15.8 ± 6.6
ZB 20%	0.07 ± 0.01	0.18 ± 0.04	5.3 ± 1.9
MMP 20%	0.08 ± 0.01	0.21 ± 0.03	5.8 ± 2.6
MMB 20%	0.07 ± 0.01	0.15 ± 0.03	4.2 ± 1.4

In their study of sawdust- and rice husk-filled polypropylene (PP) composites, Sain *et al*. [102] used magnesium hydroxide, boric acid and zinc borate as flame retardant agents. The composites were melt-blended and then injection moulded in the presence of maleated PP coupling agent. It was reported that magnesium hydroxide (i.e. 25 wt.%) effectively reduced the flammability of natural fibre/PP composites by 50% when tested using horizontal burning and LOI tests. The partial replacement of magnesium hydroxide with either boric acid or zinc borate (i.e. 5 wt.%) did not show synergy, but rather the retarding effect of the different flame retardants. A marginal decrease in the mechanical properties of flame retardant natural fibre composites when compared to non-flame retardant composites was reported. This was attributed to the poor compatibility of the flame retardants with the polymer. However, better mechanical properties were observed for these composites, with respect to neat PP.

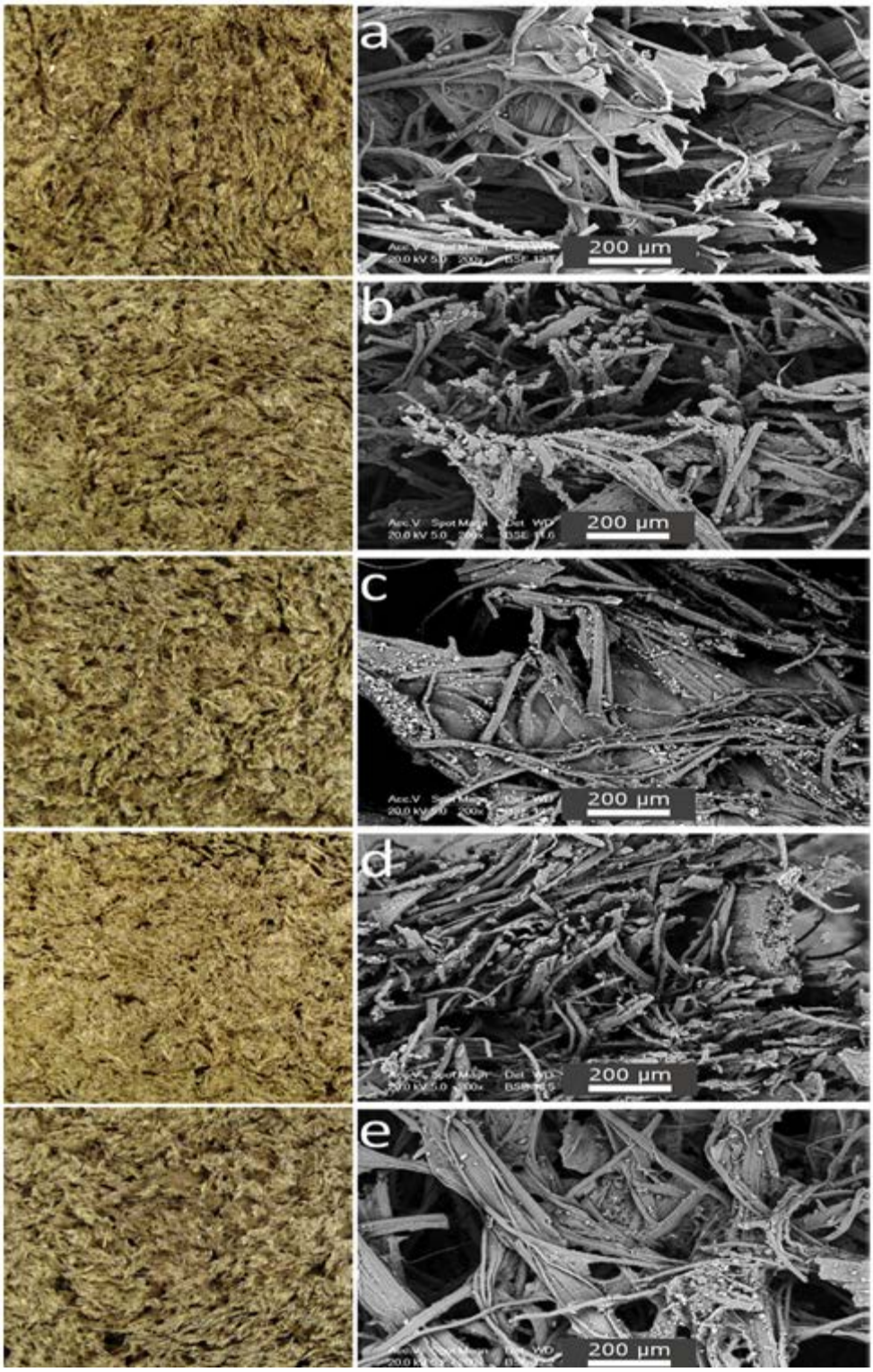

Figure 2.11 Macroscopic and SEM pictures (x200) of a) reference (untreated flax fibre), and flame retardant treated flax (fibre and pea protein binder) containing 20 wt.% of b) ATH, c) ZB, d) MMP and e) MMB. Reprinted from [140], Copyright 2013, with permission from Elsevier

A large number of studies focused on the FR properties of natural fibre based fabrics [138,139142-155]. Chai *et al*. [138] used flax-based fabrics reinforced epoxy resin and compared them with glass fibre reinforced epoxy composites of similar fabric architecture. These composite panels were prepared by a resin transfer moulding (RTM) process without any FR. The group reported, from cone calorimetry, horizontal and vertical burning tests that the flax fibre samples ignited earlier, released more heat overall, had an increased time to extinguish and increased smoke production rate (SPR) when compared to their glass fibre counterparts. This was attributed to a number of reasons, amongst others that flax fibres are themselves susceptible to ignition and combustion, that they provided additional fuel at a lower HRR, that fibres combusted exothermically and that they burned more vigorously during combustion.

Additionally, flax fibre samples showed deformation during combustion while glass fibre samples retained their integrity. It was postulated that the bulging and delamination effect of the flax fibre composites (see Figure 2.12) may be due to the internal or external forces applied to the fibres, thereby causing buckling. The authors, therefore, suggested further investigations in order to understand the mechanisms and behaviour that govern the combustion of natural fibre reinforced composites.

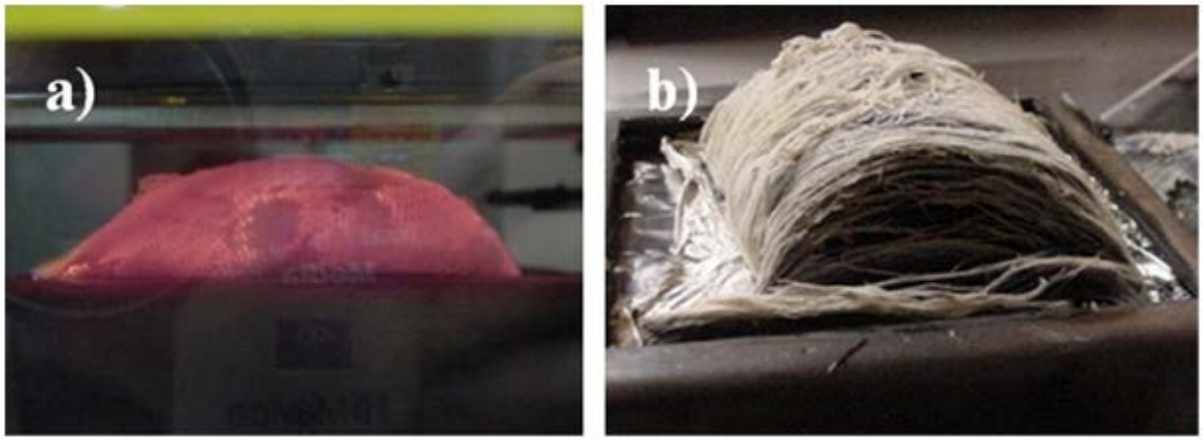

Figure 2.12 Images of (a) flax twill weave in a cone calorimeter, and (b) a burnt flax unidirectional fabric sample. Reprinted from [138], Copyright 2012, with permission from Elsevier

Kandola and Horrocks [139] looked at the nonwoven cores of flame retardant cellulose/regenerated cellulose (viscose and cotton fibres) with intumescent melamine and

phosphate-based chemicals. They investigated the mass loss and thermal barrier properties of these systems. A large quantity of char formation was observed above 500 °C. This formed char was resistant to oxidation and had better thermal insulative properties. The presence of intumescent FR led to increased activation energy (E_a) values for the full char development stage of FR/cellulosic fibre composites and reduced the thermal conductivity values. According to the authors, this revealed the existence of an interaction between different FRs and the fibre substrate and improved thermal barrier properties. Flambard *et al*. [150] used wool, flax and blends made of poly(p-phenylenediamine terephthalamide) (PPTA) with wool in textile materials for use in public transportation (i.e. buses). They studied the flame retardancy properties of these materials. The group concluded that these natural fibres can be used to manufacture fabrics that are acceptable for use in seats for transportation when they are combined with a specific flame retardant treatment or in combination with high performance fibres (wool/PPTA). The advantages offered by these materials included: good flammability and mechanical properties (abrasion and cutting resistance), dyeability and ultraviolet (UV) resistance, biodegradability and no technological problems during manufacture.

In some studies, fabric materials were generally surface coated with either commercial or laboratory synthesized flame retardants [142,149,151-155]. Abou-Okeil *et al*. [142], Nguyen *et al*. [152] and Yang *et al*. [155] developed environmentally-friendly halogen-free and formaldehyde-free FRs which were subsequently applied to cotton fabrics and evaluated for flammability performance. These were methacryloyloxyethylorthophosphorotetraethyl diamidate (MPD) [142], novel halogen and formaldehyde free flame retardants (NeoFR) [155] and phosphorus-nitrogen bond (diethyl 4-methylpiperazin-1-ylphosphoramidate) (CN-3) [152] FR compounds. In the first two studies [142,155], the performance of the novel FRs was compared with that of a commercial flame retardant (Pyrovatex) and it was concluded that the novel FRs performed better in terms of flammability and durability than the latter. NeoFR was said to have played the role of an intumescence on the flame retarding mechanism of cotton. This was due to its ability to form char. Higher tensile strength and elongation were also reported [155]. Similarly, better flame retardant properties were observed by Nguyen *et al*. [152] when print-on and twill fabrics were treated with a CN-3 flame retardant. At certain loadings, the char lengths of the FR treated fabrics were less than 50% of the original fabric with no after-flame and after-glow times. The LOI values increased from 12 vol.% (print cloth) and 18 vol.% (twill) to 28 vol.% and 29-31 vol.%, respectively. In general, the improvement

in the flammability properties of cotton fabrics emphasized the role played by char formation for treated samples, which prevented them from being completely burnt.

Extensive work on the development of novel systems, based on a sol-gel process for cotton-based fabrics was done by Alongi and co-workers [143-148]. Flame retardant finishing systems were developed in the presence of different FR compounds. The FRs were phosphorus-based compounds [145], metal alkoxide precursors (e.g. tetraethylorthosilicate, titanate, zirconate and aluminium isopropylate) [146], polyhedral oligomeric silsesquioxane (POSS) and bohemite nanoparticles [144] and compounds with smoke suppressant features (e.g. zinc oxide, zinc borate) or flame retardant properties (e.g. 9-oxa-10-phosphaphenanthrene10-oxide) [143]. The fabric exhibited improved flammability and thermooxidative stability. This was attributed to several factors, including: the homogeneous distribution and dispersion of FR additives on/and in between the cotton fibres [145], the morphology of the inorganic coatings on the fabric surface, the water content in the treated textiles [146] and the ability of the nanoparticles to release water at high temperatures, thereby forming a ceramic barrier that was able to delay the cellulose ignition and lower the heat release and corresponding rate [144]. The homogeneous distribution and fine dispersion of POSS at nanometric level [144] is said to have modified the degradation profile of cotton by playing a protective role on the thermo-oxidation of fabrics. During thermal decomposition, in the presence of POSS nanoparticles, a carbonization mechanism was favoured and the final char residue increased which slowed down the overall thermo-oxidation kinetics and hence improved the properties. The TTI was increased and the HRR was reduced by up to 40%. Based on LOI and cone calorimetry test results, nanoparticles show better performance in the flammability of cotton than the other flame retardant used. On the other hand, the major observation from the cone calorimetry tests was that in the presence of zinc-based smoke suppressants, the release of CO and CO_2 was remarkably reduced, relative to the fabrics treated with silica alone [143]. It was found that the combination of ZnO and silica showed a joint effect in reducing the release of these gases when compared to combinations of silica with phosphorus or boron based flame retardants.

The current published work by Alongi and co-workers explored the use of whey protein (folded and unfolded structures) [148] and deoxyribonucleic acid (DNA) powder from herring sperm [147] on cotton fabrics. This was achieved by deposition of whey protein on cotton fabrics and impregnation whereby cotton fabrics were dipped in a DNA solution for sometime, according to the studies. The samples so treated were assessed for their thermo-oxidative stability and

flammability characteristics. It was found that the presence of protein coating [148] significantly sensitized the degradationof cotton, but led to very high final residues. These protein-treated cotton materials were shown to have increased the total burning time as well as reducing the burning rate. The authors concluded that the system may represent a novel and promising eco-friendly finishing treatment for cellulosic substrates. Additionally, only a minimum of 10 wt.% DNA [147] loading on cotton was necessary to reach the flame-out of cotton when a methane flame was applied and that 19 wt.% DNA was able to show resistance to an irradiation heat flux of 35 kW m^{-2}. In general, this cotton/DNA sample did not burn at increased loadings, but pyrolysed due to the presence of DNA molecules that absorbed heat and released inert gases. It was concluded that although these materials displayed promising flame retardant and suppressant properties, the design of DNA-based FR needs some careful consideration and further investigation. This was due to the poor durability and resistance to washing treatments of materials, according to the ISO 6330 standard.

2.4.2 Biopolymers

Biodegradable polymer matrices are those materials with the ability to decompose into biomass, carbon dioxide, inorganic compounds, methane or water due to enzymatic action by micro-organisms when disposed-off into landfills [2,5,7]. The classification of biodegradable polymers is illustrated in Figure 2.13. They are broadly classified as natural or synthetic depending on their origin. Furthermore, they are sub-classified into those from renewable resource, the chemically synthesized, microbial synthesized and the blends systems [6,9]. The class of chemically synthesized biodegradable polymers may be further subdivided into those that are from biotechnology (i.e. polyacids, e.g. PLA) and the ones from petrochemical products (i.e. polycaprolactone, PCL, aliphatic and aliphatic-aromatic polyesters, polyester amides) [2,5,6,7,9]. These biopolymers are hydrophilic polyesters that absorb moisture. They are characterized by higher cost and lower performance than conventional plastics. Their application is mainly in the packaging industry and other applications that need low strength. Of these biopolymers, PLA is currently the most studied, both in blends and biocomposites reinforced with natural fibres [8,156,157].

Different biopolymers have been used as matrices in the investigation of various composite materials. These were compounded with additives, fillers or reinforcements. The broader goal of this was to improve their performance when compared to conventional polymeric materials,

in order to lower the market cost of their final products and to broaden their range of applications to high performance polymer sectors (including aerospace, marine and electronics). The biopolymers studied include: poly(lactic acid) (PLA), polycaprolactone (PCL), starch, cellulose, poly(3-hydroxybutyrate-co-3-hydroxyvalerate) (PHBV), poly(butylene adipate-co-terephthalate) (PBAT), poly(trimethylene terephthalate) (PTT) and polyether block amide polymers. Different properties of biopolymers, such as: mechanical, thermal, biodegradability and flammability performance, were studied [156-160].

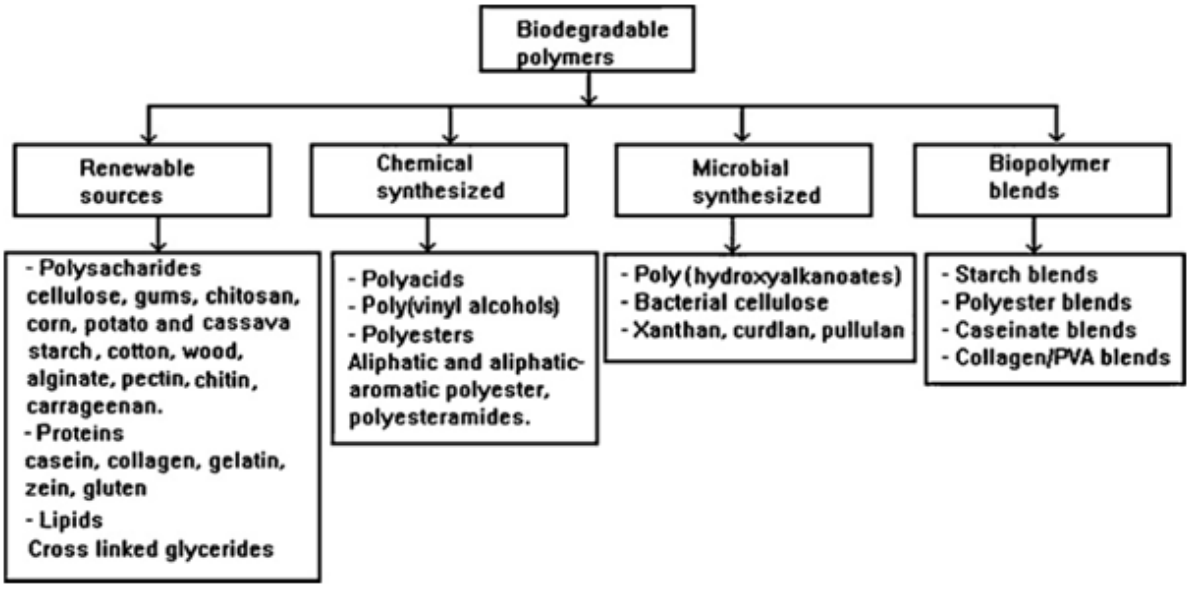

Figure 2.13 Classification of biodegradable polymers and their nomenclature. Reprinted from [9], Copyright 2009, with permission from Elsevier

A wide range of additives or reinforcements are used to fill biopolymers. The additives or reinforcements may be inorganic, organic, synthetic or natural in nature. These may include natural fibres (i.e. kenaf, flax, hemp, wool, cellulose, coconut fibre, rice husk and kraft lignin), clays, silica, metal oxides and hydroxides, phosphate compounds and graphite. The preparation of reinforced biopolymer composites and/or blends is achieved through different methods. They include: melt blending, extrusion, compression moulding and injection moulding. Of all the properties of filled biopolymer composites investigated, flammability performance is of recent research interest [21,24,159-161].

Flame retardant treated PLA composites have been investigated more than those of other biopolymers [21,24,159-161]. Ke *et al*. [21], Zhan *et al*. [161] and Zhu *et al*. [24] prepared

PLA/flame retardant composites by a melt blending/mixing method. In these studies, ammonium polyphosphate (APP) [21,24], hyperbranched polyamine charring agent (HPCA) [21], expandable graphite (EG) [24] and spirocyclic pentaerythritol bisphosphorate disphosphoryl melamine (SPDPM) [161] were used to formulate different flame retardant systems with PLA. HPCA and SPDPM were synthesized and characterized by the authors before incorporation into the PLA composites. Techniques that include UL-94, LOI, TGA, MCC (PCFC), SEM and cone calorimetry were employed, amongst others, for various tests on the composites.

These studies reported that the intumescent flame retardant (IFR)/PLA showed improved flame retardancy and anti-dripping performance. It was found that different combinations of APP/HPCA (3:2) at 30 wt.% [21], APP/EG (1:3) at 15 wt.% [24] and SPDPM at 25 wt.% [161], exhibited LOI values of 36.5 [21,24] and 38 [161] vol.%, as well as UL-94 V-0 rating (see Table 2.6). Additionally, Zhu et al. (2011) indicated that APP/EG (1:3) showed better performance than APP and EG alone. As shown in Figure 2.14 for specimens after an LOI test, the presence of different IFR additives led to the formation of charred layers. Pure PLA does not form any char and it decomposes almost completely.

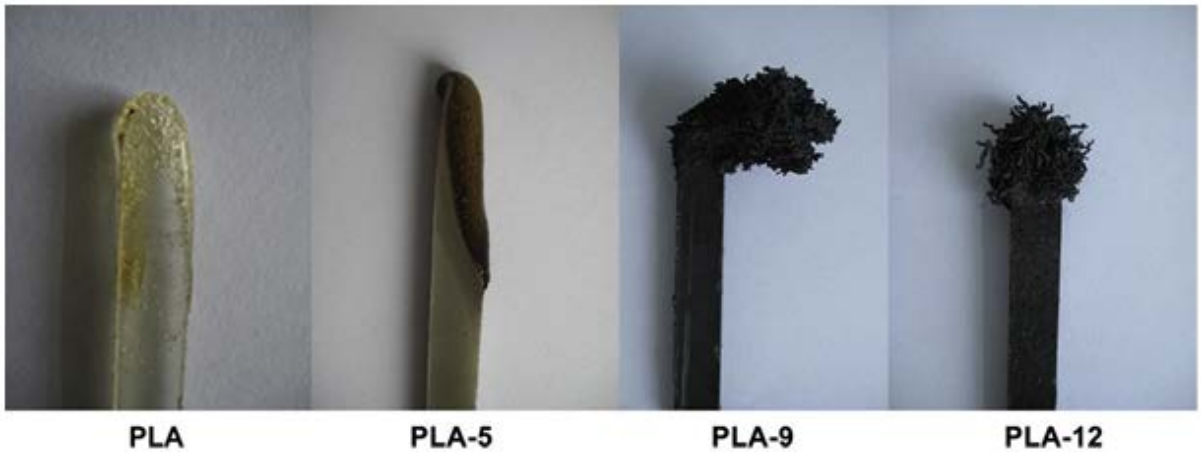

Figure 2.14 Photographs of PLA specimens after LOI tests. Reprinted from [24], Copyright 2011, with permission from Elsevier

Table 2.6 Composition of the samples and the flame retardancy of the composites Reprinted from [21], Copyright 2010, with permission from Elsevier

Sample	PLA	APP	HPCA	t1 + t2[a] (s)	LOI vol.%	UL-94 rating	Flaming dripping
PLA-1	100	–	–	–	21	Fail	Yes
PLA-2	70	30	–	10 + 5	33	V-2	Yes
PLA-3	70	20	10	0 + 1	34	V-0	No
PLA-4	70	18	12	0 + 1	36.5	V-0	No
PLA-5	70	15	15	0 + 2	28	V-0	No
PLA-6	70	12	18	0 + 13	27.5	V-1	No
PLA-7	70	10	20	1 + 14	26.5	V-1	No
PLA-8	70	–	30	–	22	Fail	Yes
PLA-9	75	15	10	0 +1	28.5	V-0	No
PLA-10	80	12	8	0 + 1	26.8	V-0	No
PLA-11	85	9	6	0 + 1	26.2	V-0	No
PLA-12	90	6	4	0 +3	25.2	V-2	Yes

[a] t1: the burning time after first ignition, t2: the burning time after second ignition.

This phenomenon of charred layer formation is further emphasized by the char residue as seen from the TGA data (see Figure 2.15). Furthermore, the cone calorimetry and microscale combustion calorimetry data were indicative of the improved fire retardancy of PLA in the presence of FR agents. This was concluded from the reduction in time to ignition (TTI), heat release rate (HRR), peak HRR, average HRR, total heat release (THR) and mass loss rate (MLR) [21,24] (see Table 2.7), and the reduction in heat release capacity (η_c) (HRC), total heat release (h_c) and the temperature at maximum pyrolysis rate (T_{max}) [161] (see Figure 2.16). From these studies, the key conclusion made by the authors is based on the efficiency and synergistic effect between different intumescent flame retardant agents. This effect led to the formation of an intumescent protective charred layer and a change in the degradation process of PLA as observed by Zhan *et al*. [161]. On the other hand, Ke *et al*. [21] arrived at the conclusion that PLA/APP/HPCA can form a char layer containing a phosphorus-oxygen-carbon (P-O-C) structure. This layer had, most possibly, hindered the transfer of heat and combustible gas, resulting in good flame retardancy without melt-dripping.

Table 2.7 Part data recorded in cone calorimeter experiments. Reprinted from [21], Copyright 2010, with permission from Elsevier

Sample	TTI (s)	Av-HRR (kW/m^2)	PHRR (kW/m^2)	TTPH (s)	Av-MLR (g/s)	THR (MJ/m^2)
PLA	60	161	272	203	0.098	65.1
PLA-2	81	125	228	146	0.072	48.6
PLA-4	65	65	153	98	0.038	35.6

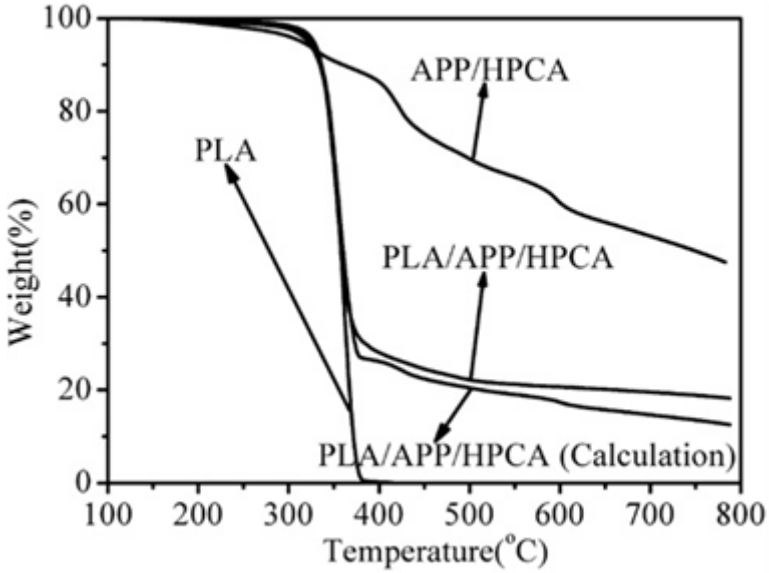

Figure 2.15 TGA curves of PLA, APP/HPCA, PLA/APP/HPCA, PLA/APP/HPCA (Calculation). Reprinted from [21], Copyright 2010, with permission from Elsevier

Zhu *et al*. [24] proposed a possible flame retardancy mechanism of PLA/APP/EG composites in which the synergism between APP and EG is explained. Figure 2.17 illustrates the phenomenon. This is explained thus: EG expands and migrates with the flow of PLA/APP. This is followed by the decomposition of APP which produces polyphosphoric and ultraphosphoric acids. These compounds catalyse PLA to form char residue. During the decomposition of EG and APP, incombustible gases, such as: SO_2, CO_2, NH_3, and H_2O are released, which diluted the fuels that originate from the degradation fragments. The flow of PLA/APP degradation products (i.e. polyphosphate) provides adhesion between the graphite flakes, consequently leading to continuous, dense and sealed char layers. These layers inhibit further degradation of PLA, APP and EG and slow down the volatilization of polyphosphoric and ultraphosphoric acids at high temperatures.

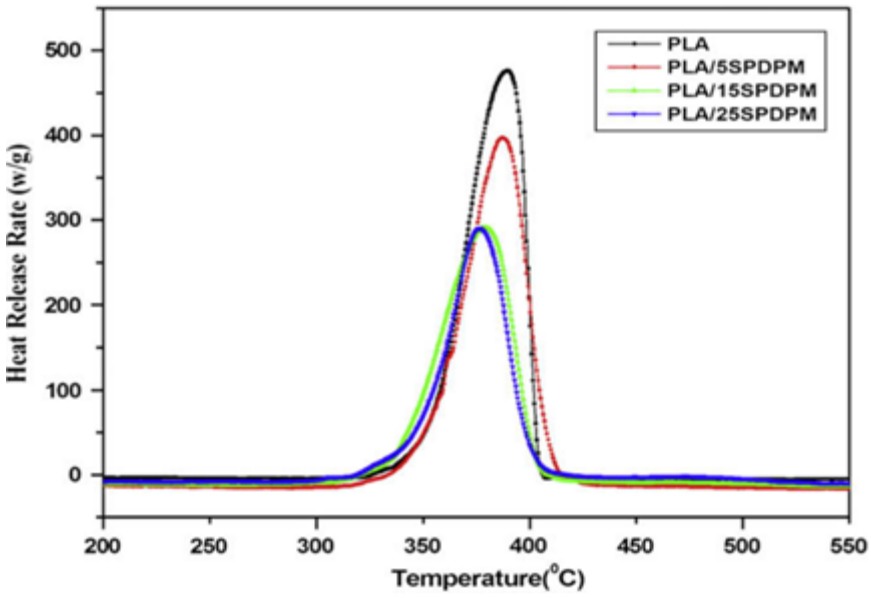

Figure 2.16 The HRR curves of PLA and its composites at 1 K/s heating rate. Reprinted from [161], Copyright 2009, with permission from Elsevier

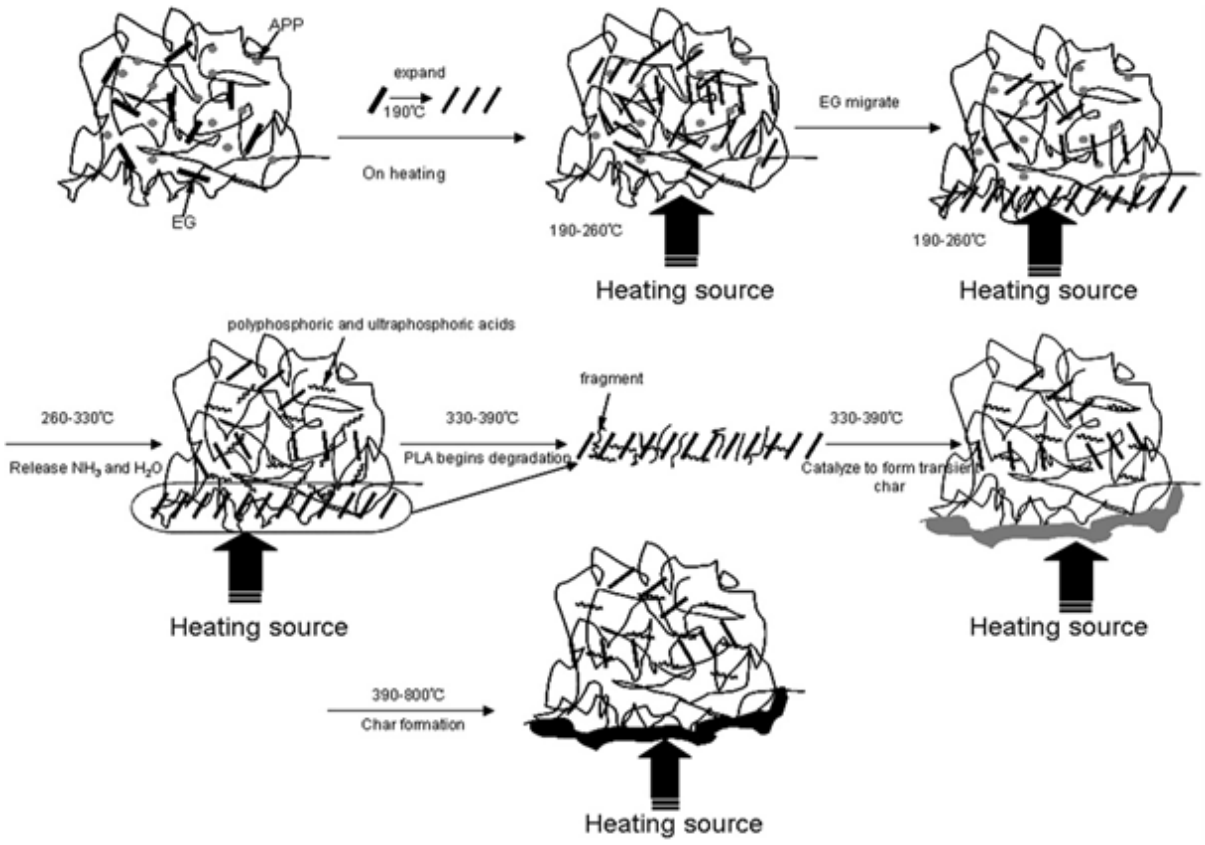

Figure 2.17 Possible flame retardant mechanism of PLA/APP/EG composite. Reprinted from [24], Copyright 2011, with permission from Elsevier

In another study, flame retardant biopolymers containing aluminium-based compounds, melamine (MA) and organoclays were investigated for their thermal, mechanical and flammability performances. These biocomposites were prepared by melt-compounding and extrusion methods. The matrices used were PLA [158-160] and polyether-block-amide (PEBAX) [162] biopolymers. In these studies, it was reported that the incorporation of flame retardant additives, such as: ammonium hypophosphite (AHP) at 30 wt.% [160], boehmite alumina at 5 wt.% [159], ATH and organoclay at 50 wt.% and 5 wt.%, respectively [158] and a maximum loading of 30 wt.% MA and 6 wt.% organoclay [162] promoted carbonization of the biopolymers. This was supported by the increased char residues of the composites as seen in TGA studies (Figure 2.18). An additional contribution to carbonization due to the presence of organoclays was also reported [158,162]. Consequently, this contributed to improved fire resistance performance of filled biopolymers, as reported from LOI, UL-94, cone calorimetry and MCC tests used in these studies.

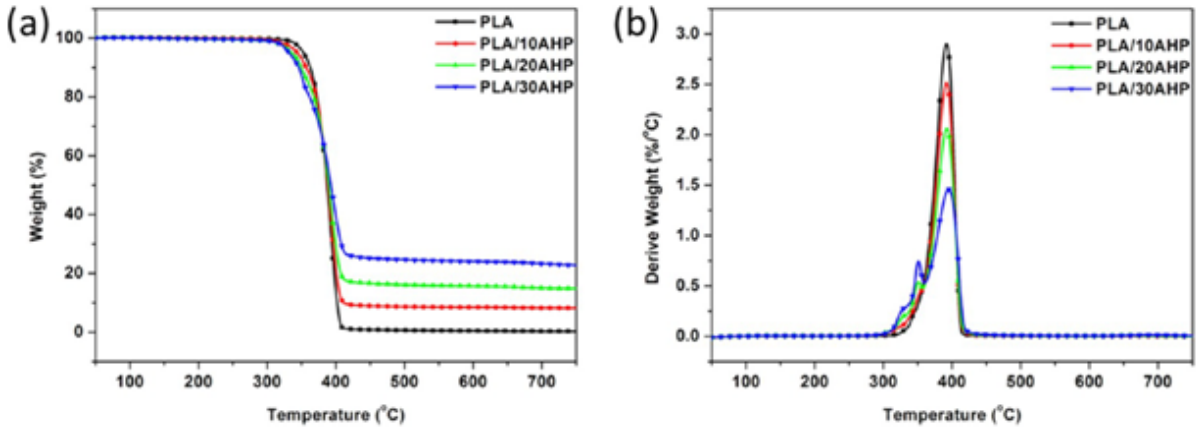

Figure 2.18 TGA and DTG curves of PLA and FR-PLA composites under nitrogen condition. Reprinted from [160], Copyright 2012, with permission from American Chemical Society

According to Cheng *et al.* [158], the addition of organoclay into a PLA/ATH system, led to further thermo-oxidative stability and the presence of organoclay and ATH increased the degradation activation energy of the composites. The authors proposed that during the UL-94 test, layered silicates and a high content of ATH in PLA were integrated to form a compact insulator on the burning surface, thus lowering the melt dripping. It was further reported that at high loadings of the conventional flame retardant ATH (i.e. 50 wt.%), the PLA composites were brittle, but improved with the addition of organoclay. On the other hand, after a series of tests, based on solid state nuclear magnetic resonance (NMR) (^{13}C and ^{27}Al) and TGA-FTIR,

Hoffendahl *et al*. [162] established the possible flame retardancy mechanisms of PEBAX/MA with and without organoclay. They concluded that MA acted by a gas phase mechanism through different routes including fuel dilution, a cooling effect due to endothermic processes and the formation of free radicals that interacted with the flame. The incorporation of organoclay to PEBAX/MA, resulted in the formation of a char layer, adding a condensed phase mechanism to the flame retardancy mechanisms.

The mechanical properties of these flame retardant PLA biocomposites were also reported. Tang *et al*. [160] reported a decreased tensile strength and elongation-at-break with the incorporation of ammonium hypophosphite (AHP) from 10 to 30 wt.% (Figure 2.19). This reduction was attributed to the rigid nature of the AHP particles, especially on the elongation-at-break. On the other hand, Das *et al*. [159] reported improved mechanical properties of PLA/Boehmite alumina (BAl) (with a maximum loading of 5 wt.%) composites, as seen in Table 2.8. This observation was explained as being due to an optimum uniform dispersion of BAl in the PLA matrix, good filler/matrix interaction and the high aspect ratio of the filler. Consequently, this led to increased rigidity and effective stress transfer between the matrix and the filler. The increased rigidity was further emphasized in the dynamic mechanical analysis (DMA) data, where the storage modulus increased inconsistently with BAl loading. The explanation was that a high D content of the neat PLA, made it less rigid and inconsistently increased the modulus.

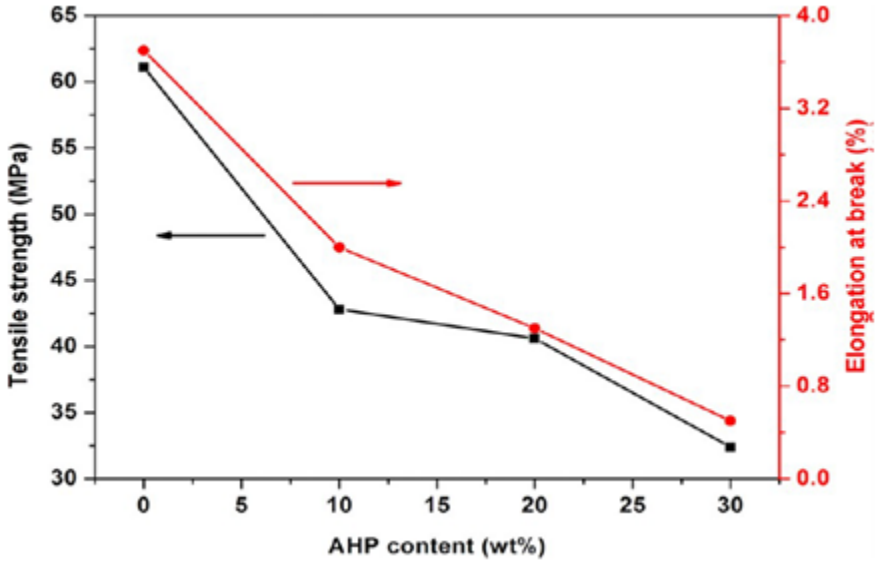

Figure 2.19 Effect of AHP loading on the mechanical properties of FR/PLA composites. Reprinted from [160], Copyright 2012, with permission from American Chemical Society

Table 2.8 Mechanical properties of the PLA/BAl composites. Reprinted from [159], Copyright 2013, with permission from American Chemical Society

Sample identification	Tensile strength (MPa)	Standard deviation	Tensile modulus (GPa)	Standard deviation	Elongation at break (%)	Standard deviation
PLA BAl 0	74.4	3.2	3.0	0.2	6.3	0.2
PLA BAl 1	84.4	2.6	3.3	0.06	5.5	0.1
PLA BAl 2	97.5	5.3	3.2	0.09	5.4	0.7
PLA BAl 3	116.4	7.8	3.1	0.1	6.1	0.5
PLA BAl 4	113.4	4.4	3.4	0.04	5.2	0.3
PLA BAl 5	107.9	8.2	3.3	0.1	4.8	0.2

Hapuarachchi and Peijs [35] developed a flame retardant system, based on PLA, multiwalled nanotubes (MWNTs), sepiolite organoclays and hemp fibres. These were prepared by an extrusion and followed by film stacking method in the case of hemp fibre reinforced biocomposites. The separate introduction of MWNTs and sepiolite nanoclays resulted in decreased onset temperatures of degradation and thermal stability of the PLA. It was attributed to a percolation threshold which caused a network of MWNTs that acted as a conducting pathway causing early onset of decomposition. The addition of sepiolite nanoclays resulted in a catalytic effect on the pyrolysis of PLA. The flame retardand biocomposites exhibited improved flammability performance with a reduction of 58% in PHRR. This was attributed to the presence of nanofillers that increased the melt viscosity of the system and eliminated the bubbling of neat PLA.

PLA-based materials were used in developing flame resistant housings for notebook computers, as reported by Kimura and Horikoshi [163]. Flame retardant PLA biocomposites, were prepared by an extrusion method with the incorporation of different flame retardants including: aromatic silicon resin, polydimethylsiloxane and aluminum hydroxide, amongst others. Due to the low rigidity of PLA, the authors used several resin additives (e.g. polystyrene, polyethylene and polypropylene) to improve its physical properties. The PLA-based materials developed showed optimal physical and flammability properties that qualified them for the purpose.

In an attempt to address the environmental concerns, Feng *et al*. [164] investigated the use of *β*-cyclodextrin (*β*-CD) as carbon agent in an intumescent flame retardant (IFR) system based on PLA/APP/melamine (MA). *β*-CD is a bio product mainly from starch. It contains many hydroxyl groups that aid the formation of char during burning. It decomposes in one major step in an inert atmosphere, leaving a char that is thermally stable and decomposes at a low rate at high temperatures. Gaseous products, such as: CO_2, CO and H_2O are released during its decomposition. The IFR complex system was prepared by mechanical grinding, whereas the IFR/PLA composites were melt-blended and then hot/melt pressed.

The authors reported that the combination of *β*-CD/APP resulted in more char formation due to the presence of APP. *β*-CD and APP contributed to the release of gaseous products, such as NH_3 and H_2O from APP, in addition to those mentioned in the case of *β*-CD. Furthermore, phosphoric and polyphosphoric acids were also formed as products from APP degradation. Melamine (MA) was reported to promote *β*-CD char formation too. On heating, intramolecular and intermolecular dehydrations were involved in the *β*-CD degradation. The char formation during decomposition of *β*-CD followed several complex pathways and this was elaborated on, by the authors. In the case of IFR/PLA composites, it was concluded that *β*-CD is an efficient green carbon agent when coupled with APP and MA at appropriate weight ratios. This was due to the improved LOI values and UL-94 rating tests. However, it was noted that MA-containing systems formed unstable char and had some degradation effect on PLA due to the basic NH_3 it produced during burning.

Gallos *et al*. [165] investigated the effect of an IFR from APP, MA and nanoclays on poly L, D lactide (PDLLA). The stereocomplexed PLA was synthesised by reactive extrusion in a two-step polymerization of L- lactide and D-lactide to yield PDLLA multiblocks and then the IFR system was incorporated to form the PDLLA/IFR nanocomposites. The group reported improved flame retardancy as observed from cone calorimetry test results, namely a decrease of 83% in the HRR peak for nanocomposites, relative to neat PDLLA. A THR of 2 MJ m^{-2} was also reported for the nanocomposites and this was related to a 95% drop with respect to the matrix (i.e. THR of 45 MJ m^{-2}). Consequently, the authors suggested the mechanism of flame retardancy to be the decomposition of APP into acids that reacted with melamine and PLA. Such a reaction led to the formation of protective intumescent char. Additionally, APP reacted with nanoclays to produce alumino phosphates, which limited the formation of large cracks at the surface of the coating and provided an efficient protection.

Similar to Feng *et al*. [164], Wang *et al*. [166] reported on the flame retardancy and thermal degradation of PLA/starch biocomposites where starch was used as the carbonizing agent. Starch is a polyol that is inexpensive, biocompatible, biodegradable and renewable and can be employed as a natural carbon source. In this study, microencapsulated ammonium polyphosphate (MCAPP) and melamine (MA) were used to formulate a MCAPP/MA/starch IFR system. The group reported improved flammability of the PLA- based biocomposites with an LOI value of 41.0 vol.% and a UL-94 V-0 rating, when 30 wt.% IFR was incorporated. This was attributed to the effectiveness of starch as a carbonizing agent. In the MCC tests, biocomposites exhibited reduced PHRR and THR. This was explained in terms of IFR catalysing the degradation of PLA with the release of low flammable gaseous products. Improved char yields and thermal stability from TGA tests were also reported and the char is believed to be made up of pyrophosphoric acid and/or polyphosphate compounds. It was due to the char layer formed that the inner polymer degradation was retarded and PLA fire resistance was improved.

Recently, Lin *et al*. [167] synthesized flame retardant poly(1,2-propanediol-2-carboxyethyl phenyl phosphinates) (PCPP) and developed PLA-based blends by melt blending. Using DMA and scanning electron microscopy (SEM) data, it was reported that PCPP/PLA blends were immiscible, with LOI values higher than 26 vol.% and at a UL-94 V-0 rating at 3 wt.% PCPP loading. The presence of PCPP was found to have simultaneously enhanced the rheology (i.e. reducing PLA brittleness and improving processability) and mechanical properties of the PLA-based blends. Finally, from the morphology of the residual material and phosphorus content measurements, it was concluded that a condensed phase and a gas phase flame retardant mechanisms existed during burning.

2.4.3 Biofibre reinforced biopolymer composites

This section deals with flammability studies of composites made of biopolymer matrices reinforced with biofibres. Various additives/agents can be incorporated in biocomposites and these include: coupling, processing, dispersion and fire retardant agents. It is the last of these agents/additives that forms the focus point of this study [2,6,7,135,160].

FR additives, as discussed earlier, have the ability to alter the flammability character of the composite material. The properties, including flammability, of the biocomposites are governed by various factors, such as: a) the structure of the composite, b) adhesion between matrix and reinforcement, c) type of natural fibre and d) type of biodegradable polymer matrix [2,6,7,135,160].

Several studies were carried out on natural fibre reinforced biopolymer composites and their thermal, morphological, mechanical and flame retardancy properties were reported [5,35,165,168,169]. Gallo *et al*. [157] investigated the performance of a multi component laminate composite, based on a biodegradable commercial blend E-PHBV reinforced with kenaf fibres. The E-PHBV consists of poly(3-hydroxybutyrate-co-3-hydroxyvalerate) (PHBV) and poly(butylene adipate-co-terephthalate) (PBAT). Furthermore, a phosphate-based additive and a metal oxide (Sb_2O_3) were incorporated in order to formulate the flame retardant biocomposites. The biocomposites were prepared by an extrusion method, followed by compression moulding. Their laminate structure and thickness are as shown in Figure 2.20.

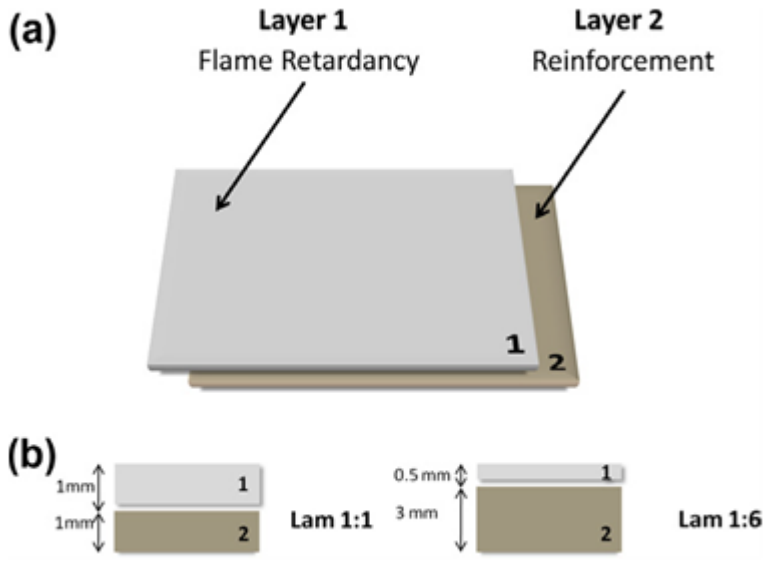

Figure 2.20 Structure (a) and laminate thickness (b) of the investigated materials. Reprinted from [157], Copyright 2013, with permission from Elsevier

Table 2.9 Mechanical properties. Reprinted from [157], Copyright 2013, with permission from Elsevier

	Flexural strength (σ_f) (MPa)	**Flexural modulus (E_f) (MPa)**	***R* (KJ m^{-2})**
E-PHBV	7.5 ± 0.4	233 ± 3	4.3 ± 0.7
Layer 1	7.0 ± 0.2	215 ± 5	2.5 ± 0.4
Layer 2	19.8 ± 1.1	804 ± 26	6.8 ± 0.8
Lam 1:1	10.7 ± 0.3	450 ± 35	4.8 ± 0.4
Lam 1:6	13.4 ± 1.5	488 ± 5	6.1 ± 1.1

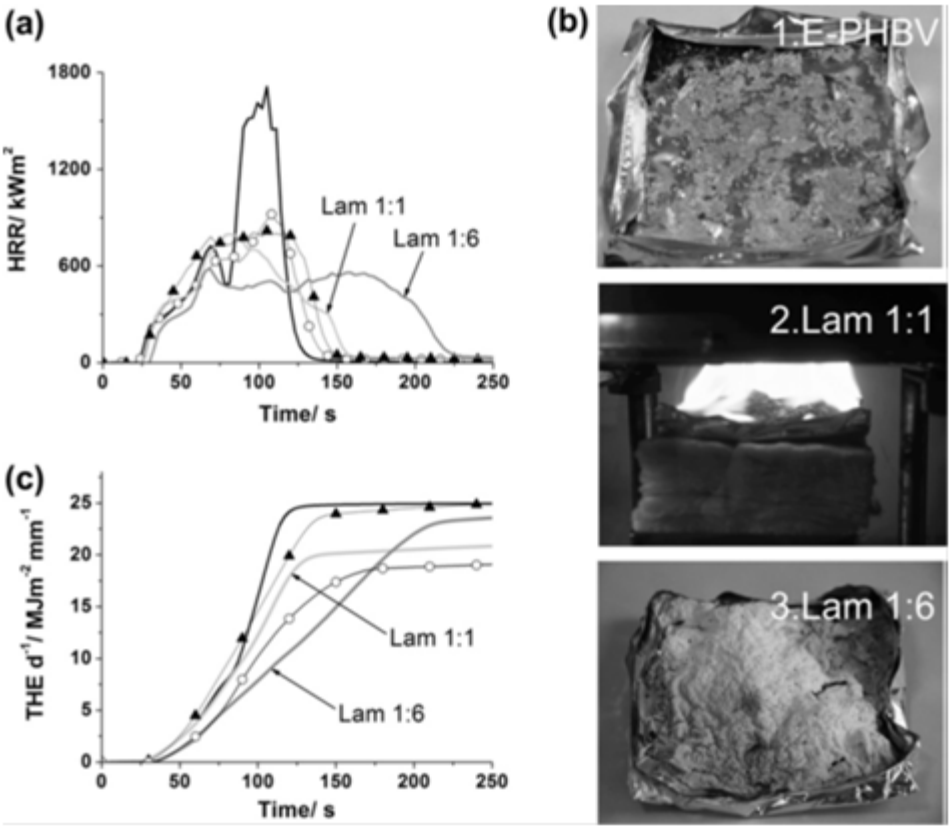

Figure 2.21 Heat release rate for E-PHBV (solid line), Layer 1 (open circles), Layer 2 (solid triangles) and laminate structures (a); fire residue after cone calorimeter test for E-PHBV (b.1), barrier formation during burning (Lam 1:1) (b.2) and fire residue for Lam 1:6 (b.3); total heat evolved (c). Reprinted from [157], Copyright 2013, with permission from Elsevier

This multi-component structure approach was reported as a successful route to balance the mechanical and fire retardancy performance in biopolymer composites. It was reported that the presence of the flame retardant and antimony oxide nanoparticles did not significantly change the flexural properties of the matrix, but reduced its resilience in comparison to the blend. On the other hand, the addition of kenaf fibres was reported to have improved all the mechanical parameters of the matrix (see Table 2.9). The different ratios in the samples (E-PHBV/Kenaf/AlPi/Sb_2O_3) were: 100/0/0/0 (E-PHBV), 90/0/8/2 (Layer 1), 70/30/0/0 (Layer 2), Layer 1/layer 2 (Lam 1:1), Layer 2/layer 1 (Lam 1:6).

A reduction in the PHRR, HRR and fire spread indices from the cone calorimetry test were reported, as shown in Figure 2.21. This was explained to be due to a combination of gas and condensed phase mechanisms from phosphorus and natural fibre. The kenaf fibres were said to have contributed by promoting the formation of an additional stable char layer during combustion. It is reported that kenaf fibres achieved this through intermolecular crosslinking and by inducing oxidation of phosphorus in the solid phase. Consequently, this prevented heat and flammable volatiles from penetrating the flame zone.

The char residue obtained after cone calorimetry tests were studied by SEM, as seen in Figure 2.22 and the relationship between the microstructure of the residue and the flame retardancy mechanism was established. It was concluded that the dense, porous structure in the residue proved that hydroxyl group rich kenaf fibres acted as a carbonization agent by forming a network of holes and cavities that affected the release of pyrolysis gases. However, the authors noted that there is a need to refine the coupling between the skin and core layer for improved interaction at the interphase.

In the study discussed previously, Hapuarachchi and Peijs [35] reinforced the flame retarded ternary system, based on PLA/MWNTs/organoclays with nonwoven needle punched hemp fibre mat (800 g m^{-2}). The authors reported that the hemp fibres reduced the HRR relative to pure PLA, but increased the THR. It was attributed to the natural fibres ability to cause the composites to burn for longer. The flame retardant effect of hemp fibres was thought to be due to the fibres charring and protecting the underlying polymer.

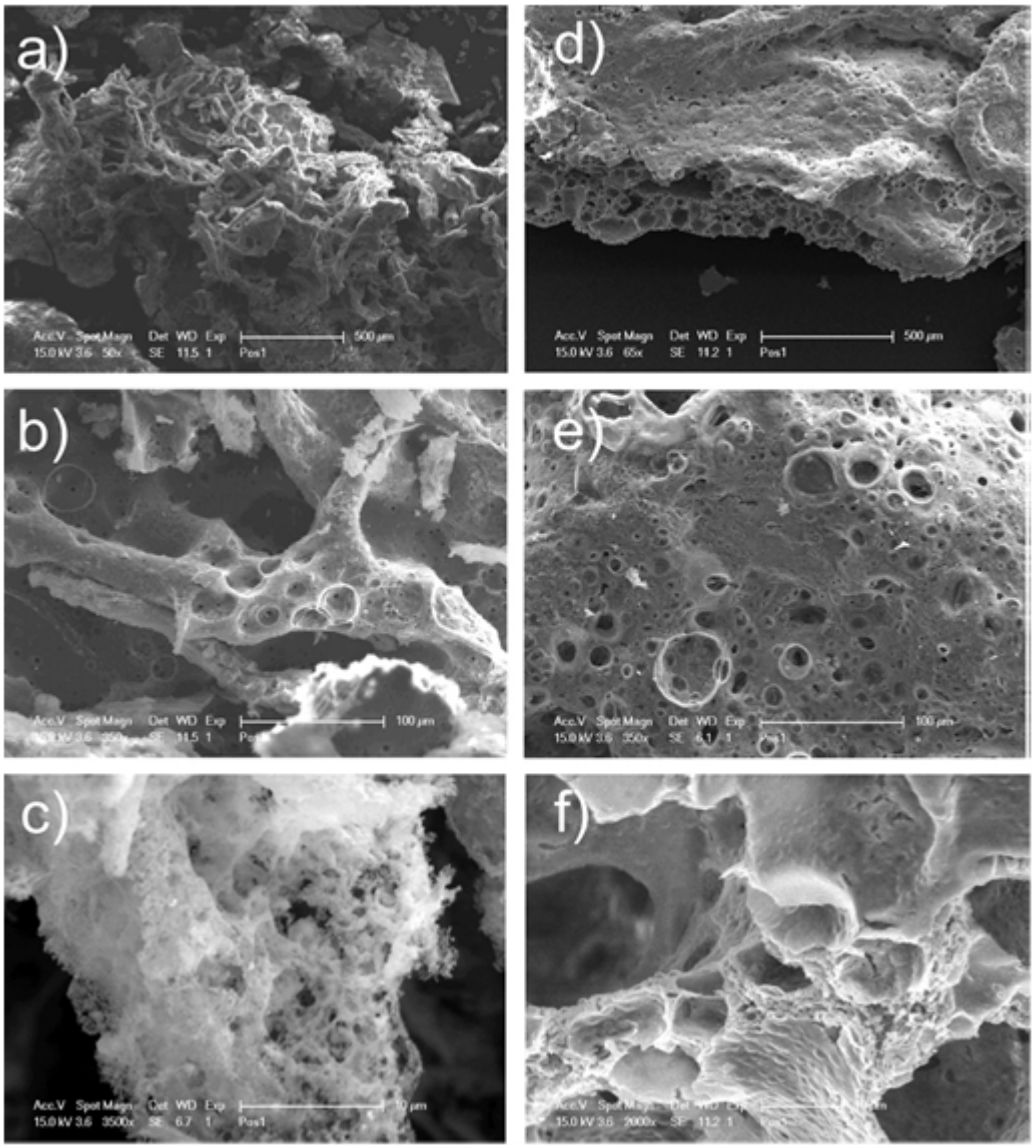

Figure 2.22 SEM micrograph of Layer 2 (a–c) and Lam 1:6 (d–f) at different magnifications. Reprinted from [157], Copyright 2013, with permission from Elsevier

Furthermore, it was reported that introducing hemp fibres, lowered the HRR when compared to the non-reinforced ternary system. In general, the authors proposed that the main flame retardant mechanism was due to a silicate char surface layer that acted as a barrier for heat and mass transportation. The group concluded by suggesting that the use of short fibre compounds are more suitable for these composites. This was to avoid thick layered structures that delaminated during cone calorimetry tests and exposed the underlying materials.

Similar results were reported by Biswal *et al*. [168] where banana fibre was used to reinforce polypropylene nanoclay composites in the presence of maleic anhydride grafted polypropylene

(MA-*g*-PP) compatibilizer. The nanocomposites were prepared by melt intercalation and the fibre reinforced nanocomposites by melt-blending, followed by compression moulding. The group reported that the tensile and flexural strengths showed linear increases as functions of clay content. This was explained as being due to the insertion of the polymer chains in the silicate clay layers, which led to an increase in the surface area necessary for the interaction between the clay and the polymer matrix. Furthermore, MA-*g*-PP facilitated the expansion of the gallery space of the nanoclay by the inclusion of polar groups to intercalate between the clay layers through hydrogen bonding with the oxygen groups of the tetrahedral clay. No considerable increase in the impact strength was observed and this was due to the presence of clay agglomerates, resulting in non-uniform dispersion within the polymer matrix. It was concluded that the better system was based on PP/clay/MA-*g*-PP (92/3/5 w/w) and it was termed optimized polypropylene (OPP).

As far as the flammability properties of these nanocomposites are concerned (Table 2.10), the incorporation of nanoclay showed a remarkable reduction in the HRR. This was attributed to i) nanoclay changing the degradation path of the polymer matrix, thus acting as a barrier by creating a roundabout path for migration and ii) the change in the thermal properties or an increase in the radiation absorptivity due to the high aspect ratio of the nanoclay. The group reported that the compatibilized banana fibre/PP/clay nanocomposites indicated a variation in reaction to fire parameters and exhibited an earlier ignition time relative to neat PP. However, the combustion process proceeded at lower HRR and mass loss rate (MLR), due to improved interfacial adhesion, but increased as a function of the fibre content in the nanocomposites. This was attributed to the typical characteristics of lignocellulosic fibres. Higher thermal stability was also reported and it was attributed to the presence of nanoclays. Finally, it was concluded that the banana fibre had some nucleating ability on the PP during crystallization, which was due to the strong interaction between the polymer matrix, fibres and nanoclays.

Jang *et al*. [5] looked at the mechanical and flammability performance of plasma treated (without any FR) coconut fibre reinforced PLA composites, prepared by the comingled yarn method. The mechanical properties were determined and flammability tests were carried out using the LOI method. It was reported that the tensile strength and Young's modulus increased with the introduction of the natural fibres, but no improvement was observed for the elongation at break. The group reported that although there was no obvious distinction between the LOI

values for the coconut fibres/PLA composites, they were above 20 vol.%, indicating a non-flammability character.

Table 2.10 Cone calorimetric parameters for the PP, OPP and banana fibre-PP (BRPP) nanocomposites. Reprinted from [168], Copyright 2012, with permission from John Wiley and Sons

Description	PP	OPP	BRPP-10	BRPP-20	BRPP-30
Time to ignition (s)	30	36	28	27	26
Time of flameout (s)	561	855	719	648	615
Total heat release (MJ/m^2)	100.5	107.3	121.7	137.4	141.5
Mass lost (g)	30.8	31	32.5	32.2	32.6
HRR (kW/m^2)	2498.2	748.3	926.4	1136.77	1256.2
Total smoke release (m^2/m^2)	1298.8	1164.5	1581.9	1746.5	1612.7
SEA (m^2/kg)	445.87	519.61	304.1	322.24	360.42

Fox *et al*. [169] investigated the flame retarding properties of PLA, using POSS modified nanofibrillated cellulose as a carbon source in IFR systems. Improved flammability was reported for the APP/cellulose and the APP/PER (pentaerythritol) systems. POSS modified cellulose showed an additional benefit by slightly lowering the PHRR and reducing the smoke. Furthermore, the use of POSS-modified cellulose in IFRs. proved effective at lowering flammability, while simultaneously inhibiting APP-induced PLA degradation, increased thermal oxidative resistance and increased composite stiffness.

Recently, researchers at the CSIR, PE (Port Elizabeth) have been involved in a project in collaboration with AIRBUS focussing on the development of natural fibre reinforced thermoset panels for use in aircraft. The research work involved the development of aqueous based flame retardant treatments for flax fabric to ensure that the composite panels comply with Federal Aviation Airworthiness (FAA) regulations. In addition to the primary flame retardant, the composite contained non fibrous natural silicate fire resistant material as well. The composite material was reported to exhibit superior flammability, smoke and toxicity properties for the aforementioned purpose [1].

2. 5 Summary

The flammability of biofibre (natural fibre) reinforced biopolymer composites and that of the biopolymer blends were succintly reviewed in this work. Different flame retardants, including: phosphorus, halogen, silicon, nanometric particles and minerals, were discussed. Their different flame retarding mechanisms, advantages and uses, disadvantages and limitations were elaborated on. Fire testing techniques, such as: cone calorimetry, pyrolysis combustion flow calorimetry, limiting oxygen index, UL-94 and Ohio State University rate of heat release apparatus, were also discussed. From this work, it could be seen that not only these testing technologies are needed to help define and come up with flame retardancy mechanisms, but other methods do play a role too. These include: burning tests, horizontal and vertical, thermal and thermo-mechanical methods of analysis (i.e. TGA, DSC), microscopic methods (i.e. SEM, transmission electron microscopy (TEM)), spectroscopic methods (i.e. FTIR and X ray diffraction (XRD)) and TGA-FTIR coupled systems.

Based on the reviewed work, a number of conclusions on the flammability of biofibre (natural fibre), biopolymers and biofibre reinforced biopolymer composites are made:

- Natural fibres (NFs) alone are a source of fuel. Thus, they are highly flammable, susceptible to ignition and combustion, combust exothermically and are burned vigorously during combustion.
- The range of NFs studied thus far from the flammability perspective is narrow and they include: wood (saw dust, particle board), flax, rice husk, regenerated cellulose (viscose), wool and mainly cotton fabric materials. There is therefore, a need to investigate other often used NFs including bamboo, coir, hemp, jute, kenaf, ramie and sisal.
- In general, the treatment of NF with various FR compounds, does indeed result in improved flame resistance.
- The flammability of biofibres is mainly dependent on their immediate environment: the nature of the polymer matrix and other FRs present, the presence or absence of coupling agents and the method of manufacturing natural fibre reinforced biocomposites. The main flammability mechanism favoured by FR treatment of NFs, is carbonization followed by increased char formation.
- Depending on the system, the mechanical properties may improve or show marginal decrease due to treatment.

- Current research has mainly focused on PLA as the preferred biopolymer matrix for the development of biofibre reinforced biocomposites. As a result, there is a need to begin exploring the use of other biopolymers {e.g. polycaprolactone (PCL), poly(3-hydroxybutyrate-co-3-hydroxyvalerate) (PHBV), poly(tetraethylene terephthalate) PTT, poly(ether ether ketone) (PEEK) and polybutylene succinate (PBS)} in this field.
- The current interest in using bio-based materials, such as: nanoclays, β CD, pea binder, starch, whey protein and DNA as participants in developing flame retardant systems (FRs) can lead to discoveries of "all green" FRs that may aid in addressing the environmental concerns. However, the important point on such systems may be two phased: the successful development of "all green" FRs on one hand and the performance and fulfilment of the required standards for the market, on the other. This poses a challenge to the scientific arena on fire retardancy.
- Finally, further studies need to be conducted to develop flame retardant biofibre reinforced biopolymer composite systems that simultaneously possess good flammability, thermal, mechanical, morphological and thermo mechanical properties for practical engineering applications.

Acknowledgements

The authors would like to acknowledge the financial support by the National Research Foundation (NRF) and Professional Development Programme (PDP). Acknowledgements are also extended to colleagues and researchers for their undivided attention and support.

References

1. Anandjiwala, R., Chapple, S.A., John, M.J., Schelling, H.-J., Michaelis, W., Döcker, M., Schoke, B. (2013). A flame-proofed artefact and a method of manufacture thereof. *World Intellectual Property Organization, International Bureau.* WO 2013/084023 A1.
2. Chapple, S., Anandjiwala, R. (2010). Flammability of natural fibre-reinforced composites and strategies for fire retardancy: A review. *Journal of Thermoplastic Composite Materials*, 23:871-893. DOI: 10.1177/0892705709356338

3. Faruk, O., Bledzki, A.K., Fink, H.-P., Sain, M. (2012). Biocomposites reinforced with natural fibers: 2000-2010. *Progress in Polymer Science*, 37:1552-1596.
DOI: 10.1016/j.progpolymsci.2012.04.003
4. Horrocks, A.R. (2011). Flame retardant challenges for textiles and fibres: New chemistry versus innovatory solutions. *Polymer Degradation and Stability*, 96:377-392.
DOI: 10.1016/j.polymdegradstab.2010.03.036
5. Jang, J.Y., Jeong, T.K., Oh, H.J., Youn, J.R., Song, Y.S. (2012). Thermal stability and flammability of coconut fiber reinforced poly(lactic acid) composites. *Composites: Part B*, 43:2434-2438.
DOI: 10.1016/j.compositesb.2011.11.003
6. John, M.J., Thomas, S. (2008). Biofibres and biocomposites. *Carbohydrate Polymers*, 71:343-364.
DOI: 10.1016/j.carbpol.2007.05.040
7. Kandola, B.K. (2012). Flame retardant characteristics of natural fibre composites. In John, M.J. and Thomas, S. (Eds.), Natural Polymers; Volume 1: Composites. The Royal Society of Chemistry, United Kingdom.
8. Sahari, J., Sapuan, S.M. (2011). Natural fibre reinforced biodegradable polymer composites. *Reviews on Advanced Materials Science*, 30:166-174.
9. Satyanarayana, K.G., Arizaga, G.G.C., Wypych, F. (2009). Biodegradable composites based on lignocellulosic fibers – An overview. *Progress in Polymer Science*, 34:982-1021.
DOI: 10.1016/j.progpolymsci.2008.12.002
10. Bourbigot, S., Fontaine, G. (2010). Flame retardancy of polylactide: an overview. *Polymer Chemistry*, 1:1413-1422.
DOI: 10.1039/c0py00106f
11. Price, D., Anthony, G., Carty, P. (2001). Introduction: polymer combustion, condensed phase pyrolysis and smoke formation. In Horrocks, A.R. and Price, D.(Eds.), Fire retardant materials. Woodhead Publishing Limited, England, pp. 1-30.
12. Kozlowski, R., Wladyka-Przybylak, M. (2001). Natural polymers, wood and lignocellulosic materials. In Horrocks, A.R. and Price, D. (Eds.), Fire retardant materials. Woodhead Publishing Limited, England.

13. Laoutid, F., Bonnaud, L., Alexandre, M., Lopez-Cuesta, J.-M., Dubois, Ph. (2009). New prospects in flame retardant polymer materials: From fundamentals to nanocomposites. *Materials Science and Engineering R*, 63:100-125.
DOI: 10.1016/j.mser.2008.09.002

14. Morgan, A.B., Gilman, J.W. (2013). An overview of flame retardancy of polymeric materials: application, technology, and future directions. *Fire and Materials*, 37:259-279.
DOI: 10.1002/fam.2128

15. Wichman, I.S. (2003). Material flammability, combustion, toxicity and fire hazard in transportation. *Progress in Energy and Combustion Science*, 29:247-299.
DOI: 10.1016/S0360-1285(03)00027-3

16. Carvel, R., Steinhaus, T., Rein, G., Torero, J.L. (2011). Determination of the flammability properties of polymeric materials: A novel method. *Polymer Degradation and Stability*, 96:314-319.
DOI: 10.1016/j.polymdegradstab.2010.08.010

17. Guillaume, E., Marquis, D., Saragoza, L. (2012). Calibration of flow rate in cone calorimeter tests. *Fire and Materials*.
DOI: 10.1002/fam.2174

18. Grexa, O., Lübke, H. (2001). Flammability parameters of wood tested on a cone calorimeter. *Polymer Degradation and Stability*, 74:427-432.
PII: S0141-3910(01)00181-1

19. Kandola, B.K. (2001). Nanocomposites. In Horrocks, A.R. and Price, D. (Eds.), Fire retardant materials. Woodhead Publishing Limited, England.

20. Kandola, B.K., Horrocks, A.R. (2001). Composites. In Horrocks, A.R. and Price, D. (Eds.), Fire retardant materials. Woodhead Publishing Limited, England.

21. Ke, C.-H., Li, J., Fang, K.-Y., Zhu, Q.-L., Zhu, J., Yan, Q., Wang, Y.-Z. (2010). Synergistic effect between a novel hyperbranched charring agent and ammonium polyphosphate on the flame retardant and anti-dripping properties of polylactide. *Polymer Degradation and Stability*, 95:763-770.
DOI: 10.1016/j.polymdegradstab.2010.02.011

22. Troitzsch, J.H. (1998). Overview of flame retardants. *Chimica Oggi/Chemistry Today*, 16:1-19.

23. Bourbigot, S., Duquesne, S. (2007). Fire retardant polymers: recent developments and opportunities. *Journal of Materials Chemistry*, 17:2283-2300.

DOI: 10.1039/b702511d

24. Zhu, H., Zhu, Q., Li, J., Tao, K., Xue, L., Yan, Q. (2011). Synergistic effect between expandable graphite and ammonium polyphosphate on flame retarded polylactide. *Polymer Degradation and Stability*, 96:183-189.
DOI: 10.1016/j.polymdegradstab.201011.017

25. Laoutid, F., Ferry, L., Lopez-Cuesta, J.M., Crespy, A. (2006). Flame-retardant action of red phosphorus/magnesium oxide and red phosphorus/iron oxide compositions in recycled PET. *Fire and Materials*, 30:343-358.
DOI: 10.1002/fam.914

26. Jimenez, M., Duquesne, S., Bourbigot, S. (2006). Intumescent fire protective coating: Toward a better understanding of their mechanism of action. *Thermochimica Acta*, 449:16-26.
DOI: 10.1016/j.tca.2006.07.008

27. Chen, L., Wang, Y.-Z. (2010). A review on flame retardant technology in China. Part I: development of flame retardants. *Polymers Advanced Technologies,* 21:1-26.
DOI: 10.1002/pat.1550

28. Hamdani, S., Longuet, C., Perrin, D., Lopez-Cuesta, J.-M., Ganachaud, F. (2009). Flame retardancy of silicone-based materials. *Polymer Degradation and Stability*, 94:465-495.
DOI: 10.1016/j.polymdegradstab.2008.11.019

29. Kashiwagi, T., Gilman, J.W., Butler, K.M., Harris, R.H., Shields, J.R., Asano, A. (2000). Flame retardant mechanism of silica gel/silica. *Fire and Materials,* 24:277-289.

30. Li, Q., Jiang, P., Wei, P. (2006). Synthesis, characteristic, and application of new flame retardant containing phosphorus, nitrogen, and silicon. *Polymer Engineering and Science*, 46:344-350.
DOI: 10.1002/pen.20472

31. Zhang, Z.X., Zhang, J., Lu, B.-X., Xin, Z.X., Kang, C.K., Kim, J.K. (2012). Effect of flame retardants on mechanical properties, flammability and foamability of PP/wood-fiber composites. *Composites: Part B*, 43:150-158.
DOI: 10.1016/j.compositesb.2011.06.020

32. Morgan, A.B. (2006). Flame retarded polymer layered silicate nanocomposites: a review of commercial and open literature systems. *Polymers for Advanced Technologies*, 17:206-217.
DOI: 10.1002/pat.685

33. Bordes, P., Pollet, E., Avérous, L. (2009). Nano-biocomposites: Biodegradable polyester/nanoclay systems. *Progress in Polymer Science*, 34:125-155.
DOI: 10.1016/j.propolymsci.2008.10.002

34. Kiliaris, P., Papaspyrides, C.D. (2010). Polymer/layered silicate (clay) nanocomposites: An overview of flame retardancy. *Progress in Polymer Science*, 35:902-958.
DOI: 10.1016/j.progpolymsci.2010.03.001

35. Hapuarachchi, T.D., Peijs, T. (2010). Multiwalled carbon nanotubes and sepiolite nanoclays as flame retardants for polylactide and its natural fibre reinforced composites. *Composites: Part A*, 41: 954-963.
DOI: 10.1016/j.compositesa.2010.03.004

36. Morgan, A.B., Harris, Jr., R.H., Kashiwagi, T., Chyall, L.J., Gilman, J.W. (2002). Flammability of polystyrene layered silicate (clay) nanocomposites: Carbonaceous char formation. *Fire and Materials*, 26:247-253.
DOI: 10.1002/fam.803

37. Manfredi, L.B., Rodríguez, E., Wladyka-Przybylak, M., Vázquez, A. (2010). Thermal properties and fire resistance of jute-reinforced composites. *Composite Interfaces*, 17:663-675.
DOI: 10.1163/092764410X513512

38. Barbosa, R., Araújo, E.M., Melo, T.J.A., Ito, E.N. (2007). Comparison of flammability behavior of polyethylene/Brazilian clay nanocomposites and polyethylene/flame retardants. *Materials Letters*, 61:2575-2578.
DOI: 10.1016/j.matlet.2006.09.055

39. Wei, P., Bocchini, S., Camino, G. (2013). Nanocomposites combustion peculiarities. A case history: Polylactide-clays. *European Polymer Journal*, 49:932-939.
DOI: 10.1016/j.eurpolymj.2012.11.010

40. Si, M., Zaitsev, V., Goldman, M., Frenkel, A., Peiffer, D.G., Weil, E., Sokolov, J.C., Rafailovich, M.H. (2007). Self-extinguishing polymer/organoclay nanocomposites. *Polymer Degradation and Stability*, 92:86-93.
DOI: 10.1016/j.polymdegradstab.2006.08.023

41. Ribeiro, S.P.S., Estevão, L.R.M., Pereira, C., Rodrigues, J., Nascimento, R.S.V. (2009). Influence of clays on the flame retardancy and high temperature viscoelastic properties of polymeric intumescent formulations. *Polymer Degradation and Stability*, 94:421-431.

DOI: 10.1016/j.polymdegradstab.2008.11.015

42. Tai, Q., Yuen, R.K.K., Song, L., Hu, Y. (2012). A novel polymeric flame retardant and exfoliated clay nanocomposites: Preparation and properties. *Chemical Engineering Journal*, 183:542-549.
DOI: 10.1016/j.cej.2011.12.095

43. Gao, F., Beyer, G., Yuana, Q. (2005). A mechanistic study of fire retardancy of carbon nanotube/ethylene vinyl acetate copolymers and their clay composites. *Polymer Degradation and Stability*, 89:559-564.
DOI: 10.1016/j.polymdegradstab.2005.02.008

44. Ye, L., Wu, Q., Qu, B. (2009). Synergistic effects and mechanism of multiwalled carbon nanotubes with magnesium hydroxide in halogen-free flame retardant EVA/MH/MWNT nanocomposites. *Polymer Degradation and Stability*, 94:751-756.
DOI: 10.1016/j.polymdegradstab.2009.02.010

45. Peeterbroeck, S., Alexandre, M., Nagy, J.B., Pirlot, C., Fonseca, A., Moreau, N., Philippin, G., Delhalle, J., Mekhalif, Z., Sporken, R., Beyer, G., Dubois, Ph. (2004). Polymer-layered silicate-carbon nanotube nanocomposites: unique nanofiller synergistic effect. *Composites Science and Technology*, 64:2317-2323.
DOI: 10.1016/j.compscitech.2004.01.020

46. Peeterbroeck, S., Laoutid, F., Taulemesse, J.-M., Monteverde, F., Lopez-Cuesta, J.-M., Nagy, J.B., Alexandre, M., Dubois, P. (2007). Mechanical properties and flame-retardant behaviour of ethylene vinyl acetate/high-density polyethylene coated carbon nanotube nanocomposites. *Advanced Functional Materials*, 17:2787-2791.
DOI: 10.1002/adfm.200600936

47. Lu, H., Wilkie, C.A. (2010). Synergistic effect of carbon nanotubes and decabromodiphenyl oxide/Sb_2O_3 in improving the flame retardancy of polystyrene. *Polymer Degradation and Stability*, 95:564-571.
DOI: 10.1016/j.polymdegradstab.2009.12.011

48. Isitman, N.A., Kaynak, C. (2010). Nanoclay and carbon nanotubes as potential synergists of an organophosphorus flame-retardant in poly(methyl methacrylate). *Polymer Degradation and Stability*, 95:1523-1532.
DOI: 10.1016/j.polymdegradstab.2010.06.013

49. Mittal, V. (2014). Functional polymer nanocomposites with graphene: A review. *Macromolecular Materials and Engineering*.
DOI: 10.1002/mame.201300394

50. Premkumar, T., Geckeler, K.E. (2012). Graphene-DNA hybrid materials: Assembly, applications, and prospects. *Progress in Polymer Science*, 37:515-529.
DOI: 10.1016/j.progpolymsci.2011.08.003

51. Hong, N., Song, L., Wang, B., Stec, A.A., Hull, T.R., Zhan, J., Hu, Y. (2014). Co-precipitation synthesis of reduced graphene oxide/NiAl-layered double hydroxide hybrid and its application in flame retarding poly(methyl methacrylate). *Materials Research Bulletin*, 49:657-664.
DOI: 10.1016/j.materresbull.2013.09.051

52. Wang, Z., Wei, P., Qian, Y., Liu, J. (2014). The synthesis of a novel graphene-based inorganic-organic hybrid flame retardant and its application in epoxy resin. *Composites: Part B*, 60:341-349.
DOI: 10.1016/j.compositesb.2013.12.033

53. Huang, G., Gao, J., Wang, X., Liang, H., Ge, C. (2012). How can graphene reduce the flammability of polymer nanocomposites? *Materials Letters*, 66:187-189.
DOI: 10.1016/j.matlet.2011.08.063

54. Huang, G., Liang, H., Wang, Y., Wang, X., Gao, J., Fei, Z. (2012). Combination effect of melamine polyphosphate and graphene on flame retardant properties of poly(vinyl alcohol). *Materials Chemistry and Physics*, 132:520-528.
DOI: 10.1016/j.matchemphys.2011.11.064

55. Huang, G., Chen, S., Tang, S., Gao, J. (2012). A novel intumescent flame retardant-functionalized graphene: Nanocomposite synthesis, characterization, and flammability properties. *Materials Chemistry and Physics*, 135:938-947.
DOI: 10.1016/j.matechemphys.2012.05.082

56. Dittrich, B., Wartig, K.-A., Hofmann, D., Mülhaupt, R., Schartel, B. (2013). Flame retardancy through carbon nanomaterials: Carbon black, multiwall nanotubes, expanded graphite, multi-layer graphene and graphene in polypropylene. *Polymer Degradation and Stability*, 98:1495-1505.
DOI: 10.1016/j.polymdegradstab.2013.04.009

57. Pandele, A.M., Ionita, M., Crica, L., Dinescu, S., Costache, M., Iovu, H. (2014). Synthesis, characterization, and *in vitro* studies of graphene oxide/chitosan-polyvinyl alcohol films. *Carbohydrate Polymers*, 102:813-820.
DOI: 10.1016/j.carbpol.2013.10.085

58. Yoon, O.J., Jung, C.Y., Sohn, I.Y., Kim, H.J., Hong, B., Jhon, M.S. (2011). Nanocomposite nanofibers of poly(D, L-lactic-co-glycolic acid) and graphene oxide nanosheets. *Composites: Part A*, 42:1978-1984.
DOI: 10.1016/j.compositesa.2011.08.023

59. Feng, Y., Zhang, X., Shen, Y., Yoshino, K., Feng, W. (2012). A mechanically strong, flexible and conductive film based on bacterial cellulose/graphene nanocomposite. *Carbohydrate Polymers*, 87:644-649.
DOI: 10.1016/j.carbpol.2011.08.039

60. Ryu, H.J., Mahapatra, S.S., Yadav, S.K., Cho, J.W. (2013). Synthesis of click-coupled graphene sheet with chitosan: Effective exfoliation and enhanced properties of their nanocomposites. *European Polymer Journal*, 49:2627-2634.
DOI: 10.1016/j.eurpolymj.2013.06.005

61. Lee, J.H., Marroquin, J., Rhee, K.Y., Park, S.J., Hui, D. (2013). Cryomilling application of graphene to improve material properties of graphene/chitosan nanocomposites. *Composites: Part B*, 45:682-687.
DOI: 10.1016/j.compositesb.2012.05.011

62. Franchini, E., Galy, J., Gérard, J.-F., Tabuani, D., Medici, A. (2009). Influence of POSS structure on the fire retardant properties of epoxy hybrid networks. *Polymer Degradation and Stability*, 94:1728-1736.
DOI: 10.1016/j.polymdegradstab.2009.06.025

63. Waddon, A.J., Coughlin, E.B. (2003). Crystal Structure of Polyhedral Oligomeric Silsequioxane (POSS) Nano-materials: A Study by X-ray Diffraction and Electron Microscopy. *Chemistry of Materials*, 15:4555-4561.
DOI: 10.1021/cm034308b

64. Devaux, E., Rochery, M., Bourbigot, S. (2002). Polyurethane/clay and polyurethane/POSS nanocomposites as flame retarded coating for polyester and cotton fabrics. *Fire and Materials*, 26:149-154.
DOI: 10.1002/fam.792

65. He, Q., Song, L., Hu, Y., Zhou, S. (2009). Synergistic effects of polyhedral oligomeric silsesquioxane (POSS) and oligomeric bisphenyl A bis(diphenyl phosphate) (BDP) on thermal and flame retardant properties of polycarbonate. *Journal of Material Science*, 44:1308-1316.
DOI: 10.1007/s10853-009-3266-5

66. Glodek, T.E., Boyd, S.E., McAninch, I.M., LaScala, J.J. (2008). Properties and performance of fire resistant eco-composites using polyhedral oligomeric silsesquioxane (POSS) fire retardants. *Composites Science and Technology*, 68:2994-3001.
DOI: 10.1016/j.compscitech.2008.06.019

67. Fina, A., Tabuani, D., Camino, G. (2010). Polypropylene-polysilsesquioxane blends. *European Polymer Journal*, 46:14-23.
DOI: 10.1016/j.eurpolymj.2009.07.019

68. Bouza, R., Barral, L., Díez, F.J., López, J., Montero B., Rico, M., Ramírez, C. (2014). Study of thermal and morphological properties of a hybrid system, iPP/POSS. Effect of flame retardance. *Composites: Part B*, 58:566-572.
DOI: 10.1016/j.compositesb.2013.11.010

69. Wang, X., Hu, Y., Song, L., Yang, H., Yu, B., Kandola, B., Deli, D. (2012). Comparative study on the synergistic effect of POSS and graphene with melamine phosphate on the flame retardance of poly(butylenes succinate). *Thermochimica Acta*, 543:156-164.
DOI: 10.1016/j.tca.2012.05.017

70. Fox, D.M., Novy, M., Brown, K., Zammarano, M., Harris Jr., R.H., Murariu, M., McCarthy, E.D., Seppala, J.E., Gilman, J.W. (2014). Flame retarded poly(lactic acid) using POSS-modified cellulose. 2. Effects of intumescing flame retardant formulations on polymer degradation and composite physical properties. *Polymer Degradation and Stability*, 106:54-62.
DOI: 10.1016/j.polymdegradstab.2014.01.007

71. Laachachi, A., Leroy, E., Cochez, M., Ferriol, M., Lopez-Cuesta, J.M. (2005). Use of oxide nanoparticles and organoclays to improve thermal stability and fire retardancy of poly(methyl methacrylate). *Polymer Degradation and Stability*, 89:344-352.
DOI: 10.1016/j.polymdegradstab.2005.01.019

72. Laachachi, A., Cochez, M., Leroy, E., Ferriol, M., Lopez-Cuesta, J.M. (2007). Fire retardant systems in poly(methyl methacrylate): Interactions between metal oxide nanoparticles and phosphinates. *Polymer Degradation and Stability*, 92:61-69.
DOI: 10.1016/j.polymdegradstab.2006.09.011

73. Gallo, E., Braun, U., Schartel, B., Russo, P., Acierno, D. (2009). Halogen-free flame retarded poly(butylene terephthalate) (PBT) using metal oxides/PBT nanocomposites

in combination with aluminium phosphinate. *Polymer Degradation and Stability*, 94:1245-1253.
DOI: 10.1016/j.polymdegradstab.2009.04.014

74. Gallo, E., Schartel, B., Acierno, D., Russo, P. (2011). Flame retardant biocomposites: Synergism between phosphinate and nanometric metal oxides. *European Polymer Journal*, 47:1390-1401.
DOI: 10.1016/j.eurpolymj.2011.04.001

75. Lewin, M. (2001). Synergism and catalysis in flame retardancy of polymers. *Polymers for Advanced Technologies*, 12:215-222.
DOI: 10.1002/pat.132

76. Wang, Z., Han, E., Ke, W. (2006). Effect of nanoparticles on the improvement in fire-resistant and anti-ageing properties of flame-retardant coating. *Surface & Coatings Technology*, 200:5706-5716.
DOI: 10.1016/j.surfcoat.2005.08.102

77. Shen, L., Chen, Y., Li, P. (2012). Synergistic catalysis effects of lanthanum oxide in polypropylene/magnesium hydroxide flame retarded system. *Composites: Part A*, 43:1177-1186.
DOI: 10.1016/j.compositesa.2012.02.014

78. Li, N., Xia, Y., Mao, Z., Wang, L., Guan, Y., Zheng, A. (2012). Influence of antimony oxide on flammability of polypropylene/intumescent flame retardant system. *Polymer Degradation and Stability*, 97:1737-1744.
DOI: 10.1016/j.polymdegradstab.2012.06.011

79. http://www.dstuns.iitm.ac.in/teaching-and-presentations/teaching/undergraduate%20courses/vy305-molecular-architecture-and-evolution-of-functions/presentations/presentations-2007/seminar-1/P4.pdf. (07/03/2014)

80. Bonnet, J., Bounor-Legaré, V., Boisson, F., Melis, F., Camino, G., Cassagnau, P. (2012). Phosphorus based organic-inorganic hybrid materials prepared by reactive processing for EVA fire retardancy. *Polymer Degradation and Stability*, 97:513-522.
DOI: 10.1016/j.polydegradstab.2012.01.018

81. Messori, M., Toselli, M., Pilati, F., Fabbri, P., Busoli, S., Pasquali, L., Nannarone, S. (2003). Flame retarding poly(methyl methacrylate) with nanostructured organic-inorganic hybrids coatings. *Polymer*, 44:4463-4470.
DOI: 10.1016/S0032-3861(03)00396-3

82. Marras, S.I., Zuburtikudis, I., Panayiotou, C. (2007). Nanostructure vs. microstructure: Morphological and thermomechanical characterization of poly(L-lactic acid)/layered silicate hybrids. *European Polymer Journal*, 43:2191-2206.
DOI: 10.1016/j.eurpolymj.2007.03.013

83. Nurul, M.S., Mariatti, M. (2013). Effect of hybrid nanofillers on the thermal, mechanical, and physical properties of polypropylene composites. *Polymer Bulletin*, 70:871-884.
DOI: 10.1007/s00289-012-0893-9

84. Vasiljević, J., Hadžić, S., Jerman, I., Černe, L., Tomšič, B., Medved, J., Godec, M., Orel, B., Simončič, B. (2013). Study of flame-retardant finishing of cellulose fibres: Organic-inorganic hybrid versus conventional organophosphonate. *Polymer Degradation and Stability*, 98:2602-2608.
DOI: 10.1016/j.polymedegradstab.2013.09.020

85. Wang, X., Pang, H., Chen, W., Lin, Y., Ning, G. (2013). Nanoengineering core/shell structured brucite@polyphosphate@amine hybrid system for enhanced flame retardant properties. *Polymer Degradation and Stability*, 98:2606-2616.
DOI: 10.1016/j.polymdegradstab.2013.09.021

86. Hollingbery, L.A., Hull, T.R. (2010). The fire retardant behaviour of huntite and hydromagnesite – A review. *Polymer Degradation and Stability*, 95:2213-2225.
DOI: 10.1016/j.polymdegradstab.2010.08.019

87. Hollingbery, L.A., Hull, T.R. (2010). The thermal decomposition of huntite and hydromagnesite – A review. *Thermochimica Acta*, 509:1-11.
DOI: 10.1016/j.tca.2010.06.012

88. Hollingbery, L.A., Hull, T.R. (2012). The thermal decomposition of natural mixtures of huntite and hydromagnesite. *Thermochimica Acta*, 528:45-52.
DOI: 10.1016/j.tca.2011.11.002

89. Laoutid, F., Gaudon, P., Taulemesse, J.-M., Lopez-Cuesta, J.M., Velasco, J.I., Piechaczyk, A. (2006). Study of hydromagnesite and magnesium hydroxide based fire retardant systems for ethylene-vinyl acetate containing organo-modified montmorillonite. *Polymer Degradation and Stability*, 91:3074-3082.
DOI: 10.1016/j.polymdegradstab.2006.08.011

90. Ahmad Ramazani, S.A., Rahimi, A., Frouchi, M., Radman, S. (2008). Investigation of flame retardancy and physical-mechanical properties of zinc borate and aluminum hydroxide propylene composites. *Materials and Design*, 29:1051-1056.

DOI: 10.1016/j.matdes.2007.04.003

91. Cárdenas, M.A., García-López, D., Gobernado-Mitre, I., Merino, J.C., Pastor, J.M., Martínez, J. de D., Barbeta, J., Calveras, D. (2008). Mechanical and fire retardant properties of EVA/clay/ATH nanocomposites – Effect of particle size and surface treatment of ATH filler. *Polymer Degradation and Stability*, 93:2032-2037.
DOI: 10.1016/j.polymdegradstab.2008.02.015

92. Durin-France, A., Ferry, L., Lopez Cuesta, J.-M., Crespy, A. (2000). Magnesium hydroxide/zinc borate/talc compositions as flame-retardants in EVA copolymer. *Polymer International*, 49:1101-1105.
DOI: 10.1002/1097-0126(200010)49:10<1101::AID-PI 523>3.0.CO;2-5

93. Focke, W.W., Molefe, D., Labuschagne, F.J.W., Ramjee, S. (2009). The influence of stearic acid coating on the properties of magnesium hydroxide, hydromagnesite, and hydrotalcite powders. *Journal of Materials Science*, 44:6100-6109.
DOI: 10.1007/s10853-009-3844-6.

94. Haurie, L., Fernández, A.I., Velasco, J.I., Chimenos, J.M., Lopez-Cuesta, J.-M., Espiell, F. (2006). Synthetic hydromagnesite as flame retardant. Evaluation of the flame behaviour in a polyethylene matrix. *Polymer Degradation and Stability*, 91:989-994.
DOI: 10.1016/j.polymdegradstab.2005.08.009

95. Haurie, L., Fernández, A.I., Velasco, J.I., Chimenos, J.-M., Lopez-Cuesta, J.M., Espiell, F. (2007). Thermal stability and flame retardancy of LDPE/EVA blends filled with synthetic hydromagnesite/aluminium hydroxide/montmorillonite and magnesium hydroxide/aluminium hydroxide/montmorillonite mixtures. *Polymer Degradation and Stability*, 92:1082-1087.
DOI: 10.1016/j.polymdegradstab.2007.02.014

96. Hull, T.R., Witkowski, A., Hollingbery, L. (2011). Fire retardant action of mineral fillers. *Polymer Degradation and Stability*, 96:1462-1469.
DOI: 10.1016/j.polymdegradstab.2011.05.006

97. Morgan, A.B., Cogen, J.M., Opperman, R.S., Harris, J.D. (2007). The effectiveness of magnesium carbonate-based flame retardants for poly(ethylene-co-vinyl acetate) and poly(ethyelene-co-ethyl acrylate). *Fire and Materials*, 31:387-410.
DOI: 10.1002/fam.950

98. Nachtigall, S.M.B., Miotto, M., Schneider, E.E., Mauler, R.S., Forte, M.M.C. (2006). Macromolecular coupling agents for flame retardant materials. *European Polymer Journal*, 42:990-999.

DOI: 10.1016/j.eurpolymj.2005.10.017

99. Pawlowski, K.H., Schartel, B., Fichera, M.A., Jäger, C. (2010). Flame retardancy mechanisms of bisphenol A bis(diphenyl phosphate) in combination with zinc borate in bisphenol A polycarbonate/acrylonitrile-butadiene-styrene blends. *Thermochimica Acta*, 498:92-99.
DOI: 10.1016/j.tca.2009.10.007

100. Qui, L., Xie, R., Ding, P., Qu, B. (2003). Preparation and characterization of $Mg(OH)_2$ nanoparticles and flame-retardant property of its nanocomposites with EVA. *Composite Structures*, 62:391-395.
DOI: 10.1016/j.compstruct.2003.09.010

101. Rothon, R.N., Hornsby, P.R. (1996). Flame retardant effects of magnesium hydroxide. *Polymer Degradation and Stability*, 54:383-385.
PII: S0141-3910(96)00067-5

102. Sain, M., Park, S.H., Suhara, F., Law, S. (2004). Flame retardant and mechanical properties of natural fibre-PP composites containing magnesium hydroxide. *Polymer Degradation and Stability*, 83:363-367.
DOI: 10.1016/S0141-3910(03)00280-5

103. Tang, H., Zhou, X.-b., Liu, X.-l. (2013). Effect of magnesium hydroxide on the flame retardant properties of unsaturated polyester resin. *Procedia Engineering*, 52:336-341.
DOI: 10.1016/j.proeng.2013.02.150

104. Witkowski, A., Stec, A.A., Hull, T.R. (2012). The influence of metal hydroxide fire retardants and nanoclay on the thermal decomposition of EVA. *Polymer Degradation and Stability*, 97:2231-2240.
DOI: 10.1016/j.polymdegradstab.2012.08.003

105. Babrauskas, V. (1993). Ten years of heat release research with the cone calorimeter. Tsukuba Building Test Laboratory, Center for Better Living. Japan symposium on heat release and fire hazard, first (1st) proceedings. Session 3. Scope for next-generation fire safety testing technology. May 10-11, Tsukuba, Japan, III/1-8 pp.
http://www.doctorfire.com/cone.html (27/09/2013)

106. Lindholm, J., Brink, A., Hupa, M. (2009). Cone calorimeter – a tool for measuring heat release rate.
www.ffrc.fi/FlameDays_2009/4B/LindholmPaper.pdf (05/05/2013)

107. Babrauskas, V., Peacock, R.D. (1992). Heat release rate: The single most important variable in fire hazard. *Fire Safety Journal*, 18:255-272.

108. Huggett, C. (1980). Estimation of rate of heat release by means of oxygen consumption measurements. *Fire and Materials*, 4(2):61-65.

109. Lyon, R.E., Walters, R. (2002). A microscale combustion calorimeter. Final Report. DOT/FAA/AR-01/117.

110. Lyon, R.E., Walters, R.N. (2004). Pyrolysis combustion flow calorimetry. *Journal of Analytical and Applied Pyrolysis*, 71:27-46.
DOI: 10.1016/S0165-2370(03)00096-2

111. Lyon, R.E., Walters, R.N., Stoliarov, S.I. (2007). Screening flame retardants for plastics using microscale combustion calorimetry. *Polymer Engineering and Science*, 47:1501-1510.
DOI: 10.1002/pen.20871

112. Morgan, A.B., Galaska, M. (2008). Microcombustion calorimetry as a tool for screening flame retardancy in epoxy. *Polymers for Advanced Technologies*, 19:530-546.
DOI: 10.1002/pat.1100

113. Morgan, A.B., Wolf, J.D., Guliants, E.A., Shiral Fernando, K.A., Lewis, W.K. (2009). Heat release measurements on micron and nano-scale aluminum powders. *Thermochimica Acta*, 488:1-9.
DOI: 10.1016/j.tca.2009.01.016

114. Schartel, B., Pawlowski, K.H., Lyon, R.E. (2007). Pyrolysis combustion flow calorimeter: A tool to assess flame retarded PC/ABS materials? *Thermochimica Acta*, 462:1-14.
DOI: 10.1016/j.tca.2007.05.021

115. Lyon, R.E., Walters, R.N. (2005). Flammability of automotive plastics. (August), pp. 1-17.
http://mvfri.org/Contracts/Final%20Reports/TRACE%20Final%20Report%209-1-05.pdf (26/09/2013).

116. Lyon, R.E., Walters, R.N., Stoliarov, S.I. (2007). Thermal analysis of flammability. *Journal of Thermal Analysis and Calorimetry*, 89(2):441-448.

117. White, R.H. (1979). Oxygen index evaluation of fire-retardant-treated wood. *Wood Science*, 12(2):113-121.
http://www.fpl.fs.fed.us/documnts/pdf1979/white79a.pdf (26/09/2013)

118. Nelson, M.I. (2001). A dynamical systems model of the limiting oxygen index test: II. Retardancy due to char formation and addition of inert fillers. *Combustion Theory and Modelling*, 5:59-83.
PII: S1364-7830(01)09402-5

119. Patel, P., Hull, T.R., Moffatt, C. (2012). PEEK polymer flammability and the inadequacy of the UL-94 classification. *Fire and Materials*, 36:185-201.
DOI: 10.1002/fam.1100

120. Wang, Y., Zhang, F., Chen, X., Jin, Y., Zhang, J. (2010). Burning and dripping behaviors of polymers under the UL94 vertical burning test conditions. *Fire and Materials*, 34:203-215.
DOI: 10.1002/fam.1021

121. Smith, E.E. (1996). Heat release rate calorimetry. *Fire Technology*, 32(4):333-347.

122. http://www.flightsimaviation.com/data/FARS/part_25-appF4.html (20/03/2013)

123. http://www.astm.org/Standards/E906.htm (06/05/2013)

124. Hirschler, M.M. (2000). "Use of Heat Release Measurements and/or Fire Hazard Assessment in Codes and Standards in the USA", Fire Risk & Hazard Assessment Symposium, National Fire Protection Research Foundation, June 28-30, 2000, Atlantic City, NJ, pp. (26/09/2013).

125. http://www.fire.tc.faa.gov/pdf/handbook/00-12_ch5-0909.pdf (06/05/2013)

126. http://www.fire-testing.com/astm-e-906-osu (05/05/2013)

127. Tran, H.C. (1988). Heat release measurement of wood products using the Ohio state university apparatus. In Proceedings of the 13th international conference on fire safety; January, 11-15, Millbrae, CA. Sunnyvale, CA. *Product Safety Corp*., 13:298-311.

128. Tran, H.C. (1990). Modifications to an Ohio state university apparatus and comparison with cone calorimeter results. In Quintiere, J.G. and Cooper, L.Y. (Eds.), Heat and mass transfer in fires. Proceedings of the AIAA/ASME thermophysics and heat transfer conference, June 18-20. The American Society of Mechanical Engineers, Seattle, WA. New York.

129. Tran, H.C., White, R.H. (1992). Burning rate of solid wood measured in a heat release rate calorimeter. *Fire and Materials*, 16:197-206.

130. White, R.H., Dietenberger, M.A. (1999). Fire Safety (Chapter 17). In Wood Handbook, Wood as an engineering material.Forest Products Laboratory, USDA Forest Service, Madison, Wisconsin.General Technical Report FPL-GTR-113.
http://www.carbeck.org/pdfs/FPL_Wood_Handbook_Ch17.pdf (06/05/2013)

131. Filipczak, R., Crowley, S., Lyon, R.E. (2005). Heat release rate measurements of thin samples in the OSU apparatus and the cone calorimeter. *Fire Safety Journal*, 40:628-645.
DOI: 10.1016/j.firesaf.2005.05.009

132. ASTM E906/E906M-10. (2010). Standard Test Method for Heat and Visible Smoke Release Rates for Materials and Products Using a Thermopile Method, ASTM International /15 April /26 pages.
http://www.techstreet.com/standards/astm/e906_e906m_10?product_id=1725917
25/03/2013)

133. Rowell, R.M., Dietenberger, M.A. (2013). Thermal properties, combustion and fire retardancy of wood. In Rowell, R.M. (Ed.), Handbook of wood chemistry and wood composites. 2nd edition. CRC Press, Taylor & Francis Group, London.

134. Kozlowski R., Wladyka-Przybylak, M. (2008). Review. Flammability and fire resistance of composites reinforced by natural fibers. *Polymers for Advanced Technologies*, 19:449-453.
DOI: 10.1002/pat.1135

135. Zavareze, E. da R., Dias, A.R.G. (2012). Relation between structural anisotropy in natural fibres and mechanical properties in composites.In John, M.J. and Thomas, S. (Eds.), Natural Polymers; Volume 1: Composites. The Royal Society of Chemistry, United Kingdom.

136. Grexa, O., Poutch, F., Manikova, D., Martvonova, H., Bartekova, A. (2003). Intumescence in fire retardancy of lignocellulosic panels. *Polymer Degradation and Stability*, 82:373-377.
DOI: 10.1016/S0141-3910(03)00215-5

137. Lewin, M. (2005). Unsolved problems and unanswered questions in flame retardance of polymers. *Polymer Degradation and Stability*, 88:13-19.
DOI: 10.1016/j.polymdegradstab.2003.12.011

138. Chai, M.W., Bickerton, S., Bhattacharyya, D., Das, R. (2012). Influence of natural fibre reinforcements on the flammability of bio-derived composite materials. *Composites: Part B*, 43:2867-2874.
DOI: 10.1016/j.compositesb.2012.04.051

139. Kandola, B.K., Horrocks, A.R. (2000). Complex char formation in flame-retarded fibre-intumescent combinations – iv. Mass loss and thermal barrier properties. *Fire and Materials*, 24:265-275.

140. Lazko, J., Landercy, N., Laoutid, F., Dangreau, L., Huguet, M.H., Talon, O. (2013). Flame retardant treatments of insulating agro-materials from flax short fibres, *Polymer Degradation and Stability*, 98:1043-1051.
DOI: 10.1016/j.polymdegradstab.2013.02.002

141. Reti, C., Casetta, M., Duquesne, S., Delobel, R., Soulestin, J., Bourbigot, S. (2009). Intumescent bio-based-polylactide films to flame retard nonwovens. *Journal of Engineered Fibers and Fabrics*, 4(2):3-39.

142. Abou-Okeil, A., El-Sawy, S.M., Abdel-Mohdy, F.A. (2013). Flame retardant cotton fabrics treated with organophosphorus polymer. *Carbohydrate Polymers*, 92:2293-2298.
DOI: 10.1016/j.carbpol.2012.12.008

143. Alongi, J., Malucelli, G. (2012). Cotton fabrics treated with novel oxidic phases acting as effective smoke suppressants. *Carbohydrate Polymers, 90*, 251 – 260.
DOI: 10.1016/j.carbpol.2012.05.032

144. Alongi, J., Brancatelli, G., Rosace, G. (2012). Thermal properties and combustion behavior of POSS- and Bohemite-finished cotton fabrics. *Journal of Applied Polymer Science*, 123:426-436.
DOI: 10.1002/app.34476

145. Alongi, J., Ciobanu, M., Malucelli, G. (2011). Novel flame retardant finishing systems for cotton fabrics based on phosphorus-containing compounds and silica derived from sol-gel processes. *Carbohydrate Polymers*, 85:599-608.
DOI: 10.1016/j.carbpol.2011.03.024

146. Alongi, J., Ciobanu, M., Malucelli, G. (2012). Thermal stability, flame retardancy and mechanical properties of cotton fabrics treated with inorganic coatings synthesized through sol-gel processes. *Carbohydrate Polymers*, 87:2093-2099.
DOI: 10.1016/j.carbpol.2011.10.032

147. Alongi, J., Carletto, R.A., Di Blasio, A., Cuttica, F., Carosio, F., Bosco, F., Malucelli, G. (2013). Intrinsic intumescent-like flame retardant properties of DNA-treated cotton fabrics. *Carbohydrate Polymers*, 96:296-304.
DOI: 10.1016/j.carbpol.2013.03.066

148. Bosco, F., Carletto, R.A., Alongi, J., Marmo, L., Di Blasio, A., Malucelli, G. (2013). Thermal stability and flame resistance of cotton fabrics treated with whey proteins. *Carbohydrate Polymers*, 94:372-377.
DOI: 10.1016/j.carbpol.2012.12.075

149. Didane, N., Giraud, S., Devaux, E. (2012). Fire performances comparison of back coating and melt spinning approaches for PET covering textiles. *Polymer Degradation and Stability*, 97:1083-1089.
DOI: 10.1016/j.polymdegradstab.2012.04.010

150. Flambard, X., Bourbigot, S., Kozlowski, R., Muzyczek, M., Mieleniak, B., Ferreira, M., Vermeulen, B., Poutch, F. (2005). Progress in safety, flame retardant textiles and flexible fire barriers for seats in transportation. *Polymer Degradation and Stability*, 88:98-105.
DOI: 10.1016/j.polymdegradstab.2004.02.024

151. Laufer, G., Kirkland, C., Morgan, A.B., Grunlan, J.C. (2012). Intumescent multilayer nanocoating, made with renewable polyelectrolytes, for flame-retardant cotton. *Biomacromolecules*, 13:2843-2848.
DOI: 10.1021/bm300873b

152. Nguyen, T.-M.D., Chang, S.C., Condon, B., Uchimiya, M., Fortier, C. (2012). Development of an environmentally friendly halogen-free phosphorus-nitrogen bond flame retardant for cotton fabrics. *Polymers Advanced Technologies*, 23:1555-1563.
DOI: 10.1002/pat.3029

153. Šimkovic, I. (2012). TG/DTG/DTA evaluation of flame retarded cotton fabrics and comparison to cone calorimeter data. *Carbohydrate Polymers*, 90:976-981.
DOI: 10.1016/j.carbpol.2012.06.030

154. Wang, L., Zhang, T., Yan, H., Peng, M., Fang, Z. (2013). Modification of ramie fabric with a metal-ion-doped flame-retardant coating. *Journal of Applied Polymer Science*, 129:2986-2997.
DOI: 10.1002/app.39015

155. Yang, Z., Wang, X., Lei, D., Fei, B., Xin, J.H. (2012). A durable flame retardant for cellulosic fabrics. *Polymer Degradation and Stability*, 97:2467-2472.
DOI: 10.1016/j.polymdegradstab.2012.05.023

156. Frone, A.N., Berlioz, S., Chailan, J.-F., Panaitescu, D.M. (2013). Morphology and thermal properties of PLA-cellulose nanofibers composites. *Carbohydrate Polymers*, 91:377-384.
DOI: 10.1016.j.carbpol.2012.08.054

157. Gallo, E., Schartel, B., Acierno, D., Cimino, F., Russo, P. (2013). Tailoring the flame retardant and mechanical performances of natural fiber-reinforced biopolymer by multi-component laminate. *Composites: Part B*, 44:112-119.

DOI: 10.1016/j.compositesb.2012.07.005

158. Cheng, K.-C., Yu, C.-B., Guo, W., Wang, S.-F., Chuang, T.-H., Lin, Y.-H. (2012). Thermal properties and flammability of polylactide nanocomposites with aluminum trihydrate and organoclay. *Carbohydrate Polymers*, 87:1119-1123.
DOI: 10.1016/j.carbpol.2011.08.065

159. Das, K., Ray, S.S., Chapple, S., Wesley-Smith, J. (2013). Mechanical, thermal, and fire properties of biodegradable polylactide/boehmite alumina composites. *Industrial & Engineering Chemistry Research*, 52:6083-6091.
DOI: 10.1021/ie4004305

160. Tang, G., Wang, X., Xing, W., Zhang, P., Wang, B., Hong, N., Yang, W., Hu, Y., Song, L. (2012). Thermal degradation and flame retardance of bio-based polylactide composites based on aluminum hypophosphite. *Industrial & Engineering Chemistry Research*, 51:12009-12016.
DOI: 10.1021/ie3008133

161. Zhan, J., Song, L., Nie, S., Hu, Y. (2009). Combustion properties and thermal degradation behavior of polylactide with an effective intumescent flame retardant. *Polymer Degradation and Stability*, 94:291-296.
DOI: 10.1016/j.polymdegradstab.2008.12.015

162. Hoffendahl, C., Fontaine, G., Bourbigot, S. (2013). Flame retardancy of bio-based polyether-block-amide polymer (PEBAX). *Polymer Degradation and Stability*, 98:1247-1255.
DOI: 10.1016/j.polymdegradstab.2013.03.002

163. Kimura, K., Horikoshi, Y. (2005). Bio-based polymers. *Fujitsu Scientific and Technical Journal*, 41(2):173-180.

164. Feng, J.-X., Su, S.-P., Zhu, J. (2011). An intumescent flame retardant system using *β*-cyclodextrin as a carbon source in polylactic acid (PLA). *Polymers Advanced Technologies*, 22:1115-1122.
DOI: 10.1002/pat.1954

165. Gallos, A., Fontaine, G., Bourbigot, S. (2013). Reactive extrusion of intumescent stereocomplexed poly-L, D-lactide: characterization and reaction to fire. *Polymers Advanced Technologies*, 24:130-133.
DOI: 10.1002/pat.3058

166. Wang, X., Hu, Y., Song, L., Xuan, S., Xing, W., Bai, Z., Lu, H. (2011). Flame retardancy and thermal degradation of intumescent flame retardant poly(lactic

acid)/starch biocomposites. *Industrial & Engineering Chemistry Research*, 50:713-720.
DOI: 10.1021/ie1017157

167. Lin, H.-J., Liu, S.-R., Han, L.-J., Wang, X.-M., Bian, Y.-J., Dong, L.-S. (2013). Effect of a phosphorus-containing oligomer on flame-retardant, rheological and mechanical properties of poly (lactic acid). *Polymer Degradation and Stability*, 98:1389-1396.
DOI: 10.1016/j.polymdegradstab.2013.03.025

168. Biswal, M., Mohanty, S., Nayak, S.K. (2012). Thermal stability and flammability of banana-fiber-reinforced polypropylene nanocomposites. *Journal of Applied Polymer Science*, 125:E432-E443.
DOI: 10.1002/app.35246

169. Fox, D.M., Lee, J., Citro, C.J., Novy, M. (2013). Flame retarded poly(lactic acid) using POSS-modified cellulose. 1. Thermal and combustion properties of intumescing composites. *Polymer Degradation and Stability*, 98:590-596.
DOI: 10.1016/j.polymdegradstab.2012.11.016

Chapter 3

Flammability, thermal decomposition and morphology of char residues of expandable graphite flame retardant poly(lactic acid) (PLA) composites

This chapter will be submitted unaltered for publication in an international journal.

Abstract

This work reports on the effect of commercial expandable graphite (EG) on the flammability and thermal decomposition properties of PLA. The PLA/EG composites were prepared by melt-mixing and their thermal stability, volatile pyrolysis products and flammability characteristics were investigated. The char residues of the composites, after combustion in a cone calorimeter, were analysed with environmental scanning electron microscopy (ESEM). The thermal decomposition stability of the composites improved in the presence of EG. However, the char content was less than expected as per the combination of the wt.% EG added into PLA and the % residue of PLA. The flammability performance of the PLA/EG composites improved, especially at 15 wt.% EG content, due to a thick and strong worm-like char structure. The peak heat release rate (PHRR) improved by 74%, the total smoke production (TSP) by 40% and the specific extinction area (SEA) by 55%. The improvements are attributed to the ability of EG to exfoliate at increased temperatures during which time, three effects occurred: i) cooling effect due to an endothermic exfoliation process, ii) dilution effect due to release of H_2O, SO_2 and CO_2 gases and iii) formation of a protective intumescent char layer. However, the CO and CO_2 yields were found to be unfavourably high due to the presence of EG.

Keywords: polylactic acid; expandable graphite; thermal stability; flammability.

3.1 Introduction

The development of biodegradable polymer composite materials with fire resistance ability and thermal stability can create new uses and extend their industrial applications. Biodegradable polymers in general and poly(lactic acid) (PLA) in particular, have recently gained considerable research interest due to environmental concerns, as well as the shortage and high cost of fossil fuel. Being produced from biobased monomers that are derived from agricultural products, PLA is eco-friendly. In addition, when compounded with additives and made into composite materials, it possesses improved chemical and physical properties. These properties include, but are not limited to, thermal stability and fire resistance when appropriate micro- and/or nano-fillers, such as graphite and expandable graphite (EG) in particular is employed [1-11].

Poly(lactic acid) (PLA) is an aliphatic polyester, generally made from α-hydroxy acid. It is produced by classical synthesis using a bio-based 2-hydroxy propionic acid (i.e. lactic acid) monomer. The latter can be derived from corn or potato starch, cane or beet sugar and cheese whey. PLA is applied in various fields, such as medical and pharmaceuticals, textiles, packaging and composites. It is the most highly produced degradable aliphatic polyester with relatively modest cost. It has advantages that include: eco-friendliness, biocompatibility, compostability, processability and energy efficiency during production. It is, however, marred by several inherent limitations, such as: poor toughness, hydrophobicity and slow crystallization rate, lack of side-chain groups, poor thermal stability and flammability performance. Consequently, there is a need to pursue its modification through additives, such as expandable graphite, in order to achieve properties equivalent and/or superior to the conventional petroleum-based polymers [3-11].

Expandable graphite (EG) is an intercalated compound produced by the chemical or electrochemical intercalation of molecular or atom guests between the layers of graphite. Its structure consists of graphene sheets/layers within which chemical compounds (i.e. oxidants such as H_2SO_4 or HNO_3, and $KMnO_4$) are intercalated [6,12-15]. When exposed to high temperatures (i.e. >190 °C), EG layers are able to exfoliate and expand rapidly in an accordion-like pattern. This is due to the decomposition of the intercalation compounds (e.g. sulfuric acid, H_2SO_4) into water and sulphur dioxide gas. EG further undergoes oxidation by H_2SO_4 with the production of carbon dioxide and sulphur dioxide gases. This exfoliation process is said to

be endothermic. Thus, when used as a flame retardant in a polymer matrix, it triggers temperature decreases in the system to below the polymer combustion temperature. Since the decomposition of an acid and the redox reaction between an acid and graphite result in the production of inert gases (i.e. H_2O, CO_2 and SO_2), it leads to dilution of a mixture of combustible gases. The latter gases limit the concentration of the reagents and the possibility of materials to ignite when exposed to fire. Finally, the resultant carbonaceous intumescent char will form a protective layer between the gaseous and the solid combustible phases. Consequently, the transfer of combustible volatile gases is limited and the oxygen necessary for combustion is excluded, thus the quantity of decomposition gases is reduced [16,17]. This is referred to as a physical mode of action, manifested by a cooling and fuel dilution effect, as well as the formation of a protective barrier [8]. Since EG begins to exfoliate at temperatures below the onset of thermal decomposition of PLA at ~280 °C, EG will act before the thermal decomposition of the biopolymer. It will therefore modify the thermal decomposition pathway of PLA to yield some char and lower the evolution of flammable pyrolysis products [6,13,14,18].

A number of studies were conducted where expandable graphite was used as a flame retardant in various polymer matrices. EG was either used alone or with other additives, in polymers, such as: polyolefins (i.e. low density polyethylene, LDPE; linear low density polyethyele, LLDPE; polypropylene, PP and ethylene vinyl acetate, EVA), polyurethanes, polyamide and PLA [5,12,16,17,19-28]. The polymer/EG composites were generally prepared either by solution-mixing, melt extrusion/blending, milling or injection moulding. For instance, Xie and Qu [19,20] investigated the synergistic effect and the thermo-oxidative degradation behaviour of expandable graphite with halogen-free flame retardant additives (i.e. ammonium polyphosphate, zinc borate, phosphorus-nitrogen compounds and micro-encapsulated red phosphorus) in LLDPE and EVA-based systems. It was found that the combination of EG with other flame retardant additives increased the LOI values, improved flammability performance and increased the thermo-oxidative degradation temperature while reducing the oxidation heat [19]. It was concluded that the phosphorus-nitrogen compound was an efficient synergist, whereas zinc borate acted as smoke suppressant in the polyolefin/EG flame resistant system. On the other hand, the presence of EG in LLDPE [20] improved the thermo-oxidative degradation by lowering the decomposition rates. In another study by Wang *et al*. [17], the fire and water resistance of coatings, based on expandable graphite and an intumescent flame retardant additive composed of ammonium polyphosphate, pentaerythritol and melamine were

compared. It was reported that EG (with 74 μm particle size) showed better anti-oxidation and fire resistance properties and that EG coating (at 8.5%) retained the material fire resistance ability, even after 500 hours of water immersion.

Focke and co-workers [16,21-23] reported on the characterization [16] and use of expandable graphite in thermally conductive phase-change materials [21] and in fire retardant LDPE [22] and poly(vinyl chloride) (PVC) [23] systems, prepared by extrusion and high shear mixing and followed by curing at elevated temperatures. It was reported that although EG more effectively lowered the smoke emission and peak heat release rate (PHRR) than the novel intumescent additive (i.e. phosphate salt of 3,5-diaminobenzoic acid) synthesized in LDPE, the combination of these two led to a further reduction in PHRR. This was attributed to the formation of a heat insulating protective barrier at the solid surface, thus limiting the heat transfer to the substrate and slowing down the material's rate of thermal degradation [22]. In the case of a PVC/EG system (where PVC was plasticized with 60 phr phosphorus ester), it was found that the PHRR and total heat release (THR) were reduced with only 5 wt.% EG inclusion. This was said to be due to an excellent match between the exfoliation onset temperature of EG and the onset of decomposition of the PVC [23].

Only few studies have been reported on the use of expandable graphite as a flame retardant in a PLA matrix [5,29,30]. Wei *et al*. [5] investigated the thermal stability and combustion behaviour of extruded PLA/expandable graphite composites. They reported that the PLA/EG composites showed the highest V-0 ranking (UL-94 flammability test) with a 5 wt.% EG content, whereas 10 wt.% EG was adequate for a lowered rate of combustion, as observed from cone calorimetry. Mu *et al*. [29] reported improved thermal stability, flame retardancy, synergistic effect and anti-dripping performance of melt-blended PLA/EG/{poly(bis(phenoxy)phosphazene)} composites. This was attributed to the combined effect of the gas and condensed phase flame retardant mechanism of EG and phosphazene polymer. On the other hand, Zhu *et al*. [30] observed a synergistic effect of EG/ammonium polyphosphate (APP) (1:3) at 15 wt.% in melt-blended PLA composites and this was attributed to the formation of compact, dense and stable char protection layers that resulted from the filling of gaps between EG flakes with the viscous decomposition products from APP/PLA.

The aim of this study is to investigate the thermal degradation and combustion properties of Cereplast PLA, loaded with commercial grade expandable graphite (EG). This was achieved

by melt blending PLA with EG at 5, 10 and 15 wt.% loadings and characterizing the PLA/EG composites for their: thermal stability, evolved volatile pyrolysis products and flammability performance. This investigation is the basis of a series of studies on the use of a commercial expandable graphite grade as a halogen-free flame retardant for biopolymers and their blends.

3.2 Materials and methods

3.2.1 Materials

Polylactic acid (PLA) is a sustainable 1001 injection molding grade, containing additives derived from starch and other renewable resources, with physical properties as shown in Table 3.1. The commercial expandable graphite (EG) used was an ES250 B5 grade, consisting of 90-95% carbon content, expansion rate of 250-500 cm^3 g^{-1} at a starting temperature range of between 180-300 °C and a particle size of 80% (of the particles) > 300 µm and was supplied by Qingdao Kropfmuehl Graphite, China. The EG used consists of $KMnO_4$ as an oxidant and H_2SO_4 as an intercalant [23,31]. The materials were used as received from the suppliers without any modification/purification, except for drying at 50 °C prior to the compounding.

Table 3.1 Physical properties of PLA, Cereplast Sustainable Resin 1001 grade [32]

Physical property	ASTM Test method	Values
Tensile strength at maximum	D 638	49.6 MPa
Tensile elongation at break	D 638	5.1 %
Tensile modulus	D 638	3,590 MPa
Flexural modulus	D 790	3,360 MPa
Flexural strength	D 790	80 MPa
Gardner impact	D 5420	1.13 J
Notched Izod impact strength (at 23 °C)	D 256	40 J m^{-1}
Temperature deflection under 0.45 MPa	D 648	44 °C
Melt Flow Index 190 °C at 2.16 kg	D 1238	8 g/10min
Density	D792 Method A	1.28 g ml^{-1}

3.2.2 Sample preparation

The samples were compounded (according to the ratios shown in Table 3.2) after drying overnight and were prepared by melt-mixing, using a Brabender-Plastograph with a mixing volume of 55 cm^3. The mixing temperature was 180 °C at a rotational speed of 60 rpm for 12 minutes. This was followed by hot melt-pressing at the temperature of 180 °C under 50 bar for 5 min. in order to obtain 140 x 140 x 2 mm square sheets.

Table 3.2 Sample compositions of the PLA/EG composites

Sample	Composition [wt.%]
PLA	100
PLA/EG-5	95/5
PLA/EG-10	90/10
PLA/EG-15	85/15

3.2.3 Sample analysis

The TGA analyses were carried out in a PerkinElmer STA 6000 simultaneous thermal analyzer. The samples (mass range between 20-25 mg) were heated from 30 to 700 ºC, at a heating rate of 10 ºC min^{-1} under flowing nitrogen (flow rate 20 mL min^{-1}). In this study, the TGA technique was mainly employed to examine the thermal stability and char content of the samples.

The thermal decomposition volatiles of the samples were analysed using the TGA connected to a PerkinElmer Spectrum 100 Fourier-transform infrared (FTIR) spectrometer (TGA-FTIR). The same temperature range and heating rate were used as in the case of TGA analysis and the volatiles were transferred to the FTIR by a Perkin Elmer TL 8000 balanced flow FT-IR EGA system. The spectra were collected continuously during the degradation process.

The flammability tests were performed using a cone calorimeter (FTT, UK) according to ISO 5660-1 at a heat flux of 35 kW m^{-2}. The samples have dimensions of 100 mm x 100 mm x 2 mm and were prepared by compression molding. The samples were wrapped with an aluminum foil on the sides and at the bottom and placed in a retainer frame over low density ceramic wool and then secured on the specimen holder. The following quantities were measured using the cone calorimeter: heat release rate, time to ignition, mass loss rate, as well as carbon monoxide and carbon dioxide yields.

In order to determine the morphology of the char residues after combustion in the cone calorimeter, an FEI Quanta 200 environmental scanning electron microscope (ESEM) was used and the analysis was done at room temperature. The samples were gold-coated by sputtering in order to obtain conductive coatings onto the samples.

3.3 Results and discussion

3.3.1 Thermogravimetric analysis (TGA)

The TGA and DTG results of PLA/EG composites are depicted in Figure 3.1 and the data therefore are summarized in Table 3.3. $T_{2\%}$ and $T_{60\%}$ represent the mass loss temperatures at 2 and 60 wt.% mass loss, respectively, while T_{max} is the temperature at maximum degradation rate. The $T_{2\%}$ is normally considered as the onset temperature of thermal degradation. Furthermore, the char residue % for the composites at 700 °C is also reported.

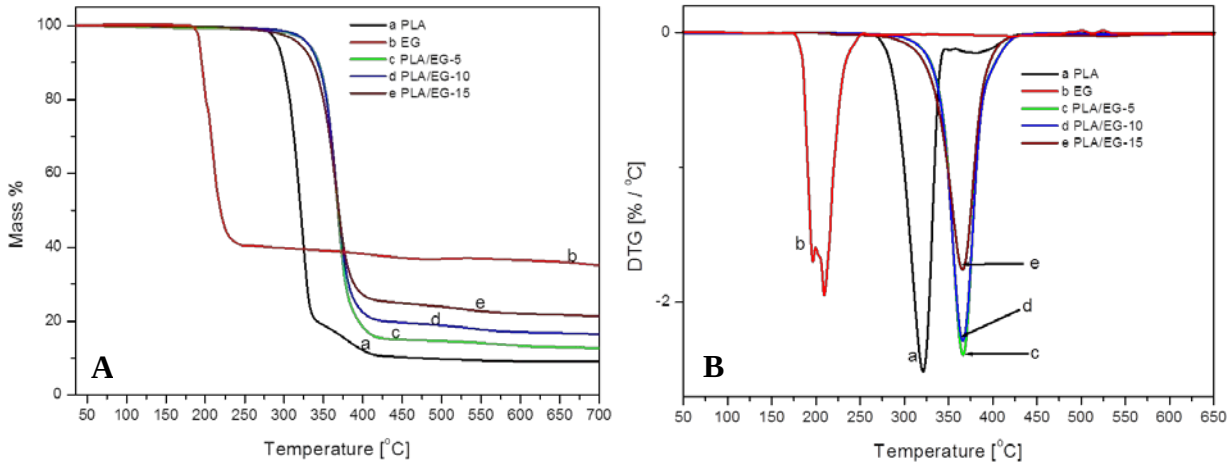

Figure 3.1 TGA (A) and DTG (B) thermograms of PLA/EG composites

Table 3.3 TGA results of investigated PLA/EG composite materials

Sample	$T_{2\%}$ [°C]	$T_{60\%}$ [°C]	T_{max}[a] [°C]	Residue at 700 °C [%]
PLA	282	325	321 & 381	9.1
EG	190	-	196 & 209	35
PLA/EG-5	306	372	368	12.7 (21)
PLA/EG-10	310	374	374	16.4 (25)
PLA/EG-15	291	376	376	21.7 (29)

$T_{2\%}$ and $T_{60\%}$, temperatures at 2 and 60% weight loss, respectively; [a] Temperature at maximum mass loss rate from DTG. The values in parenthesis are the expected residue % (at 700 °C) calculated from: {residue % of PLA (e.g. 9.1%) × weight fraction of the blend (e.g. 0.95) + weight fraction of EG (e.g. 5%) = 21%}.

From Figure 3.1A, it is observed that PLA degrades in two steps and leaves some residues. The first major step occurs over the temperature range of between 270-337 °C and its T_{max} is 321 °C. This major step is due to the thermal degradation of PLA. The thermal degradation of PLA is reported to be a complex process, involving several reaction mechanisms with at least one dominating [33]. The reaction mechanisms may include non-radical and radical reactions, viz: i) random chain scission, ii) depolymerization, iii) thermo-oxidative degradation, iv) intra-molecular and inter-molecular trans-esterifications, v) hydrolytic degradation, vi) pyrolytic elimination and vii) radical reactions. It is, however, considered that the main thermal degradation mechanism for PLA is due to intra-molecular transesterification reactions [34]. In addition, there is a simultaneous recombination of the cyclic oligomers that were formed with linear polyesters through insertion reactions [33]. This led to the formation of cyclic oligomers of lactic acid and lactide. Other thermal decomposition products of PLA that include carbon monoxide and carbon dioxide, acetaldehyde (i.e. believed to decompose into methane and butanedione), methyleketene (i.e. very reactive specie) and water are reported in literature [35]. The second minor thermal degradation step occurs between 337-460 °C with T_{max} of 381 °C. This is due to the degradation of the char from the starch and other renewable resources-based additives in PLA. The thermal degradation of PLA yielded a char residue of about 9.1% at 700 °C, which is attributable to the presence of starch and other renewable resources additives in PLA [36]. Likewise, EG degrades via a two step process with a maximum decomposition temperature of 209 °C. This relates to the exfoliation process of the expandable graphite starting at around 190 °C, due to the escape of SO_2 and CO_2 inert gases [16,22,23].

In the case of PLA/EG composites, all the composites decompose in one major step, occurring over a temperature range of between 258-420 °C (Figures 3.1A & B). It is observed that the incorporation of EG micro-particles in PLA, shifts the thermal degradation curves to higher temperatures (Table 3.3: $T_{2\%}$, $T_{60\%}$ and T_{max}). This is attributed to the good barrier effect of the graphite micro-sheets [37]. It seems that this step has overlapped with the second minor degradation step observed for PLA, since they occur within a similar temperature range. The onset temperature of thermal decomposition ($T_{2\%}$) is higher for the composites when compared with the PLA (Table 3.3), but the increase is inconsistent with EG loadings. The PLA/EG-10 composition recorded the highest value of 310 °C, whereas the PLA/EG-15 yielded the lowest of the composites (i.e. 291 °C). This may be attributed to the quick degradation of EG since the reaction between H_2SO_4 and graphite produces blowing gases above 190 °C. Similar findings were reported by Zhu *et al*. [30] who investigated the synergistic effect between

expandable graphite and ammonium polyphosphate on flame retarded PLA. Furthermore, $T_{60\%}$ and T_{max} increased with EG loadings. This is attributable to the presence of EG, which improved the thermal stability of the PLA/EG composites. The char residue of the composites is higher than that of neat PLA. However, the experimentally observed % residue is less than the calculated % residue (Table 3.3: values in parenthesis). This is probably due to thermal degradation reaction(s) that are not in favour of yielding carbon, instead proceeding by the formation of CO and CO_2 volatile gases. From the TGA results, it can be seen that the presence of EG improved the thermal stability of PLA/EG composites.

3.3.2 Volatile products of PLA and PLA/EG composites: TGA-FTIR analysis

The FTIR spectra of PLA and the PLA/EG composites at temperatures, where the maximum pyrolysis products were given-off, are illustrated in Figure 3.2. It is observed that there are different absorption regions labelled (a to g) consisting of ranges of wavenumbers; a: 3747-3573 cm^{-1}, b: 3008-2500 cm^{-1}, c: 2500-2300 cm^{-1}, d: 2300-2000 cm^{-1}, e: 2000-1700 cm^{-1}, f: 1500-900 cm^{-1} and g: 900-600 cm^{-1}. From this, it may be inferred that the main pyrolysis products are made up of compounds that contain –OH groups (regions a and f), C–H (hydrocarbons, $–CH_3$ and $–CH_2$ groups, both stretching and bending modes) (region b), CO_2 (regions c & g), CO (region d); C=O (carbonyl) containing groups (region e) and aliphatic esters (C–O–C) and C–O stretch (region f) [38-40]. It can be observed that EG exhibits absorption spectra at regions: c, e, f and g, indicating the evolution of CO_2, C–O and carbonyl-containing compounds (C=O), as well as water or acid (–OH) based groups. The bands associated with CO_2 (regions c and g) are strong for EG, showing that EG produces more carbon dioxide gas. On the other hand, PLA exhibits characteristic absorption bands in most of the regions, except at g. This indicates that the pyrolysis products of PLA are possiblely: water, aldehydes, CO_2 and CO and aliphatic esters.

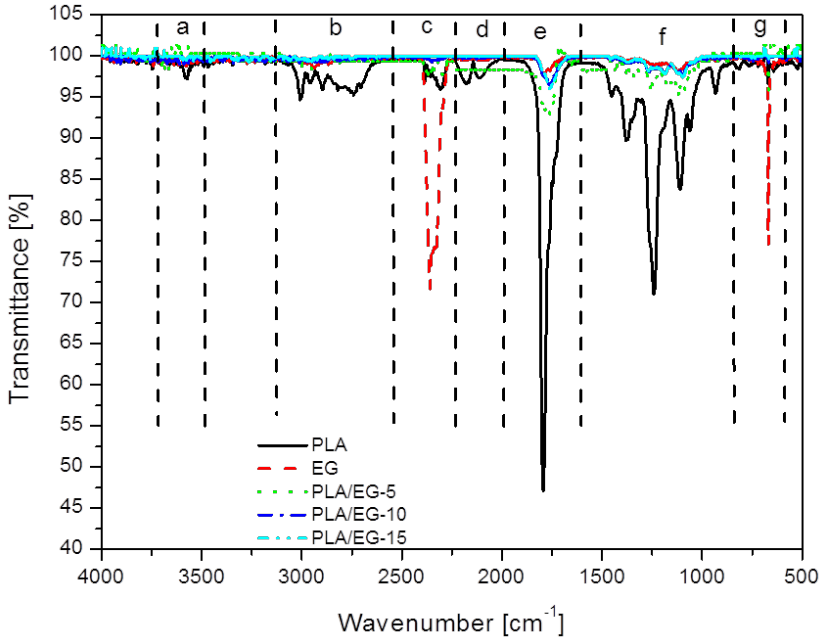

Figure 3.2 FTIR spectra of the PLA/EG composites at the temperatures where the maximum pyrolysis products were given off

For the PLA/EG composites, it is observed that there are fewer pyrolysis products when compared with those of PLA and EG alone. The incorporation of EG in PLA (i.e. 5 wt.% EG), resulted in less intense absorption bands in all the regions. However, at higher EG contents (i.e. 10 and 15 wt.%), only regions (i.e. e and f) associated with carbonyl and aliphatic ester groups, respectively, are observed. This indicates the fact that EG is effective at hindering the formation and evolution of pyrolysis products of the PLA/EG composites.

3.3.3 Cone calorimetry

The cone calorimetric results of the PLA/EG composites are shown in Figures 3.3 to 3.6 and the data are summarized in Tables 3.4 and 3.5. FPI was calculated according to Equation 1 [41]:

$$FPI = \frac{TTI}{PHRR} \qquad (3.1)$$

It can be seen that the incorporation of EG into PLA reduces the time to ignition (TTI) of the composites. The reduction is nonetheless inconsistent with the EG content. TTI is lowered from 44 s for PLA to 31 s for the PLA/EG-5 composite. The lower TTI is attributed to the low thermal stability and quick decomposition of EG, occurring at a lower temperature (i.e. 190

°C, as seen from TGA results in section 3.3.1) than for PLA (i.e. onset temperature of decomposition is 282 °C) [42]. In this case, sufficient quantities of flammable volatiles were released at an earlier stage in order to initiate ignition. Similar findings were reported by Focke *et al*. [22], who observed a decrease in TTI from ~58 s for low-density polyethylene (LDPE) to ~46 s for 10 wt. % EG filled-LDPE.

Table 3.4 Cone calorimetric results (at 35 kW m^{-2} heat flux) of all the investigated samples

Parameter	PLA	PLA/EG-5	PLA/EG-10	PLA/EG-15
TTI [s]	44 ± 0	31 ± 0.9	35 ± 1	33 ± 1
PHRR [kW m^{-2}]	363 ± 0 414 ± 0.01	276 ± 2 224± 2	194 ± 4	109 ± 5
THR [MJ m^{-2}]	30 ± 2	45 ± 1	36 ± 2	26 ± 3
EHC [MJ kg^{-1}]	16 ± 0.1	18 ± 0.6	20 ± 0.1	17 ± 2
av-MLR [g s^{-1} m^{-2}]	8.6 ± 0.3	8.9 ± 0.6	4.7 ± 0.3	2.9 ± 0
MARHE [kW m^{-2}]	199 ± 6	175 ± 3.0	100 ± 2	58 ± 4
FPI [kW m^{-2} s^{-1}]	0.11	0.11	0.18	0.30

TTI, time to ignition; PHRR, peak heat release rate; THR, total heat release; EHC, effective heat of combustion; av-MLR, average mass loss rate; MARHE, maximum average rate of heat emission; and FPI, fire performance index.

The dynamic curves of heat release rate (HRR) in Figure 3.3 for PLA show the characteristic shape of a thermally thin sample [22]. Thermally thin samples are characterised by sharp peak HRR curves when the whole sample is pyrolyzed at once. The HRR curves for thermally thick, char-forming samples, exhibit a sudden rise to a plateau value [22] and this phenomenon is observed in the flame-retarded samples. The HRR is clearly lowered for the PLA/EG composites with respect to the PLA matrix. It is observed that PLA shows a peak shoulder at 363 kW m^{-2} (i.e. at 75 s), which may be related to the starch component, whereas the maximum peak at 414 kW m^{-2} (i.e. at 90 s) relates to PLA. Likewise, the PLA/EG-5 composite shows two clearly defined peaks at 276 (i.e. at 60 s) and 224 kW m^{-2} (i.e. at 130 s). The peak heat release rate (PHRR) values, as a function of EG content of the composites, decreased from 414 kW m^{-2} for PLA to 109 kW m^{-2} (Table 3.4). This shows a reduction of 33, 53 and 74% for the 5, 10 and 15 wt.% EG contents, respectively. The improved fire performance with respect to PHRR is due to the formation of an insulating protective intumescent char barrier at the solid surface of the composites. This is shown in Figure 3.4, where the exfoliated intumescent graphite char layer was formed consistently with EG loadings. This formed a barrier that has limited the transfer of heat from the source to the substrate and consequently slowed down the thermal degradation of the composites, thus minimizing the rate at which flammable volatiles

are evolved [16,22]. This is further confirmed by the average mass loss rate (av-MLR) data in Table 3.4, whereby a reduction is observed from 8.9 g s^{-1} m^{-2} for PLA to 2.9 g s^{-1} m^{-2} for the PLA/EG-15 composite, although the 5 wt.% EG sample proves to be different. Furthermore, the exfoliation of EG is an endothermic process with the attendant consequence of lowering the temperature of the medium, manifesting in a cooling effect of a physical mode of action. The reduction in PHRR is also attributed to a dilution effect of the CO_2 and H_2O, produced during the exfoliation of the EG in the composites [17,42].

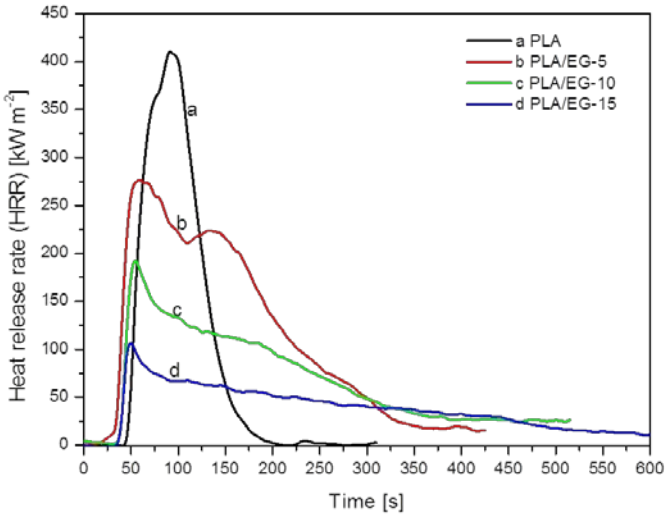

Figure 3.3 Heat release rate (HRR) curves for PLA and PLA/EG composites at various EG contents

As shown in Figure 3.4 for the samples after combustion using the cone calorimeter, PLA left a grey powdery ash with some oily-like molten material on the edges of the retainer frame (Figure 3.4A). In the presence of 5 wt.% EG, a cracked and very lightly covered surface composed of grey ash and carbonaceous exfoliated graphite, is observed (Figure 3.4B). The ash is limited within the frame. At high EG contents (i.e. 10 and 15 wt.%), it is observed that the ash content is high and it even overflowed beyond the retainer frame. As discussed in the introduction, the entire process described for the exfoliation of EG, played a key role in lowering the temperature of the medium, diluting the evolved flammable volatile gases by producing inert gases and forming a barrier of carbonaceous exfoliated graphite. These have aided in improving the flammability performance of the PLA/EG composites.

Figure 3.5 and Table 3.4 illustrate the total heat release (THR) of PLA and the PLA/EG composites. The slope of the THR curve is assumed to be representative of the flame spread rate [42]. It is observed that PLA showed a higher flame spread (i.e. steeper slope) with a THR

value of 30 MJ m^{-2}. The incorporation of EG at 5 and 10 wt.% into PLA, respectively led to 33 and 17% increases in THR compared to PLA. It can be seen that the flame spread rates of the PLA/EG composites were less than that of PLA. A decrease in THR to 26 MJ m^{-2}, corresponding to a 17% reduction was observed for the 15 wt.% EG composite. The results indicate that the composite, at the highest EG loading, is partially protected by the exfoliated EG without complete combustion. At 5 and 10 wt.% EG loadings, however, it seems that the barrier is insufficient to prevent the release of volatile combustion products [5]. Furthermore, from Table 3.4, it can be seen that the effective heat of combustion (EHC) is high for all the composites (i.e. around 17-20 MJ kg^{-1}) when compared to that of PLA (i.e. 16 MJ kg^{-1}). This indicates that the carbon and hydrogen atoms in the composite samples can easily react with oxygen in air to produce carbon dioxide and water and hence release a large amount of heat during combustion [19,20].

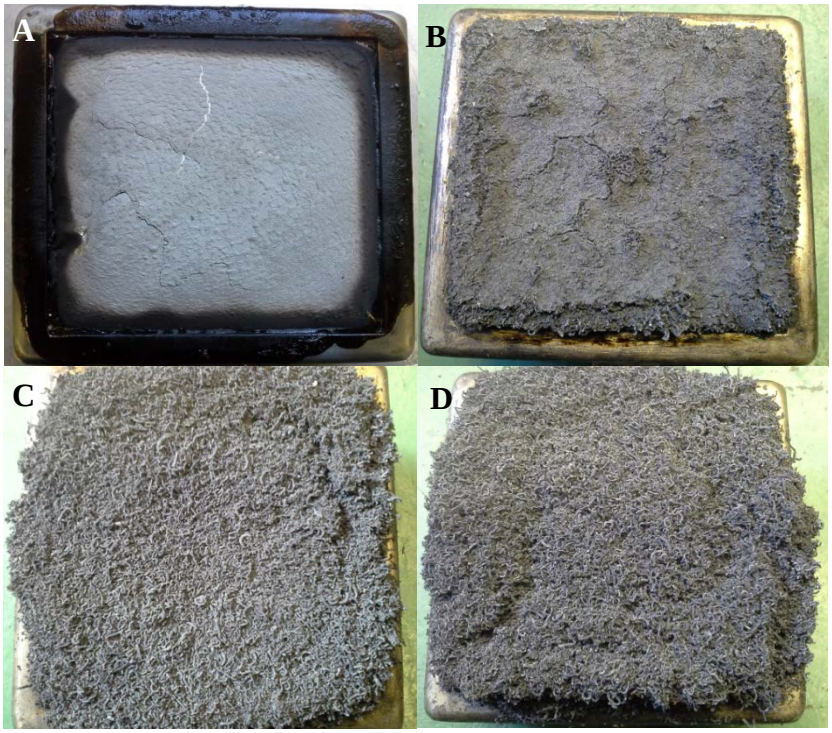

Figure 3.4 Images of ash samples after cone calorimetry tests of (A) PLA, and PLA/EG composites at (B) 5, (C) 10 and (D) 15 wt.% EG

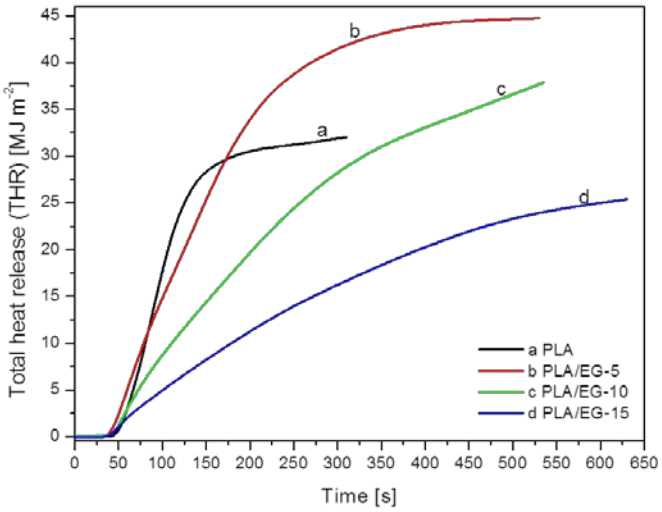

Figure 3.5 Total heat release (THR) curves of PLA and PLA/EG composites

The maximum average rate of heat emission (MARHE) and fire performance index (FPI) are also reported in Table 3.4. The MARHE parameter provides a measure of the inclination for fire development under real scale conditions [22]. Generally, it can be seen that the MARHE is reduced with the incorporation of EG, i.e. from 199 kW m^{-2} for PLA to 58 kW m^{-2} at the highest EG content. It corresponds to 12, 50 and 71% reduction in MARHE at 5, 10 and 15 wt.% EG levels, respectively. This indicates that the PLA/EG composites have less tendency for fire development under real scale conditions. The FPI parameter, which is closely related to a real fire situation, further provides for the estimation of the predicted fire spread rate and size of a real fire. It is considered a good indicator of the contribution of fire growth of materials [41]. The results show no change in the FPI value for the 5 wt.% EG containing sample, while a reduction of 39 and 63% in FPI was observed for the 10 and 15 wt.% EG containing samples, respectively. It is concluded that the PLA/EG composites at high EG loadings (i.e. 10 and 15 wt.%) have little contribution to fire growth in a real fire situation.

Table 3.5 Smoke emission parameters of neat PLA and the PLA/EG composites from cone calorimetry (35 kW m^{-2} heat flux)

Parameter	PLA	PLA/EG-5	PLA/EG-10	PLA/EG-15
TSR [m^2 m^{-2}]	25.5 ± 0.7	31.3 ± 3	21.9 ± 0	15.3 ± 3
SEA [m^2 kg^{-1}]	18 ± 2	11.5 ± 1	11 ± 0	8.1 ± 2
CO (× 10^{-3}) [kg kg^{-1}]	13 ± 0.003	41.7 ± 5	89.4 ± 1	119 ± 1
CO_2 [kg kg^{-1}]	1.3 ± 0.01	1.6 ± 0.01	1.4 ± 0.03	1.3 ± 0.01
CO/CO_2 (× 10^{-3})	10	26.1	63.9	91.4

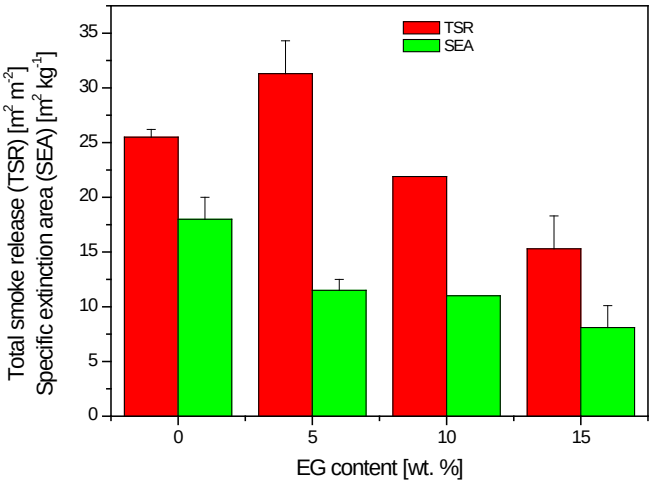

Figure 3.6 Total smoke release (TSR) and specific extinction area (SEA) versus EG content

On the smoke emission behaviour (see Table 3.5 and Figure 3.6) of the samples investigated, it can be seen that the TSR and SEA were improved in the presence of EG. Although the TSR at 5 wt.% EG loading was increased by 19%, it was reduced by 14 and 40% at 10 and 15 wt.% EG contents, respectively. The SEA, which signifies the smoke density, was lowered by 36, 39 and 55% at 5, 10 and 15 wt.% EG loadings, respectively. This indicates that EG acted as a smoke suppressant in the PLA/EG composites. The composites exhibited high CO yields as a function of EG content when compared to PLA. This is related to the presence of EG. Likewise, the CO_2 yield was high in the presence of EG, but comparable to that of PLA at the highest EG content. The CO/CO_2 ratio (Table 3.5) was increased as a function of EG loading. This signifies the incomplete combustion of the composites in the presence of the EG micro-filler.

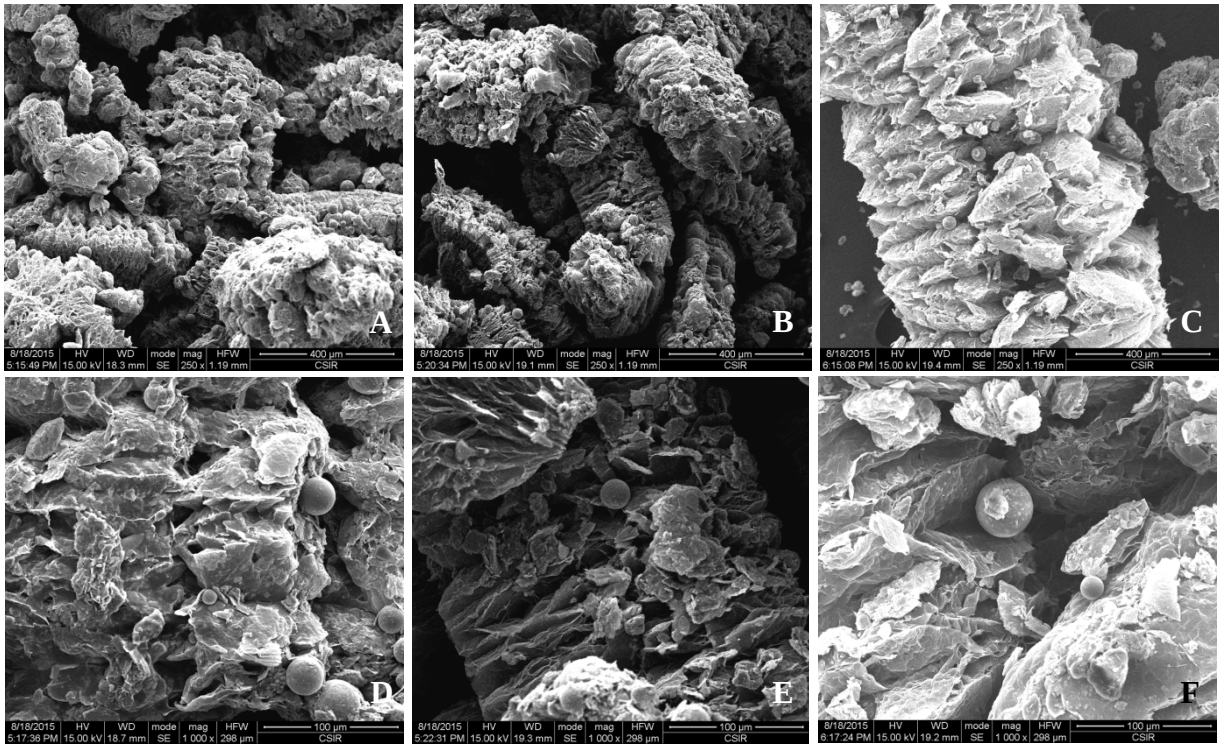

Figure 3.7 SEM micrographs of the char residues after combustion from the cone calorimetry: A & D: PLA/EG-5; B & E: PLA/EG-10, and C & F: PLA/EG-15

In order to further clarify the flame retardancy mechanism of PLA/EG composites, the morphology and structure of the char residues of the composites after combustion, were investigated by ESEM. As shown in Figure 3.7, an exfoliated structure of the residues with embedded microspheres is observed for all the composites investigated after cone calorimetry tests. A weak, short and lighter char structure with numerous holes are seen for the 5 wt.% EG containing composite (Figure 3.7A & D). The presence of holes is believed to originate from the blowing gases in the redox reaction between residual H_2SO_4 and the graphite, according to the reaction equation 3.2 [25]. The surface is covered by grey ash (as seen from Figure 3.4), owing to a large quantity of polymeric material when compared to EG content. Since there was some level of incomplete combustion (i.e. 62%, Table 3.5), this observation is due to char residue from starch and other renewable resource materials and the silicon-based materials (i.e. glass) [36] present in PLA. There is a fairly long, brittle and continuous exfoliated char structure, the surface of which has some pocket-like structures, for the 10 wt.% EG composite (Figure 3.7B & E). A thick and strong worm-like structure is observed for the 15 wt.% EG content composite (Figure 3.7C & F). This formed an effective protective char layer that accounts for the improved fire resistance performance, as observed from the cone calorimetry results.

$$C + 2H_2SO_4 \rightarrow CO_2 + 2SO_2 + 2H_2O \quad (3.2)$$

3.4 Conclusions

Expandable graphite flame retardant Cereplast PLA polymer composites were prepared by melt-blending and their thermal degradation stability, volatile pyrolysis products and flammability properties were studied. The thermal degradation stability of the PLA/EG composites was improved as a function of EG micro-filler. Although, the char content increased with filler loading, the experimental % char content of the composites was less than the sum of the % residue from PLA and the wt.% EG initially mixed with PLA. The flammability performance of the PLA/EG composites was improved, especially at 15 wt.% EG content. The peak heat release rate (PHRR) was improved by 74%, the total smoke production (TSP) reduced by 40% and the specific extinction area (SEA) reduced by 55%. The improvements were due to the key property and ability of EG to exfoliate at elevated temperatures, during which time, three effects (i.e. via physical mode of action) were in place: i) cooling effect due to the endothermic exfoliation process, thus lowering the temperature of the medium, ii) dilution effect due to the release of H_2O, SO_2 and CO_2 inert gases that have diluted the concentration of evolved flammable volatiles and iii) the formation of an effective protective intumescent char layer that prevented heat transfer from the source to the composites substrates and mass transfer from the composite to the flame zone are experienced. This has further excluded the oxygen necessary for combustion. However, since the combustion of EG resulted in CO, CO_2 and heat, the composites were characterized by high CO and CO_2 yields, as well as high THR and EHC.

Acknowledgements

The authors would like to acknowledge the financial support by the National Research Foundation (NRF) and Professional Development Programme (PDP). Acknowledgements are also extended to colleagues and researchers for their undivided attention and support.

References

1. Garlotta, D. (2001). A literature review of poly(lactic acid). *Journal of Polymers and the Environment*, 9(2):63-83.

DOI: 10.1023/A:1020200822435

2. Gupta, A.P., Kumar, V. (2007). New emerging trends in synthetic biodegradable polymers – Polylactide: A critique. *European Polymer Journal*, 43:4053-4074. DOI: 10.1016/j.eurpolymj.2007.06.045
3. Rasal, R.M., Janorkar, A.V., Hirt, D.E. (2010). Poly(lactic acid) modifications. *Progress in Polymer Science*, 35:338-356. DOI: 10.1016/j.progpolymsci.2009.12.003
4. Saeidlou, S., Huneault, M.A., Li, H., Park, C.B. (2012). Poly(lactic acid) crystallization. *Progress in Polymer Science*, 37:1657-1677. DOI: 10.1016/j.progpolymsci.2012.07.005
5. Wei, P., Bocchini, S., Camino, G. (2013). Flame retardant and thermal behavior of polylactide/expandable graphite composites. *Polimery*, 58(5):361-364. DOI: 10.14314/polimery.2013.361
6. Fukushima, K., Murariu, M., Camino, G., Dubois, P. (2010). Effect of expanded graphite/layered-silicate clay on thermal, mechanical and fire retardant properties of poly(lactic acid). *Polymer Degradation and Stability*, 95:1063-1076. DOI: 10.1016/j.polymdegradstab.2010.02.029
7. Huang, G., Gao, J., Wang, X., Liang, H., Ge, C. (2012). How can graphene reduce the flammability of polymer nanocomposites? *Materials Letters*, 66:187-189. DOI: 10.1016/j.matlet.2011.08.063
8. Mngomezulu, M.E., John, M.J., Jacobs, V., Luyt, A.S. (2014). Review on flammability of biofibres and biocomposites. *Carbohydrate Polymers*, 111:149-182. DOI: 10.1016/j.carbpol.2014.03.071
9. Murariu, M., Dechief, A.L., Bonnaud, L., Paint, Y., Gallos, A., Fontaine, G., Bourbigot, S., Dubois, P. (2010). The production and properties of polylactide composites filled with expanded graphite. *Polymer Degradation and Stability*, 95:889-900. DOI: 10.1016/j.polymdegradstab.2009.12.019
10. Vogel, C., Siesler, H.W. (2008). Thermal degradation of poly(ε-caprolactone), poly(L-lactic acid) and their blends with poly(3-hydroxy-butyrate) studies by TGA/FT-IR spectroscopy. *Macromolecular Symposia*, 265:183-194. DOI: 10.1002/masy.200850520
11. Wu, D., Zhang, Y., Zhang, M., Zhou, W. (2008). Phase behaviour and its viscoelastic response of polylactide/poly(ε-caprolactone) blend. *European Polymer Journal*, 44:2171-2183.

DOI: 10.1016/j.eurpolymj.2008.04.023

12. Bai, G., Guo, C., Li, L. (2014). Synergistic effect of intumescent flame retardant and expandable graphite on mechanical and flame-retardant properties of wood flour-polypropylene composites. *Construction and Building Materials*, 50:148-153.
DOI: 10.1016/j.conbuildmat.2013.09.028
13. Lee, J.D. (1995). Concise Inorganic Chemistry. 4th Edition. Chapman & Hall Ltd. Singapore.
14. Sengupta, R., Bhattacharya, M., Bandyopadhyay, S., Bhowmick, A.K. (2011). A review on the mechanical and electrical properties of graphite and modified graphite reinforced composites. *Progress in Polymer Science*, 36:638-670.
DOI: 10.1016/j.progpolymsci.2010.11.003
15. Weil, E.D., Levchik, S.V. (2008). Flame retardants in commercial use or development for polyolefins. *Journal of Fire Sciences*, 26:5-43.
DOI: 10.1177/0734904107083309
16. Focke, W.W., Badenhorst, H., Mhike, W., Kruger, H.J., Lombaard, D. (2014). Characterization of commercial expandable graphite fire retardants. *Thermochimica Acta*, 584:8-16.
DOI: 10.1016/j.tca.2014.03.021
17. Wang, Z., Han, E., Ke, W. (2007). Influence of expandable graphite on fire resistance and water resistance of flame-retardant coatings. *Corrosion Science*, 49:2237-2253.
DOI: 10.1016/j.corsci.2006.10.024
18. Bourbigot, S., Fontaine, G. (2010). Flame retardancy of polylactide: An overview. *Polymer Chemistry*, 1:1413-1422.
DOI: 10.1039/c0py00106f
19. Xie, R., Qu, B. (2001). Synergistic effects of expandable graphite with some halogen-free flame retardants in polyolefin blends. *Polymer Degradation and Stability*, 71:375-380.
PII: S0141-3910(00)00188-9
20. Xie, R., Qu, B. (2001). Thermo-oxidative degradation behaviours of expandable graphite-based intumescent halogen-free flame retardant LLDPE blends. *Polymer Degradation and Stability*, 71:395-402.
PII: S0141-3910(00)00190-7

21. Mhike, W., Focke, W.W., Mofokeng, J.P., Luyt, A.S. (2012). Thermally conductive phase-change materials for energy storage based on low-density polyethylene, soft Fischer-Tropsch wax and graphite. *Thermochimica Acta*, 527:75-82.
DOI: 10.1016/j.tca.2011.10.008
22. Focke, W.W., Kruger, H.J., Mhike, W., Taute, A., Roberson, A., Ofosu, O. (2014). Polyethyelene flame retarded with expandable graphite and a novel intumescent additive. *Journal of Applied Polymer Science*, 40493:1-8.
DOI: 10.1002/app.40493
23. Focke, W.W., Muiambo, H., Mhike, W., Kruger, H.J., Ofosu, O. (2014). Flexible PVC flame retarded with expandable graphite. *Polymer Degradation and Stability*, 100:63-69.
DOI: 10.1016/j.polymedegradstab.2013.12.024
24. Uhl, F.M., Yao, Q., Nakajima, H., Manias, E., Wilkie, C.A. (2005). Expandable graphite/polyamide-6 nanocomposites. *Polymer Degradation and Stability*, 89:70-84.
DOI: 10.1016/j.polymdegradstab.2005.01.004
25. Pang, X.-Y., Weng, M.-Q. (2014). Preparation of expandable graphite composite under the auxiliary intercalation of zinc sulfate and its flame retardancy for ethylene/vinyl acetate copolymer. *International Journal of ChemTech Research*, 6(2):1291-1298.
26. Gao, L., Zheng, G., Zhou, Y., Hu, L., Feng, G., Xie, Y. (2013). Synergistic effect of expandable graphite, melamine polyphosphate and layered double hydroxide on improving the fire behavior of rosin-based rigid polyurethane foam. *Industrial Crops and Products*, 50:638-647.
DOI: 10.1016/j.indcrop.2013.07.050
27. Gao, L., Zheng, G., Zhou, Y., Hu, L., Feng, G., Zhang, M. (2014). Synergistic effect of expandable graphite, diethyl ethylphosphonate and organically-modified layered double hydroxide on flame retardancy and fire behavior of polyisocyanurate-polyurethane foam nanocomposite. *Polymer Degradation and Stability*, 101:92-101.
DOI: 10.1016/j.polymdegradstab.2013.12.025
28. Qian, L., Feng, F., Tang, S. (2014). Bi-phase flame-retardant effect of hexa-phenoxy-cyclotriphosphazene on rigid polyurethane foams containing expandable graphite. *Polymer*, 55:95-101.
DOI: 10.1016/j.polymer.2013.12.015
29. Mu, X., Yuan, B., Hu, W., Qiu, S., Song, L., Hu, Y. (2015). Flame retardant and anti-dripping properties of polylactic acid/poly(bis(phenoxy)phosphazene)/expandable graphite composite and its flame retardant mechanism. *RSC Advances*, 5:76068-76078.

DOI: 10.1039/c5ra12701g

30. Zhu, H., Zhu, Q., Li, J., Tao, K., Xue, L., Yan, Q. (2011). Synergistic effect between expandable graphite and ammonium polyphosphate on flame retarded polylactide. *Polymer Degradation and Stability*, 96:183-189.
DOI: 10.1016/j.polymdegradstab.2010.11.017
31. http://www.gk-graphite.cn/fileadmin/user_upload/PDF/List_standard.pdf (26/10/2015).
32. http://trellisbioplastic.com/wp-content/uploads/2014/08/Sustainable-1001-Property-Guide.pdf (26/10/2015).
33. Carrasco, F., Pagès, P., Gámez-Pérez, J., Santana, O.O., Maspoch, M.L. (2010). Processing of poly(lactic acid): Characterization of chemical structure, thermal stability and mechanical properties. *Polymer Degradation and Stability*, 95:116-125.
DOI: 10.1016/j.polymdegradstab.2009.11.045
34. Nicolae, C.-A., Grigorescu, M.A., Gabor, R.A. (2008). An investigation of thermal degradation of poly(lactic acid). *Engineering Letter*, 16:4, EL_16_4_16.
35. Kopinke, F.-D. Remmler, M. Mackenzie, K. Milder, M. Wachsen, O. (1996). Thermal decomposition of biodegradable polyesters – II. Poly(lactic acid). *Polymer Degradation and Stability*, 43:329-342.
PII: S0141-3910(96)00102-4
36. Chapple, S., Anandjiwala, R., Ray, S.S. (2013). Mechanical, thermal, and fire properties of polylactide/starch blend/clay composites. *Journal of Thermal Analysis and Calorimetry*, 113:703-712.
DOI: 10.1007/s10973-012-2776-6
37. Wang Y., Lin, C.-S. (2014). Preparation and characterization of maleated polylactide-functionalized graphite oxide nanocomposites. *Journal of Polymer Research*, 21:334 (pp: 1-14).
DOI: 10.1007/s10965-013-0334-y
38. Pavia, D.L., Lampman, G.M., Kriz, Jr. G.S. (1979). Introduction to Spectroscopy: A Guide for Students of Organic Chemistry. Saunders College Publishing, Harcourt Brace Jovanovich College Publishers, Philadelphia.
39. Persenaire, O., Alexandre, M., Degée, P., Dubois, P. (2001). Mechanisms and kinetics of thermal degradation of poly(ε-caprolactone). *Biomacromolecules*, 2:288-294.
DOI: 10.1021/bm0056310

40. Liu, X., Khor, S., Petinakis, E., Yu, L., Simon, G., Dean, K., Bateman, S. (2010). Effects of hydrophilic fillers on the thermal degradation of poly(lactic acid). *Thermochimica Acta*, 509:147-151.
DOI: 10.1016/j.tca.2010.06.015
41. Wu, X., Wang, L., Wu, C., Yu, J., Xie, L., Wang, G., Jiang, P. (2012). Influence of char residues on flammability of EVA/EG, EVA/NG and EVA/GO composites. *Polymer Degradation and Stability*, 97:54-63.
DOI: 10.1016/j.polymdegradstab.2011.10.011
42. Jin, J., Dong, Q.-x., Shu, Z.-j., Wang, W.-j., He, K. (2014). Flame retardant properties of polyurethane/expandable graphite composites. *Procedia Engineering*, 71:304-309.
DOI: 10.1016/j.proeng.2014.04.044

Chapter 4

Morphology, thermal and dynamic mechanical properties of poly(lactic acid/expandable graphite (PLA/EG) flame retardant composites

This chapter will be submitted unaltered for publication in an international journal.

Abstract

This work reports on the effect of expandable graphite (EG) on the morphology, thermal and dynamic mechanical properties of flame retardant PLA/EG composites. The composites were prepared by melt-mixing and their structure, morphology, melting and crystallization behaviour, as well as their dynamic mechanical properties were investigated by X-ray diffraction (XRD), scanning electron microscopy (SEM), differential scanning calorimetry (DSC) and dynamic mechanical analysis (DMA) techniques. It was found that graphite layers still existed in an aggregate structure with poor filler dispersion resulting in the lack of interfacial adhesion between EG and the PLA matrix. The presence of EG micro-particles did not favour the crystallization of PLA, increased the glass transition temperature and showed a reduction in the crystallinity of the composites. The composites showed enhanced storage and loss moduli, especially at higher EG contents (i.e. 10 and 15 wt.%). The glass transition from the loss modulus and damping factor varied inconsistently with EG content. The use of commercial expandable graphite as filler in PLA can preserve the thermal properties of injection molding grade Cereplast PLA, while improving the fire resistance of PLA/EG flame retardant composites.

Keywords: polylactic acid, expandable graphite, morphology, melting, crystallization, dynamic mechanical analysis.

4.1 Introduction

Of recent, the development and characterization of biodegradable polymer composites is of intense research interest due to their potential applications in industry. Among all the biodegradable polymers, poly(lactic acid) (PLA) is the most highly produced biodegradable aliphatic polyester and it is available at a relatively modest cost. It is applied in the medical and pharmaceuticals, textiles, packaging and composites industries. PLA has advantages of eco-friendliness, biocompatibility, processability and energy efficiency during production. There are limitations inherent to PLA that include: poor toughness, hydrophobicity, slow crystallization rate, lack of side-chain groups and poor flammability performance. However, the development of PLA/filler composites is one approach to improve these flaws. For example, in our previous study, it was reported that PLA/expandable graphite (EG) composites showed improved fire resistance, reduced smoke density and better thermal degradation stability (see Chapter 3). It is, therefore, important to further examine the effect of EG on the morphology and structure, melting and crystallization behaviour, as well as dynamic mechanical properties of PLA/EG composites [1-10].

The structure and morphology of a polymer/filler composite are fundamental to the understanding and furthering of, the applicability of composite materials. The valuable information provided by these properties include: i) the spatial arrangement of atoms, molecules and layers of polymer and platelet-like filler material, such as PLA and EG, ii) the distribution and/or dispersion of filler within the polymer matrix, iii) the intercalation and/or exfoliation of a filler and iv) the level of interaction (i.e. interfacial adhesion) between the filler and the matrix. Different technologies are used to obtain the above mentioned and include *inter alia*, X-ray diffraction (XRD) and scanning electron microscopy (SEM). XRD is widely used to investigate the dispersion of clays and/or graphite, whereby intercalated and/or exfoliated polymer/filler composites may be classified on the basis of the change in peak position due to inter-gallery/layer spacing of the filler [11]. For instance, it was reported that the melt-mixing process, during the fabrication of PLA/filler (i.e. clay and/or graphite) composites, can not separate the graphite layers in which the majority still existed in an aggregate structure [3,12]. In the case of graphite, the structure and morphology of EG was characterized through Raman spectroscopy, SEM and XRD. EG is, by definition, an intercalated compound produced by the chemical or electrochemical intercalation of molecular or atom guests between the layers of graphite. Its structure consists of graphene sheets/layers within which chemical compounds

(i.e. oxidants such as H_2SO_4 or HNO_3 and $KMnO_4$) are intercalated [3,13-16]. Focke *et al*. [17] reported that commercial expandable graphite exhibited a characteristic reflection peak and/or, at least, a shoulder similar to that of natural graphite due to the presence of extra unreacted or partial sulphate intercalated graphite layers. They also identified other low angle reflection peaks that were attributed to sulfuric acid intercalated graphite and graphite oxide phases. Other authors reported that EG particles were uniformly dispersed in PLA and that the composites showed flat surfaces with some holes. This was explained thus: that the EG particles were large and presented poor compatibility with the PLA matrix [18]. Such structural and morphological characteristics have an influence on other properties, such as thermal transitions (i.e. melting and crystallization) of the polymer composite.

The thermal transition temperatures of polymers and their composites are an integral part of the understanding of the possible working temperatures (e.g. processing) of materials. They are influenced by the structure and morphology of the materials. These provide information on the melting and crystallization properties (i.e. temperatures and enthalpies). For instance, the melting temperature (T_m) of a polymer crystal is dependent on the crystal and/or the lamellar thickness (l) [19]. Furthermore, melting is affected by various factors including i) chemical structure (i.e. stiffness of the main polymer chain, presence of polar groups, as well as the type and size of side groups present on the polymer backbone), ii) molar mass and degree of chain branching and iii) copolymerization. For example, the melting of PLA was influenced by the incorporation of filler [3]. In the study where the effect of two layered silicate clays (montmorillonite and fluoro-hectorite) on the thermal, mechanical and degradation properties of PLA were investigated, Fukushima *et al*. [3] reported that the presence of clays led to PLA melting with double peaks. This they explained as being due to the presence of the α- and β-crystal structures. The former is said to be highly ordered, as it melts at high temperatures and is the most prevalent polymorph of PLA. The latter was related to a low melting endotherm with imperfect crystal structure. Cereplast PLA and its clay composites also exhibited two endotherms and they were attributed to the melting of crystallites with different sizes and/or perfection ordering [20].

The degree of crystallinity was also found to have an important effect on the physical properties of a polymer. Crystallization, defined as the process whereby an ordered structure is produced from a disordered phase (e.g. a melt), is said to be a two-step process of nucleation and growth of the crystal nucleus. This is influenced by various crystallization thermodynamic and kinetic

theories. From this, the crystallization temperature (T_c) of polymeric materials (e.g. PLA) is obtained [19,21]. Generally, PLA may not crystallize on cooling since its crystallization is typically too slow to develop significant crystallinity. It may, however, be induced by strain such as in processes used to produce bottles [3]. Its crystallization may be mainly observed on heating by DSC where a cold-crystallization exotherm is observed above T_g. Fukushima *et al*. [3] and Chapple *et al*. [20] reported an enhanced cold-crystallization rate in the presence of clays, as shown by a reduced cold-crystallization temperature (T_{cc}), especially at high filler loadings [3]. This was related to the effective nucleation role played by clays [20]. It was also reported that the overall crystallinity of the PLA/clay composites was increased in the presence of clays due to the combination of crystallization during cooling and heating stages [3] and the d-isomer content of the pure PLA [20].

The transition from a glass to a rubber-like state, known as the glass transition temperature (T_g), marks a region where dramatic changes in the physical properties (e.g. hardness and elasticity) are observed [21]. It is affected by several factors including i) chemical structure (i.e. chain flexibility, steric effects and/or nature of side groups), ii) copolymerization and iii) molecular architecture (i.e. molar mass, branching and crosslinking). The value of T_g may: i) increase with increasing molar mass, ii) either be reduced in the presence of a small number of branches or increased when high density branching, is present on a polymer chain and iii) be increased in the presence of chemical crosslinks due to reduced specific volume, thus reduced free volume and difficulty in molecular motion [19,21]. For example, the T_g of PLA/clay composites (i.e. 10 wt.% montmorillonite and fluoro-hectorite) was lowered by 7 and 16 °C, respectively and this was attributed to a reduction in the molecular weight of PLA during melt processing [22]. Chapple *et al*. [20] reported a slight reduction in T_g of pure and Cereplast PLA/clay composites and was explained by the plasticizing effect of the organic modifier in the clay. There are two measurement techniques used to detect this transition (T_g): the dynamic and static measurements. The static measurement technique uses the traditional differential scanning calorimetry (DSC), whereby the change in heat capacity as a function of temperature is followed. On the other hand, the dynamic measurement technique uses the dynamic mechanical analysis (DMA), where T_g is obtained by a rapid change in modulus, which is dependent on the frequency of the applied force [19,21].

The dynamic mechanical properties of a polymer are also dependent on the presence of filler in the polymer/filler systems. It is generally expected that the addition of fillers to polymer

matrices would result in improved properties, including better tensile and flexural strengths, higher modulus, dimensional stability and higher heat distortion temperature [23]. In the DMA, different modulus values: complex modulus (E*), elastic modulus (E´) and loss (i.e. imaginary) modulus (E˝) are calculated from the material response to the sine wave. Consequently, the ability of a material to return or store energy, its ability to lose energy and the ratio of these effects (i.e. tan δ, also called damping factor), may be examined [24]. For example, the addition of clay in PLA was reported to have a considerable effect on the elastic properties of the composites. The storage modulus as a function of temperature increased in the presence of clay (i.e. 5 and 10 wt.%), below and above T_g. This was associated with the i) reinforcement effect of clays, ii) good clay dispersion level, iii) increased polymer composite crystallinity and iv) more restricted movements of the polymer chains above T_g [22]. Although expandable graphite has been used as a flame retardant in LDPE [25], PVC [26] and PLA [27], relatively less work has been presented on the effect of commercial EG on the morphology and structure, melting and crystallization, as well as the dynamic mechanical properties of PLA/EG flame retardant composites.

The aim of this study is to investigate the morphology, structure, melting and crystallization, and the dynamic mechanical properties of flame retardant PLA/EG composites. The objectives are: i) to prepare PLA/EG biocomposites by melt-mixing at 5, 10 and 15 wt.% EG loadings and ii) to characterize the biocomposites using X-ray diffraction (XRD), scanning electron microscopy (SEM), differential scanning calorimetry (DSC) and dynamic mechanical analysis (DMA).

4.2 Materials and methods

4.2.1 Materials

The poly(lactic acid) (PLA) used in this study was a Cereplast Sustainable 1001 injection molding grade containing additives derived from starch and other renewable resources as well as silicon-based naterials (i.e. glass) [20] with physical properties as shown in Table 4.1. The commercial expandable graphite (EG) used was an ES250 B5 grade consisting of 90-95% carbon content, expansion rate of 250-500 $cm^3\ g^{-1}$ at a starting temperature range of between 180-300 °C and a particle size (of 80% of the particles) > 300 µm, supplied by Qingdao Kropfmuehl Graphite, China. The EG contained $KMnO_4$ as an oxidant and H_2SO_4 as an

intercalant [17,28]. The materials were used as received from the suppliers without any modification/purification except for drying in an oven at 50 °C overnight prior to the sample preparation.

Table 4.1 Physical properties of PLA, Cereplast Sustainable Resin 1001 grade [29]

Physical property	ASTM Test method	Values
Tensile strength at maximum	D 638	49.6 MPa
Tensile elongation at break	D 638	5.1%
Tensile modulus	D 638	3,590 MPa
Flexural modulus	D 790	3,360 MPa
Flexural strength	D 790	80 MPa
Gardner impact	D 5420	1.13 J
Notched Izod impact strength (at 23 °C)	D 256	40 J m^{-1}
Temperature deflection under 0.45 MPa	D 648	44 °C
Melt Flow Index 190 °C at 2.16 kg	D 1238	8 g/10min
Density	D792 Method A	1.28 g ml^{-1}

4.2.2 Sample preparation

Samples were compounded according to the ratios shown in Table 4.2 after drying overnight. They were prepared by melt-mixing technique using a Brabender-Plastograph with a mixing volume of 55 cm^3. The mixing temperature was 180 °C at a rotational speed of 60 rpm for 12 minutes. This was followed by hot melt pressing at 180 °C under 50 bar for 5 min. in order to obtain 140 mm x 140 mm x 2 mm square sheets.

Table 4.2 Sample compositions of PLA/EG composites

Sample	Composition [wt.%]
PLA	100
PLA/EG-5	95/5
PLA/EG-10	90/10
PLA/EG-15	85/15

4.2.3 Sample analysis

The crystalline structures of EG and PLA/EG were determined through X-ray diffraction (XRD). A D8 Advance diffractometer (BRUKER AXS, Germany) with PSD Vantec-1 detectors and Cu K_α radiation (λ = 1.5406 Å = 0.15406 nm), a tube voltage of 40 kV, a current of 40 mA and a V20 slit were used. The samples were scanned in locked couple mode with

2θ increments (2θ range of 0-100°) in 0.5 s steps. The inter-layer distance (i.e. *d*-spacing) of the EG in the composites was calculated using the Bragg's diffraction Equation 4.1 [20].

$$2d \sin\theta = n\lambda \qquad \text{(i.e. where n = 1)} \qquad (4.1)$$

DSC analyses were done on a PerkinElmer Pyris-1 differential scanning calorimeter under nitrogen flow (20 mL min^{-1}). Samples were held at 0 °C for 1 min., heated from 0 to 180 °C at a heating rate of 10 °C min^{-1}, cooled at the same rate and then heated again under similar conditions. The peak temperatures of melting and crystallization, as well as the melting and crystallization enthalpies, were determined from the second scansin order to eliminate any thermal history effects. Also reported are the glass transition temperature values as determined from the heating curves. Results are reported as average values of three tests with standard deviations.

In order to determine the morphology of the cryo-fractured samples, a TESCAN VEGA3 scanning electron microscope (SEM) was used and the analysis was done at room temperature. The samples were gold coated by sputtering for 60 s in order to produce conductive coatings onto the samples.

The dynamic mechanical properties of the samples were tested using a PerkinElmer Diamond DMA dynamic mechanical analyser. The tests were performed in a bending (dual cantilever) mode at a frequency of 1 Hz and a heating rate of 3 °C min^{-1}, under nitrogen atmosphere. The samples were heated from -90 to 130 °C.

4.3 Results and discussion

4.3.1 X-ray diffraction (XRD)

The XRD results for the composites investigated are shown in Figures 4.1 and 4.2. The corresponding data are summarized in Table 4.3. EG exhibits diffraction peaks with different intensities within a 2θ range of 24-30° (Figure 4.1A). From these, three reflection peaks are noted. Firstly, a strong peak is observed at 2θ = 25.8°, which is related to an interlayer distance of 0.35 nm. Since EG consists of an acid (H_2SO_4) intercalated within its layers [17], this major peak is attributed to the acid-intercalated layers of expandable graphite [30]. Secondly, a peak

shoulder is observed at $2\theta = 26.6°$ with a *d*-spacing of 0.34 nm (Table 4.3) between the graphite sheets. This is due to the stacking of single layers of graphite with a (002) basal reflection [3,4,12,17]. Finally, a broad peak at around $2\theta = 28.1°$ with a *d*-spacing value of 0.33 nm is also noted. PLA shows different peaks at $2\theta = 9.5$, 16.6, 19 and 28.7° (Figure 4.1B). The second and third peaks (i.e. $2\theta = 16.6$ and 19°), respectively, correspond to *d*-spacing values of 0.27 and 0.24 nm, with (200/110) and (203) basal reflections. Both are attributed to the stable α-form of PLA with an orthorhombic crystalline structure [31-33]. The other diffraction peaks at $2\theta = 9.5$ and 28.6° are related to the additives derived from starch and other renewable resource (see section 4.2.1) [20]. Additionally, it is observed that the XRD diffractogram of PLA consists of a broad halo within a 2θ range of 10-26° and this is attributed to the amorphous structure of the PLA matrix [20,34,35].

Table 4.3 Basal spacing of neat EG, PLA and PLA/EG composites

Sample	2θ [degree]	*d*-spacing [nm]
EG	25.8, 26.6 & 28.1	0.35, 0.34 & 0.33
PLA	9.5, 16.6, 19 & 28.7	0.47, 0.27, 0.24 & 0.32
PLA/EG-5	9.4, 16.5, 19.0, 26.5 & 28.6	0.47, 0.27, 0.24, 0.34 & 0.32
PLA/EG-10	9.4, 16.4, 19.0, 26.4 & 28.6	0.47, 0.27, 0.24, 0.34 & 0.32
PLA/EG-15	9.4, 16.4, 18.9, 26.4 & 28.6	0.47, 0.27, 0.24, 0.34 & 0.32

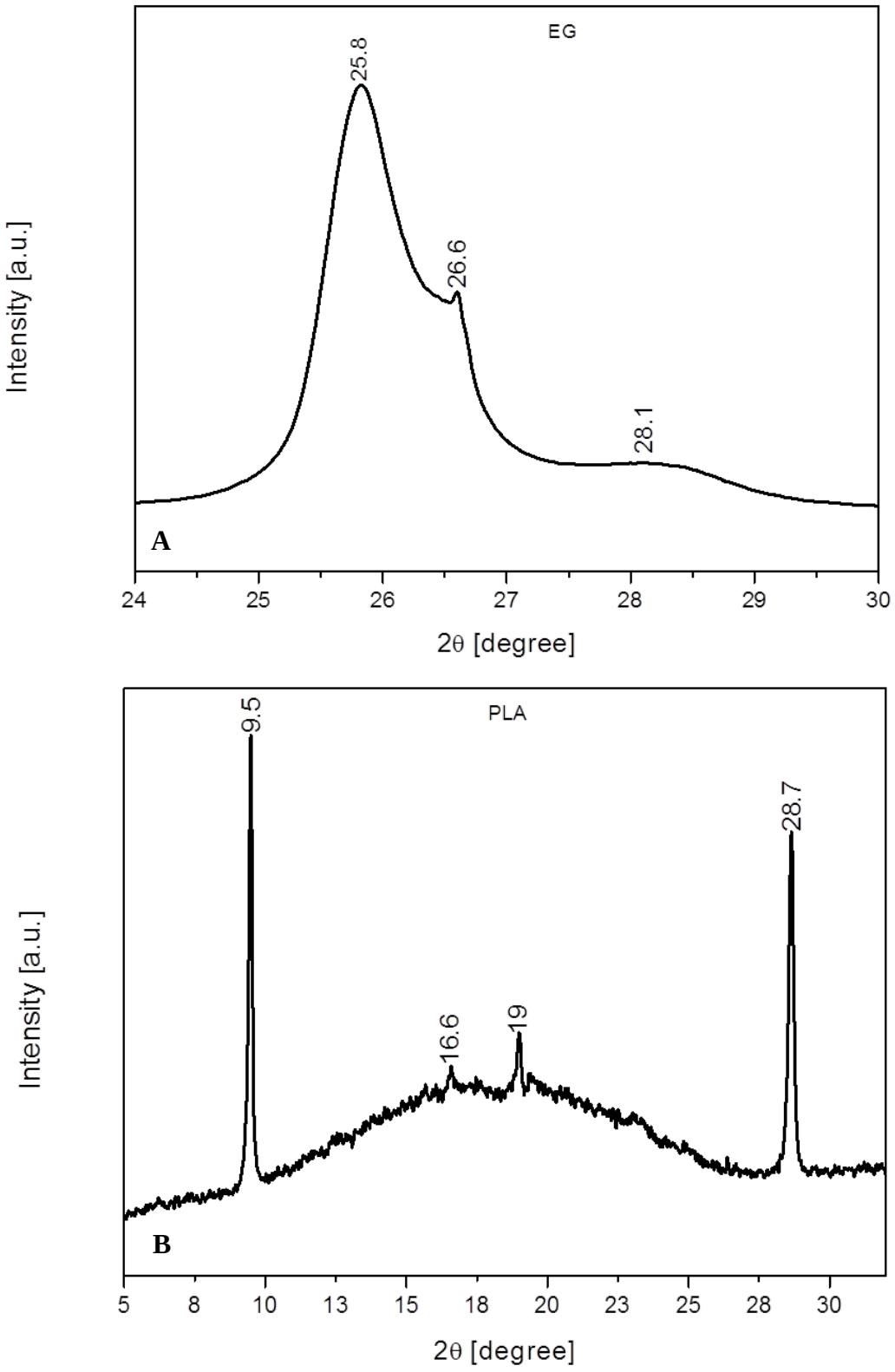

Figure 4.1 X-ray diffraction spectra of (A) EG and (B) PLA

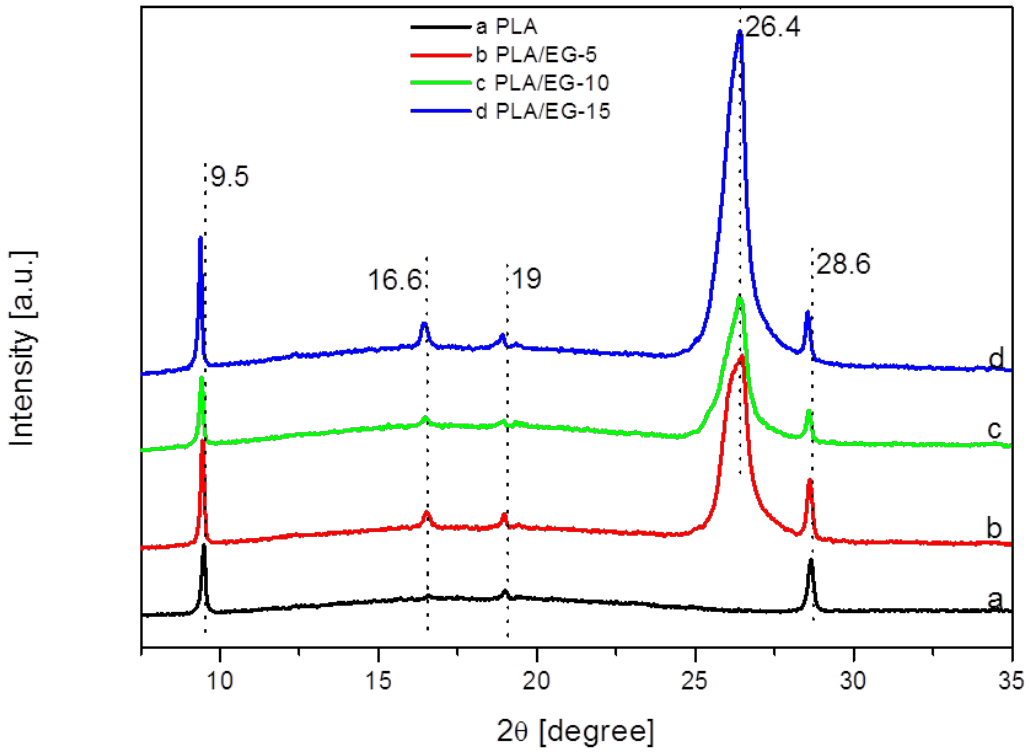

Figure 4.2 X-ray diffraction spectra of PLA/EG composites

The XRD patterns of the PLA/EG composites are shown in Figure 4.2. It can be seen that they are characterized by a broad halo (i.e. 2θ range of between 10-26°) and several diffraction peaks. The existence of a diffraction peak at $2\theta \sim 26.5°$, in addition to those attributed to PLA (i.e. $2\theta = 9.4$, 16.5, 19.0 and 28.7°), is related to the EG within the PLA matrix. Generally, the peak at $2\theta \sim 26.5°$, due to EG occurs at the same position in all the composites. This suggests that the melt-mixing process could not separate the graphite layers, thus the majority of them still exist in the aggregate structure (i.e. EG layered stacks). Similar findings were reported by Fukushima *et al*. [3] and Narimissa *et al*. [12] in their studies of melt-processed PLA/nano-filler composites. In the case of the EG component of the composites, some peaks (especially $2\theta = 25.8$ and 28.1°) are absent after melt-mixing, which suggests that the acid intercalated layers may have arranged themselves into agglomerates that are distributed throughout the matrix. As seen from Table 4.3, there was generally no change in the 2θ angles of the PLA/EG composites with respect to the neat materials. The diffraction peak intensities related to EG from the PLA/EG composites increased at high EG loadings in the order: EG-10 < EG-5 < EG-15 (Figure 4.2). From the results, it is concluded that melt-mixing of EG with PLA did not separate the graphite layers and that they were still present in an aggregate form in the composites.

4.3.2 Scanning electron microscopy (SEM)

The SEM images of the cryo-fractured surfaces of neat PLA and PLA/EG composites at different magnifications are shown, respectively, in Figures 4.3 and 4.4. The PLA consists of various additives and/or components (Figure 4.3). These additives are in different shapes and sizes with varying degrees of interfacial adhesion with the matrix. Firstly, there are micro-spherical materials (i.e. micro-spheres) that are fairly well distributed in the PLA matrix, as indicated with arrows in Figure 4.3A. Figure 4.3B shows that there is a reasonably good interfacial adhesion between the micro-spheres and the matrix (indicated with an arrow). Secondly, platelet-like materials of different sizes are also recognized (Figure 4.3C) and although there are some gaps between these and the matrix, some level of adhesion can be seen. Thirdly, some droplet-like morphology with good interfacial adhesion and an even distribution are observed (see arrows marked 1 in Figure 4.3D). This is attributed to the presence of starch-derived additives in Cereplast PLA [20,29]. Lastly, little beads-like materials in circular formations (as indicated with arrows marked 2 in Figure 4.3D) are observed. These are attributed to the presence of silicon-based materials (i.e. glass). Such silicon-based materials were identified by Chapple *et al*. [20] in their study of the fire, thermal and mechanical properties of PLA/starch/clay composites.

Figure 4.4 shows the SEM images of the PLA/EG composites with varying EG contents at different magnifications. Generally, the incorporation of EG into PLA shows stacks of graphite layers that exist in the polymer matrix. Specifically from the figure, a number of factors can be alluded to. Firstly, the incorporation of EG into PLA shows a composite surface with the EG filler aggregates (i.e. EG layered stacks) for all the compositions (see arrows marked 1 in Figure 4.4A, C & E). This was also observed in the XRD results (discussed in section 4.3.1). Although these aggregates (i.e. agglomerates) are dispersed in the polymer matrix (especially at 10 and 15 wt.% EG), there is generally a lack of uniformity in the EG dispersion. Secondly, the EG filler exists in different orientations in the PLA matrix i.e. i) normal to- and ii) parallel to-the surfaces of the cryo-fractured composites. The normal to-surface orientation is illustrated by arrows marked 1, while the parallel-to-surface orientation is indicated by arrows marked 2 throughout Figure 4.4. Thirdly, there is an existence of holes on composite surfaces (see arrows marked 3 in Figure 4.4A, C & E). Similar findings were reported by Tang *et al*. [18] for

PLA/EG composites at 20 wt.% EG content. This was attributed to the fact that EG particles were large and presented poor compatibility with PLA [18].

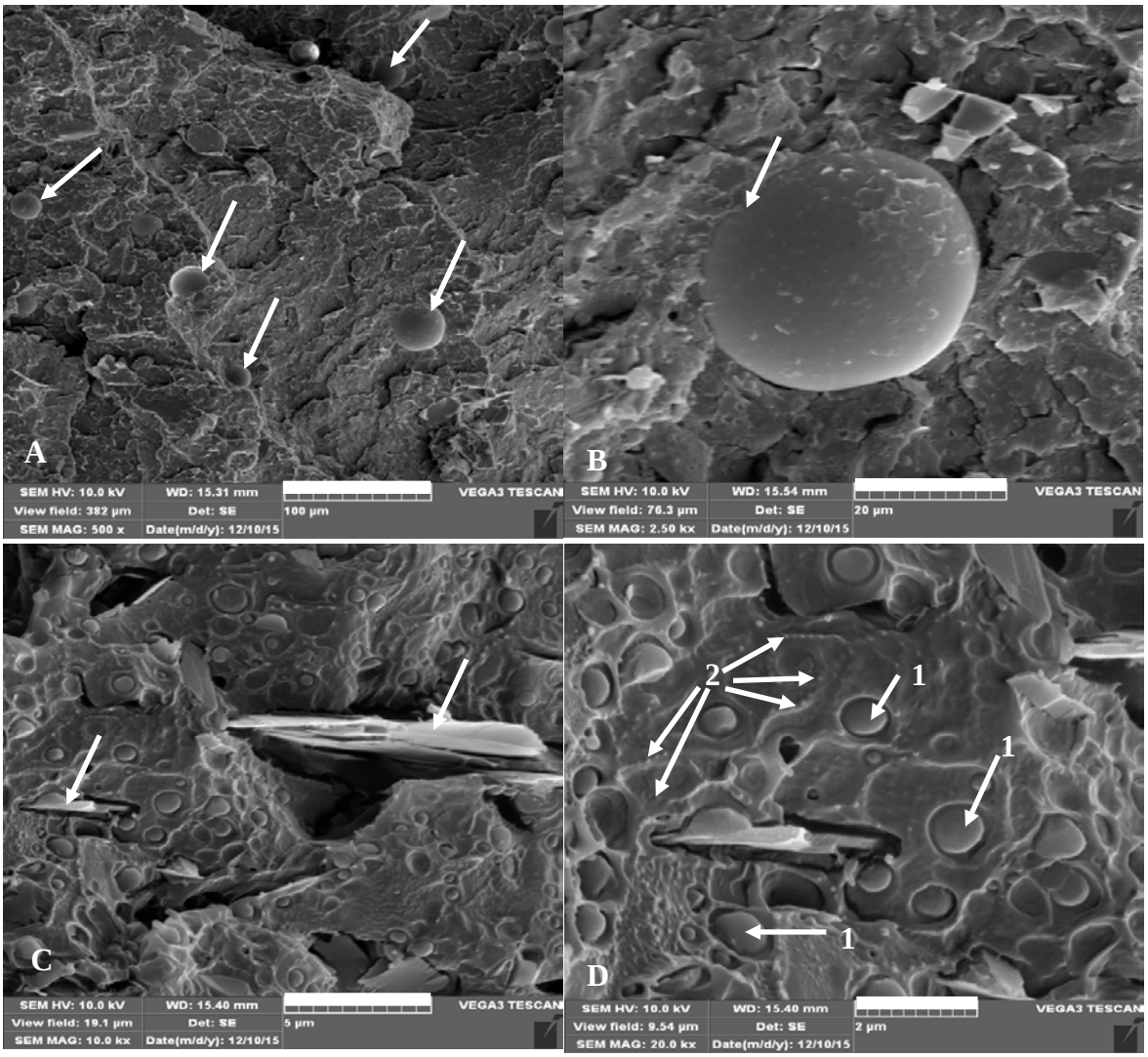

Figure 4.3 SEM micrographs of cryo-fractured surface of PLA at various magnifications: (A) 500x, (B) 2500x, (C) 10 000x and (D) 20 000x

Fourthly, EG filler pull-outs are evident from the cryo-fractured surfaces of the composites, and these increased in frequency with the filler loading (see arrows marked 4 in Figure 4.4A, C, D & E). This suggests the existence of poor interfacial adhesion between EG and PLA [18]. Lastly, the micro-spherical materials are still observed in the PLA/EG composites and they do not seem to be affected by the presence of EG. It can be inferred that although the EG layered stacks were dispersed in the PLA matrix, the PLA/EG flame retardant composites show a lack of i) uniform dispersion of EG, ii) poor compatibility of EG particles with the PLA matrix and thus iii) lack of interfacial adhesion between the PLA matrix and the EG filler.

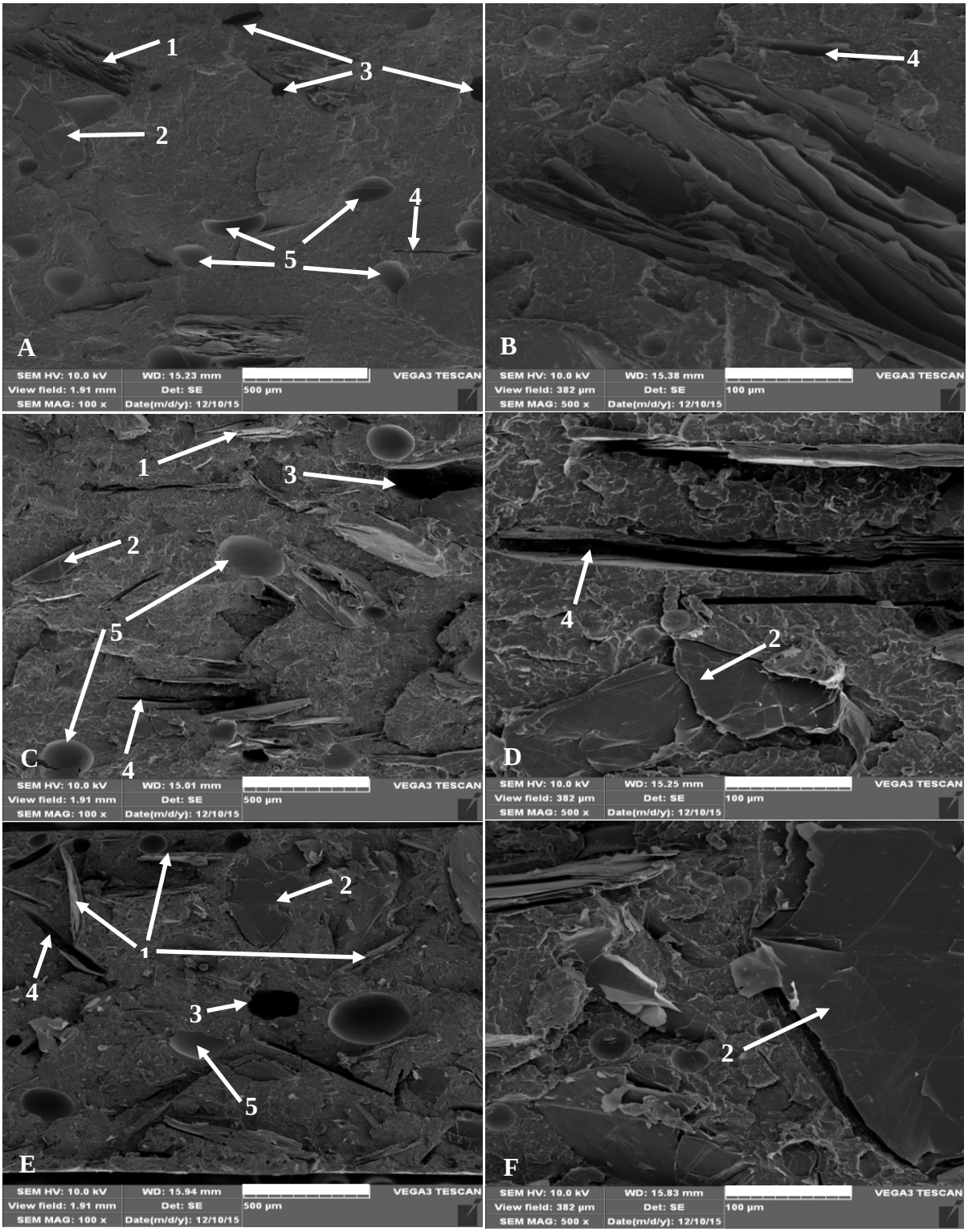

Figure 4.4 SEM micrographs of cryo-fractured surfaces of PLA/EG biocomposites at 5 (A & B), 10 (C & D) and 15 (E & F) wt.% EG at different magnifications of 100, 500 and 1000x

4.3.3 Differential scanning calorimetry (DSC)

The DSC results of the PLA/EG flame retardant composites are presented in Figures 4.5 and 4.6, while their data are summarized in Table 4.4. The data are presented as the average values of three tests (with standard deviations) of: i) peak temperatures of melting, cold-crystallization and crystallization and ii) enthalpies of melting, cold-crystallization and crystallization. The glass transition temperature (T_g) values obtained from the heating curves are also presented in the table. The degree of crystallinity (X_c) was calculated according to equation 4.2:

$$X_c(\%) = \frac{\Delta H_m}{\Delta H_m^0} \times 100\% \qquad (4.2)$$

where ΔH_m and ΔH_m^0 are respectively the experimental melting enthalpy and the melting enthalpy of a 100% crystalline PLA, the latter with a value of 93 J g^{-1} [20,23].

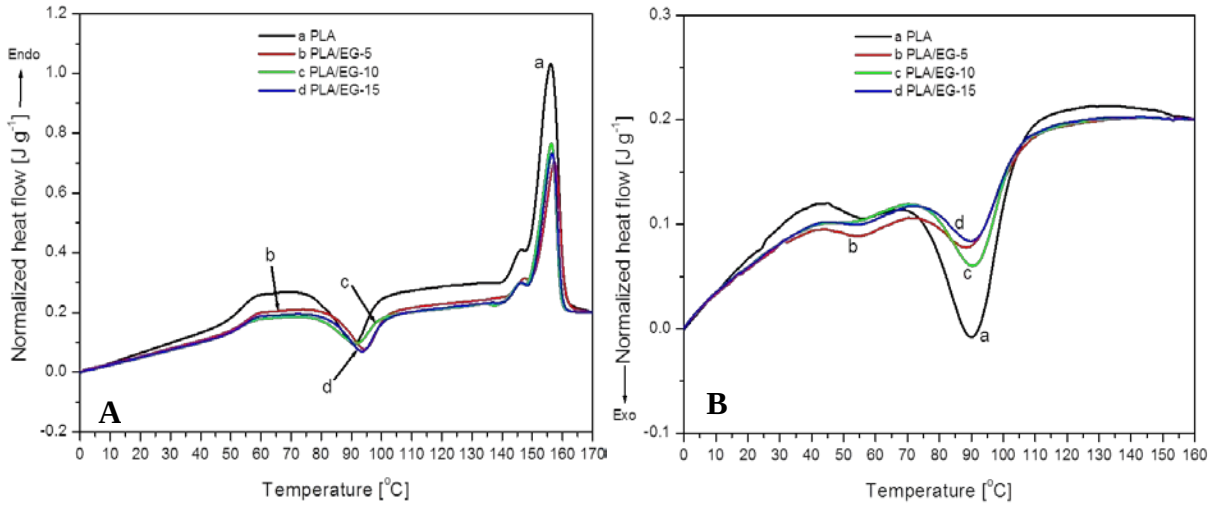

Figure 4.5 DSC curves of PLA and PLA/EG composites: (A) heating and (B) cooling

The heating and cooling curves of PLA and the PLA/EG composites are presented in Figure 4.5. On heating, PLA shows endothermic and exothermic thermal transitions within the experimental temperature range. The first endothermic transition is observed between 50-60 °C (i.e. 53.5 °C). This is due to the glass transition of the amorphous phase of the semicrystalline PLA [22]. The second (exothermic) transition at around 89 °C, relates to the cold-crystallization of PLA. The endothermic peak observed at 157 °C is associated with the melting of the PLA crystallites. There is also a peak shoulder at 145 °C, which is related to the melting of smaller crystallites within the amorphous regions of the polymer. These would melt

first due to an excess of free energy associated with the disordered chains that emerge from the ends of the ordered crystallites, which is relatively greater for the smaller crystallites [20-23]. Chapple *et al*. [20] observed the double melting phenomenon for Cereplast PLA/clay composites and attributed this to the melting of crystallites that have different sizes and/or order of perfection. Fukushima *et al*. [22], however, reported that the dual endothermic peaks of PLA relate to different crystal structures of the α- and β-forms. The α-form is said to melt at higher temperatures and it is the most common polymorph of PLA, while the latter form, melting at lower temperatures, relates to an imperfect crystal structure.

Table 4.4 DSC data of PLA/EG bio-based polymer composites

Parameter	PLA	PLA/EG-5	PLA/EG-10	PLA/EG-15
T_g [°C]	53.5 ± 0.0	54.8 ± 0.2	53.9 ± 0.2	54.9 ± 0.04
T_m [°C]	145 ± 0.4[a] 157 ± 0.1[b]	144 ± 0.8[a] 157 ± 0.3[b]	145 ± 1.2[a] 158 ± 0.7[b]	146 ± 0.3[a] 157 ± 0.7
ΔH_m [J g^{-1}]	22.7 ± 0.9	20 ± 0.6	22.1 ± 0.2	21 ± 0.1
ΔH_m^n [J g^{-1}]	22.7	21.6	20.4	19.3
T_{cc} [°C]	88.8 ± 1	94 ± 0.3	92 ± 0.5	94 ± 0.2
$-\Delta H_{cc}$ [J g^{-1}]	5.3 ± 1	11 ± 0.3	7.6 ± 0.3	10.6 ± 0.3
T_c [°C]	91.8 ± 0.4	91.4 ± 0	91.5 ± 0.1	91.4 ± 0.7
$-\Delta H_c$ [J g^{-1}]	14.9 ± 3	7.3 ± 0.3	9.7 ± 0.2	7.4 ± 1
X_c [%]	24.4	21.5	23.8	22.6

where T_m, T_{cc} and T_c are peak temperatures of melting, cold-crystallization and cooling; whereas ΔH_m and ΔH_m^n, ΔH_{cc} and ΔH_c are enthalpies of melt from experiments and normalized, enthalpies of cold-crystallization and cooling; and X_c is crystallinity degree in percentages. [a] and [b] respectively denote the melting temperature and shoulder peak of PLA. The normalized enthalpy, ΔH_m^n was calculated by multiplying the experimental enthalpy, ΔH_m, by weight fraction, wt.% of the polymer in a specific composition.

The same transitions are observed for the PLA/EG composites. From Table 4.4 it can be seen that the glass transition temperatures (T_g) are slightly higher for the composites, and this is better observed from Figure 4.6. This suggests that the presence of EG micro particles in the amorphous phase of PLA have a stiffening effect, thus lowering the polymer chain mobility. On the other hand, the melting temperatures (T_m) for both the peak shoulder and the maximum melting peak are consistently within the ranges of 144-146 °C and 157-158 °C, respectively. These values are well within the experimental error, as seen from Table 4.4. Similar findings were reported by Narimissa *et al*. [12] in their study of the influence of nano-graphite platelet concentration on the onset of crystalline degradation in PLA composites.

The crystallization temperature (T_c) (in the range of 91.4-91.8 °C) of the PLA/EG composites is the same as that of PLA, within experimental error. On the other hand, the cold-

crystallization temperatures (T_{cc}) of the PLA/EG composites are higher than that of PLA. A similar trend is observed for the cold-crystallization enthalpy (ΔH_{cc}) (Table 4.4). The observed increases are inconsistent with the EG micro-filler loadings. This suggests that the presence of the EG micro particles did not favour cold-crystallization, thus implying the reduction in polymer chain mobility of PLA by EG. The results indicate that the EG micro filler particles had no nucleation effect.

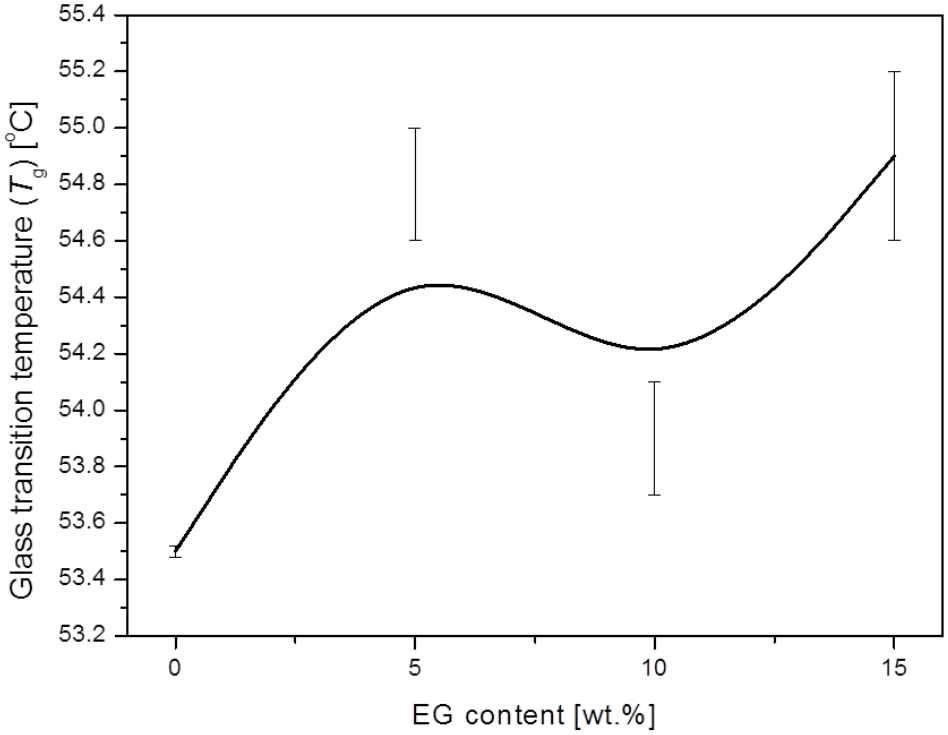

Figure 4.6 The dependence of glass transition temperature (T_g) on EG content

Furthermore, it is observed that the melting enthalpies (ΔH_m) of PLA in the PLA/EG composites, generally, do not exceed that of PLA i.e. slightly lower. Similarly, the degree of crystallinity, X_c of these composites was generally lower than for PLA, although the observed effects of EG on PLA were inconsistent with EG micro-filler content. This reduction effect in enthalpy and degree of crystallinity is attributed to the possible aggregation and poor dispersion of EG micro-filler single layers within PLA matrix, as revealed by the XRD and SEM results (discussed in sections 4.3.1 & 4.3.2). The normalized enthalpy values, ΔH_m^n for PLA in the composites were also determined and presented in Table 4.4. It is observed that ΔH_m^n was reduced in the presence of EG micro-filler particles. This is also attributed to a lack of: i) uniform dispersion of EG, ii) poor compatibility of EG particles with the PLA matrix and thus iii) lack of interfacial adhesion between the PLA matrix and the EG filler, as reported from

XRD and SEM results (see sections 4.3.1 and 4.3.2). Although the crystallization temperatures of the composites were similar to those of PLA, the enthalpies of crystallization were generally reduced inconsistently, suggesting that EG micro-particles did not promote crystallization of PLA.

4.3.4 Dynamic mechanical analysis (DMA)

The DMA results of PLA and the PLA/EG flame retardant composites are shown in Figures 4.7 and 4.8, while the data are summarized in Tables 4.5 and 4.6. The DMA storage modulus (E′), loss modulus (E″) and damping factor (tan δ) are reported.

The storage modulus (E′) of PLA and the PLA/EG flame retardant composites is shown in Figure 4.8A and the data tabulated in Table 4.5. It can be seen that the E′ is a decreasing function of temperature due to increases in the free volume as samples pass through various regions. These regions include: i) sub-glass transition, ii) glass transition, iii) rubbery plateau, iv) cold crystallization and v) pre-melting regions. For PLA, at low temperatures (i.e. below -80 °C), the polymer molecules are tightly compressed. As the sample warms up and expands (i.e. above -80 °C), a transition (i.e. γ-transition) with subsequent decline in E′ is observed. This is due to the increased free volume and localized bond (bending and stretching) movement and side chain movement. At temperatures between -40 to -25 °C, another transition is noted. This is due to the movement of the whole side chains and localized groups of backbone atoms that now have sufficient space to move and the material has developed some toughness. This transition is known as the β-transition and is the glass transition of a secondary component present in PLA. As discussed in sections 4.3.1 and 4.3.2, the PLA used in this study contains various additives, including starch [20]. Consequently, this transition is related to the starch component present in PLA. At temperatures, starting around 50 °C, there is a transition accompanied by an exponential drop in E′ up to ~65 °C. This relates to the glass transition of PLA and it is due to the polymer chains in an amorphous phase beginning to coordinate large-scale motions. After this, a rubbery plateau is reached (i.e. temperature range of between 65-120 °C), within which a slight increase in E′ accompanied by a transition peak is noted between 87 to 97 °C. This is attributed to the cold-crystallization transition [21,24,36]. This was also observed in the DSC (discussed in section 4.3.3).

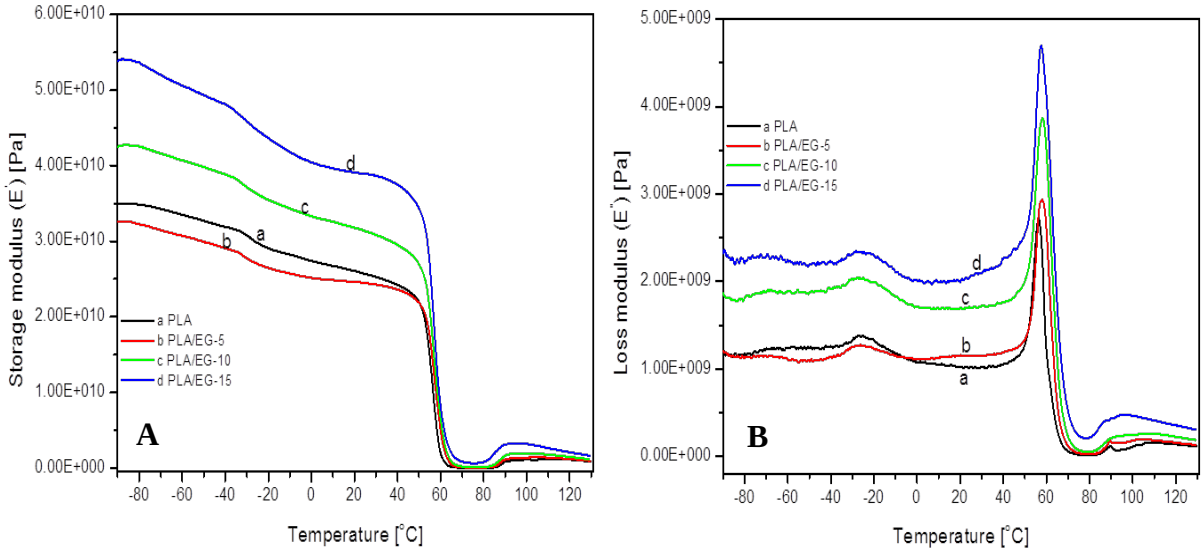

Figure 4.7 Temperature dependence of (A) storage modulus (E´) and (B) loss modulus (E˝) of PLA and the PLA/EG composites

The PLA/EG composites exhibit similar transitions to PLA in the E´ curves as observed in Figure 4.8A. Generally, the presence of EG micro-filler particles in PLA resulted to increased storage modulus throughout the experimental temperature range (Table 4.5). This is attributed to the reinforcing effect by EG and the high restricted movements of the polymer chains in the presence of EG micro-particles [22]. Similar findings were reported by Fukushima *et al*. [37] in their study to evaluate the effect of different nanoparticles on the thermal and thermo-mechanical properties of PLA.

Table 4.5 Storage modulus (E´) value of PLA and PLA/EG composites at different temperature ranges

Sample	E´ at 25 °C [MPa]	E´ at 60 °C [MPa]	E´ at 80 °C [MPa]
PLA	25692	1851	24
PLA/EG-5	24481	4202	64
PLA/EG-10	31309	6308	157
PLA/EG-15	38909	7934	809

The loss modulus (E˝) exhibits some transitions within the experimental temperature range (Figure 4.8B). In the sub-glass transition region, a transition around -27 °C (Table 4.6, see T_1), is observed which is due to the glass transition of the starch component (see XRD, SEM and DSC discussions in sections 4.3.1, 4.3.2 and 4.3.3, respectively). As seen in Table 4.6, the peak temperature values of this transition alternate between -26.1 and -27.9 °C in the presence of

EG. A transition peak is also observed between 50-70 °C (i.e. ~57 °C, Table 4.6, see T_2) and it is due to the glass transition of PLA. In this case, the peak temperature values showed an increase from 56.8 to 58.4 °C, as a function of EG content up to 10 wt.%, after which it declined to 57.4 °C at 15 wt.% EG content. This is explained by the immobilization effect of PLA polymer chains by EG micro filler. Finally, a transition between 85-100 °C, due to the cold-crystallization process, is also observed (see DSC discussion in section 4.3.3).

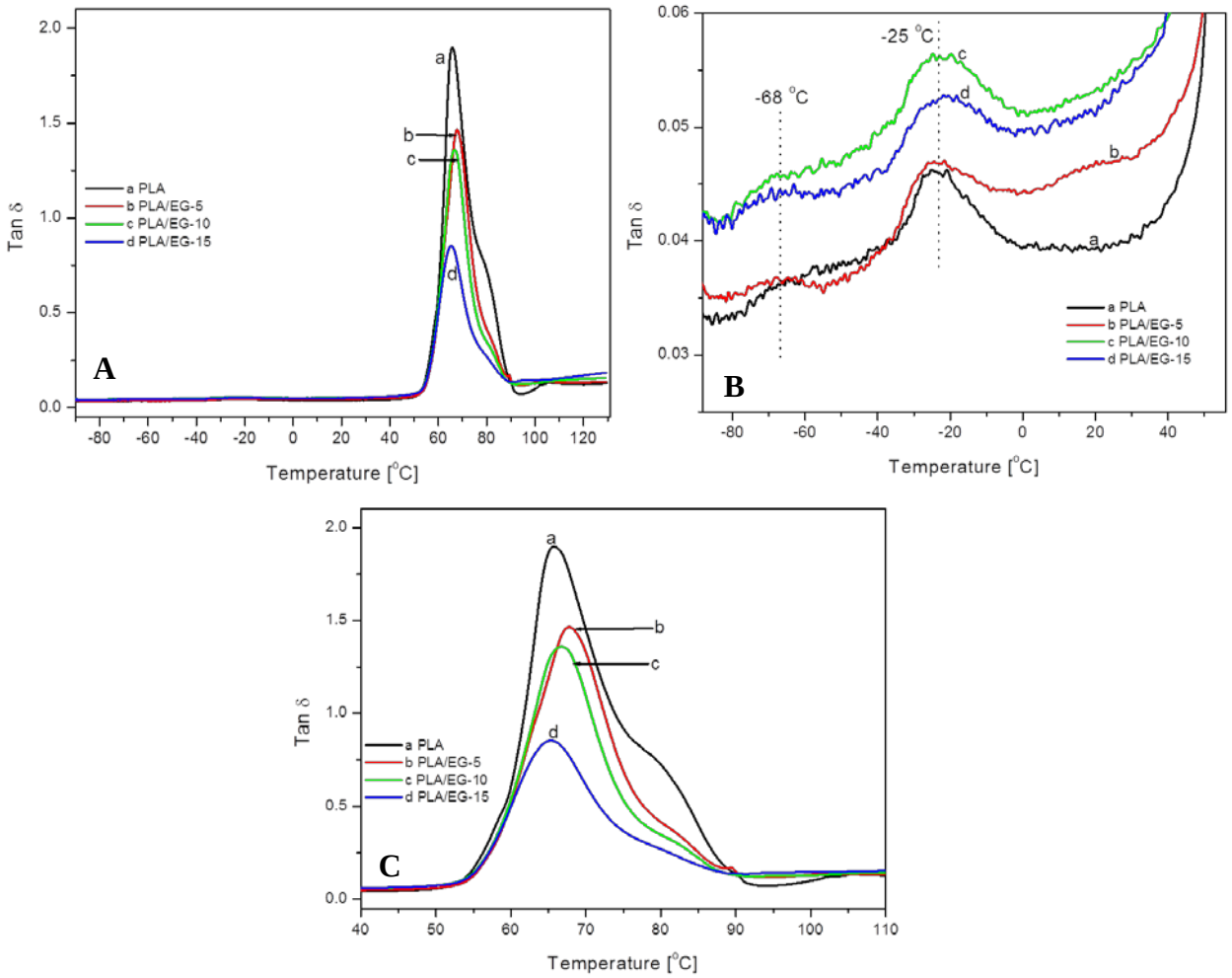

Figure 4.8 Temperature dependence of tan δ (damping factor) of PLA and the PLA/EG composites shown at (A) the entire experimental temperature range, (B) below the glass transition and (C) at and above the glass transition

Table 4.6 Transition temperature values obtained from loss modulus (E″) and damping factor (tan δ) curves of PLA and the PLA/EG composites

Sample	Peak E″, T_1 [°C]	Peak E″, T_2 [°C]	Peak tan δ [°C]
PLA	-27.6	56.8	65.8
PLA/EG-5	-26.3	57.7	67.8
PLA/EG-10	-27.9	58.4	66.7
PLA/EG-15	-26.1	57.4	65.1

The damping factor (tan δ) is shown in Figure 4.9 and the peak transition values are tabulated in Table 4.6. Various transitions are observed between -68 °C and -25 °C (Figure 4.9B), as well as around 66 °C (Figure 4.9A & C). The transitions observed at low temperatures are due to the presence of other additives derived from renewable resources with the transition around -25 °C, related to the starch component in PLA. All the samples show peaks between 65-68 °C and this is related to the glass transition of PLA (Figure 4.9C, Table 4.6). Furthermore, PLA shows a shoulder peak at temperatures above 80 °C which is related to the cold crystallization transition of PLA, and this diminished with the addition of EG. The PLA/EG flame retardant composites are generally characterized by high storage and loss moduli, with slight variations in T_g.

4.4 Conclusions

The effect of expandable graphite (EG) on the morphology, structure and thermal and the dynamic mechanical properties of melt-mixed flame retardant PLA/EG composites was investigated. It was found that the graphite layers still existed in aggregate form (i.e. EG layered stacks) with a lack of EG single layers dispersion in the composites because of poor interfacial adhesion between EG and the PLA matrix. The presence of EG in PLA showed increased glass transition temperatures and there were no changes in the melting and crystallization temperatures. The presence of EG micro-particles also gave rise to reduced crystallinity of PLA in the composites, indicating the fact that their immobilizing effect dominated over their nucleating effect. The PLA/EG composites showed increasing storage moduli with increasing filler content, which was due to the inherent stiffness of the filler rather than to significant interaction between the filler and polymer. The glass transition temperature from the loss modulus and damping factor curves, varied inconsistently with EG content. These results suggest that the incorporation of the commercial expandable graphite into PLA could stiffened

the materials and preserved some of the thermal properties of injection molding grade Cereplast PLA, while improving the fire resistance of PLA/EG flame retardant composites.

Acknowledgements

The authors would like to acknowledge the financial support by the National Research Foundation (NRF) and Professional Development Programme (PDP). Acknowledgements are also extended to colleagues and researchers for their undivided attention and support.

References

1. Mngomezulu, M.E., John, M.J., Jacobs, V., Luyt, A.S. (2014). Review on flammability of biofibres and biocomposites. *Carbohydrate Polymers*, 111:149-182. DOI: 10.1016/j.carbpol.2014.03.071
2. Huang, G., Gao, J., Wang, X., Liang, H., Ge, C. (2012). How can graphene reduce the flammability of polymer nanocomposites? *Materials Letters*, 66:187-189. DOI: 10.1016/j.matlet.2011.08.063
3. Fukushima, K., Murariu, M., Camino, G., Dubois, P. (2010). Effect of expanded graphite/layered-silicate clay on thermal, mechanical and fire retardant properties of poly(lactic acid). *Polymer Degradation and Stability*, 95:1063-1076. DOI: 10.1016/j.polymdegradstab.2010.02.029
4. Murariu, M., Dechief, A.L., Bonnaud, L., Paint, Y., Gallos, A., Fontaine, G., Bourbigot, S., Dubois, P. (2010). The production and properties of polylactide composites filled with expanded graphite. *Polymer Degradation and Stability*, 95:889-900. DOI: 10.1016/j.polymdegradstab.2009.12.019
5. Rasal, R.M., Janorkar, A.V., Hirt, D.E. (2010). Poly(lactic acid) modifications. *Progress in Polymer Science*, 35:338-356. DOI: 10.1016/j.progpolymsci.2009.12.003
6. Vogel, C., Siesler, H.W. (2008). Thermal degradation of poly(ε-caprolactone), poly(L-lactic acid) and their blends with poly(3-hydroxy-butyrate) studies by TGA/FT-IR spectroscopy. *Macromolecular Symposia*, 265:183-194. DOI: 10.1002/masy.200850520

7. Wu, D., Zhang, Y., Zhang, M., Zhou, W. (2008). Phase behaviour and its viscoelastic response of polylactide/poly(ε-caprolactone) blend. *European Polymer Journal*, 44:2171-2183.
DOI: 10.1016/j.eurpolymj.2008.04.023
8. Garlotta, D. (2001). A literature review of poly(lactic acid). *Journal of Polymers and the Environment*, 9(2):63-83.
DOI: 10.1023/A:1020200822435
9. Gupta, A.P., Kumar, V. (2007). New emerging trends in synthetic biodegradable polymers – Polylactide: A critique. *European Polymer Journal*, 43:4053-4074.
DOI: 10.1016/j.eurpolymj.2007.06.045
10. Saeidlou, S., Huneault, M.A., Li, H., Park, C.B. (2012). Poly(lactic acid) crystallization. *Progress in Polymer Science*, 37:1657-1677.
DOI: 10.1016/j.progpolymsci.2012.07.005
11. Tai, Q., Yuen, K.K.R., Song, L., Hu, Y. (2012). A novel polymeric flame retardant and exfoliated clay nanocomposites: Preparation and properties. *Chemical Engineering Journal*, 183:542-549.
DOI: 10.1016/j.cej.2011.12.095
12. Narimissa, E., Gupta, R., Bhaskaran, M., Sriram, S. (2012). Influence of nano-graphite platelet concentration on onset of crystalline degradation in polylactide composites. *Polymer Degradation and Stability*, 97:829-832.
DOI: 10.1016/j.polymdegradstab.2012.02.010
13. Bai, G., Guo, C., Li, L. (2014). Synergistic effect of intumescent flame retardant and expandable graphite on mechanical and flame-retardant properties of wood flour-polypropylene composites. *Construction and Building Materials*, 50:148-153.
DOI: 10.1016/j.conbuildmat.2013.09.028
14. Lee, J.D. (1995). Concise Inorganic Chemistry. 4th Edition. Chapman & Hall Ltd. Singapore.
15. Sengupta, R., Bhattacharya, M., Bandyopadhyay, S., Bhowmick, A.K. (2011). A review on the mechanical and electrical properties of graphite and modified graphite reinforced composites. *Progress in Polymer Science*, 36:638-670.
DOI: 10.1016/j.progpolymsci.2010.11.003
16. Weil, E.D., Levchik, S.V. (2008). Flame retardants in commercial use or development for polyolefins. *Journal of Fire Sciences*, 26:5-43.
DOI: 10.1177/0734904107083309

17. Focke, W.W., Badenhorst, H., Mhike, W., Kruger, H.J., Lombaard, D. (2014). Characterization of commercial expandable graphite fire retardants. *Thermochimica Acta*, 584:8-16.
DOI: 10.1016/j.tca.2014.03.021
18. Tang, G., Zhang, R., Wang, X., Wang, B., Song, L., Hu, Y., Gong, X. (2013). Enhancement of flame retardant performance of bio-based polylactic acid composites with the incorporation of aluminum hypophosphite and expanded graphite. *Journal of Macromolecular Science, Part A: Pure and Applied Chemistry*, 50:255-269.
DOI: 10.1080/10601325.2013.742835
19. Young, R.J., Lovell, P.A. (2011). Introduction to Polymers. 3rd Edition. CRC Press, Taylor & Francis Group. Boca Raton.
20. Chapple, S., Anandjiwala, R., Ray, S.S. (2013). Mechanical, thermal, and fire properties of polylactide/starch blend/clay composites. *Journal of Thermal Analysis and Calorimetry*, 113:703-712.
DOI: 10.1007/s10973-012-2776-6
21. Cowie, J.M.G. (1991). Polymers: Chemistry & Physics of Modern Materials. 2nd Edition. CRC Press. Boca Raton.
22. Fukushima, K., Tabuani, D., Arena, M., Gennari, M., Camino, G. (2013). Effect of clay type on thermal, mechanical properties and biodegradation of poly(lactic acid) nanocomposites. *Reactive & Functional Polymers*, 73:540-549.
DOI: 10.1016/j.reactfunctpolym.2013.01.003
23. Murariu, M., Dechief, A.-L., Paint, Y., Peeterbroeck, S., Bonnaud, L., Dubois, P. (2012). Polylactide (PLA)-halloysite nanaocomposites: Production, morphology and key-properties. *Journal of Polymers and the Environment*, 20:932-943.
DOI: 10.1007/s10924-0488-4
24. Menard, K.P. (1999). Dynamic Mechanical Analysis. A Practical Introduction. CRC Press LLC. Boca Raton.
25. Focke, W.W., Kruger, H.J., Mhike, W., Taute, A., Roberson, A., Ofosu, O. (2014). Polyethyelene flame retarded with expandable graphite and a novel intumescent additive. *Journal of Applied Polymer Science*, 40493:1-8.
DOI: 10.1002/app.40493
26. Focke, W.W., Muiambo, H., Mhike, W., Kruger, H.J., Ofosu, O. (2014). Flexible PVC flame retarded with expandable graphite. *Polymer Degradation and Stability*, 100:63-69.
DOI: 10.1016/j.polymedegradstab.2013.12.024

27. Wei, P., Bocchini, S., Camino, G. (2013). Flame retardant and thermal behavior of polylactide/expandable graphite composites. *Polimery*, 58(5):361-364.
DOI: 10.14314/polimery.2013.361
28. http://www.gk-graphite.cn/fileadmin/user_upload/PDF/List_standard.pdf (26/10/2015)
29. http://trellisbioplastic.com/wp-content/uploads/2014/08/Sustainable-1001-Property-Guide.pdf (26/10/2015)
30. Uhl, F.M., Yao, Q., Nakajima, H., Manias, E., Wilkie, C.A. (2005). Expandable graphite/polyamide-6 nanocomposites. *Polymer Degradation and Stability*, 89:70-84.
DOI: 10.1016/j.polymdegradstab.2005.01.004
31. Park, J.W., Im, S.S. (2002). Phase behavior and morphology in blends of poly(L-lactic acid) and poly(butylene succinate). *Journal of Applied Polymer Science*, 86:647-655.
DOI: 10.1002/app.10923
32. Xiao, H.W., Li, P., Ren, X., Jiang, T. Yeh, J.-T. (2010). Isothermal crystallization kinetics and crystal structure of poly(lactic acid): Effect of triphenyl phosphate and talc. *Journal of Applied Polymer Science*, 118:3558-3569.
DOI: 10.1002/app.32728
33. Wang Y., Lin, C.-S. (2014). Preparation and characterization of maleated polylactide-functionalized graphite oxide nanocomposites. *Journal of Polymer Research*, 21:334 (pp: 1-14).
DOI: 10.1007/s10965-013-0334-y
34. Pluta, M., Galeski, A., Alexandre, M., Paul, M.-A., Dubois, P. (2002). Polylactide/montmorillonite nanocomposites and microcomposites prepared by melt blending: Structure and some physical properties. *Journal of Applied Polymer Science*, 86:1497-1506.
DOI: 10.1002/app.11309
35. Fukushima, K., Tabuani, D., Camino, G. (2009). Nanocomposites of PLA and PCL based on montmorillonite and sepiolite. *Materials Science and Engineering C*, 29:1433-1441.
DOI: 10.1016/j.msec.2008.11.005
36. Kowalczyk, M., Piorkowska, E., Kulpinski, P., Pracella, M. (2011). Mechanical and thermal properties of PLA composites with cellulose nanofibers and standard size fibers. *Composites: Part A*, 42:1509-1514.
DOI: 10.1016/j.compositesa.2011.07.003

37. Fukushima, K., Tabuani, D., Camino, G. (2012). Poly(lactic acid)/clay nanocomposites: effect of nature and content of clay on morphology, thermal and thermo-mechanical properties. *Materials Science and Engineering C*, 32:1790-1795.
DOI: 10.1016/j.msec.2012.04.047

Chapter 5

Effect of expandable graphite on fire resistance and thermal stability of PLA/PCL blend

This chapter will be submitted unaltered for publication in an international journal.

Abstract

The effect of expandable graphite (EG) on the flammability and thermal stability of a poly(lactic acid) (PLA)/poly(ε-caprolactone) (PCL) blend was investigated. The samples were prepared by melt-mixing and characterized by thermogravimetric analysis (TGA), simultaneous TGA-Fourier transform infrared spectroscopy and cone calorimetry. The char residues of the composites after combustion from cone calorimeter were analysed with environmental scanning electron microscopy (ESEM). The thermal degradation stability of the composites improved and the char content was found to be increased. The flammability performance results indicated that the PLA/PCL blend was successfully modified with the EG micro-filler in order to obtain fire resistant composites, especially at high filler loadings, due to the formation of intumescent carbonaceous char. This was confirmed by reductions of the up to 64% in the peak heat release rate (PHRR) and the total smoke release (TSR) and 54% in the specific extinction area (SEA). This is due to the effect of EG acting mainly through a physical mode by cooling and fuel dilution and through the formation of an intumescent char layer. However, the effective heat of combustion (EHC) and carbon monoxide (CO) yields did not improve favourably.

Keywords: poly(lactic acid), poly(ε-caprolactone), expandable graphite, thermal properties, flammability, bio-based polymer blends

5.1 Introduction

The development of biopolymer blends with better fire resistance performance and thermal properties may see biopolymers replacing petroleum-based materials in applications of advanced engineering. In the automotive and electric and electronics industries, there are strict requirements on fire safety of materials, therefore mainly high performing petroleum-based materials are used. The current research interest is, therefore, on the use of bio-based materials as alternatives to petroleum-based types. This is because the latter have challenges, such as: high cost, shortage of fossil fuel, lack of biodegradability and a negative impact on the environment. Bio-based materials are obtained from renewable resources and include: i) those extracted directly from biomass (e.g. cellulose, protein and starch), ii) those produced by classical synthesis using either renewable bio-based monomers (e.g. poly(lactic acid), PLA) or oil-based monomers (e.g. polycaprolactones, PCL) and iii) those produced by microorganisms and genetically-modified bacteria (e.g. polyhydroxyalkanoates, PHA). They do offer advantages, such as: biodegradability, being eco-friendly, recyclability, better mechanical properties and easy processability by conventional methods (e.g. blow and injection moulding and thermoforming) [1-5].

However, biopolymers, such as PLA and PCL, have inherent physical and/or chemical limitations that may be remedied by either blending and/or composite formation approaches. PLA is one of the most common bio-based, aliphatic polyesters with a relatively modest cost. It is produced from renewable lactic acid monomer, which is obtained from the fermentation of starch and other polysaccharides (i.e. beet, sugar cane, potatoes and other biomasses) [5]. It is applied in various fields, such as: composites, drug delivery, orthopaedics, packaging, pharmaceuticals, sutures, textiles and tissue engineering. In the case of composites, it may be used for cutlery, disposable plates and cups, toys, thermoformed trays for fruits and vegetables, home furnishings, household articles and fibre composites. Despites its widespread use, it has some drawbacks that include poor: toughness, hydrophobicity, slow crystallization rate, lack of side-chain groups and poor flammability performance [4-11]. PCL, on the other hand, is a biodegradable, semi-crystalline linear aliphatic commercial polyester, produced from ε-caprolactone, which has good mechanical properties [10,11].

Blending PLA with PCL, either by melt-mixing or solution casting, provides an important property complementarity. In this case, the glassy PLA with low thermal stability and high

degradation rate, exhibits better tensile strength, while the rubbery PCL with high thermal stability and relatively slower degradation rate shows better toughness [2,3,10-16]. Other than PCL, polymers such as: poly(butylene succinate) (PBS), polycarbonate (PC), polystyrene (PS), polyethylene (PE) and polypropylene (PP), may also be used to modify the properties of PLA [14,17-20].

Studies on PLA/PCL bio-blends have focused mainly on biodegradation, structure, morphology, static and dynamic mechanical, rheology and thermal properties. Thus there is a need to investigate the fire resistance properties of PLA/PCL-based systems in order to advance the research in this field.

Generally, modification of the individual biopolymers and their blends by the incorporation of additives/fillers to form composites is of utmost benefit. The manufacture of composites can be achieved either by solution mixing, melt extrusion/blending or injection moulding. PLA has been compounded with ammonium polyphosphate, boehmite, clays, halloysite, talc, silica and graphite and the resulting materials were characterized to have better thermal, mechanical and fire resistance performance [6,8,21-31]. For instance, PLA was reported as flammable and burning with intense dripping during combustion; however, the incorporation of clay and/or expanded graphite rendered PLA composites fire resistant [6]. In another study, Kimura and Horikoshi [20] reported on the development of PLA-based flame resistant housings for notebook computers. PLA biocomposites were prepared by extrusion with the incorporation of various flame retardants (e.g. aromatic silicon resin, polydimethylsiloxane and aluminum hydroxide). Furthermore, due to the low rigidity of PLA, other resin additives (e.g. polystyrene, polyethylene and polypropylene) were used to improve its physical properties. It was reported that the PLA-based materials developed, showed optimal physical and flammability properties qualifying them for the intended purpose.

The flammability properties of blends (e.g. PLA/PCL, PLA/PC, PHBV/PBAT) have also been improved through the use of various additives, including: clays, graphite, aluminium hypophosphate and glass fibres [6,19,32,33]. Gallo *et al*. [33] investigated the synergism between aluminium phosphinate and metal oxides (i.e. antimony oxide, Sb_2O_3 and iron oxide, Fe_2O_3) nano-particles on the flammability and thermal properties of melt blended biodegradable nanocomposites, based on a commercial poly(3-hydroxybutyrate-co-3-hydroxyvalerate) (PHBV)/poly(butylene adipate-co-terephthalate) (PBAT) blend. They found

that the co-addition of both additives/fillers (i.e. at 10 wt.%) led to improved flame retardancy and increased char content. Lin *et al*. [19] reported improved mechanical properties, heat and fire resistance of melt blended glass fibre reinforced 70/30 w/w PLA/PC filled with aluminium hypophosphite. Xie and Qu [34] reported that the incorporation of EG, phosphorus-based compounds and zinc borate in EVA/LDPE blends, gave flame retardant-polyolefin materials with good mechanical and flammability properties due to the synergistic effect of flame retardants and EG.

Graphite is a layered material consisting of strong interlayer covalent bonds within the carbon layers and weak van der Waals interaction between successive carbon layers. It combines the layered structure of clays with the superior electrical properties and thermal characteristics of carbon nanotubes and metals. It is suitable for applications where its characteristics, such as: heat stability, lubricant ability, thermal and electrical conductivity are required. Graphite intercalated compounds (GIC) are a subclass of graphite and are formed by the chemical or electrochemical intercalation of molecular or atom guests, e.g. sulphuric acid, between the layers of graphite. Expandable graphite (EG) is an example of a GIC that exfoliates when heated. At temperatures from ~180 °C, the intercalated acid can be driven-off as reduction products, with an accompanied expansion of the graphite interlayers. When used as a polymer additive, this produces a protective, foamed, exfoliated graphite covering on the burning polymer surface. Since EG starts exfoliating at temperatures below the onset of thermal decomposition of PLA, ~280 °C, EG will act before degradation of the biopolymer. It will therefore, modify the thermal degradation pathway of PLA to yield some char and probably lower the evolution of flammable pyrolysis products [6,32,35,36].

The use of EG for flame retardancy has several advantages, such as: excellent flame retardant effect with low material use, reduction of fumes and it is free from heavy metals, non-polluting, suitable for a wide range of applications and has low cost. The application fields of expandable graphite include insulation foam (e.g. polyurethane rigid foam plates), soft foams (e.g. in furniture, mattresses), carpets, textiles, coatings, plastic foils, rubber products (e.g. conveyer belts) and pipe closing systems. Different studies have been reported on the use of EG (i.e. either alone or in conjunction with other additives) as an intumescent and halogen-free flame retardant in different polymer matrices, including: ethylene vinyl acetate (EVA) [34,37,38], low-density polyethylene (LDPE) [34,39], polyvinyl chloride (PVC) [40] and PLA [6,8,28,41]. For instance, Focke *et al*. [40] reported on the successful use of expandable graphite as flame

retardant in plasticized PVC, even at a low loading (i.e. 5 wt.%). This was attributed to the EG providing a barrier layer, as well as a good match between the exfoliation onset temperatures of EG and the onset of decomposition of PVC. In addition, Zhu *et al*. [28] observed a synergistic effect between expandable graphite and ammonium polyphosphate (i.e. 1:3 APP/EG, 15 wt.%) incorporated in PLA. A high LOI value and UL-94 V-0 rating, improved char content and a ~38% lower PHRR were reported, which were attributed to the formation of a stable and dense char protection layer.

The current study investigates the influence of expandable graphite (EG) on the fire resistance and thermal stability of a PLA/PCL blend system. Samples were prepared by melt-mixing PLA with PCL, followed by the incorporation of EG (at 5, 10 and 15 wt.% loading). The resultant samples were then characterized for their thermal and flammability properties.

5.2 Materials and methods

5.2.1 Materials

The PLA used in this study was a Cereplast Sustainable 1001 injection moulding grade, containing additives derived from starch and other renewable resources, with physical properties as shown in Table 5.1. The polymer contains fillers, including silicon-based materials (i.e. glass) and microspheres [42]. PCL in flakes form was purchased from Sigma-Aldrich, South Africa. It has an average molecular weight ($\bar{M}_w$) and number average molecular weight ($\bar{M}_n$) of 14 000 and 10 000 g mol^{-1}, respectively, a melting point (T_m) temperature of 60 °C and a density (ρ) of 1.146 g ml^{-1}. The commercial EG used was an ES250 B5 grade consisting of 90-95 % carbon content, expansion rate of between 250-500 cm^3 g^{-1} at a starting temperature range of between 180-300 °C, particle size: 80 % of the particles > 300 µm and was supplied by Qingdao Kropfmuehl Graphite, China. The EG consists of $KMnO_4$ as an oxidant and H_2SO_4 as an intercalant [40,43]. Materials were used as received from the suppliers without any modification/purification, except for drying, prior to the compounding.

Table 5.1 Physical properties of PLA, Cereplast Sustainable Resin 1001 grade [44]

Physical property	ASTM Test method	Values
Tensile strength at maximum	D 638	49.6 MPa
Tensile elongation at break	D 638	5.1%
Tensile modulus	D 638	3,590 MPa
Flexural modulus	D 790	3,360 MPa
Flexural strength	D 790	80 MPa
Gardner impact	D 5420	1.13 J
Notched Izod impact strength (at 23 °C)	D 256	40 J m^{-1}
Temperature deflection under 0.45 MPa	D 648	44 °C
Melt Flow Index 190 °C at 2.16 kg	D 1238	8 g/10 min
Density (ρ)	D792 Method A	1.28 g ml^{-1}

5.2.2 Sample preparation

Samples were compounded according to the ratios shown in Table 5.2. The ratio of PLA/PCL was set at 85/15 w/w, while the EG content was varied. 85/15 w/w PLA/PCL was selected due to its good tensile modulus and strength, as determined during preliminary tests. The components were dried overnight in an oven at 50 °C. The composites were then prepared by melt-mixing, using a Brabender Plastograph 55 cm^3 internal mixer at a temperature of 180 °C and speed of 60 rpm. for 12 min. This was followed by hot melt pressing under a pressure of 50 bar at a temperature of 180 °C for 5 min. in order to obtain 140 mm x 140 x mm 2 mm sheets.

Table 5.2 Sample ratios of PLA/PCL/EG composites

Sample	Composition [wt.%]
PLA	100
PCL	100
PLA/PCL	85/15
PLA/PCL/EG-5	80.75/14.25/5
PLA/PCL/EG-10	76.5/13.5/10
PLA/PCL/EG-15	72.25/12.75/15

5.2.3 Sample analysis

The thermal degradation behaviour of the composites was analysed using a PerkinElmer STA6000 Simultaneous Thermal Analyzer. The samples (mass range 20-25 mg) were heated from 30 to 700 ºC at a rate of 10 ºC min^{-1} under flowing nitrogen (20 ml min^{-1}). In this study, the TGA technique was mainly used to examine the thermal stability and char content of the samples.

The thermal decomposition volatiles of the samples were analysed using the TGA connected to a PerkinElmer Spectrum 100 Fourier-transform infrared (FTIR) spectrometer (TGA-FTIR). As in the case of TGA analysis, the same temperature range and heating rate were used and the volatiles were transferred to the FTIR by a PerkinElmer TL 8000 balanced flow FT-IR EGA system. Spectra were collected continuously during the degradation process.

The flammability tests were performed using a cone calorimeter (FTT, UK) according to ISO 5660-1 at a heat flux of 35 kW m^{-2}. The test samples, with dimensions of 100 mm x 100 mm x 2 mm, were prepared by compression moulding. The samples were wrapped with an aluminium foil on the sides and at the bottom and placed (i.e. horizontal orientation) in a retainer frame over low density ceramic wool and then secured on the specimen holder. The following quantities were measured using the cone calorimeter: Time to ignition (TTI), peak heat release rate (PHRR), total heat release (THR), effective heat of combustion (EHC), maximum average rate of heat emission (MARHE), the average specific mass loss rate (av-MLR), the fire performance index (FPI), the CO and CO_2 yields and the CO/CO_2 weight ratio.

In order to determine the morphology of the char residues after combustion using cone calorimeter, an FEI Quanta 200 environmental scanning electron microscope (ESEM) was used and the analysis was done at room temperature. The samples were gold coated by sputtering in order to produce a conductive coating on the samples.

5.3 Results and discussion

5.3.1 Thermogravimetric analysis (TGA)

The TGA and DTG curves for neat PLA, PCL and the PLA/PCL/EG composites are depicted in Figure 5.1 and their data summarized in Table 5.3. The thermal stability of the samples was characterized in terms of the temperatures at 2 wt.% ($T_{2\%}$) and 60 wt.% ($T_{60\%}$) mass loss, the temperature at maximum mass loss rate (T_{max}) and the char residue at 700 °C. The $T_{2\%}$ is normally considered as the onset temperature of thermal degradation. It is observed that neat PLA starts to decompose at around 282 °C ($T_{2\%}$), proceeding in two steps and yielding some char residue (~9.1%). The first degradation step occurring within the temperature range of between 270-337 °C with T_{max} = 321 °C (Table 5.3) is attributed to the thermal degradation of the PLA matrix. The thermal degradation of PLA, in addition to other radical reaction

mechanisms [45-48], is considered to be mainly due to non-radical, backbiting ester interchange reaction that involves hydroxyl chain ends. Amongst the pyrolysis products of PLA, cyclic oligomers of lactic acid, lactide, acetaldehyde, carbon monoxide (CO) and carbon dioxide (CO_2) are cited in literature [35,46,47,49]. The second step, occurring between 337-650 °C, with T_{max} of 381 °C, is attributed to the degradation of the char residues formed due to the additives derived from starch and other renewable resource-based materials present in the PLA matrix (see section 5.2.1). The neat PCL showed an early onset in thermal degradation at 265 °C, degrading completely in one step within the temperature range of between 243-450 °C, with T_{max} = 410 °C (Table 5.3). This is due to the rupture of the polyester chains through an ester pyrolysis reaction with the release of CO_2, H_2O, carboxylic acid and 5-hexenoic acid [50]. Although PCL exhibits an early onset temperature of thermal degradation of 265 °C, it is more thermally stable than PLA by about 89 °C.

For the 85/15 w/w PLA/PCL blend, a two-step degradation mechanism is noted with a char residue of about 8.3%. The first step occurred at 346 °C, while the second step occurred at 398 °C (Table 5.3). These steps correspond to the degradation of PLA and PCL, respectively, in the blend. It is noted that the first step occurs at a higher temperature than that for neat PLA, while the second step occurs at a lower temperature than that for neat PCL. This important result suggests that melt-mixing PLA with PCL led to improved thermal stability of PLA in the blend due to the presence of the more thermally stable PCL component.

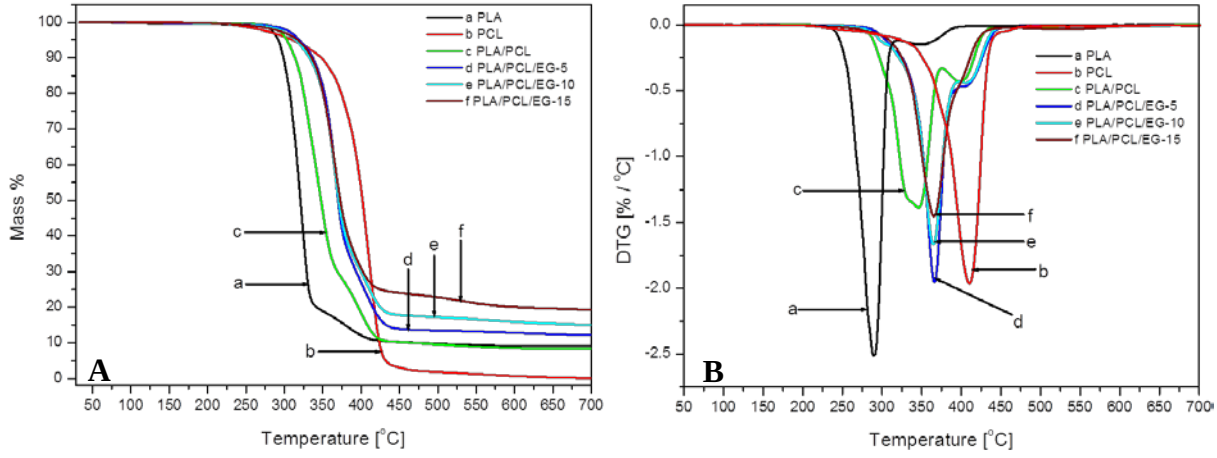

Figure 5.1 TGA (A) and DTG (B) curves of PLA, PCL and the PLA/PCL/EG composites

Table 5.3 TGA result of investigated PLA/PCL/EG composite materials

Sample	$T_{2\%}$ [°C]	$T_{60\%}$ [°C]	T_{max}[a] [°C]	Residue at 700 °C [%]
PLA	282	325	321 & 381	9.1
PCL	265	405	410	0.1
PLA/PCL	290	353	346 & 398	8.3
PLA/PCL/EG-5	298	375	366 & 404	12.1 (13)
PLA/PCL/EG-10	290	377	365 & 406	15.0 (17)
PLA/PCL/EG-15	282	380	366	19.3 (22)

$T_{2\%}$ and $T_{60\%}$ are temperatures at 2 and 60% weight loss; [a] Temperature at maximum weight loss from DTG. The values in parenthesis are the expected residue % (at 700 °C) calculated from {residue % of the blend (e.g. 8.3%) × weight fraction of the blend (e.g. 0.95) + weight fraction of EG (e.g. 5%) = 13%}.

For the PLA/PCL/EG system shown in Figure 5.1 and Table 5.3, it is observed that the composites showed higher temperatures of degradation ($T_{2\%}$) at 5 wt.% EG, which may be due to the fairly even distribution of EG layers and/or stacks at lower content within the PLA/PCL matrix. At higher loadings (i.e. 10 and 15 wt.% EG), a decrease in $T_{2\%}$ is observed, and this is attributed to the presence of H_2SO_4 acid within the EG layers which, when released, catalysed the initiation of thermal degradation of the PLA/PCL matrix [8,28,51]. These composites showed significant higher $T_{60\%}$ values than the PLA/PCL blend and these values marginally increased with increasing filler content. The temperatures at maximum degradation rate were generally higher than those for the neat blend, indicating better thermal stability. It is interesting to note that at the highest EG loading (i.e. 15 wt.%), the composite exhibited only one thermal decomposition step, with T_{max} = 366 °C. Although the temperatures at maximum degradation rate for the composites are higher than those for the blend, they fall within the same temperature range of between 365-366 °C, irrespective of the size of the EG content. The better thermal stability of these composites is attributed to the shielding effect of EG with its flake-like structure, which hindered the diffusion of the volatile decomposition products by increasing their diffusion pathway [8]. The insignificant changes in the thermal stability at higher EG loadings is attributed to the release of degradation products by residual acid at lower temperatures [51]. On the other hand, the char content was obviously increased in the presence of EG, which formed part of the residue. However, the % residue from the composites does not generally correlate with a combination of wt.% EG, initially mixed into PLA/PCL blend and the % residue left by PLA/PCL blend. This is shown by the high calculated % residue values (values in parenthesis from Table 5.3) than the experimentally observed. This may, probably, indicate that the chemical reactions involved in the thermal decomposition of PLA/PCL/EG composites were in favour of the formation of CO and CO_2 rather than yielding carbon. The formation of CO and CO_2 gases is supported by TG-IR results as discussed below.

5.3.2 Volatile products of PLA/PCL and the PLA/PCL/EG composites: TGA-FTIR analysis

Simultaneous TG-FTIR aids in analysing the evolved gas products during thermal decomposition. The TG-FTIR spectra of the volatile thermal decomposition products of PLA/PCL and the PLA/PCL/EG composites are presented in Figure 5.2. Figure 5.2A shows, with labelled regions (from a to i) all the characteristic absorption spectra of the blend and composites. The regions consist of ranges of wavenumbers, a: 3740-3572 cm^{-1}, b: 3000-2744 cm^{-1}, c: 2356-2343 cm^{-1}, d: 2173-2104 cm^{-1}, e: 1792-1763 cm^{-1}, f: 1497-1300 cm^{-1}, g: 1309-1033 cm^{-1}, h: 940-930 cm^{-1} and i: 529-669 cm^{-1}. From this, it can be seen that the thermal decomposition pyrolysis products for the blend and composites consist of compounds that contain –OH groups (regions a and h), C–H (hydrocarbons, $–CH_3$ and $–CH_2$ groups, both stretching and bending modes) (regions b and f), CO_2 (regions c & i), CO (region d), aliphatic esters (C–O–C) and C–O stretch (region g) and C=O (carbonyl) containing groups (region e) [52-54].

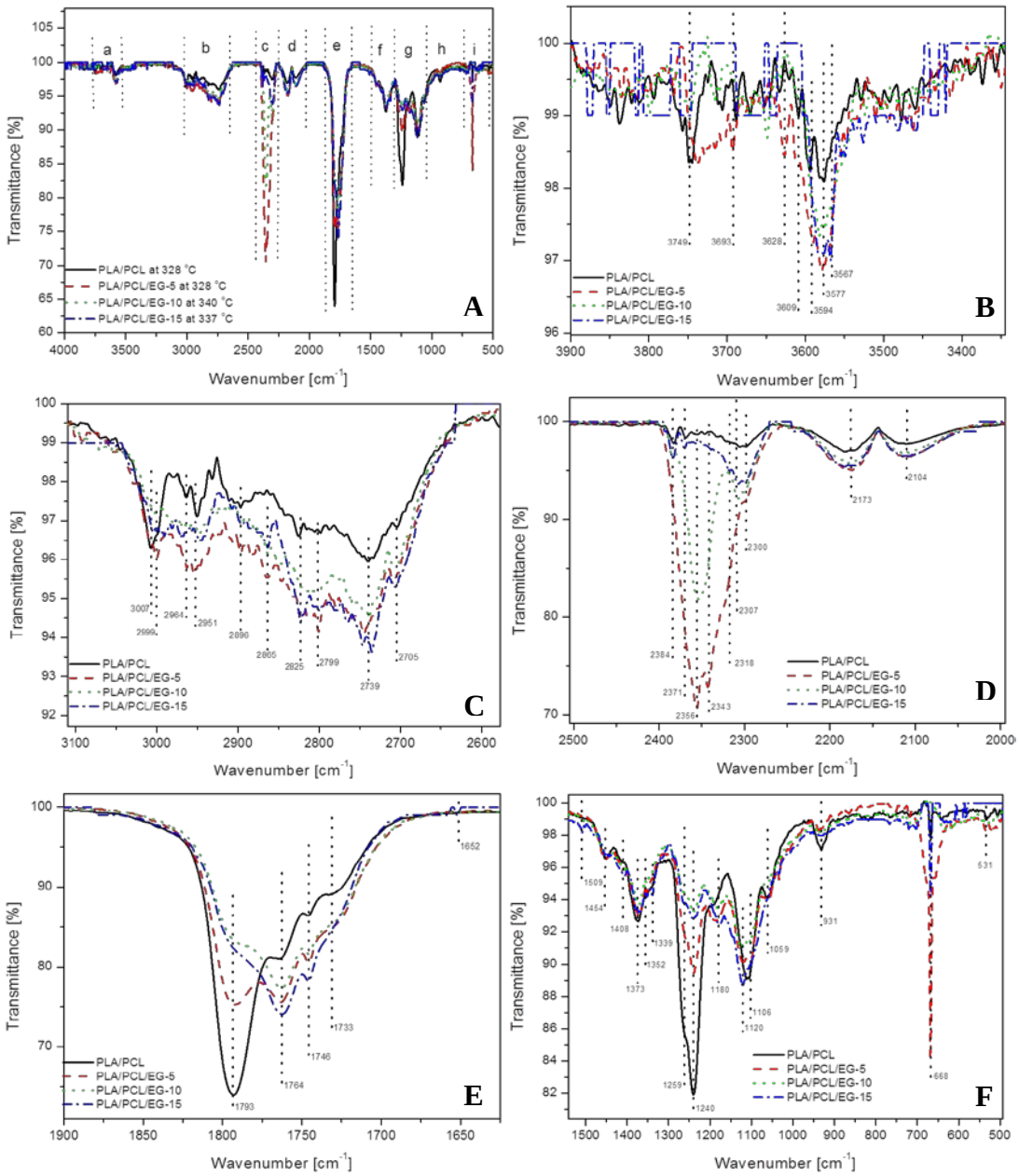

Figure 5.2 FTIR spectra of the blend and composites at the temperatures where the maximum pyrolysis products were given off: (A) PLA/PCL blend and PLA/PCL/EG composites, (B to F) spectra at various absorption regions

From Figure 5.2E, the bands at: 1793, 1764, 1746 and 1733 cm^{-1} indicate the presence of C=O (carbonyl) functional group. Furthermore, other groups can be identified thus: –OH near 3750-3400 cm^{-1} (Figure 5.2B) which may indicate the presence of an acid or water, C–O near 1240-1108 cm^{-1} (Figure 5.2F) indicative of esters, aldehyde C-H represented by two weak absorption peaks at 2825 and 2739 cm^{-1} (Figure 5.2C). This is in line with studies in literature [10,55,56] that the main volatile decomposition products, in addition to water, CO_2 and CO, include an aldehyde, lactide and methane for PLA and 5-hexenoic acid and ε-caprolactone (characteristic

band at 1733 cm^{-1}) for PCL (Figure 5.2E). The composites show relatively high peak intensities for –OH (Figure 5.2B), hydrocarbons (Figure 5.2C) and CO_2 and CO (Figure 5.2D) when compared to the PLA/PCL blend. This indicates that the incorporation of EG in the PLA/PCL blend favoured the formation of compounds containing these functional groups [52-54].

5.3.3 Cone calorimetry

The cone calorimetry results for neat PLA and PCL are shown in Figures 5.3 to 5.5 and their data are summarized in Tables 5.4 and 5.5. The FPI was calculated according to Equation 5.1 [38]:

$$FPI = \frac{TTI}{PHRR} \tag{5.1}$$

Figure 5.3 illustrates the HRR for neat PLA, PCL and the PLA/PCL/EG composites at different EG loadings. The neat PLA in Figure 5.3A shows a peak shoulder at 363 kW m^{-2} followed by a PHRR at 414 kW m^{-2}. The combustion was complete after 350 s with some char residue left. PCL shows a PHRR and a shoulder at 250 and 175 kW m^{-2}, respectively, with complete combustion in 250 s. PLA and PCL showed some dripping behaviour during the test. Similar to neat the biopolymers, the PLA/PCL bio-blend shows a maximum peak and a shoulder (Figure 5.3B and Table 5.4). The PHRR was only 4% less than that for PLA (i.e. 398 kW m^{-2} when compared with 414 kW m^{-2}) and the shoulder followed as was observed for PCL. It is considered that HRR is an important parameter and normally a high HRR may lead to shorter ignition time [8]. This was observed for the PLA and PLA/PCL blend samples which had a shorter TTI when compared to the PCL sample.

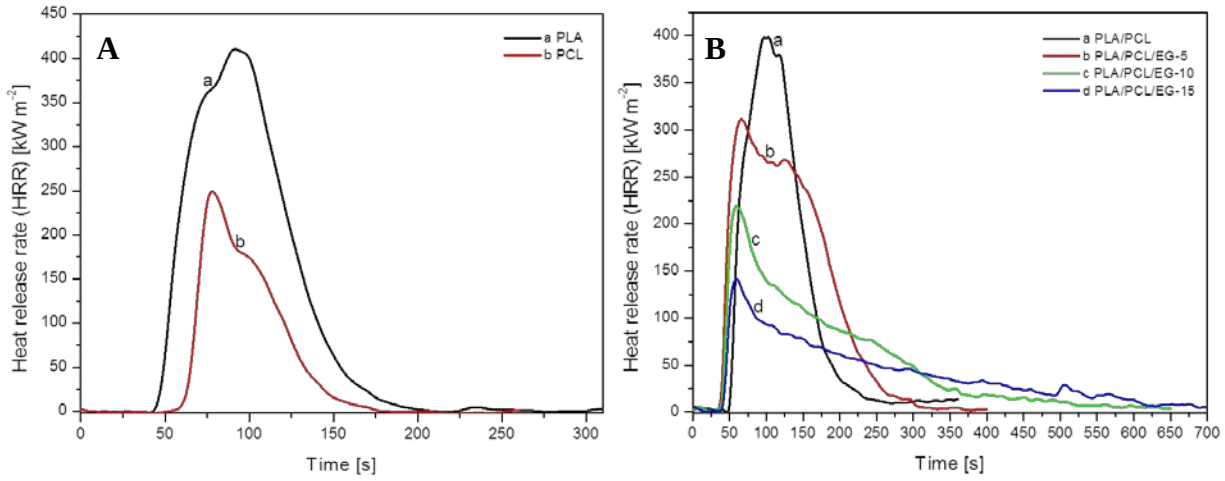

Figure 5.3 Heat release rate (HRR) curves for (A) neat PLA and PCL, and (B) PLA/PCL/EG composites at various EG contents

Table 5.4 Cone calorimetric results (at 35 kW m^{-2} heat flux) of all the investigated samples

Sample	TTI [s]	PHRR [kW m^{-2}]	THR [MJ m^{-2}]	EHC [MJ kg^{-1}]	av-MLR [g s^{-1} m^{-2}]	MARHE [kW m^{-2}]	FPI [m^2 s kW^{-1}]
PLA	44 ± 0	414 ± 0 363 ± 0	30 ± 2	16 ± 0.1	8.6 ± 0.3	203 ± 3	0.11
PCL	55 ± 1	250 ±3 175 ± 0	12 ± 1	5 ± 0.2	22 ± 0.1	87 ± 5	0.22
PLA/PCL	47 ± 0	398 ± 4 382 ± 1	37 ± 0.2	16 ± 0.1	12 ± 0.4	199 ± 2	0.12
PLA/PCL/EG-5	40 ± 0	311 ± 9 266 ± 2	43 ± 1	19 ± 0.5	12 ± 0.2	196 ± 4	0.13
PLA/PCL/EG-10	36 ± 1	225 ± 5	33 ± 0.2	18 ± 0.4	4 ± 0.2	111 ± 2	0.16
PLA/PCL/EG-15	38 ± 1	145 ± 1	29 ± 1	17 ± 0.1	3 ± 0.1	71 ± 1	0.26

TTI, time to ignition; PHRR, peak heat release rate; THR, total heat release; EHC, effective heat of combustion; av-MLR, averge specific mass loss rate; MARHE, maximum average rate of heat emission and FPI, fire performance index.

The TTI for the PLA/PCL/EG composites was lowered with the incorporation of EG (Table 5.4) and this is attributed to the effect of acid present within the EG layers. As is observed in Figure 5.3B, the presence of EG in the composites led to a remarkable decrease in PHRR. The combustion times of the PLA/PCL/EG composites increased with increasing EG content. At 5 wt.% EG content, the HRR is characterized by a PHRR (~311 kW m^{-2}) and a shoulder (~266 kW m^{-2}), similar to the blend. However, at 10 and 15 wt.% EG loadings, only one HRR peak maximum was observed. An increase in EG content showed a 22, 43 and 64% reduction in PHRR at 5, 10 and 15 wt.% EG, respectively. This is attributed to the ability of EG to exfoliate

during combustion and form a protective intumescent char layer on the composite surface as shown in Figure 5.6. During heating of EG (expandable graphite), the intercalated acid anions decompose with the consequent quick expansion of the EG interlayers. This leads to the formation of a porous carbonaceous (i.e. expanded graphite) char layer which protects the substrate from air/oxygen, heat and fuel production [57]. Thus, the exfoliated graphite layers produced acted as a barrier for heat transfer from the source (cone) to the PLA/PCL/EG composite materials. This behaviour has been reported in several studies, where graphite was used either alone or with other flame retardant additives in PLA [6,8], polypropylene (PP) [58] and EVA [38]. In their study, Murariu *et al*. [8] observed that the PHRR of melt-mixed PLA/EG (i.e. 6 wt.% EG) nano-composites decreased by ~30% with char formation and non-dripping behaviour.

Figure 5.4 illustrates the THR curves of PLA, PCL and PLA/PCL/EG composites. The slope of the THR curve is assumed to be representative of flame spread rate [38]. As observed in Figure 5.4A, PLA exhibited a higher flame spread (steeper slope) and a THR value of 30 MJ m^{-2}, while PCL had a lower flame spread and a THR of 12 MJ m^{-2} (Table 5.4). Surprisingly, the PLA/PCL blend showed a 19% increase in THR when compared to PLA. It can be seen in Figure 5.4B that the flame spread rates were similar for the 5 wt.% EG composite and the PLA/PLC blend, but the THR of the 5 wt.% EG composite increased from 37 to 43 MJ m^{-2}. Decreases in THR to 33 MJ m^{-2} and 29 MJ m^{-2} were observed for the 10 and 15 wt.% EG composites, respectively and the flame spread rate was lower. When compared to the PLA/PCL blend, there was a 14% increase and an 11 and 29% decreases in THR for the 5, 10 and 15 wt.% EG containing samples, respectively. The results indicate that the composites, at higher EG levels, are partially protected by the exfoliated EG without complete combustion. At 5 wt.% EG level, however, the barrier is insufficient to prevent the release of volatile combustion products [27].

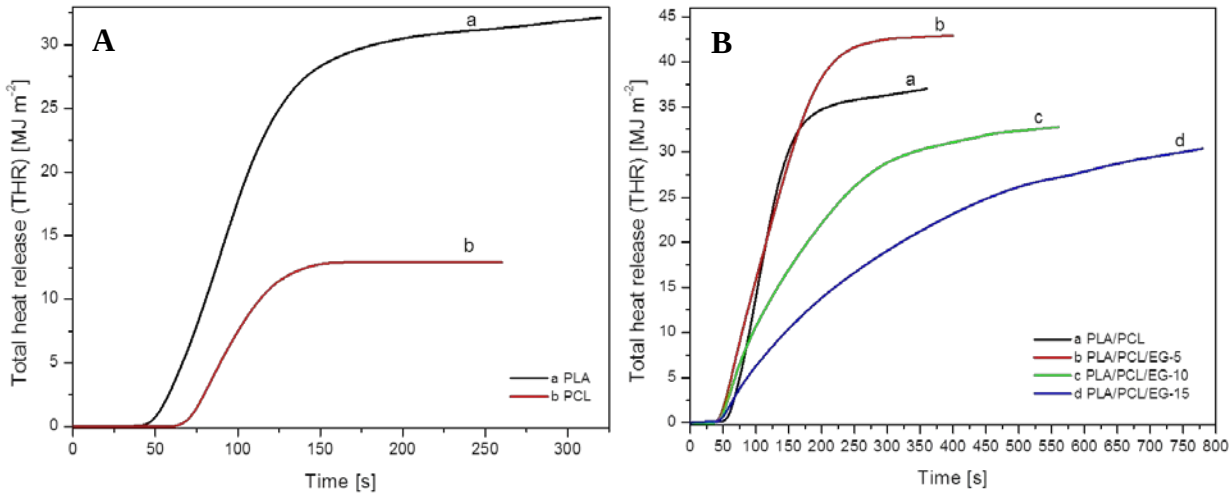

Figure 5.4 Total heat release (THR) curves for (A) neat PLA and PCL, and (B) PLA/PCL/EG composites at various EG contents

The effective heat of combustion (EHC) was higher for PLA when compared to PCL and for the blend, the EHC resembled that of PLA (Table 5.4). The EHC for the composites was higher than that for the blend, but decreased with increase in EG content. Turku *et al*. [59] and Wei *et al*. [27] reported similar findings. Blending PLA with PCL led to a 40% increase in av-MLR when compared to PLA alone and this is probably due to the presence of PCL with a high av-MLR. The av-MLR of the composites was only reduced at higher 10 and 15wt.% EG loadings, corresponding to 67 and 75% reductions in av-MLR when compared to the PLA/PCL blend. The reduced av-MLR relates to slower pyrolysis of the samples because of the formation of a intumescent char layer.

The maximum average rate of heat emission (MARHE) is defined as the peak value of the cumulative heat emission over time. It provides a measure of the tendency for fire development under real fire scale conditions [39]. For the PLA/PCL blend, a 2% reduction (with respect to PLA) in MARHE was observed. The MARHE values for the 5, 10 and 15 wt.% EG containing composites were reduced, respectively by 1.5, 44 and 64%. This indicates that the composites, at higher EG levels, may have a low tendency for fire development under real state conditions. The fire performance index (FPI) presented in Table 5.4 is also closely related to a real fire situation and enables the estimation of the predicted fire spread rate and size of the fire. Thus, it is a good indicator of the contribution to fire growth of materials [38]. The FPI increased by 8, 19 and 54% for the respective EG loadings, indicating that these composite materials would probably have less contribution to fire growth in a real fire situation.

The smoke emission behaviour results of the composites investigated are illustrated in Figure 5.5 and Table 5.5. It is observed that PLA exhibited low total smoke release (TSR) (Figure 5.5A) and specific extinction area (SEA) values (Table 5.5). This may be attributed to the presence of additives as discussed in section 5.3.1. These enabled the PLA to form a char residue that might have aided in reducing the yield of pyrolyzates and hence, decreasing smoke reduction [60]. However, high yields of CO and CO_2 are observed for PLA. This is because CO and CO_2 are amongst the main thermal decomposition products of PLA (section 5.3.1) [61]. PCL showed a converse behaviour to PLA, by exhibiting high TSR and SEA values, as well as low CO and CO_2 yields. It is clear from the smoke emission behaviour results that PLA generates more combustion gases, while PCL contributes more, towards visible smoke. In the case of the blend, the TSR, SEA and CO_2 yield increased by 79, 48 and 7%, respectively, while the CO yield decreased by 12%, relative to that of PLA. It can be inferred from the fire performance and smoke emission behaviour that the blend is a highly flammable material that may benefit from the incorporation of fire retardant fillers, such as expandable graphite.

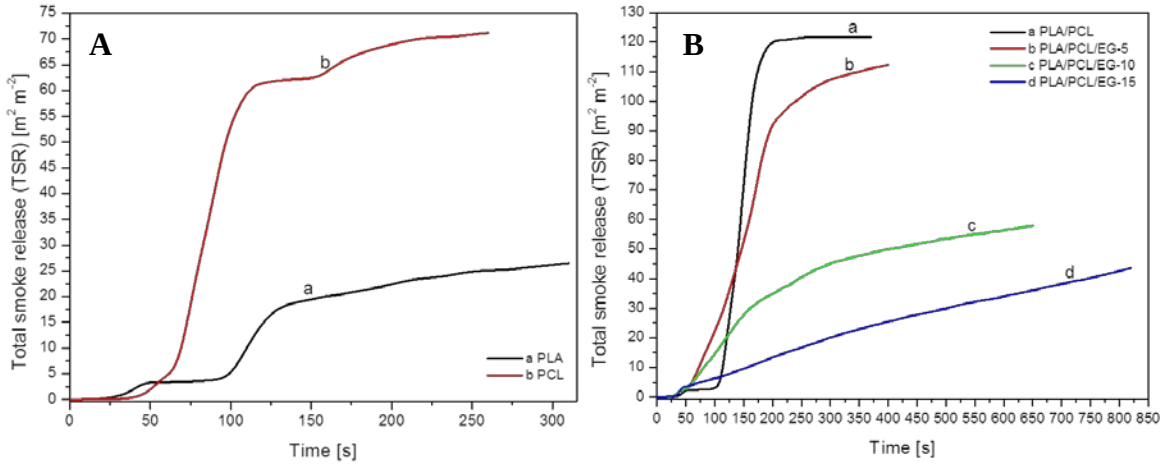

Figure 5.5 Total smoke release (TSR) curves for (A) neat PLA and PCL, and (B) PLA/PCL/EG composites at various EG contents

Table 5.5 Smoke emission behaviour of neat PLA, PCL and the PLA/PCL/EG biocomposites by cone calorimeter (35 kW m^{-2} heat flux)

Sample	TSR [m^2 m^{-2}]	SEA [m^2 kg^{-1}]	CO (× 10^{-3}) [kg kg^{-1}]	CO_2 [kg kg^{-1}]	CO/CO_2 (×10^{-3})
PLA	23 ± 1	18 ± 2	15 ± 3	1.3 ± 0.01	11.5
PCL	60 ± 8	21 ± 4	5.2 ± 0.1	0.4 ± 0.02	13.7
PLA/PCL	111 ± 9	48 ± 3	12 ± 1	1.4 ± 0.04	8.6
PLA/PCL/EG-5	113 ± 3	50 ± 2	32 ± 0.01	1.7 ± 0.04	18.8
PLA/PCL/EG-10	58 ± 1	28 ± 2	102 ± 3	1.6 ± 0.04	63.7
PLA/PCL/EG-15	40 ± 3	22 ± 1	142 ± 6	1.4 ± 0.02	101

The smoke emission characteristics of the biocomposites show that the presence of EG led to a reduction in TSR and SEA (Figure 5.5 and Table 5.5). The TSR was reduced by 48 and 64% at 10 and 15 wt.% EG loadings, respectively. Although the TSR value at 5 wt.% EG is 2% higher than that for the blend, it is within the cone calorimeter experimental error and 5% EG made no difference to the TSR. Similar to the TSR, the SEA values were lower by 42 and 54% at the 10 and 15 wt.% EG loadings, with respect to that of the blend. These results imply that EG performed an important smoke suppression role for the composites, especially at high loadings. Similar findings were reported for TSR by Wu *et al*. [38] in their study of the potential flame retardancy action of expanded graphite, natural graphite and graphite oxide in EVA-based composites.

CO yields increased consistently with EG content. This may be due to the high level of oxidation during manufacture of expandable graphite (EG), which when heated above ~200 °C, produces carbon monoxide as one of the products [62]. On the other hand, although the CO_2 yields generally showed a decreasing trend as a function of EG content, however they were higher at 5 and 10 wt.% EG contents and equal to that of the blend at 15 wt.% EG content. The CO/CO_2 weight ratio presented in Table 5.5 is a useful parameter that gives an indication of the extent of combustion completeness in a system. The greater this ratio, the lower is the combustion completeness. From the table, it can be seen that the blend shows the lowest CO/CO_2 weight ratio, implying a high degree of completeness of the combustion. For the composites, the values of this parameter increased as a function of EG content. This clearly indicates that the combustion reaction was not complete in the presence of EG, which implies that some of the molten materials could not be completely converted to gaseous flammable volatiles and transferred to the flame zone, but remained trapped within the exfoliated graphite.

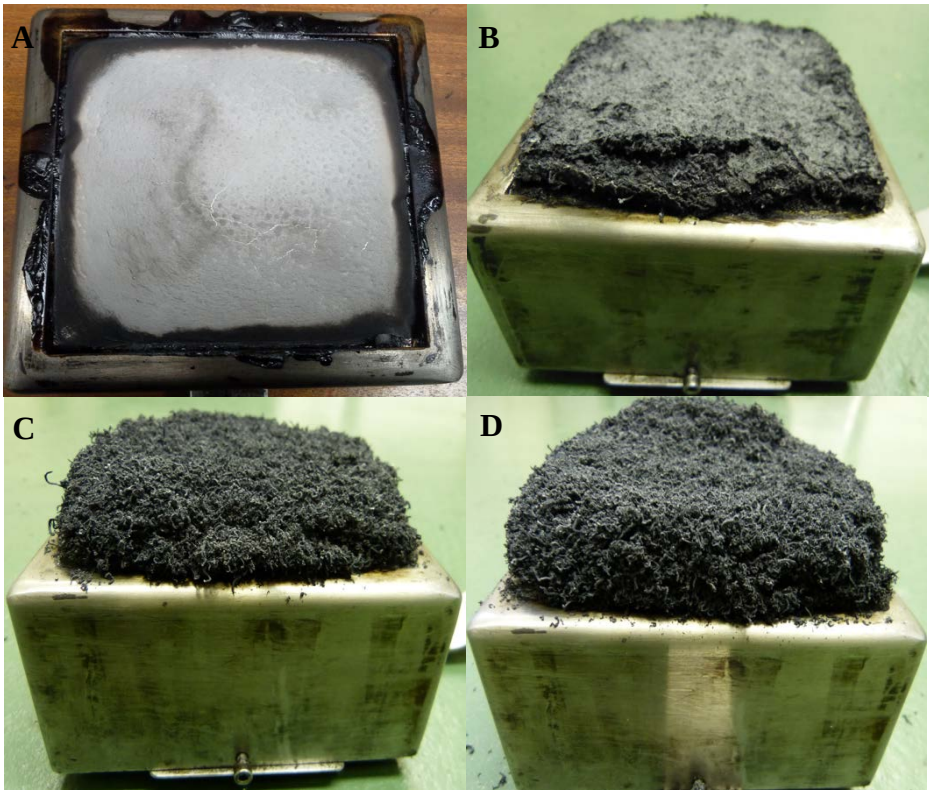

Figure 5.6 Images of the char residues obtained after cone calorimetry tests of the (A) PLA/PCL blend and the (B) PLA/PCL/EG-5, (C) PLA/PCL/EG-10 and (D) PLA/PCL/EG-15 composites

Figure 5.6 shows the images of the char obtained after the cone calorimetry test of the different samples investigated. It can be seen, for the blend (Figure 5.6A) that only a grey ash remained. In the presence of EG, an intumescent multicellular worm-like char is observed. This comes as a result of the exfoliation of the expandable graphite during heating due to the release of CO_2 and SO_2 gases [40]. It is during this endothermic exfoliation process of EG that the decrease in temperature of the system is triggered, thus manifesting a cooling effect. It is also noted that during exfoliation, CO_2 and H_2O gases were released which diluted the concentration of the mixture of combustible gases *via* fuel dilution. The multicellular worm-like char formed provided a solid protective layer limiting the transfer of heat and combustible volatile gases [4,37]. The amount of char increased with EG content in the composites, as discussed in section 5.3.1.

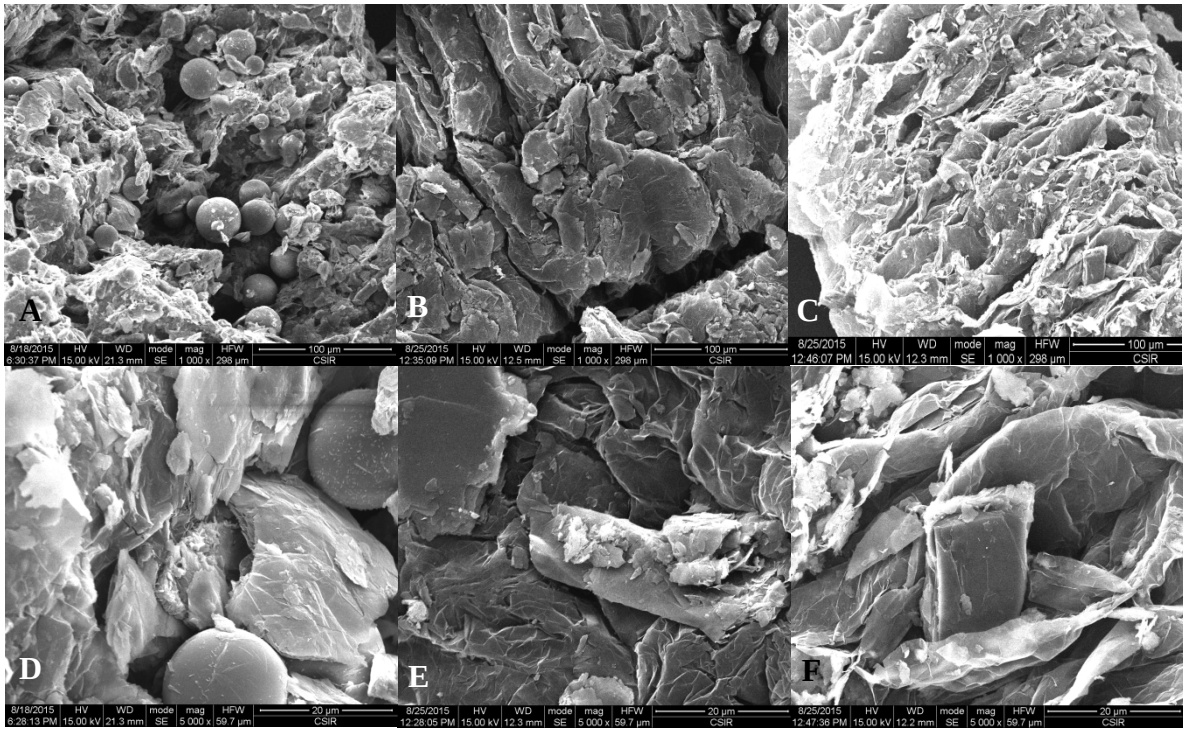

Figure 5.7 SEM micrographs of the char layers after the cone calorimetry test: (A & D) PLA/PCL/EG-5; (B & E) PLA/PCL/EG-10; (C & F) PLA/PCL/EG-15

The SEM micrographs of the char layers of the different samples after the cone calorimetry test are presented in Figure 5.7. All the composites' char layers contain some flake-like structures on their surfaces with some microspheres "beads" embedded within the char [42]. For the 5 wt.% EG containing composite (Figure 5.7A & D), the char layer microstructure is discontinuous and has some pores. For the 10 wt.% EG content, an improved char microstructure is observed. However, the char consists of some visible cracks (Figure 5.7B & E). For the 15 wt.% EG loading, a worm-like structure with the multicellular surface of the exfoliated graphite can be seen (Figure 5.7C). In Figure 5.7F, at a high magnification, a greater continuous char microstructure is noted. The char varies from discontinuous and porous, continuous and cracked to multicellular and smooth microstructural surfaceemanating from the 5 to 15 wt.% EG contents, respectively. It is reported in literature that an effective protective char layer improves flame retardancy [37]. It can be concluded that the 10 and 15 wt.% EG loaded compositions have effective protective char morphology, which accounts for the good fire resistance properties of these composites.

5.4 Conclusions

The effect of expandable graphite on the flammability and thermal stability properties of a PLA/PCL blend was investigated. It was found that the thermal stability of the composites was improved, relative to the blend. Although, the char content of the composites was generally increased with EG loadings, however the combined % residue from the blend and wt.% EG initially added to the blend was higher than the observed % residue because of the thermal degradation mechanism that favoured the formation of CO and CO_2 volatile gases, rather than carbon. From the flammability performance observations, the composite systems had high EHC and CO yields and therefore, require further improvements. However, it can be concluded that the biocomposite materials manufactured, possessed better fire resistance characteristics due to the ability of EG to exfoliate and intumesce, thereby forming a barrier that protects the underlying composite material from heat, air/oxygen and further pyrolysis and combustion. The cone calorimetry investigations showed that the PLA/PCL blend was successfully modified by the EG micro-filler in order to obtain bio-based materials with improved fire resistant properties. This was confirmed by the reduced flammability parameters: 64% in PHRR, 65% in MARHE, 22% in THR, 64% in TSR and 54 % reduction in SEA. The av-MLR and FPI were also reduced by 75 and 55%, respectively, in the presence of EG. For possible applications in the electrical and electronics fields, in addition to the observed challenges, it will be necessary to further investigate the electrical and thermal conductivity characters, rheology, as well as the static and dynamic mechanical properties of the PLA/PCL/EG composites.

Acknowledgements

The authors would like to acknowledge the financial support by the National Research Foundation (NRF) and the Professional Development Programme (PDP). Acknowledgements are also extended to colleagues and researchers for their undivided attention and support.

References

1. Yu, L., Dean, K., Li, L. (2006). Polymer blends and composites from renewable resources. *Progress in Polymer Science*, 31:576-602.
   DOI: 10.1016/j.progpolymsci.2006.03.002

2. Cabedo, L., Feijoo, J.L., Villanueva, M.P., Lagarón, J.M., Giménez, E. (2006). Optimization of biodegradable nanocomposites based on aPLA/PCL blends for food packaging applications. *Macromolecular Symposia*, 233:191-197.
DOI: 10.1002/masy.200650124
3. Takayama, T., Todo, M., Tsuji, H. (2011). Effect of annealing on the mechanical properties of PLA/PCL and PLA/PCL/LTI polymer blends. *Journal of the Mechanical Behavior of Biomedical Materials*, 4:255-260.
DOI: 10.1016/j.jmbbm.2010.10.003
4. Mngomezulu, M.E., John, M.J., Jacobs, V., Luyt, A.S. (2014). Review on flammability of biofibres and biocomposites. *Carbohydrate Polymers*, 111:149-182.
DOI: 10.1016/j.carbpol.2014.03.071
5. Gupta, A.P., Kumar, V. (2007). New emerging trends in synthetic biodegradable polymers – Polylactide: A critique. *European Polymer Journal*, 43:4053-4074.
DOI: 10.1016/j.eurpolymj.2007.06.045
6. Fukushima, K., Murariu, M., Camino, G., Dubois, P. (2010). Effect of expanded graphite/layered-silicate clay on thermal, mechanical and fire retardant properties of poly(lactic acid). *Polymer Degradation and Stability*, 95:1063-1076.
DOI: 10.1016/j.polymdegradstab.2010.02.029
7. Huang, G., Gao, J., Wang, X., Liang, H., Ge, C. (2012). How can graphene reduce the flammability of polymer nanocomposites? *Materials Letters*, 66:187-189.
DOI: 10.1016/j.matlet.2011.08.063
8. Murariu, M., Dechief, A.L., Bonnaud, L., Paint, Y., Gallos, A., Fontaine, G., Bourbigot, S., Dubois, P. (2010). The production and properties of polylactide composites filled with expanded graphite. *Polymer Degradation and Stability*, 95:889-900.
DOI: 10.1016/j.polymdegradstab.2009.12.019
9. Rasal, R.M., Janorkar, A.V., Hirt, D.E. (2010). Poly(lactic acid) modifications. *Progress in Polymer Science*, 35:338-356.
DOI: 10.1016/j.progpolymsci.2009.12.003
10. Vogel, C., Siesler, H.W. (2008). Thermal degradation of poly(ε-caprolactone), poly(L-lactic acid) and their blends with poly(3-hydroxy-butyrate) studies by TGA/FT-IR spectroscopy. *Macromolecular Symposia*, 265:183-194.
DOI: 10.1002/masy.200850520

11. Wu, D., Zhang, Y., Zhang, M., Zhou, W. (2008). Phase behaviour and its viscoelastic response of polylactide/poly(ε-caprolactone) blend. *European Polymer Journal*, 44:2171-2183.
DOI: 10.1016/j.eurpolymj.2008.04.023
12. Patrício T., Domingos M., Gloria, A., Bártolo, P. (2013). Characterisation of PCL and PCL/PLA scaffolds for tissue engineering. *Procedia CIRP*, 5:110-114.
DOI: 10.1016/j.procir.2013.01.022
13. Patrício, T., Bártolo, P. (2013). Thermal stability of PCL/PLA blends produced by physical blending process. *Procedia Engineering*, 59:292-297.
DOI: 10.1016/j.proeng.2013.05.124
14. Todo, M., Park, S-D., Takayama, T., Arakawa, K. (2007). Fracture micromechanisms of bioabsorbable PLLA/PCL polymer blends. *Engineering Fracture Mechanics*, 74:1872-1883.
DOI: 10.1016/j.engfracmech.2006.05.021
15. Li, H., Huneault, M.A. (2011). Comparison of sorbitol and glycerol as plasticizers for thermoplastic starch in TPS/PLA blends. *Journal of Applied Polymer Science*, 119:2439-2448.
DOI: 10.1002/app.32956
16. Chavalitpanya, K., Phattanarudee, S. (2013). Poly(lactic acid)/polycaprolactone blends compatibilized with block copolymer. *Energy Procedia*, 34:542-548.
DOI: 10.1016/j.egypro.2013.06.783
17. Park, J.W., Im, S.S. (2002). Phase behavior and morphology in blends of poly(L-lactic acid) and poly(butylene succinate). *Journal of Applied Polymer Science*, 86:647-655.
DOI: 10.1002/app.10923
18. Wu, D., Lin, D., Zhang, J., Zhou, W., Zhang, M., Zhang, Y., Wang, D., Lin, B. (2011). Selective localization of nanofillers: Effect on morphology and crystallization of PLA/PCL blends. *Macromolecular Chemistry and Physics*, 212:613-626.
DOI: 10.1002/macp.201000579
19. Lin, L., Deng, C., Lin, G.-P., Wang, Y.-H. (2014). Mechanical properties, heat resistance and flame retardancy of glass fiber-reinforced PLA-PC alloys based on aluminum hypophosphite. *Polymer-Plastics Technology and Engineering*, 53:613-625.
DOI: 10.1080/03602559.2013.866244
20. Kimura K., Horikoshi Y. (2005). Bio-based polymers, *Fujitsu Scientific and Technical Journal*, 41(2):173-180.

21. Das K., Ray, S.S., Chapple, S., Wesley-Smith, J. (2013). Mechanical, thermal, and fire properties of biodegradable polylactide/boehmite alumina composites. *Industrial & Engineering Chemistry Research*, 52:6083-6091.
DOI: 10.1021/ie4004305
22. Fukushima, K., Tabuani, D., Camino, G. (2012). Poly(lactic acid)/clay nanocomposites: Effect of nature and content of clay on morphology, thermal and thermo-mechanical properties. *Materials Science and Engineering C*, 32:1790-1795.
DOI: 10.1016/j.msec.2012.04.047
23. Fukushima, K., Tabuani, D., Arena, M., Gennari, M., Camino, G. (2013). Effect of clay type on thermal, mechanical properties and biodegradation of poly(lactic acid) nanocomposites. *Reactive & Functional Polymers*, 73:540-549.
DOI: 10.1016/j.reactfunctpolym.2013.01.003
24. Hapuarachchi T.D., Peijs, T. (2010). Multiwalled carbon nanotubes and sepiolite nanoclays as flame retardants for polylactide and its natural fibre reinforced composites. *Composites: Part A*, 41:954-963.
DOI: 10.1016/j.compositesa.2010.03.004
25. Murariu, M., Dechief, A.-L., Paint, Y., Peeterbroeck, S., Bonnaud, L., Dubois, P. (2012). Polylactide (PLA)-halloysite nanaocomposites: Production, morphology and key-properties. *Journal of Polymers and the Environment*, 20:932-943.
DOI: 10.1007/s10924-0488-4
26. Tang, G., Wang, X., Xing, W., Zhang, P., Wang, B., Hong, N., Yang, W., Hu, Y., Song, L. (2012). Thermal degradation and flame retardance of biobased polylactide composites based on aluminum hypophosphite. *Industrial & Engineering Chemistry Research*, 51:12009-12016.
DOI: 10.1021/ie3008133
27. Wei, P., Bocchini, S., Camino, G. (2013). Flame retardant and thermal behavior of polylactide/expandable graphite composites. *Polimery*, 58(5):361-364.
DOI: 10.14314/polimery.2013.361
28. Zhu, H., Zhu, Q., Li, J., Tao, K., Xue, L., Yan, Q. (2011). Synergistic effect between expandable graphite and ammonium polyphosphate on flame retarded polylactide. *Polymer Degradation and Stability*, 96:183-189.
DOI: 10.1016/j.polymdegradstab.2010.11.017
29. Pluta, M., Galeski, A., Alexandre, M., Paul, M.-A., Dubois, P. (2002). Polylactide/montmorillonite nanocomposites and microcomposites prepared by melt

blending: Structure and some physical properties. *Journal of Applied Polymer Science*, 86:1497-1506.
DOI: 10.1002/app.11309

30. Jain, S., Misra, M., Mohanty, A.K., Ghosh, A.K. (2012). Thermal, mechanical and rheological behavior of poly(lactic acid)/talc composites. *Journal of Polymers and the Environment*, 20:1027-1037.
DOI: 10.1007/s10924-012-0500-z
31. Dorigato, A., Sebastiani, M., Pegoretti, A., Fambri, L. (2012). Effect of silica nanoparticles on the mechanical performances of poly(lactic acid). *Journal of Polymers and the Environment*, (2012) 20:713-725.
DOI: 10.1007/s10924-012-0425-6
32. Sengupta, R., Bhattacharya, M., Bandyopadhyay, S., Bhowmick, A.K. (2011). A review on the mechanical and electrical properties of graphite and modified graphite reinforced composites. *Progress in Polymer Science*, 36:638-670.
DOI: 10.1016/j.progpolymsci.2010.11.003
33. Gallo, E., Schartel, B., Acierno, D., Russo, P. (2011). Flame retardant biocomposites: Synergism between phosphinate and nanometric metal oxides. *European Polymer Journal*, 47:1390-1401.
DOI: 10.1016/j.eurpolymj.2011.04.001
34. Xie, R., Qu, B. (2001). Synergistic effects of expandable graphite with some halogen-free flame retardants in polyolefin blends. *Polymer Degradation and Stability*, 71:375-380.
PII: S0141-3910(00)00188-9
35. Bourbigot, S., Fontaine, G. (2010). Flame retardancy of polylactide: An overview. *Polymer Chemistry*, 1:1413-1422.
DOI: 10.1039/c0py00106f
36. Lee, J.D. (1995). Concise Inorganic Chemistry. 4th Edition. Chapman & Hall Ltd. Singapore.
37. Pang, X.-Y., Weng, M.-Q. (2014). Preparation of expandable graphite composite under the auxiliary intercalation of zinc sulfate and its flame retardancy for ethylene/vinyl acetate copolymer. *International Journal of ChemTech Research*, 6(2):1291-1298.
38. Wu, X., Wang, L., Wu, C., Yu, J., Xie, L., Wang, G., Jiang, P. (2012). Influence of char residues on flammability of EVA/EG, EVA/NG and EVA/GO composites. *Polymer Degradation and Stability*, 97:54-63.

DOI: 10.1016/j.polymdegradstab.2011.10.011

39. Focke, W.W., Kruger, H.J., Mhike, W., Taute, A., Roberson, A., Ofosu, O. (2014). Polyethyelene flame retarded with expandable graphite and a novel intumescent additive. *Journal of Applied Polymer Science*, 40493:1-8.
DOI: 10.1002/app.40493
40. Focke, W.W., Muiambo, H., Mhike, W., Kruger, H.J., Ofosu, O. (2014). Flexible PVC flame retarded with expandable graphite. *Polymer Degradation and Stability*, 100:63-69.
DOI: 10.1016/j.polymedegradstab.2013.12.024
41. Tang. G., Zhang, R., Wang, X., Wang, B., Song, L., Hu, Y., Gong, X. (2013). Enhancement of flame retardant performance of bio-based polylactic acid composites with the incorporation of aluminum hypophosphite and expanded graphite. *Journal of Macromolecular Science, Part A: Pure and Applied Chemistry*, 50:255-269.
DOI: 10.1080/10601325.2013.742835
42. Chapple, S., Anandjiwala, R., Ray, S.S. (2013). Mechanical, thermal, and fire properties of polylactide/starch blend/clay composites. *Journal of Thermal Analysis and Calorimetry*, 113:703-712.
DOI: 10.1007/s10973-012-2776-6
43. http://www.gk-graphite.cn/fileadmin/user_upload/PDF/List_standard.pdf (26/10/2015)
44. http://trellisbioplastic.com/wp-content/uploads/2014/08/Sustainable-1001-Property-Guide.pdf (26/10/2015)
45. Kopinke, F.-D., Remmler, M., Mackenzie, K., Milder, M., Wachsen, O. (1996). Thermal decomposition of biodegradable polyesters – II. Poly(lactic acid). *Polymer Degradation and Stability*, 53:329-342.
PII: S0141-3910(96)00102-4
46. Carrasco, F., Pagès, P., Gámez-Pérez, J., Santana, O.O., Maspoch, M.L. (2010). Processing of poly(lactic acid): Characterization of chemical structure, thermal stability and mechanical properties. *Polymer Degradation and Stability*, 95:116-125.
DOI: 10.1016/j.polymdegradstab.2009.11.045
47. Nicolae, C.-A., Grigorescu, M.A., Gabor, R.A. (2008). An investigation of thermal degradation of poly(lactic acid). *Engineering Letter*, 16:4, EL_16_4_16.
48. Gupta, M.C., Deshmukh, V.G. (1982). Thermal oxidative degradation of poly-lactic acid. *Colloid & Polymer Science*, 260:514-517.

49. Westphal, C., Perrot, C., Karlsson, S. (2001). Py-GC/MS as a means to predict degree of degradation by giving microstructural changes modelled on LDPE and PLA. *Polymer Degradation and Stability*, 73:281-287.
PII: S0141-3910(01)00089-1

50. Fukushima, K., Tabuani, D., Camino, G. (2009). Nanocomposites of PLA and PCL based on montmorillonite and sepiolite. *Materials Science and Engineering C*, 29:1433-1441.
DOI: 10.1016/j.msec.2008.11.005

51. Uhl, F.M., Yao, Q., Nakajima, H., Manias, E., Wilkie, C.A. (2005). Expandable graphite/polyamide-6 nanocomposites. *Polymer Degradation and Stability*, 89:70-84.
DOI: 10.1016/j.polymdegradstab.2005.01.004

52. Pavia, D.L., Lampman, G.M., Kriz, Jr. G.S. (1979). Introduction to Spectroscopy: A Guide for Students of Organic Chemistry. Saunders College Publishing, Harcourt Brace Jovanovich College Publishers, Philadelphia.

53. Persenaire, O., Alexandre, M., Degée, P., Dubois, P. (2001). Mechanisms and kinetics of thermal degradation of poly(ε-caprolactone). *Biomacromolecules*, 2:288-294.
DOI: 10.1021/bm0056310

54. Liu, X., Khor, S., Petinakis, E., Yu, L., Simon, G., Dean, K., Bateman, S. (2010). Effects of hydrophilic fillers on the thermal degradation of poly(lactic acid). *Thermochimica Acta*, 509:147-151.
DOI: 10.1016/j.tca.2010.06.015

55. Chen, X., Zhuo, J., Jiao, C. (2012). Thermal degradation characteristics of flame retardant polylactide using TG-IR. *Polymer Degradation and Stability*, 97: 2143-2147.
DOI: 10.1016/j.polymdegradstab.2012.08.016

56. Wang, X., Hu, Y., Song, L., Xuan, S., Xing, W., Bai, Z., Lu, H. (2011). Flame retardancy and thermal degradation of intumescent flame retardant poly(lactic acid)/starch biocomposites. *Industrial & Engineering Chemistry Research*, 50:713-720.
DOI: 10.1021/ie1017157

57. Weil, E.D., Levchik, S.V. (2008). Flame retardants in commercial use or development for textiles. *Journal of Fire Sciences*, 26:243-281.
DOI: 10.1177/0734904108089485

58. Bai, G., Guo, C., Li, L. (2014). Synergistic effect of intumescent flame retardant and expandable graphite on mechanical and flame-retardant properties of wood flour-polypropylene composites. *Construction and Building Materials*, 50:148-153.

DOI: 10.1016/j.conbuildmat.2013.09.028

59. Turku, I., Nikolaeva, M., Kärki, T. (2014). The effect of fire retardants on the flammability, mechanical properties, and wettability of co-extruded PP-based wood-plastic composites. *BioResources*, 9(1):1539-1551.
DOI: 10.15376/biores.9.1.1539-1551

60. Price, D., Anthony, G., Carty, P. (2001). Introduction: Polymer combustion, condensed phase pyrolysis and smoke formation. In Horrocks, A.R. & Price, D. (Eds.), Fire Retardant Materials. Woodhead Publishing Limited, England.

61. Zou, H., Yi, C., Wang, L., Liu, H., Xu, W. (2009). Thermal degradation of poly(lactic acid) measured by thermogravimetry coupled to Fourier transform infrared spectroscopy. *Journal of Thermal Analysis and Calorimetry*, 97:929-935.
DOI: 10.1007/s10973-009-0121-5.

62. Focke, W.W., Badenhorst, H., Mhike, W., Kruger, H.J., Lombaard, D. (2014). Characterization of commercial expandable graphite fire retardants. *Thermochimica Acta*, 584:8-16.
DOI: 10.1016/j.tca.2014.03.021

Chapter 6

Morphology, thermal and dynamic mechanical characteristics of fire resistant poly(lactic acid)/poly(ε-caprolactone)/expandable graphite (PLA/PCL/EG) composites

This chapter will be submitted unaltered for publication in an international journal.

Abstract

The effect of expandable graphite (EG) on the morphology, thermal and dynamic mechanical properties of flame retardant poly(lactic acid)/poly(ε-caprolactone)/expandable graphite (PLA/PCL/EG) composites was investigated in this study. The composites were prepared by melt-mixing and then characterized via X-ray diffraction (XRD), scanning electron microscopy (SEM), differential scanning calorimetry (DSC) and dynamic mechanical analysis (DMA) techniques. It was found that the melt-mixing process could not separate the graphite layers, which existed as aggregate structures (i.e. EG layered stacks and/or lumps). In the composites, PCL was favoured to crystallize, mainly on the surface of the microspheres and EG. The PLA/PCL blend showed an immiscibility feature even in the presence of EG filler. Incorporation of EG in PLA/PCL blend influenced the melting and crystallization behaviours of PCL than that of the PLA component. Both the PCL and EG hindered the crystallization of PLA component. From DSC and DMA data, the glass transition of the composites occurred at high temperatures, suggesting that PLA polymer chains were immobilized in the presence of EG micro filler. Both the storage and loss moduli were low for the composites when compared to PLA/PCL. The results suggest that the PLA/PCL/EG flame retardant composites have low thermal and thermo-mechanical properties, due to the aggregation of EG and the lack of interfacial adhesion between EG lumps and the polymer blend matrix.

Keywords: polylactic acid, poly-ε-caprolactone, expandable graphite, blends, composites, morphology, thermal properties, dynamic mechanical properties

6.1 Introduction

The development of biodegradable polymer blends and composites is of research interest, in recent times, from both academic and industrial domains. This important step is motivated by several factors due to the different/various properties and applications of biopolymers and commodity polymers. The latter polymers are marred by lack of biodegradability, which has raised environmental concerns. Additionally, depletion of fossil fuel resources and high cost, related to petroleum-based polymers are other factors motivating the development of biopolymer blends and composites. As a consequence, there is a need for alternative high performance materials that are eco-friendly. Biopolymers are obtained from bio-based renewable resources. They include those extracted directly from biomass (e.g. starch), those synthesised using either renewable bio-based monomers (e.g. polylactide, PLA) or oil-based monomers (e.g. poly-ε-caprolactone, PCL) and those produced by micro-organisms and genetically-modified bacteria (e.g. polyhydroxyalkanoates, PHA). Although biopolymers are characterized by eco-friendly properties, they have shortcomings, such as: lack of thermal stability, poor fire resistance and low mechanical properties. Therefore, the modification of biopolymers into useful blends and composite materials with sufficient properties for wide industrial applications, is indeed a necessity. There are different ways to the improve properties of biodegradable polymer systems. They include: blending, incorporation of fillers and/or reinforcement materials (i.e. composite formation), plasticization and impact modification [1-9]. For instance, the incorporation of commercial expandable graphite (EG) filler into a PLA/PCL blend, resulted in composites with improved fire resistance and thermal stability due to the intumescent nature of EG and its high thermal stability (see Chapter 5). Thus, the current study further investigates other properties (i.e. morphology and structure, thermal and thermo-mechanical properties) of these fire resistant and thermally-stable PLA/PCL/EG composites.

Biodegradable polymers, such as PLA and PCL, have inherent physical and/or chemical limitations that may be remedied by either blending and/or composite formation approaches. PLA is the most common bio-based, aliphatic polyesters produced from renewable lactic acid monomer, which is based on the fermentation of starch and other polysaccharides (i.e. from beet, sugar cane, potatoes and other biomasses) [2]. Although it is widely used, it has some flaws, such as: poor toughness, hydrophobicity and slow crystallization rate, lack of side-chain groups and poor flammability performance [2-8]. PCL, on the other hand, is a biodegradable, semi-crystalline linear aliphatic commercial polyester, produced from ε-caprolactone which

has good mechanical properties [8,9]. Blending PLA with PCL, either by melt mixing or solution casting, provides an important property complementarity. In this case, the glassy PLA with low thermal stability and high degradation, rate exhibits better tensile strength, while the rubbery PCL with high thermal stability and relatively slower degradation rate, shows better toughness [8-14].

Different biopolymer blend systems have been prepared and characterized for their morphology, structure, thermal and thermo-mechanical characteristics. For the morphology and structural properties, techniques including *inter alia* atomic force microscopy (AFM), XRD, SEM and transmission electron microscopy (TEM) are used, for thermal properties DSC and thermogravimetric analysis (TGA), while DMA and rheology testing techniques are used for thermo-mechanical characteristics. These provide valuable information on the surface topology and morphology, structural arrangements of the atoms and molecules within samples, melting and crystallization behaviour, thermal decomposition/degradation stability, and visco-elastic response relative to contributions of the viscous and elastic components of visco-elastic materials [9,15-21].

PLA was successfully blended with other different biopolymers, including: thermoplastic starch (i.e. PLA/TPS blends) [15], poly(butylene adipate-co-terephthalate) (i.e. PLA/PBAT blends) [16], poly(butylene succinate-b-ethylene succinate) multi block copolymer (i.e. PLA/PBES blends) [17], natural rubber (i.e. PLA/NR blends) [18], poly(ethylene glycol) (i.e. PLA/PEG blends) [19] and poly(ε-caprolactone) (i.e. PLA/PCL blends) [9,15,20,21]. The blends were prepared either via solution blending and casting or melt mixing processing methods. Amongst the studied systems, the PLA/PCL blends are of current research interest. For instance, Wu *et al*. [9], Sarazin *et al*. [15] and Hoidy *et al*. [21] reported on melt mixed PLA/PCL blend systems and found that these blends were immiscible at various compositions. Generally, most polymers are immiscible with other polymers because of the unfavourable factors, including entropy and enthalpy. This then leads to heterogeneous blend systems with multiphase morphology having very useful properties. It is also noted that the properties of such blends are not only dependent on the physical properties of each component, but also on the dispersed phase microstructure and their interfacial chemistry [18]. Wu *et al*. [9] showed that PLA/PCL blends morphology changed depending on the content of the component phases. From the etched (using acetic acid as the etchant) samples morphology, according to the authors, three different morphologies were possible viz.: i) spherical droplet, ii) elongated or

fibrous structure and iii) co-continuous structure. From this, it was concluded that 60 wt.% PLA, with respect to PLC, was the phase inversion region.

The successful development of PLA-based systems involving the incorporation of a third component in the binary biodegradable polymer blends has been reported. The third component(s), usually flexible material(s) when compared with PLA, may take a form of fillers, plasticizers and/or other biopolymers in order to improve the thermal, mechanical and visco-elastic properties of the blends. For instance, Sarazin *et al*. [15], Rodriguez-Llamazares *et al*. [19], Wu *et al*. [20] and Hoidy *et al*. [21], respectively reported on the resulting morphology and properties of PLA/PCL/TPS binary and ternary blends, the effect of PEG content on the structural and thermal properties of melt mixed PLA/PEG/clay nanocomposites, selective localization of carbon nanotubes (CNTs) and clay on PLA/PCL blends and the use of different organoclays on PLA/PCL/clay nanocomposites.

Based on XRD, SEM and TEM results, Hoidy *et al*. [21] reported that the silicate layers of the clay used were intercalated by PLA/PCL in both the solution cast and melt-blended PLA/PCL/clay composites. Rodríguez-Llamazares *et al*. [19] found that PEG molecules could co-intercalate between silicate layers of the clay, as well as with the PLA chains. This was found advantageous in that it allowed for better parallel stacking of silicate layers and interaction between them, hence the improved properties. Sarazin *et al*. [15] reported on significant improvements in impact and elongation-at-break properties of PLA through the addition of starch and PCL. It was attributed to the synergy between starch (i.e. at high glycerol contents) and PCL giving PLA/PCL/TPS ternary blends with improved properties. From viscosity measurements, the authors found that high glycerol contents in TPS showed viscosity reduction phenomenon, indicating an added benefit of TPS as a processing aid during melt processing of PLA/PCL/TPS blends. Furthermore, the glass transition temperature obtained via tan δ peak temperature from DMA was found independent of TPS composition and that the presence of PCL in the PLA/PCL/TPS ternary blend had insignificant effect on the blend transition [15]. In the case of the thermal properties of filled blends, Wu *et al*. [20] found that nanofiller localized in the PCL phase had a nucleation effect on the PCL melt crystallization, whereas for the cold crystallization of PLA component, both the PLA phase localized clay tactoids and the phase interface localized CNTs could promote crystallization of PLA. To the best of our knowledge, little or no work has been reported on the effect of the commercial expandable graphite (EG) micro-filler particles, as a third component on the: morphology,

structure, melting and crystallization behaviour as well as the dynamic mechanical properties of fire resistant PLA/PCL/EG composites.

The aim of this study is to investigate the: morphology, structure, melting and crystallization, and dynamic mechanical properties of flame retardant PLA/PCL/EG composites. The objectives are: i) to prepare PLA/PCL/EG samples by melt-mixing technique at 5, 10 and 15 wt.% EG loadings and ii) to characterize the biocomposites using X-ray diffraction (XRD), scanning electron microscopy (SEM), differential scanning calorimetry (DSC) and dynamic mechanical analysis (DMA).

6.2 Materials and methods

6.2.1 Materials

The polylactic acid (PLA) used in this study was a Cereplast Sustainable 1001 injection molding grade, containing additives derived from starch and other renewable resources, with physical properties as shown in Table 6.1. The polymer contains fillers, including silicon-based (i.e. glass) and microspheres [22]. Poly(ε-caprolactone) (PCL), in flakes form, was purchased from Sigma-Aldrich, South Africa. The PCL used had an average molecular weight ($\bar{M}_w$) and number average molecular weight ($\bar{M}_n$) of 14 000 and 10 000 g mol^{-1}, respectively. It has a melting point temperature (T_m) of 60 °C and a density (ρ) of 1.146 g ml^{-1}. The commercial expandable graphite (EG) used was an ES250 B5 grade, consisting of between 90-95% carbon content, with an expansion rate of between 250-500 cm^3 g^{-1} at the starting temperature range of between 180-300 °C, particle size: 80% of the particles > 300 µm and was supplied by Qingdao Kropfmuehl Graphite, China. The EG consists of $KMnO_4$ as an oxidant and H_2SO_4 as an intercalant [23,24]. Materials were used as received from the suppliers without any modification/purification, except for drying prior to the compounding.

Table 6.1 Physical properties of PLA, Cereplast Sustainable Resin 1001 grade [25]

Physical property	ASTM Test method	Values
Tensile strength at maximum	D 638	49.6 MPa
Tensile elongation at break	D 638	5.1%
Tensile modulus	D 638	3,590 MPa
Flexural modulus	D 790	3,360 MPa
Flexural strength	D 790	80 MPa
Gardner impact	D 5420	1.13 J
Notched Izod impact strength (at 23 °C)	D 256	40 J m^{-1}
Temperature deflection under 0.45 MPa	D 648	44 °C
Melt Flow Index 190 °C at 2.16 kg	D 1238	8 g/10min
Density (ρ)	D792 Method A	1.28 g ml^{-1}

6.2.2 Sample preparation

Samples were compounded according to the ratios shown in Table 6.2. The ratio of PLA/PCL was set at 85/15 w/w while the EG content was varied. PLA/PCL 85/15 w/w was selected due to its better tensile modulus and tensile strength as determined during preliminary tests. Components were dried overnight in an oven at 50 °C. The composites were then prepared by melt-mixing method, using Brabender-Plastograph with a mixing volume of 55 cm^3. The mixing temperature was 180 °C at a rotational speed of 60 rpm for 12 minutes. This was followed by hot melt pressing under 50 bar at 180 °C for 5 min. in order to obtain 140 mm x 140 mm x 2 mm sheets.

In order to establish the morphology of the blend and composites, samples were etched with acetic acid in order to dissolve the PCL component of the blend and composites. Etched samples were immersed in sufficient quantities of acetic acid in order to cover the samples at 50 °C for 24 hours. They were then dried in an oven for 24 hours prior to morphology analysis by SEM.

Table 6.2 Sample ratios of PLA/PCL/EG composites

Sample	Composition [wt.%]
PLA	100
PCL	100
PLA/PCL	85/15
PLA/PCL/EG-5	80.75/14.25/5
PLA/PCL/EG-10	76.5/13.5/10
PLA/PCL/EG-15	72.25/12.75/15

6.2.3 Sample analysis

The crystalline structures of EG and PLA/PCL/EG composites were determined through X-ray diffraction (XRD). A D8 Advance diffractometer (BRUKER AXS, Germany) with PSD Vantec-1 detectors and Cu K_α radiation (λ= 1.5406 Å), a tube voltage of 40 kV, a current of 40 mA and a V20 slit were used. The samples were scanned in a locked couple mode with 2θ increments (2θ range: 0-80°) and 0.5 s steps. The inter-layer distance (i.e. *d*-spacing) of the EG in the composites was calculated using the Bragg's diffraction equation 6.1 [22]:

$$2d \sin\theta = n\lambda \qquad \text{(i.e. where n = 1)} \qquad (6.1)$$

In order to determine the morphology of the cryo-fractured samples, the VEGA3 TESCAN scanning electron microscope (SEM) was used and the analysis was done at room temperature. The samples were gold coated by sputtering for 60 s in order to produce conductive coatings onto the samples.

DSC analyses were done in a PerkinElmer Pyris-1 differential scanning calorimeter under nitrogen flow (flow rate 20 mL min^{-1}). Samples were held at 0 °C for 1 min., heated from 0 to 180 °C at a heating rate of 10 °C min^{-1}, cooled at the same rate and then heated again under similar conditions. The peak temperatures of melting and crystallization, as well as melting and crystallization enthalpies, were determined from the second scans in order to eliminate any thermal history effects. Measurements were repeated three times on different samples for each composition. The melting and crystallization temperatures and enthalpies, were reported as average values of three tests with standard deviations.

The dynamic mechanical properties of the samples were tested using a PerkinElmer Diamond DMA dynamic mechanical analyser. The test was performed in a bending (dual cantilever) mode at a frequency of 1 Hz and a heating rate of 3 °C min^{-1} under nitrogen atmosphere. The samples were heated from -90 to 130 °C. The storage (E′) and loss (E″) moduli and the damping factor (tan δ) are reported.

6.3 Results and discussion

6.3.1 X-ray diffraction (XRD)

The XRD results for the composites under investigation are shown in Figures 6.1 and 6.2. The corresponding data is summarized in Table 6.3. From Figure 6.1A, EG exhibits diffraction peaks with different intensities within a 2θ range of 24-30°. From these, three reflection peaks are noted. Firstly, a strong peak is observed at 2θ = 25.8° that has an interlayer (*d*-spacing) distance of 0.35 nm. Since EG consists of an acid (H_2SO_4) intercalated within its layers [24], this major peak is attributed to acid-intercalated layers of expandable graphite [26]. Secondly, a shoulder peak is observed at 2θ = 26.6° with a *d*-spacing of 0.34 nm (Table 6.3) between graphite sheets. This is due to the stacking of single layers of graphite with a (002) basal reflection [3,7,24,27]. Finally, a broad peak around 2θ = 28.1° with a *d*-spacing value of 0.33 nm is also noted. PLA shows different peaks at 2θ = 9.5, 16.6, 19 and 28.7° (Figure 6.1B). The second and third peaks (i.e. 2θ = 16.6 and 19°), respectively correspond to *d*-spacing values of 0.27 and 0.24 nm, with (200/110) and (203) basal reflections. They are attributed to the stable α-form of PLA with an orthorhombic crystal structure [28-30]. The other diffraction peaks, i.e. 2θ = 9.5 and 28.7° are related to the additives derived from starch and other renewable resource (see section 6.2.1) [22]. Additionally, it is observed that the XRD diffractogram of PLA consists of a broad halo within a 2θ range of 10-26° and this is attributable to the amorphous structure of the PLA matrix [22,30,31]. PCL exhibits XRD peaks at 2θ = 21.5 and 23.8° that correspond respectively with the (110) and (200) planes. These indicate an orthorhombic crystal lattice structure of PCL [31,32]. A shoulder peak at 2θ = 22.1° is also noted. From the XRD reflection of PLA/PCL 85/15 w/w blend in Figure 6.1D, two aspects may be noted: i) the presence of characteristic reflection peaks of the neat biopolymers and ii) the absence and/or insignificance of the reflection peaks at 16.6 and 22.1° that are respectively related to PLA and PCL components in the blend. The former observation is attributed to the immiscibility character of PLA/PCL blend, whereas the latter is due to the existing level of interaction between the PLA and PCL components.

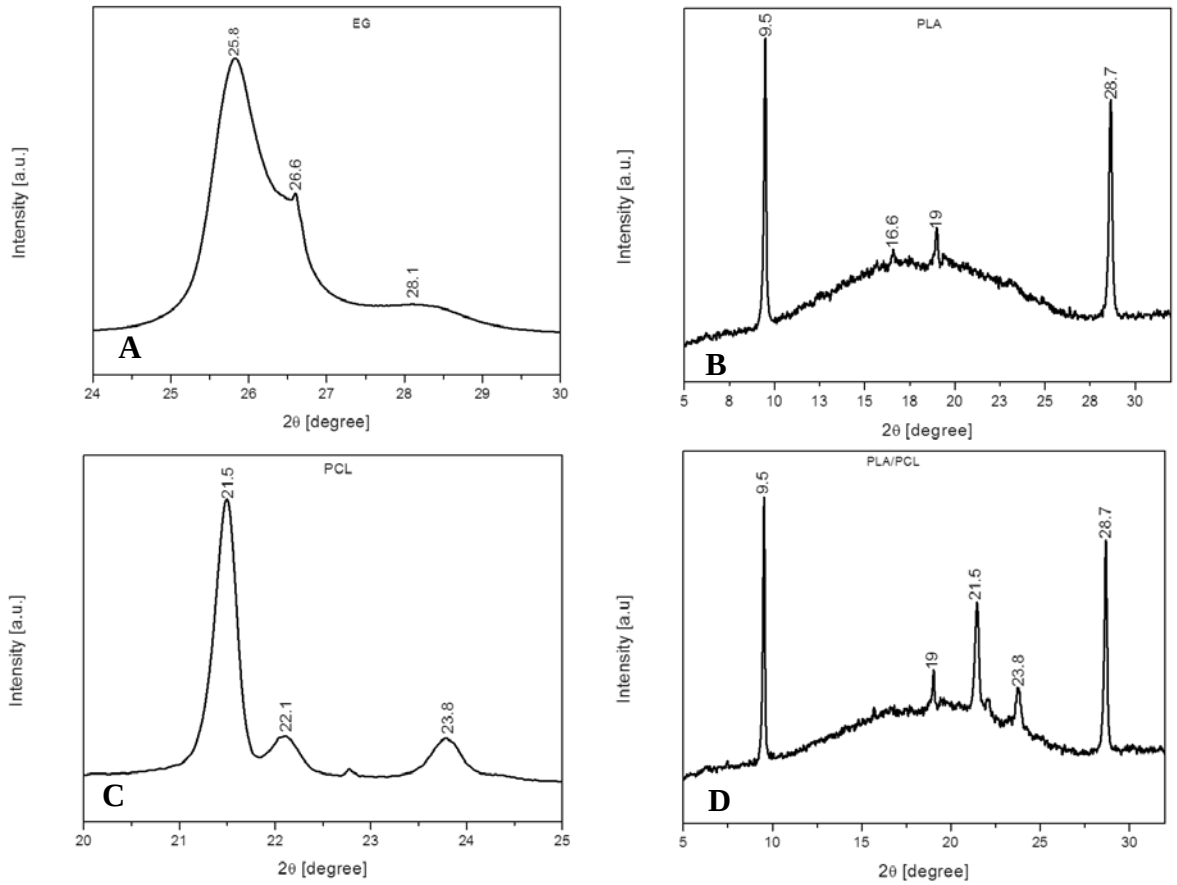

Figure 6.1 X-ray diffraction patterns of (A) EG, (B) PLA, (C) PCL and (D) PLA/PCL blend

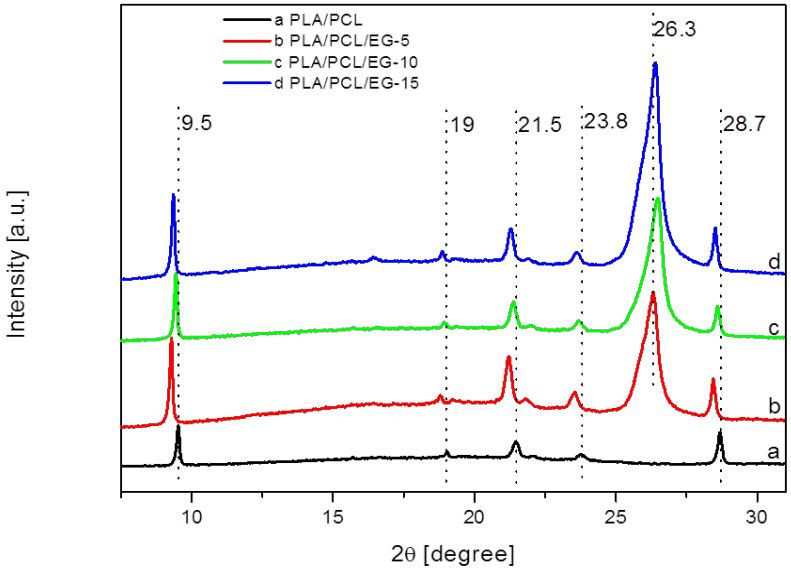

Figure 6.2 X-ray diffraction patterns of PLA/PCL and PLA/PCL/EG composites at different EG contents

Table 6.3 XRD results of PLA/PCL/EG biocomposite samples

Sample	2θ [°]	*d*-Spacing [nm]
EG	25.8, 26.6 & 28.1	0.35, 0.34 0.33
PLA	9.5, 16.6, 19 & 28.7	0.47, 0.27, 0.24 & 0.32
PCL	21.5, 22.1 & 23.8	0.42, 0.41 & 0.38
PLA/PCL	9.5, 19, 21.5, 23.8 & 28.7	0.47, 0.24, 0.42, 0.38 & 0.32
PLA/PCL/EG-5	26.3 & 28.4	0.35 & 0.32
PLA/PCL/EG-10	26.5 & 28.6	0.34 & 0.32
PLA/PCL/EG-15	26.4 & 28.5	0.35 & 0.32

The XRD patterns of PLA/PCL/EG composites are shown in Figure 6.2. The composites show characteristic reflection peaks of the individual constituents. This is evidenced by the presence of peaks at 2θ = 9.5, 19 and 28.7° relating to PLA, peaks around 21.5 and 23.8° that relate to PCL and the one at 26.3°, associated with EG in PLA/PCL/EG composites. Generally, the peak around 2θ ~ 26.3° due to EG occurs at the same position in all the composites. This suggests that the melt-mixing process could not separate the graphite layers, thus the majority of them still exist in the aggregate structure (i.e. EG layered stacks). Similar findings were reported by Fukushima *et al*. [3] and Narimissa *et al*. [33] in their studies of melt processed PLA/nano-filler composites. In the case of the EG component from the composites, certain peaks (i.e. 2θ = 25.8 and 28.1°) are absent after the melt-mixing exercise, which suggests that the acid intercalated layers may have arranged themselves into agglomerates that are distributed throughout the matrix. As seen from Table 6.3, there was a slight shift to low values in the 2θ angles of the PLA/PCL/EG composites, with respect to the neat EG (i.e. at 5 and 15 wt.% contents). This led to increased *d*-spacing from 0.34 to 0.35 nm (Table 6.3), suggesting the existence of EG layered stacks, within which single graphite layers were spread out, within the polymer blend matrix. However, at 10 wt.% EG content, a comparable *d*-spacing value (i.e. 0.34 nm) to neat EG was obtained, suggesting the existence of EG layered stacks with individual EG layers packed close to one another. The diffraction peak intensities that are related to the EG from the PLA/PCL/EG composites, increased consistently with EG loadings (Figure 6.2). From the results, it may be concluded that melt-mixing of EG with PLA/PCL blend showed no effect on the structure of the blend and that EG existed as aggregates in the composites.

6.3.2 Scanning electron microscopy (SEM)

Figure 6.3 presents the SEM micrographs of cryo-fractured surfaces of neat materials (i.e. PLA and PCL) and PLA/PCL blend from two different areas. In Figure 6.3A, neat PLA shows spherical droplet morphology due to the presence of starch (see arrows marked 1 from the figure). The starch component is well dispersed within the PLA continuous phase. There are also some platelet-like materials of different sizes embedded within the matrix (see an arrow marked 2 from the same figure). Around these platelet-like materials, some gaps (see an arrow marked 3) may be observed suggesting the lack of interfacial adhesion. It is also recognized that the PLA used in this study contains microspheres (see Chapter 4) and silicon-based materials (i.e. glass) (see an arrow marked 4 from Figure 6.3A) [22]. On the other hand, PCL shown in Figure 6.3B exhibits smooth and continuous surface that contains long leafy structure. In the case of PLA/PCL blend (Figures 6.3C & D), a fairly smooth and continuous surface, resembling that of PCL, is observed. This suggests that part of the PCL phase resides on the surface of the continuous PLA phase, suggesting some compatibility between the PLA and PCL phases. Furthermore, there were little or no gaps around the platelet-like materials (see an arrow marked 2 from Figure 6.3C). From Figure 6.3D, it can be observed that i) the starch micro droplets were fairly covered with the matrix (see an arrow marked 1) and ii) the microspheres were also well covered by PCL (see arrows marked 5). This shows that a part of PCL did crystallize on the surface of the microspheres separate from PLA, implying that the microspheres act as nucleating sites. This indicates that PLA/PCL 85/15 w/w blend is immiscible. Similar findings were reported by Wu *et al*. [9] and Todo *et al*. [12] in their studies on the development of PLA and PCL blends. The authors observed phase a separation and the presence of spherical structures, the size of which increased with PCL content (i.e. up to 15 wt.% PCL) [12]. Based on SEM results, it can be inferred that although PLA and PCL display some partial miscibility, probably in the amorphous phase, generally they are immiscible in the crystalline phase.

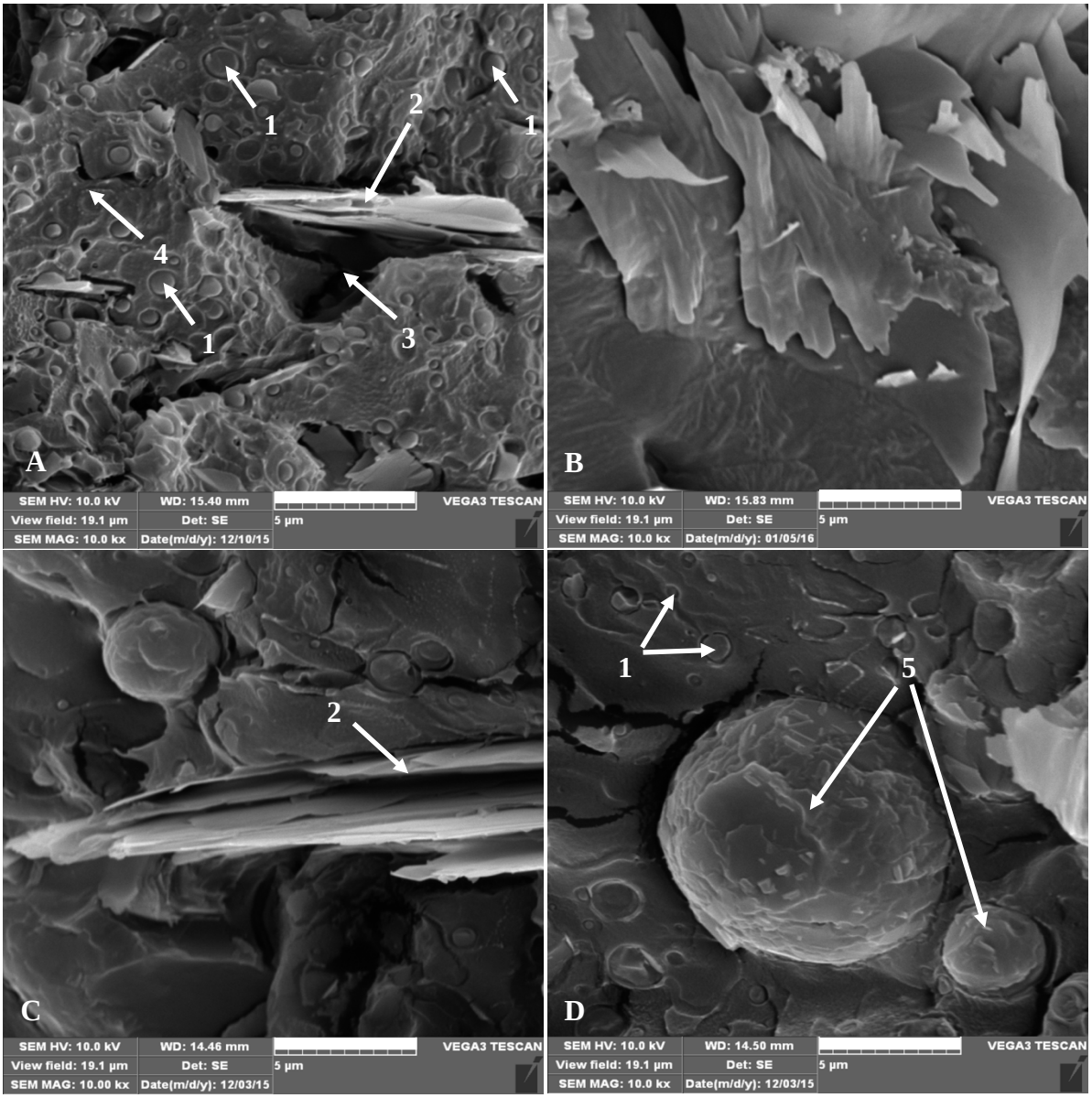

Figure 6.3 SEM micrographs of cryo-fractured (A) PLA, (B) PCL, (C & D) PLA/PCL blend

In order to observe the morphology of the immiscible PLA/PCL blend more clearly, the cryo-fractured surface of the samples was etched with acetic acid in order to dissolve the PCL component. The SEM micrographs of the etched sample are presented in Figure 6.4. The surface showed a collapsed, cracked and porous structure of the PLA matrix (see arrows from Figures 6.4A & D). It is also noted from Figure 6.4B that the microspheres were clear (an arrow marked 1) and appeared loose with voids around them after the PCL phase was dissolved (see an arrow marked 2). This confirmed the observation that PCL crystallized on and around the microspheres. It seems that the starch component was not influenced by PCL, since it remained fairly adhered to PLA even after etching (see arrows from Figure 6.4C).

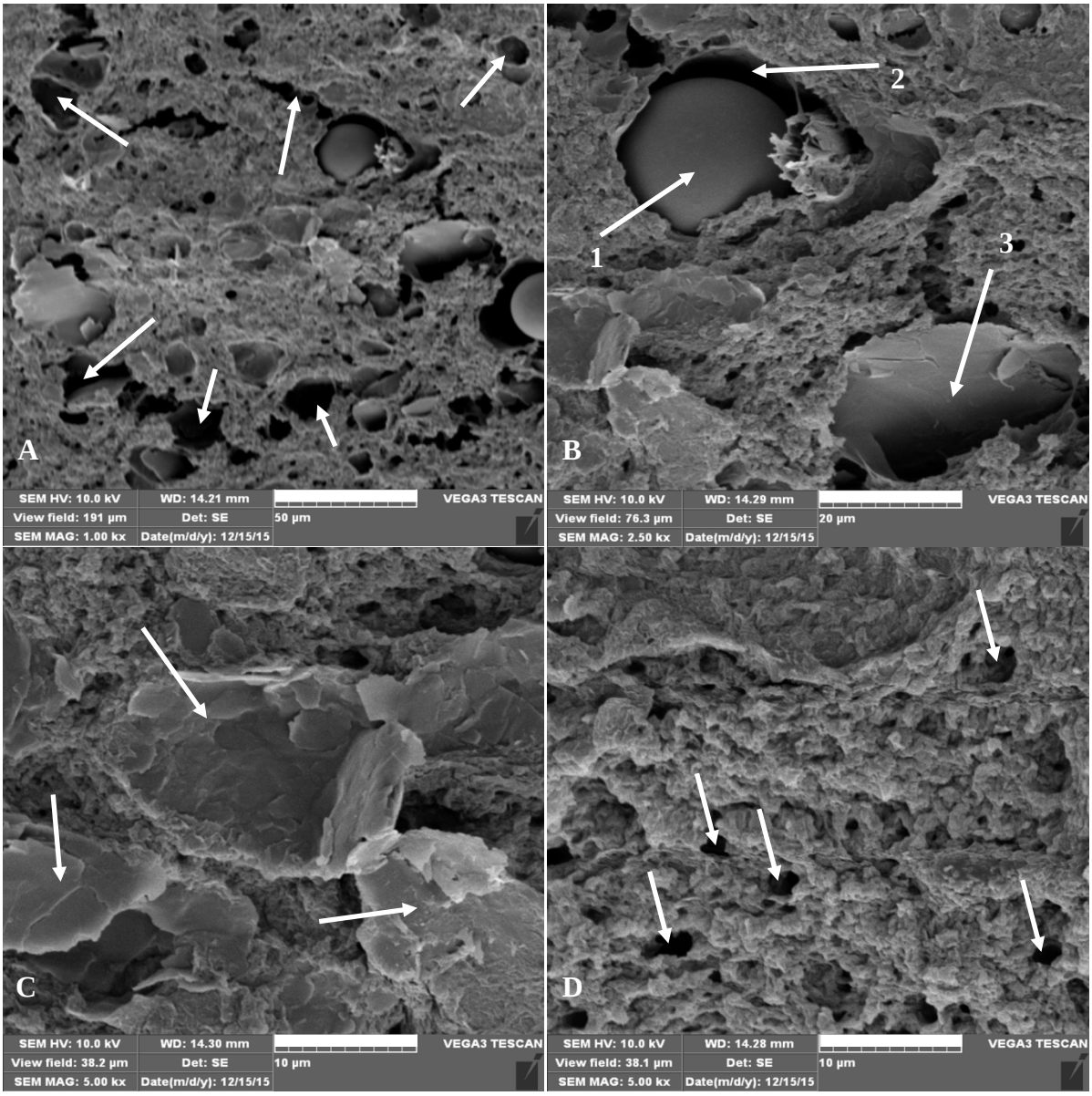

Figure 6.4 SEM micrographs of cryo-fractured etched 85/15 w/w PLA/PCL blend at various magnifications

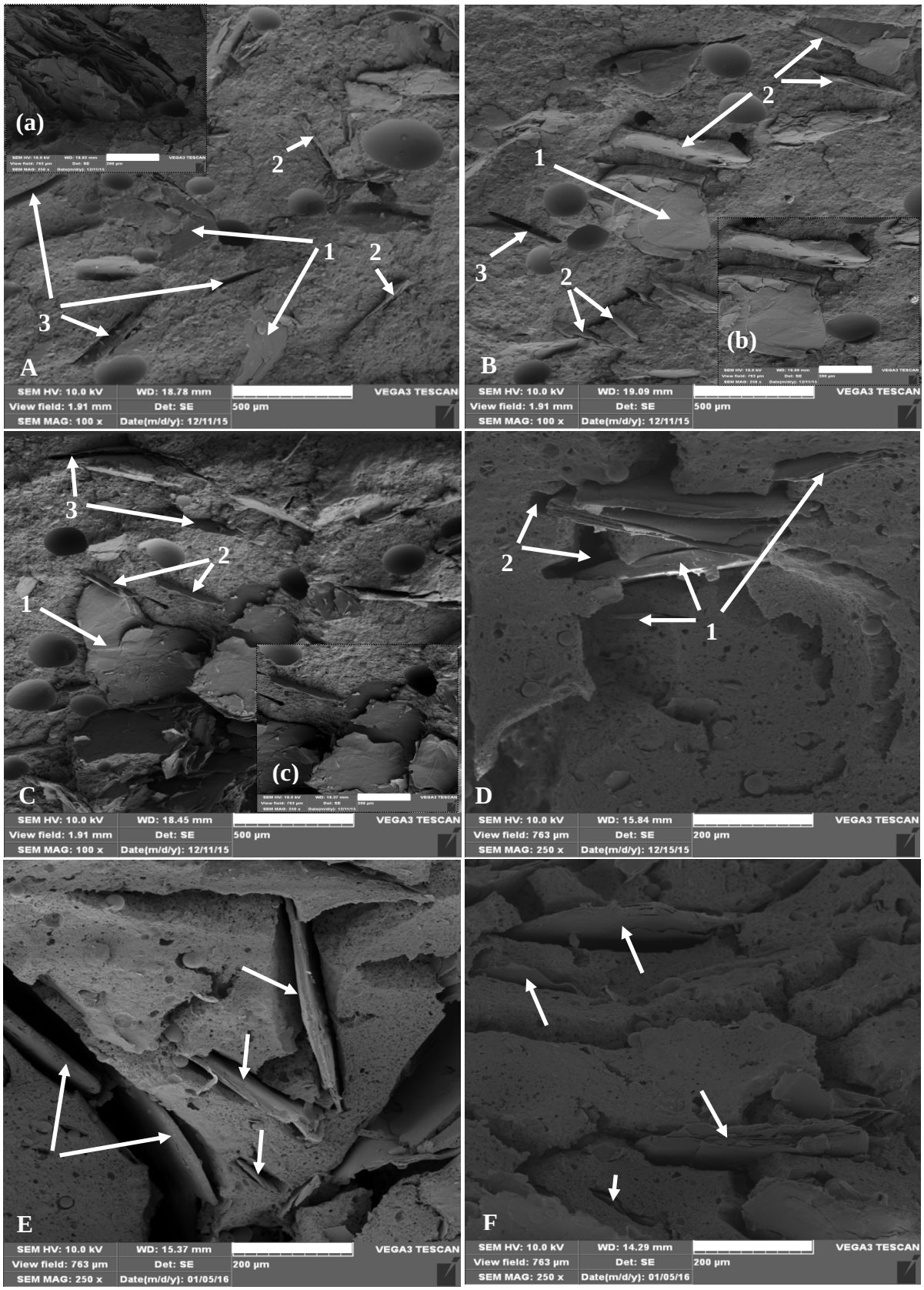

Figure 6.5 SEM micrographs of cryo-fractured samples: Un-etched: (A) 5, (B) 10 and (C) 15 wt.% EG and etched: (D) 5, (E)10 and (F) 15 wt.% EG PLA/PCL/EG composites

The SEM micrographs of the un-etched and etched PLA/PCL/EG composites at different EG contents are shown in Figure 6.5. It can be seen that EG is embedded in a smooth surface of PLA/PCL blend matrix and exists as small and large layered stacks. Generally, from Figure 6.5A, B & C, these layered stacks are oriented in parallel (see arrows marked 1) and normal (see arrows marked 2) relative to the cryo-fractured surface. Although small EG layered stacks were fairly dispersed within the matrix, the agglomeration of EG layered stacks was observed especially at low {i.e. 5 wt.%, see insert Figure 6.5(a)} and high {i.e. 15 wt.%, see insert Figure 6.5(c)} EG contents. However, the 10 wt.% EG loading shows the presence of large EG layered stacks {i.e. lumps of EG as seen from the insert, Figure 6.5(b)} with fair distribution within the matrix (Figure 6.5B). All the micrographs show some degree of interfacial adhesion between the EG layered stacks and the matrix, however there is evidence of filler pull-out during fracture (see arrows marked 3 from Figure 6.5A, B & C). When the PCL component was dissolved as seen from the micrographs of the etched composites (Figure 6.5D, E & F), the surface was discontinuous, rough and porous and there were gaps around the microspheres and EG layered stacks embedded within the composites. This confirmed that some of the PCL phase did adhere on the surface of the continuous PLA phase and mainly onto the EG and microspheres.

6.3.3 Differential scanning calorimetry (DSC)

The DSC results of the PLA/PCL/EG composites are illustrated in Figures 6.6 and 6.7. The peak temperatures of the glass transition, melting, cold-crystallization and cooling, the enthalpies of melting, cold-crystallization and cooling and the degree of crystallization are summarized in Tables 6.4 and 6.5. The degree of crystallinity, X_c of the biopolymer phases was calculated using Equation 6.2:

$$X_c(\%) = \frac{\Delta H_m}{\Delta H_m^0} \times \frac{100}{wt.\%} \qquad (6.2)$$

where ΔH_m is the experimental enthalpy heat of fusion/melting, ΔH_m^0 is the enthalpy heat of melting per gram of 100% crystalline material, and $\Delta H_{m,PLA}^0$ = 93 J g^{-1} while $\Delta H_{m,PCL}^0$ = 137 J g^{-1} [20] and $wt.\%$ is the weight fraction of the polymer.

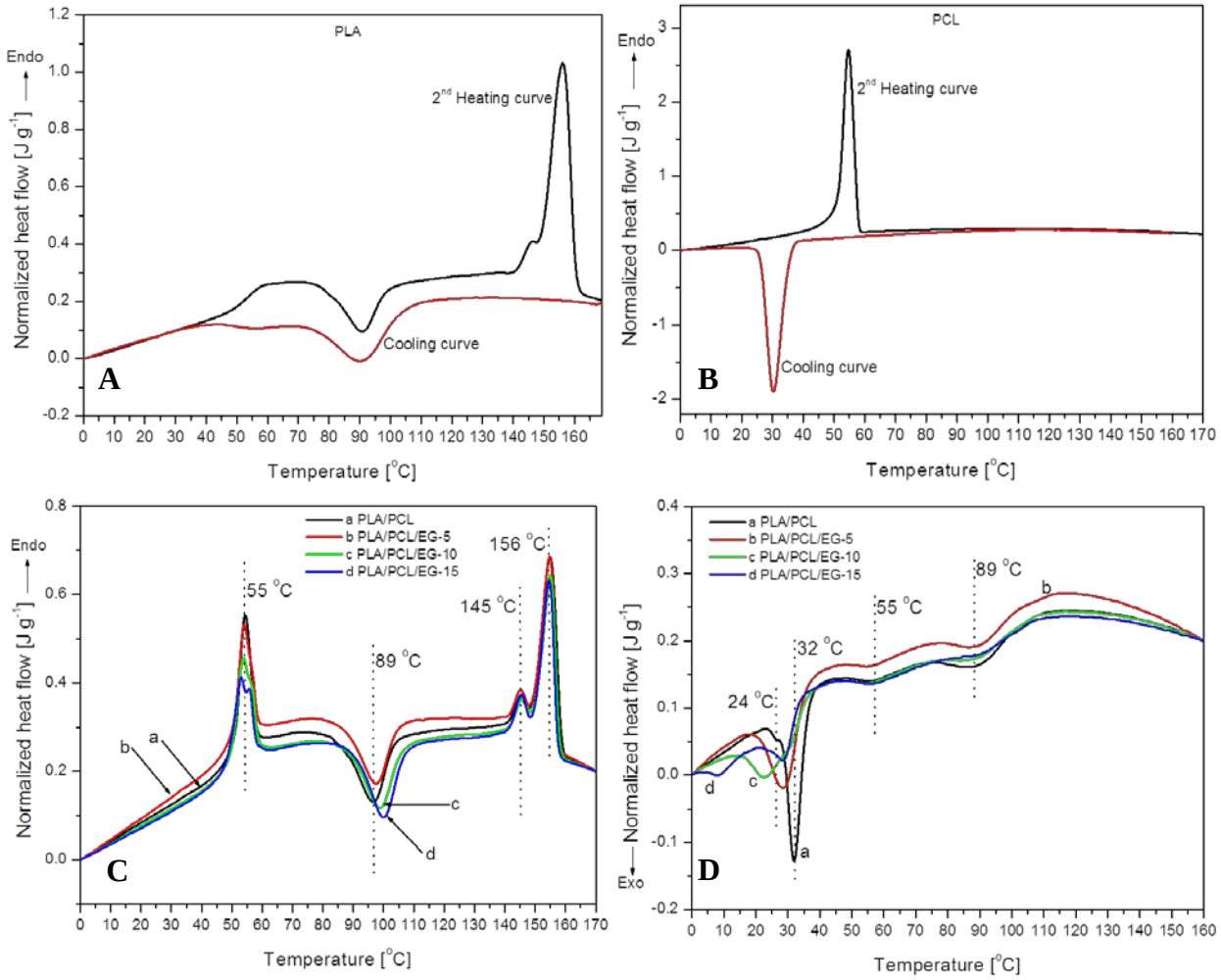

Figure 6.6 DSC heating and cooling thermograms of (A) PLA, (B) PCL, (C) heating and (D) cooling curves of PLA/PCL/EG composites

In Figure 6.6A, the DSC heating and cooling thermograms of neat PLA are shown. On heating, PLA shows endothermic and exothermic thermal transitions within the experimental temperature range. The first endothermic transition is observed between 50-60 °C (i.e. 53.5 °C). This is due to the glass transition of the amorphous phase of the semicrystalline PLA [34]. The second (exothermic) transition around 89 °C, relates to the cold-crystallization of PLA. The endothermic peak observed at 157 °C is associated with the melting of the PLA crystallites. There is also a peak shoulder at 145 °C, which may be related to the melting of smaller crystallites within the amorphous regions of the polymer. These would melt first due to an excess of free energy associated with the disordered chains that emerge from the ends of the ordered crystallites, which is relatively greater for the smaller crystallites [22,35,36]. Chapple *et al.* [22] observed the double melting phenomenon for Cereplast PLA/clay composites and attributed this to the melting of crystallites having different sizes and/or order of perfection.

Fukushima *et al*. [34], however, reported that the dual endothermic peaks of PLA relate to different crystal structures of the α- and β-forms. The α-form is said to melt at higher temperatures and is the most common polymorph of PLA, while the latter form, melting at lower temperatures, relates to an imperfect crystal structure. PLA has a melting enthalpy (ΔH_m) as low as 22.7 J g^{-1} (Table 6.5). On cooling, PLA exhibits crystallization peak temperature (T_c) at 91.8 °C with crystallization enthalpy (ΔH_c) of 14.9 J g^{-1}. On the other hand, PCL in Figure 6.6B shows peak T_m and T_c of 54.7 and 30.3 °C, respectively and has the highest ΔH_m of 71 J g^{-1}.

Table 6.4 DSC thermal transition peak temperatures of PLA/PCL/EG samples

Sample	T_g [°C]	T_{m1} [°C]	T_{m2} [°C]	T_{m3} [°C]	ΔH_m [J g^{-1}]	ΔH_m^n[J g^{-1}]
PLA	46.7 ± 0.5	-	145 ± 0.4	157 ± 0.1	22.7 ± 0.9	22.7
PCL	-	54.7 ± 0.04	-	-	71 ± 0.6	71
PLA/PCL 85/15	62.3 ± 0.1	54.9 ± 1.1	145 ± 1	156 ± 1.8	10.7 ± 0.4[a] 16 ± 0.8[b]	1.6[a] 13.6[b]
PLA/PCL/EG-5	64.6 ± 0.1	54.2 ± 0.3	145 ± 0.3	156 ± 0.4	9.4 ± 0.5[a] 15.3 ± 0.6[b]	1.3[a] 12.3[b]
PLA/PCL/EG-10	64.3 ± 0.2	53.7 ± 0.1 57 ± 0.04	145 ± 0.2	156 ± 0.3	9.5 ± 0.2[a] 13.8 ± 0.3[b]	1.3[a] 10.6[b]
PLA/PCL/EG-15	63.2 ± 0.1	53.5 ± 0.4 56.3 ± 0.5	146 ± 0.6	156 ± 0.7	8.3 ± 0.03[a] 14.5 ± 0.1[b]	1.1[a] 10.5[b]

Where T_g, T_{m1}, T_{m2} and T_{m3} are peak temperatures of glass transition, melting transitions relating to PCL, PLA shoulder and PLA main peak, respectively. ΔH_m is the enthalpy heat of melting, determined experimentally. [a] and [b] denote the values of melting enthalpies related to PCL and PLA components, respectively. The normalized enthalpy, ΔH_m^n was calculated by multiplying the experimental enthalpy (ΔH_m), by the weight fraction (wt.%) of the polymer in a specific composition.

For the PLA/PCL blend shown in Figure 6.6C, all the characteristic transitions of the individual components are reflected, except for the glass transition related to the PLA component on heating. Since the glass transition due to the PLA component was located around 53.5 °C and the crystalline melting transition related to the PCL was around 54.7 °C, the two endothermic transitions seem to have overlapped and occurred simultaneously [13]. The glass transition temperature (T_g) values, were consequently determined from the cooling curves and tabulated in Table 6.4. It can be seen that the blending of PLA with PCL shifted this transition to higher temperatures i.e. from 46.7 °C to 62.3 °C. The result suggests that the rotational motion of PLA polymer chain segments in the amorphous phase were restricted by the PCL phase, leading to increased T_g values [37]. This result indicates some miscibility feature of the blend in the

amorphous state. PLA/PCL blend exhibits two separate maximum melting peaks around 55 and 157 °C, respectively related to the PCL and PLA components. Additionally, a well-defined shoulder peak (~146 °C), when compared with the neat PLA, is observed from the blend (see Figures 6.6A & C). The crystalline melting transitions due to the individual polymer components were generally not influenced by melt blending of PLA with PCL, suggesting that there was no change in the crystallite sizes and/or lamellar thickness. It can be inferred from this that the blend is immiscible in the crystalline state at 85/15 w/w PLA/PCL [9,12,38]. This was also observed in SEM (see section 6.3.2).

Table 6.5 DSC melting and crystallization enthalpies of PLA/PCL/EG samples

Sample	T_{cc} [°C]	$-\Delta H_{cc}$ [J g^{-1}]	T_c [°C]	$-\Delta H_c$ [J g^{-1}]	X_c [%]
PLA	88.8 ± 1.3	5.3 ± 1.1	91.8 ± 0.4	14.9 ± 2.7	24.4
PCL	-	-	30.3 ± 0.03	71.3 ± 0.4	51.8
PLA/PCL 85/15	97 ± 1	12.2 ± 0.8	31.5 ± 0.3	8.7 ± 0.8	52.1[a] 20.2[b]
PLA/PCL/EG-5	97.7 ± 0.6	11.2 ± 0.5	29.7 ± 0.1	6.9 ± 0.3	48.1[a] 20.4[b]
PLA/PCL/EG-10	98.8 ± 0.1	11.9 ± 0.2	23.4 ± 0.5 31.1 ± 0.2	5.9 ± 0.1	51.4[a] 19.4[b]
PLA/PCL/EG-15	100 ± 0.3	11.9 ± 0.1	6.2 ± 0.1 29.1 ± 0.1	2.9 ± 0.04	47.5[a] 21.6[b]

whereT_{cc} and T_c are peak temperatures of cold-crystallization and cooling, respectively. ΔH_{cc} and ΔH_c are respectively the enthalpies of cold-crystallization and cooling and χ_c is the crystallinity degree, in percentages, for bio-blend components. [a] and [b] denote the values of melting enthalpies and crystallinity related to PCL and PLA components, respectively.

ΔH_m and the degree of crystallinity of PLA phase were lowered in the presence of the PCL phase from the PLA/PCL blend, while those of the latter phase were not influenced (Tables 6.4 & 6.5). This means that PLA could not crystallize effectively in the presence of the PCL phase (Tables 6.4 & 6.5). On cooling, the crystallization transition due to PLA was suppressed from the blend and only that due to PCL was recorded by DSC. As observed in Figure 6.6D and Table 6.5, the crystallization transition of PCL component in the blend showed marginal shift to high temperatures with respect to neat PCL. This behaviour is attributed to the presence of: mainly the microspheres, platelet-like materials, silicon-based materials (i.e. glass) or starch which acted as active substrate(s) that promoted crystallization of the PCL [20]. Additionally, a shoulder peak is noted ~24 °C, suggesting the possible formation of less ordered and/or small separate crystals. In case of cold crystallization transition temperature (T_{cc}) and its enthalpy (ΔH_{cc}) due to PLA, the blend showed higher values with respect to neat PLA component. This indicates that the presence of molten PCL phase around these temperatures could not promote

crystallization of PLA component from the amorphous state during heating. This suggests that the presence of PCL may have reduced the polymer chain mobility within PLA (i.e. immobilization effect) [38].

The heating and cooling thermograms of the PLA/PCL/EG biocomposites are illustrated in Figure 6.6C and D, while the dependence of glass transition temperature on EG content is depicted in Figure 6.7. It can be seen that the glass transition temperatures of the composites generally occurred at higher temperatures than for PLA/PCL blend, although it dropped slightly at the highest filler loading. This is explained thus: the presence of EG micro-filler in the amorphous phase of the matrix had a stiffening effect, thus lowering the polymer chain mobility. On the other hand, the T_m relating to the PCL component, remained within experimental error of the blend indicating that the EG filler had insignificant effect on the crystallites of PCL at low EG content (Table 6.4). However, at increased filler loadings, the crystalline melting transition displayed two peaks. The development of a shoulder peak located around 57 °C at 10 wt.% EG content and a second peak around 56 °C for 15 wt.% EG loading, are observed. This may be due to the formation of other separate crystallites with different lamellar thicknesses as by the PCL phase, in which case EG micro-particles may have acted as heterogeneous nucleating sites. It is also noted that the peak height of the melting transitions corresponding with the PCL component is reduced with EG loading. This indicates a reduction in the amount of crystallites due to the PCL component in the presence of EG micro-filler. The ΔH_m of PCL component and hence its crystallinity (Table 6.4) were reduced in the presence of EG due to the reduced perfection and amount of crystallites. Similarly, it is observed that the T_c of the composites was lowered as EG content increased. Similar to melting, the composites containing 10 and 15 wt.% EG contents, respectively, showed, the presence of a shoulder and a crystallization peak. ΔH_c was also reduced as a function of EG content. This is attributed to the immobilization effect by EG micro-particles of polymer chains, which does not promote the crystallization process of the blend.

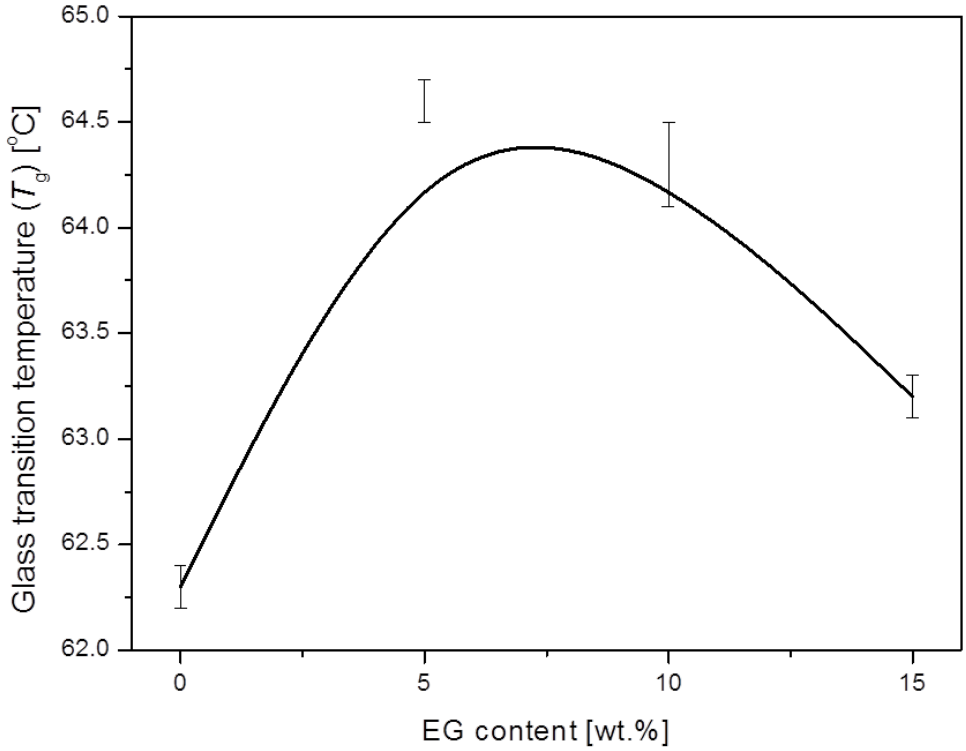

Figure 6.7 The dependence of glass transition temperature (T_g) on EG content

In case of the PLA component, the incorporation of EG showed no significant changes in T_m. It is also observed that its ΔH_m was slightly reduced. Furthermore, it is observed that the presence of EG micro-particles in PLA/PCL blend led to increased T_{cc} of the composites, but generally no change in ΔH_{cc} (Table 6.5). This may be explained thus: the EG micro-filler does not promote crystallization process in the composites. From these results, it is clear that the presence of EG micro-filler particles have an immobilization effect on PLA phase of the composites. The normalized enthalpy values ΔH_m^n for both PLA and PCL components of the composites were also determined and presented in Table 6.4. It is observed that ΔH_m^n was reduced for both polymers in the presence of EG micro-filler particles. This is attributed to EG filler aggregation, low level of dispersion of single and/or small EG layered stacks and non-existent or lack of interfacial adhesion, as reported in the XRD and SEM results (see sections 6.3.1 and 6.3.2). It can be generally concluded that the incorporation of EG micro-filler particles into PLA/PCL blend had more influence on the melting and crystallization behaviour of the PCL component than the PLA component of the blend.

6.3.4 Dynamic mechanical analysis (DMA)

The DMA results of the PLA/PCL blend and PLA/PCL/EG flame retardant composites are shown in Figures 6.8 and 6.9, while the data is summarized in Tables 6.6 and 6.7. The DMA storage modulus (E′), loss modulus (E″) and damping factor (tan δ) are reported.

The storage modulus (E′) of PLA/PCL and PLA/PCL/EG composites is shown in Figure 6.8A and the data tabulated in Table 6.6. It can be seen that the E′ is a decreasing function of temperature due to increases in the free volume as samples passed through various regions. These regions include: i) sub-glass transition, ii) glass transition (T_g), iii) rubbery plateau, iv) cold crystallization and v) pre-melting regions. For the PLA/PCL blend, at low temperatures (i.e. below -80 °C), the polymer molecules are tightly compressed and the sample undergoes the solid-state transition. As the sample warms up and expands, a transition occurred over a broad temperature range (i.e. between -80 to -30 °C) with the subsequent decline in E′ is observed. This is due to the movement of the whole side chains and localized groups of backbone atoms, which now have sufficient space to move and the material developed some toughness. This transition is known as the β-transition and it is due to the glass transition of a secondary component(s) present in PLA [39]. As discussed in the XRD and SEM data (see sections 6.3.1 & 6.3.2, respectively), the PLA used in this study contains various additives, including starch [22]. In addition, the PCL present in the blend exhibits glass transition around this region [15]. Consequently, this broad transition is related to the overlapping of the glass transitions of starch and the PCL components in the blend. From the figure, at temperatures starting at around 50 °C, there is a transition accompanied by an exponential drop in E′ up to ~65 °C. This relates to the glass transition of the PLA component and this is due to the polymer chains in the amorphous, phase beginning to coordinate large scale motions. After this, a rubbery plateau is reached (i.e. temperature range of 65-100 °C) within which a slight increase in E′ is accompanied by a transition peak observed between 87 to 97 °C. This is attributed to the cold-crystallization transition due to PLA [34,36,40]. This was also observed in the DSC data (discussed in section 6.3.3). From the results, it can be inferred that the Cereplast PLA used in this study is an immiscible blend of PLA and starch. It can also be concluded that the Cereplast PLA/PCL blend is immiscible due to the development of separate glass transitions of the individual components.

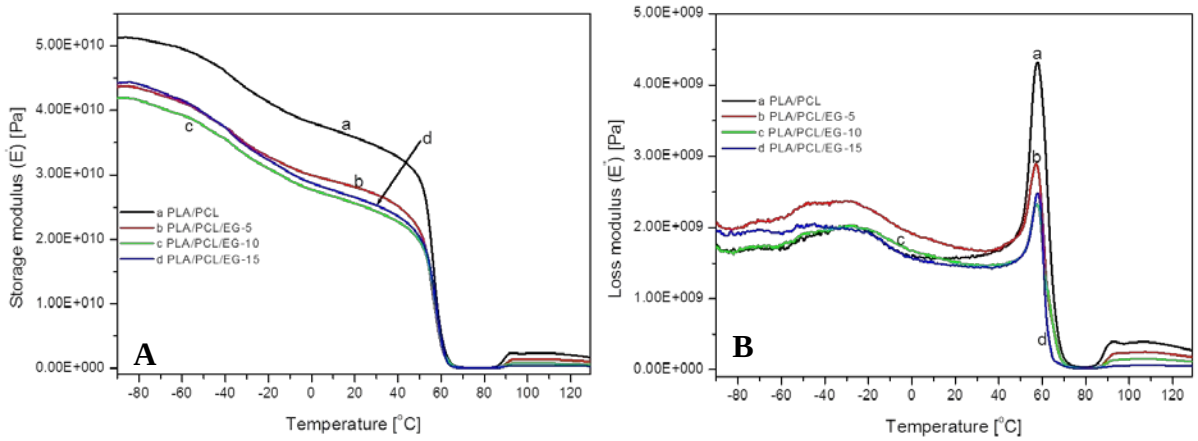

Figure 6.8 Temperature dependence of (A) storage modulus (E´) and (B) loss modulus (E″) curves of PLA/PCL and PLA/PCL/EG composites

The PLA/PCL/EG composites exhibit similar behaviour to the PLA/PCL blend in the E´ curves as observed in Figure 6.8A. From Table 6.6, it is further observed that the E´ was low with respect to the PLA/PCL blend in the presence EG micro-particles. The reduction in the storage modulus is independent of the EG filler, especially at lower temperatures (i.e. sub-glass transition region) while the clear filler dependency is noted around 90 °C (i.e. around cold crystallization), whereby the modulus decreased as a function of the EG content. This is attributed to less interaction between PLA and EG, due to the isolation by PCL phase which has crystallized on and/or around EG micro-filler particles as observed in the SEM micrographs (discussed in section 6.3.2).

Table 6.6 Storage modulus (E´) value of PLA/PCL blend and PLA/PCL/EG composites at different temperature ranges

Sample	E´ at 25 °C [MPa]	E´ at 60 °C [MPa]	E´ at 80 °C [MPa]
PLA/PCL	35137	5039	80.6
PLA/PCL/EG-5	27524	3504	36.2
PLA/PCL/EG-10	25937	3228	39.9
PLA/PCL/EG-15	24956	3999	26.3

As seen in Figure 6.8B, the loss modulus (E″) exhibits some transitions within the experimental temperature range. In the sub-glass region, a transition around the maxima of ~ -27 °C is observed, which occurs over a broad temperature range (i.e. between -60 to 1 °C). This is due to the overlapped glass transitions of the PCL (i.e. ~ -47 °C) and starch (i.e. ~ -27 °C) components [15]. E″ was slightly high in the presence of EG filler at the sub-glass transition region, while the opposite is observed at and above the glass transition region of PLA phase.

This may be due to stiffening effect by the solid PCL phase and EG micro filler particles, whereas at high temperatures, it is due to the PCL component which melts at ~55 °C. In this case, the peak temperature values showed an insignificant decrease from ~58 to 57 °C and this was inconsistent with EG content. This is attributed to the presence of low melting PCL (i.e. T_m = 55 °C) in the amorphous phase of PLA. Finally, a transition between 85-100 °C due to cold-crystallization is also observed (see DSC discussion in section 4.3.3).

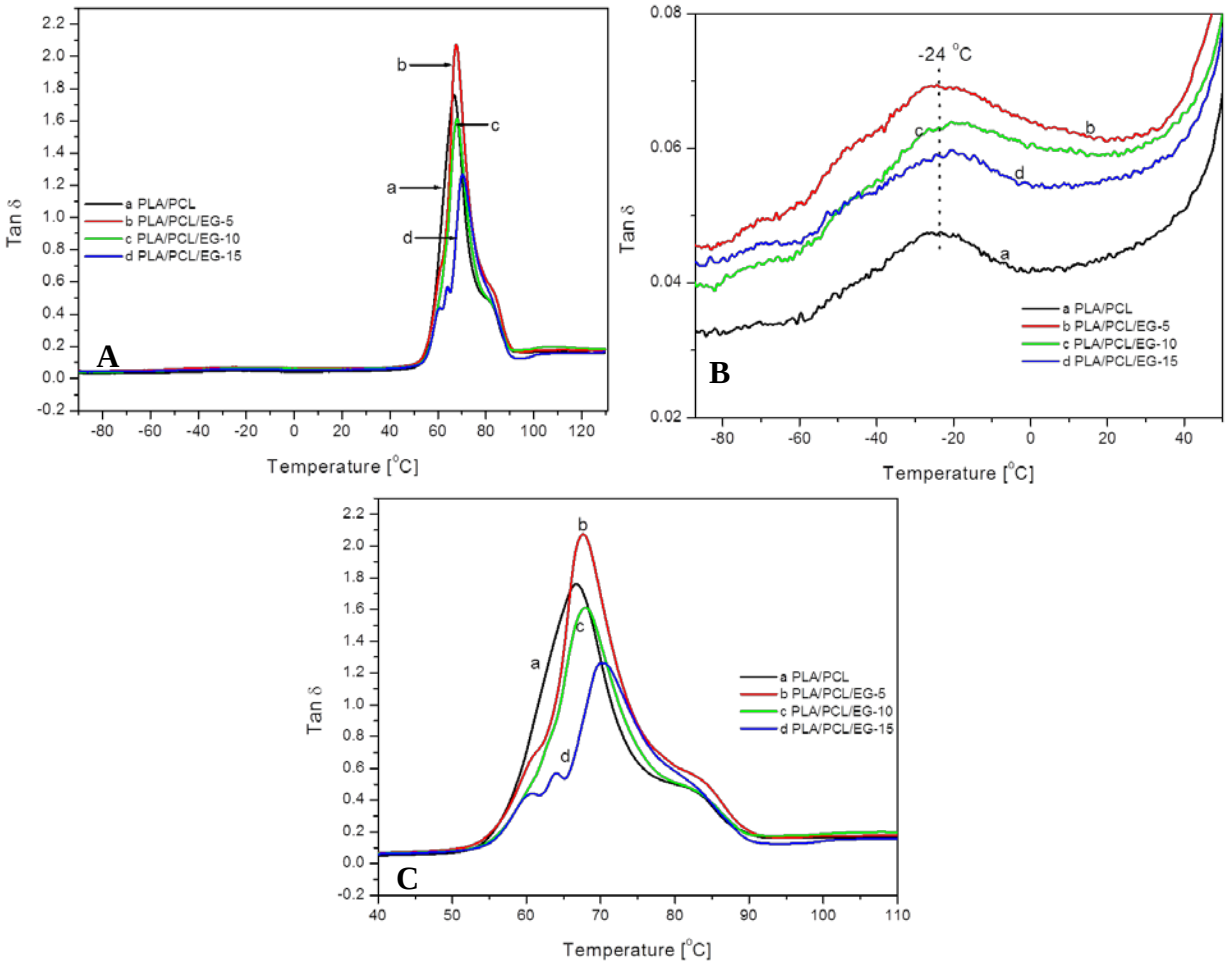

Figure 6.9 Temperature dependence of tan δ (damping factor) curves of PLA/PCL and PLA/PCL/EG composites shown at (A) entire experimental temperature range, (B) below glass transition region and (C) at and above glass transition region

Table 6.7 Transition temperature values obtained from the loss modulus (E″) and damping factor (tan δ) curves of PLA/PCL blend and the PLA/PCL/EG composites

Sample	Peak E″, T_1 [°C]	Peak E″, T_2 [°C]	Peak tan δ [°C]
PLA/PCL	-27	58.1	66.6
PLA/PCL/EG-5	-28.3	56.9	67.6
PLA/PCL/EG-10	-26.4	57.8	68.1
PLA/PCL/EG-15	-27.6 & -44.6	57.5	70.4 (60.7 & 64)

The damping factor (tan δ) is shown in Figure 6.9 and the peak transition values are tabulated in Table 6.7. From the figure, transitions may be observed approximately between -60 to -10 °C (i.e. with peak maxima at -25 °C, see Figure 6.9B) and at around 67 °C (Figure 6.8A & C). The transition observed at lower temperatures occurs over a broad temperature range, indicating an overlapping of two transitions related to starch present in PLA and glass transition of PCL (i.e. T_g ~ -47 °C) [15]. Sarazin *et al*. [15] reported similar findings in their study of binary and ternary blends of PLA, PCL and TPS. From the DMA results, the authors observed a tan δ peak located at around -57 °C for the blends and they related this to the overlapping of the β relaxation for the plasticized starch and the glass transition for PCL. On the other hand, the transition located at around 66.6 °C (Figure 6.9A & C), relates to the glass transition of PLA (Table 6.7) [15]. From Table 6.7, it is observed that the tan δ peak values shifted to high temperatures as a function of EG micro-filler particle in the PLA/PCL/EG composites. This indicates an increase in the glass transition temperature of PLA component in the presence of EG filler. It is attributed to the stiffening effect due to the solid EG micro-filler particles that have immobilized the amorphous polymer chains of the PLA component in the composites. This concurs in the DSC experiments on the glass transition (discussed in section 6.3.3). Furthermore, at temperatures between 60-64 °C, the tan δ curves show the presence of little shoulder peaks, observable in the composite with 15 wt.% EG content. Lastly, the presence of a shoulder around 84 °C is attributed to the cold crystallization transition due to the PLA component. The PLA/PCL/EG flame retardant composites are generally characterized by low storage and loss moduli, with high T_g due to the polymer chain immobilization effect by the solid PCL phase with low melting point and the EG micro-particles.

6.4 Conclusions

The effect of commercial expandable graphite (EG) on the morphology, structure, melting and crystallization behaviour as well as the dynamic mechanical properties of melt-mixed flame retardant PLA/PCL/EG composites was investigated. It was found that the melt mixing process could not separate the graphite layers, thus the majority of EG existed in the aggregate structure (i.e. EG layered stacks and/or lumps). Although PCL had some level of adhering onto the surface of PLA phase, it was mainly onto the EG and micro spherical materials components surfaces, indicating that the PLA/PCL blend was immiscible even in the presence of EG micro filler. The incorporation of EG filler had an influence on the melting and crystallization

behaviours of the PCL than the PLA component of the composites. PCL and EG did not favour crystallization of PLA component in the PLA/PCL/EG composites. From the DSC and DMA results, the glass transition of the composites occurred at high temperature, suggesting the immobilization effect of the PLA polymer chain by EG filler. The PLA/PCL/EG flame retardant composites are generally characterized by low storage and loss moduli due to the aggregation, lack of EG layered stacks (i.e. lumps) dispersion and the lack of interfacial adhesion of EG layers with PLA/PCL blend. Further kinetic studies based on melting and crystallization characteristics and rheology and static mechanical properties are suggested, to further shed light on the properties of these flame retardant PLA/PCL/EG composites.

Acknowledgements

The authors would like to acknowledge the financial support by the National Research Foundation (NRF) and Professional Development Programme (PDP). Acknowledgements are also extended to colleagues and researchers for their undivided attention and support.

References

1. Imre, B., Pukánszky, B. (2013). Compatibilization in bio-based and biodegradable polymer blends. *European Polymer Journal*, 49:1215-1233. DOI: 10.1016/j.eurpolymj.2013.01.019
2. Gupta, A.P. and Kumar, V. (2007). New emerging trends in synthetic biodegradable polymers – Polylactide: A critique. *European Polymer Journal*, 43:4053-4074. DOI: 10.1016/j.eurpolymj.2007.06.045
3. Fukushima, K., Murariu, M., Camino, G., Dubois, P. (2010). Effect of expanded graphite/layered-silicate clay on thermal, mechanical and fire retardant properties of poly(lactic acid). *Polymer Degradation and Stability*, 95:1063-1076. DOI: 10.1016/j.polymdegradstab.2010.02.029
4. Huang, G., Gao, J., Wang, X., Liang, H., Ge, C. (2012). How can graphene reduce the flammability of polymer nanocomposites? *Material Letters*, 66:187-189. DOI: 10.1016/j.matlet.2011.08.063
5. Mngomezulu, M.E., John, M.J., Jacobs, V.N., Luyt, A.S. (2014). Review on flammability of biofibres and biocomposites. *Carbohydrate Polymers*, 111:149-182. DOI: 10.1016/j.carbpol.2014.03.071

6. Murariu, M., Dechief, A.L., Bonnaud, L., Paint, Y., Gallos, A., Fontaine, G., Bourbigot, S., Dubois, P. (2010). The production and properties of polylactide composites filled with expanded graphite. *Polymer Degradation and Stability*, 95:889-900.
DOI: 10.1016/j.polymdegradstab.2008.12.019
7. Rasal, R.M., Janorkar, A.V., Hirt, D.E. (2010). Poly(lactic acid) modifications. *Progress in Polymer Science*, 35:338-356.
DOI: 10.1016/j.progpolymsci.2009.12.003
8. Vogel, C. and Siesler, H.W. (2008). Thermal degradation of poly(ε-caprolactone), poly(L-lactic acid) and their blends with poly(3-hydroxy-butyrate) studies by TGA/FT-IR spectroscopy. *Macromolecular Symposia*, 265:183-194.
DOI: 10.1002/masy.200850520
9. Wu, D., Zhang, Y., Zhang, M., Zhou, W. (2008). Phase behaviour and its viscoelastic response of polylactide/poly(ε-caprolactone) blend. *European Polymer Journal*, 44:2171-2183.
DOI: 10.1016/j.eurpolymj.2008.04.023
10. Cabedo, L., Feijoo, J.L., Villanueva, M.P., Lagarón, J.M., Giménez, E. (2006). Optimization of biodegradable nanocomposites based on aPLA/PCL blends for food packaging applications. *Macromolecular Symposia*, 233:191-197.
DOI: 10.1002/masy.200650124
11. Patrício, T., Bártolo, P. (2013). Thermal stability of PCL/PLA blends produced by physical blending process. *Procedia Engineering*, 59:292-297.
DOI: 10.1016/j.proeng.2013.05.124
12. Todo, M., Park, S-D., Takayama, T., Arakawa, K. (2007). Fracture micromechanisms of bioabsorbable PLLA/PCL polymer blends. *Engineering Fracture Mechanics*, 74:1872-1883.
DOI: 10.1016/j.engfracmech.2006.05.021
13. Chavalitpanya, K. and Phattanarudee, S. (2013). Poly(lactic acid)/polycaprolactone blends compatibilized with block copolymer. *Energy Procedia*, 34:542-548.
DOI: 10.1016/j.egypro.2013.06.783
14. Takayama, T., Todo, M., Tsuji, H. (2011). Effect of annealing on the mechanical properties of PLA/PCL and PLA/PCL/LTI polymer blends. *Journal of the Mechanical Behavior of Biomedical Materials*, 4:255-260.
15. Sarazin, P., Li, G., Orts, W.J., Favis, B.D. (2008). Binary and ternary blends of polylactide, polycaprolactone and thermoplastic starch. *Polymer*, 49:599-609.

DOI: 10.1016/j.polymer.2007.11.029

16. Gu, S.-Y., Zhang, K., Zhan, H. (2008). Melt rheology of polylactide/poly(butylene adipate-*co*-terephthalate) blends. *Carbohydrate Polymers*, 74:79-85.
DOI: 10.1016/j.carbpol.2008.01.017

17. Jiao, L., Huang, C.-L., Zeng, J.-B., Wang, Y.-Z., Wang, X.-L. (2012). Miscibility, crystallization and mechanical properties of biodegradable blends of poly(L-lactic acid) and poly(butylene succinate-b-ethylene succinate) multiblock copolymer. *Thermochimica Acta*, 539:16-22.
DOI: 10.1016/j.tca.2012.03.019

18. Bitinis, N., Verdejo, R., Cassagnau, P., Lopez-Manchado, M.A. (2011). Structure and properties of polylactide/natural rubber blends. *Materials Chemistry and Physics*, 129:823-831.
DOI: 10.1016/j.matchemphys.2011.05.016

19. Rodríguez-Llamazares, S., Rivas, B.L., Pérez, M., Perrin-Sarazin, F. (2012). Poly(ethylene glycol) as a compatibilizer and plasticizer of poly(lactic acid)/clay nanocomposites. *High Performance Polymers*, 24(4):254-261.
DOI: 10.1177/0954008311433605

20. Wu, D., Lin, D., Zhang, J., Zhou, W., Zhang, M., Zhang, Y., Wang, D., Lin, B. (2011). Selective localization of nanofillers: effect on morphology and crystallization of PLA/PCL blends. *Macromolecular Chemistry and Physics*, 212:613-626.
DOI: 10.1002/macp.201000579

21. Hoidy, W.H., Ahmad, M.B. Al-Mulla, E.A.J., Bt Ibrahim, N.A. (2010). Preparation and characterization of polylactic acid/polycaprolactone clay nanocomposites. *Journal of Applied Science*, 10(2):97-106.
ISSN 1812-5654

22. Chapple, S., Anandjiwala, R., Ray, S.S. (2013). Mechanical, thermal, and fire properties of polylactide/starch blend/clay composites. *Journal of Thermal Analysis and Calorimetry*, 113:703-712.
DOI: 10.1007/s10973-012-2776-6

23. http://www.gk-graphite.cn/fileadmin/user_upload/PDF/List_standard.pdf
(29/01/2016)

24. Focke, W.W., Badenhorst, H., Mhike, W., Kruger, H.J., Lombaard, D. (2014). Characterization of commercial expandable graphite fire retardants. *Thermochimica Acta*, 584:8-16.

DOI: 10.1016/j.tca.2014.03.021

25. http://trellisbioplastic.com/wp-content/uploads/2014/08/Sustainable-1001-Property-Guide.pdf (26/10/2015)
26. Uhl, F.M., Yao, Q., Nakajima, H., Manias, E., Wilkie, C.A. (2005). Expandable graphite/polyamide-6 nanocomposites. *Polymer Degradation and Stability*, 89:70-84. DOI: 10.1016/j.polymdegradstab.2005.01.004
27. Bai, G., Guo, C., Li, L. (2014). Synergistic effect of intumescent flame retardant and expandable graphite on mechanical and flame-retardant properties of wood flour-polypropylene composites. *Construction and Building Materials*, 50:148-153. DOI: 10.1016/j.conbuildmat.2013.09.028
28. Xiao, H.W., Li, P., Ren, X., Jiang, T. Yeh, J.-T. (2010). Isothermal crystallization kinetics and crystal structure of poly(lactic acid): Effect of triphenyl phosphate and talc. *Journal of Applied Polymer Science*, 118:3558-3569. DOI: 10.1002/app.32728
29. Wang Y., Lin, C.-S. (2014). Preparation and characterization of maleated polylactide-functionalized graphite oxide nanocomposites. *Journal of Polymer Research*, 21:334 (pp: 1-14). DOI: 10.1007/s10965-013-0334-y
30. Pluta, M., Galeski, A., Alexandre, M., Paul, M.-A., Dubois, P. (2002). Polylactide/montmorillonite nanocomposites and microcomposites prepared by melt blending: Structure and some physical properties. *Journal of Applied Polymer Science*, 86:1497-1506. DOI: 10.1002/app.11309
31. Fukushima, K., Tabuani, D., Camino, G. (2009). Nanocomposites of PLA and PCL based on montmorillonite and sepiolite. *Materials Science and Engineering C*, 29:1433-1441. DOI: 10.1016/j.msec.2008.11.005
32. Liu, J.Y., Reni, L., Wei, Q., Wu, J.L., Liu, S., Wang, Y.J., Li, G.Y. (2011). Fabrication and characterization of polycaprolactone/calcium sulfate whisker composites. *eXPRESS Polymer Letters*, 5(8):742-752. DOI: 10.3144/expresspolymlett.2011.72
33. Narimissa, E., Gupta, R., Bhaskaran, M., Sriram, S. (2012). Influence of nano-graphite platelet concentration on onset of crystalline degradation in polylactide composites. *Polymer Degradation and Stability*, 97:829-832.

DOI: 10.1016/j.polymdegradstab.2012.02.010

34. Fukushima, K., Tabuani, D., Arena, M., Gennari, M., Camino, G. (2013). Effect of clay type on thermal, mechanical properties and biodegradation of poly(lactic acid) nanocomposites. *Reactive & Functional Polymers*, 73:540-549.
DOI: 10.1016/j.reactfunctpolym.2013.01.003

35. Cowie, J.M.G. (1991). Polymers: Chemistry & Physics of Modern Materials. 2nd Edition. CRC Press. Boca Raton.

36. Murariu, M., Dechief, A.-L., Paint, Y., Peeterbroeck, S., Bonnaud, L., Dubois, P. (2012). Polylactide (PLA)-halloysite nanaocomposites: Production, morphology and key-properties. *Journal of Polymers and the Environment,* 20:932-943.
DOI: 10.1007/s10924-0488-4

37. Menczel, J.D., Prime, R.B. (2009). Thermal Analysis of Polymers. Fundamentals and Applications. John Wiley and Sons, New Jersey.

38. Dell' Erba, R., Groeninckx, G., Maglio, G., Malinconico, M., Migliozzi, A. (2001). Immiscible polymer blends of semicrystalline biocompatible components: thermal properties and phase morphology analysis of PLLA/PCL blends. *Polymer,* 42:7831-7840.
PII: S0032-3861(01)00269-5

39. Menard, K.P. (1999). Dynamic Mechanical Analysis. A Practical Introduction. CRC Press LLC. Boca Raton.

40. Fukushima, K., Tabuani, D., Camino, G. (2012) Poly(lactic acid)/clay nanocomposites: effect of nature and content of clay on morphology, thermal and thermo-mechanical properties. *Materials Science and Engineering C,* 32:1790-1795.
DOI: 10.1016/j.msec.2012.04.047

Chapter 7

General conclusions

This study was primarily concerned with the flammability properties of biopolymers and their blends. Flame retarded samples were prepared by melt-mixing, using Brabender Plastograph and the samples were characterized for their fire resistance performance, using cone calorimetry technique. Additionally, morphology and structural characteristics, thermal and dynamic mechanical properties were also evaluated.

This study was pivoted around the question: What influence will commercial expandable graphite (EG) have on the: flammability, thermal, morphology and structure, as well as thermo-mechanical characteristics of Cereplast PLA and its blend with PCL? The current study was aimed at the extension of the possible applications (such as aeroplane, automotive, electric and electronic devices) of PLA/EG and PLA/PCL/EG composites and the addition to the knowledge base in the polymer composites field.

The aims of this study were: i) to investigate whether the incorporation of commercial EG in PLA and a PLA/PCL blend can improve their flammability properties and thermal stability, ii) to determine the influence of blending PLA with PCL on the foregoing properties and iii) to determine the melting and crystallization phenomena, morphology, structure and thermo-mechanical properties of the melt blended PLA/EG and PLA/PCL/EG composites. The objectives were therefore: i) to develop PLA/EG and PLA/PCL/EG at 5, 10 and 15 wt.% EG flame retardant composites and ii) to characterize the composites developed for their flammability performance, thermal decomposition stability, pyrolysis volatile products, morphology, structure, melting and crystallization behaviour and dynamic mechanical properties.

From the first system of PLA/EG composites, it was found that the thermal degradation stability of the PLA/EG composites was improved as a function of EG micro-filler. Although the char content increased with filler loading, the experimental % char content of the composites was less than the sum of the % residue from PLA and the wt.% EG initially mixed with PLA. The flammability performance of the PLA/EG composites was improved, especially

at 15 wt.% EG content. The peak heat release rate (PHRR) was reduced by 74%, the total smoke production (TSP) by 40% and the specific extinction area (SEA) by 55%. The improvements were due to the key ability of EG to exfoliate at elevated temperatures, during which three effects (i.e. via physical mode of action) were in place: i) cooling effect due to the endothermic exfoliation process, thus lowering the temperature of the medium; ii) dilution effect due to the release of H_2O, SO_2 and CO_2 inert gases that have diluted the concentration of evolved flammable volatiles and iii) the formation of an effective protective intumescent char layer that prevented heat transfer from the source to the composites substrates and mass transfer from the composite to the flame zone. This has further excluded the oxygen necessary for combustion. However, since the combustion of EG resulted in CO, CO_2 and heat, the composites were characterized by high CO and CO_2 yields, as well as high THR and EHC.

On morphology, structure, thermal and dynamic mechanical properties of melt-mixed flame retardant PLA/EG composites system, it was found that graphite layers still existed in aggregate form (i.e. EG layered stacks) with poor interfacial adhesion between EG and PLA matrix and the lack of EG single layers dispersion in the composites. The presence of EG in PLA showed no significant changes on glass transition, melting and crystallization temperature from the melt. Furthermore, the presence of EG micro-particles did not favour crystallization of PLA with the consequent reduction in crystallinity of the composites. PLA/EG composites showed enhanced storage and loss moduli at increased temperatures, especially at higher EG contents (i.e. 10 and 15 wt.%). Similar to the DSC results, both the loss modulus and tan δ peaks positions were generally not changed in the presence of EG, confirming that the glass transition temperature of PLA remained unaffected by the EG. These results suggested that the incorporation of the commercial expandable graphite into PLA can preserve most of the thermal properties of the injection molding grade Cereplast PLA, while improving the fire resistance of PLA/EG flame retardant composites.

On the other hand, from the second system of PLA/PCL/EG composites, it was found that the thermal stability of the composites was improved relative to the blend. Although, the char content of the composites, generally increased with EG loadings, but the combined % residue from both the blend and wt.% EG, initially added into the blend was higher than the observed % residue because of thermal degradation mechanism that favoured the formation of CO and CO_2 volatile gases, rather than carbon. From the flammability performance observations, the composite systems had high EHC and CO yields and may require further improvements.

However, it can be concluded that the manufactured materials possessed better fire resistance characteristics due to the ability of EG to exfoliate and intumesce, thereby forming a barrier that protects the underlying composite material from heat, air/oxygen and further pyrolysis and hence combustion. The cone calorimetry investigations showed that the PLA/PCL blend was successfully modified by the EG micro-filler in order to obtain bio-based materials with improved fire resistant properties. This was confirmed by the reduced flammability parameters: 64% in PHRR, 65% in MARHE, 22% in THR, 64% in TSR, and 54 % reduction in SEA. The average-MLR and FPI were, respectively reduced by 75 and 55% in the presence of EG.

The melt-mixing process could not separate the graphite layers, thus the majority of EG existed in the aggregate structure (i.e. EG layered stacks and/or lumps) as observed from XRD and SEM analyses. Although, PCL had some level of adherence onto the surface of PLA phase, it was mainly onto the EG and micro-spherical material components surfaces, indicating that the PLA/PCL blend was immiscible even in the presence of EG micro filler. The incorporation of EG filler had an influence on the melting and crystallization behaviour of PCL than PLA component of the composites. Both the PCL and EG did not favour crystallization of PLA component in the PLA/PCL/EG composites. From the DSC and DMA results, the glass transition temperature of the composites occurred at high temperature, suggesting the PLA chain immobilization effect by EG filler. The PLA/PCL/EG flame retardant composites were generally characterized by low storage and loss moduli, due to aggregation, lack of EG layered stacks (i.e. lumps) dispersion as well as the lack of interfacial adhesion of EG layers with PLA/PCL blend. Further kinetic studies based on the melting and crystallization characteristics and rheology, as well as the static mechanical properties are suggested to be carried out in order to further understand the properties of these flame retardant PLA/PCL/EG composites.

For future work, systems based on different flame retardants, such as vermiculite, diammonium phosphate, magnesium hydroxide nano and micro fillers, zinc borate, aluminum trihydroxide, magnesium carbonate and calcium carbonate, either alone or in collaboration with EG have already been prepared and experiments are ongoing and in some cases discussions of results have begun. Chemical modification of EG will also be attempted in order to improve the dispersion.